

eNOS and Oxidative Stress in the Remodeling Heart

a delicate balance

Elza Dianne van Deel

eNOS and Oxidative Stress in the Remodeling Heart: a delicate balance

Cover design: Vincent J. de Beer en Elza D. van Deel

©2012 Elza D. van Deel
Thesis Erasmus Medical Center, Rotterdam

ISBN: 978-94-6191-158-2

Printed by: Ipskamp Drukkers

eNOS and Oxidative Stress in the Remodeling Heart

a delicate balance

eNOS en Oxidatieve Stress in het Remodellerende Hart

een delicate balans

Proefschrift

ter verkrijging van de graad van doctor aan de
Erasmus Universiteit Rotterdam

op gezag van de rector magnificus
Prof.dr. H.G. Schmidt
en volgens besluit van het College voor Promoties.

De openbare verdediging zal plaatsvinden op
woensdag 25 januari 2012 om 11.30 uur

door

Elza Dianne van Deel

geboren te Rotterdam



Promotiecommissie:

Promotoren: Prof.dr. D.J.G.M. Duncker
Prof.dr. J.H.J. Hoeijmakers

Overige leden: Prof.dr. A.H.J. Danser
Prof.dr. F.W. Prinzen
Dr. J. van der Velden

The studies in this thesis have been performed at the Laboratory for Experimental Cardiology, ErasmusMC Faculty, the Netherlands and at the Center for Vascular Biology and Cardiovascular Division, Department of Medicine, University of Minnesota Medical School, Minneapolis, USA.

Financial support for the publication of this thesis was generously provided by:

the Dutch Heart Foundation
J.E. Jurriaanse stichting
UNO Roestvaststaal BV

The research described in this thesis was supported by a grant from the Dutch Heart Foundation (DHF-2007B024)

Contents

Chapter 1	General Introduction and Outline of this Thesis	9
Chapter 2	Inducible Nitric Oxide Synthase Deficiency Protects the Heart From Systolic Overload-Induced Ventricular Hypertrophy and Congestive Heart Failure.	25
Chapter 3	Reduction of Blood Pressure, Plasma Cholesterol and Atherosclerosis by Elevated Endothelial Nitric Oxide.	45
Chapter 4	Vasomotor Control in Mice Overexpressing Human Endothelial Nitric Oxide Synthase.	59
Chapter 5	Exercise Training does not Improve Cardiac Function in Compensated or Decompensated Left Ventricular Hypertrophy Induced by Aortic Stenosis.	77
Chapter 6	eNOS Overexpression is Detrimental in LV Pressure-Overload by Enhancing Oxidative Stress	99
Chapter 7	Extracellular Superoxide Dismutase Deficiency Exacerbates Pressure Overload-Induced Left Ventricular Hypertrophy and Dysfunction.	117
Chapter 8	Extracellular Superoxide Dismutase Protects the Heart against Oxidative Stress and Hypertrophy after Myocardial Infarction.	131
Chapter 9	Accelerated Aging in Xpd ^{TTD} Mutant Mice is Associated with Increased Vulnerability to Pressure-Overload but not to Myocardial Infarction.	147
Chapter 10	General Conclusions	163
Chapter 11	Summary	181
	Nederlandse Samenvatting	187
	PhD Portfolio	193
	List of Publications	199
	Curriculum Vitae	205
	Dankwoord	207



A grayscale photograph of a hand pointing towards the left, set against a background of a white grid pattern on a dark surface. The hand is positioned in the lower half of the frame, with the index finger extended. The grid pattern consists of white lines forming a series of squares.

General Introduction and Outline of this Thesis

1

1

List of abbreviations:

HF:	heart failure
MI:	myocardial infarction
LV:	left ventricle
SR:	sarcoplasmic reticulum
ROS:	reactive oxygen species
SERCA2a:	SR calcium-ATPase 2a
MAPK:	mitogen-activated protein kinase
TGF β :	transforming growth factor beta
NO:	nitric oxide
NOS:	NO synthase
BH ₄ :	tetrahydrobiopterin
nNOS:	neuronal NOS
iNOS:	inducible NOS
eNOS:	endothelial NOS
SOD:	superoxide dismutase
EC-SOD:	extracellular-SOD
TTD:	trichothiodystrophy
PI3K:	phosphoinositide-3 kinase
TAC:	transverse aortic constriction

Epidemiology of Heart Failure

Cardiovascular disease has become the leading cause of death worldwide.¹ Although typically characterized as a major burden in the Western world, heart related diseases are also rapidly expanding in developing countries. In the Netherlands, cardiovascular diseases are responsible for 30% of all deaths and are the main cause of death in woman.² Paradoxically, improved treatment of cardiovascular diseases reduced acute mortality but greatly increased the number of patients suffering from insufficient cardiac pump function referred to as heart failure (HF). HF is the final common stage of all cardiac diseases and considerably increases the risk for morbidity and mortality. Moreover, the prevalence (proportion of the population affected by the disease) and incidence (number of new cases in a period of time) are still increasing.³⁻⁴ With a prevalence of over 23 million globally,⁵ HF has become a chronic disease epidemic. Large cohort studies like the Framingham Heart Study, the Rochester Epidemiologic Project in Olmsted County and the Rotterdam Study consistently show that the prevalence of HF is higher in men than in woman and substantially increases with age⁶⁻¹⁰ reaching 1% in those 55-64 years of age and 13% in those aged over 75 years in the Rotterdam Study.⁶ Additionally race appears to play a role in the prevalence of HF as death rates of HF have shown to be higher in black than in white patients.⁸

The most important cause of HF is myocardial infarction (MI) secondary to ischemic heart disease.^{5,11} Prolonged ischemia in the heart due to occlusion of the coronary artery results in necrosis of the heart muscle. Loss of viable myocardial tissue impairs cardiac function that can ultimately result in chronic HF. Reperfusion therapy within 12 hours after MI decreases the severity of MI and as such would reduce the patient's risk for HF.¹² However, results from the Framingham Heart Study show that improved survival after MI coincides with increased incidence of HF by increasing the population at risk.¹³ A second prominent cause for HF is chronic pressure-overload as a consequence of systemic hypertension^{10,14} or obstruction of the aortic outflow track by aortic stenosis.¹⁵ In pressure-overload, the elevated hemodynamic afterload forces the heart to enhance its contractile force and develop hypertrophy in order to maintain cardiac output. However, over time the heart is unable to maintain this continuous increased workload, resulting in myocardial dysfunction which eventually leads to cardiac failure. Beside stenotic valve disease, cardiac valves can also become incapable to close properly resulting in valvular leakage or regurgitation. Valve regurgitation induces volume-overload to the heart and consequently forces the heart to increase stroke volume to maintain forward flow despite the regurgitation.¹⁶ Over time also this form of chronic burden to the heart will increase the risk for HF. An additional risk factor with increasing prevalence in the general population is diabetes mellitus. Diabetes mellitus, a metabolic disease characterized by high blood sugar levels, increases the risk of HF independent of coronary heart disease, hypertension or any other recognized cardiac cause.¹⁷⁻¹⁹ The relative risk of HF in diabetes mellitus patients is approximately 2 fold higher in men and 5 fold higher in women than it is for non diabetic patients.^{9-10,19} Moreover, diabetes is not only a risk factor for developing HF, but also worsens outcomes in the presence of HF. Finally, several gene mutations have been found to contribute to the development of HF.²⁰

Although all these risk factors eventually predispose the heart to HF they do not all induce identical symptoms or similarly affect the heart. In fact two distinct phenotypic forms of HF can be distinguished, although both forms regularly present themselves simultaneously. Systolic HF is characterized by impaired contractile force of the cardiac muscle resulting in reduced stroke volume and LV dilation,²¹ whereas in diastolic HF reduced stroke volume is principally caused by impaired filling of the heart due to LV stiffening with no or minimal increase in LV dimensions.²²⁻²³ These distinct underlying pathologies subsequently lead to correspondingly distinct adaptations of the heart characterized by typical cardiac hypertrophic remodeling.

Pathological cardiac remodeling

Cardiac hypertrophic remodeling is induced as an adaptive response to cope with increased hemodynamic load.²⁴ However, over time the persistent overloading of the heart directs the cardiac remodeling from a compensatory towards a pathological decompensated response, characterized by excessive hypertrophy, dilation and cardiac dysfunction that ultimately results in chronic heart failure^{16,24}. Prolonged LV failure can induce pulmonary congestion that is characterized by buildup of fluid in the lungs.²⁵ This will increase pulmonary pressure and subsequently result in right ventricular failure and further deterioration of cardiac function.

Classically two separate pathological hypertrophic phenotypes can be distinguished.^{16,26} Pressure-overload caused by hypertension or aortic stenosis induces concentric hypertrophy that is typical for diastolic HF²⁷ and characterized by myocyte thickening, normal or slightly decreased left ventricular (LV) volume and parallel addition of sarcomeres^{24,28} (Figure 1). Consequently, the pressure increase is offset by an increase in wall thickness to normalize wall tension in this type of remodeling. On the other hand, eccentric hypertrophy induced by volume-overload or MI, is more pronounced in systolic HF^{27,29} and characterized by LV dilation. In this form of hypertrophy, myocyte lengthening with sarcomeres added in series results in LV dilation,^{24,28} that acts as a compensatory mechanism to maintain stroke volume in spite of reduced LV function.^{16,30} However, over time the compensatory hypertrophy will evolve into pathological remodeling and concomitant cardiac dysfunction.

In the healthy heart a dense network of capillaries ensures sufficient oxygen supply to meet the high energy demand of properly contracting myocytes. Contractile function of cardiac myocytes is regulated by Ca^{2+} triggered release of Ca^{2+} from the sarcoplasmic reticulum (SR) that induces contraction by binding to the myofilaments. Reuptake of Ca^{2+} in the SR and release of Ca^{2+} from the myofilaments subsequently causes cardiac muscle relaxation. Additionally, neurohumoral systems allow the heart to rapidly adapt heart rate and cardiac contractility in response to changes in oxygen demand of the body. However, under pathological conditions alterations in hemodynamic loading conditions initiate neurohumoral and energetic alterations as well as numerous cross-talking intracellular signaling pathways that lead to the complex multifactorial process of adverse cardiac remodeling^{24,31-34} (Figure 2). Activation of G-protein-coupled receptors by ligands such as angiotensin II, endothelin, stimulation of β -adrenergic receptor by catecholamines and

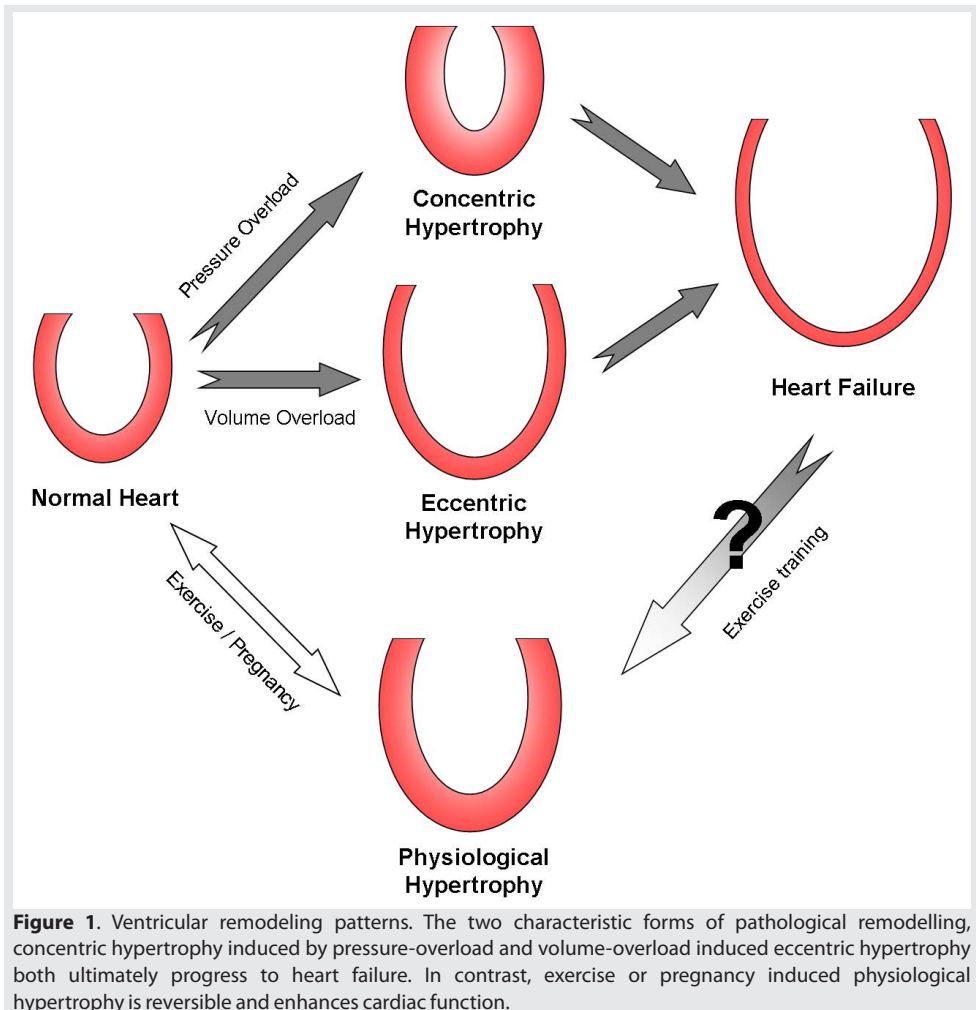


Figure 1. Ventricular remodeling patterns. The two characteristic forms of pathological remodelling, concentric hypertrophy induced by pressure-overload and volume-overload induced eccentric hypertrophy both ultimately progress to heart failure. In contrast, exercise or pregnancy induced physiological hypertrophy is reversible and enhances cardiac function.

activation of natriuretic peptide receptors and cytokine receptors boost a multitude of signaling pathways. Subsequently, these pathways stimulate the production of reactive oxygen species (ROS) that induce cellular damage, fibrosis and apoptosis and activate numerous transcription factors inducing cardiac hypertrophy.^{30,34-35} Myocyte hypertrophy reduces the capillary density and increases vascular length, resulting in impaired oxygen supply to the heart. This reduced oxygen supply becomes even more problematic in the failing heart, in which as a consequence of an increased heart rate and wall stress the demand for oxygen is increased. Additionally, disturbed β -adrenergic signaling impairs cardiomyocyte Ca^{2+} handling and thereby reduces contractile function³⁸ by down regulating SR calcium-ATPase 2a (SERCA2a)³⁹ and the ryanodine receptor⁴⁰ as well as reducing phospholamban phosphorylation⁴¹ and increasing Ca^{2+} sensitivity of the myofilaments⁴² (Figure 2).

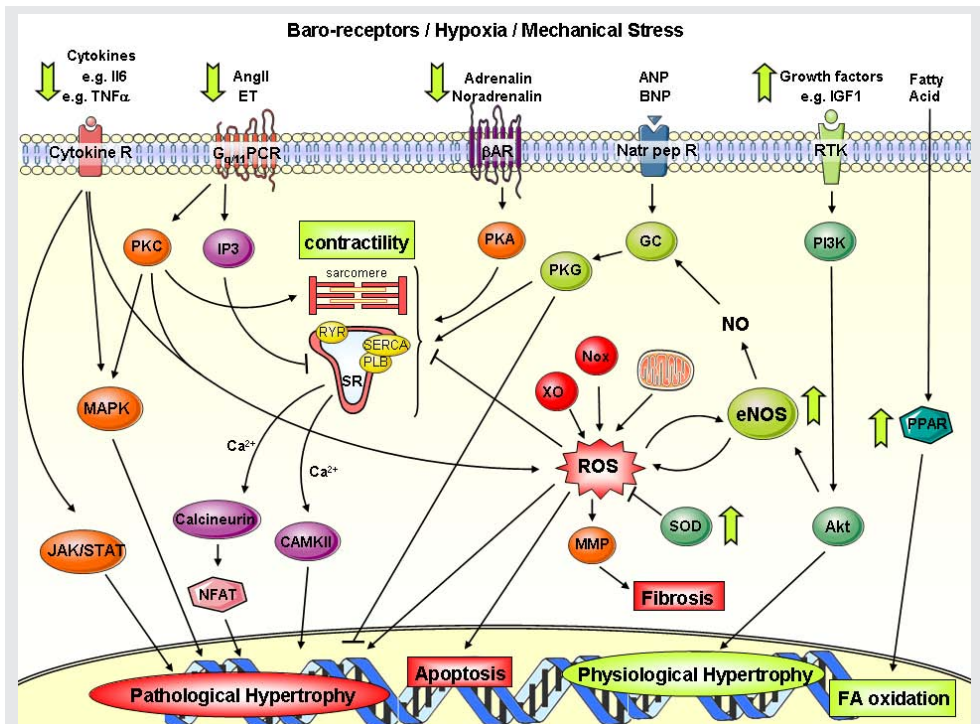


Figure 2. Signalling pathways involved in pathological and physiological cardiac remodelling. Cytokines including interleukin(IL)-6 and tumor necrosis factor (TNF), impair myocardial contractility by disturbing Ca²⁺ handling and induce pathological remodelling via the mitogen-activated protein kinase (MAPK) and the JAK/STAT pathways. Ligands such as angiotensin (Ang II), endothelin (ET)-1 and noradrenalin activate G-protein-coupled receptors (Gq/11PCR) that in turn activate several proteins involving protein kinases C, MAPK, the calcineurin-nuclear factor of activated T cells (NFAT) pathway and Ca²⁺/calmodulin-dependent kinase II (CAMKII). Subsequently, numerous transcription factors are activated to induce the development of cardiac hypertrophy. Impaired β-adrenergic signaling through PKA reduces cardiomyocyte contractile function by impairing Ca²⁺ handling through down regulation of sarcoplasmic reticulum calcium-ATPase2a (SERCA2a) and the ryanodine receptor (RyR) and upregulation of phospholamban (PLB) levels and increasing Ca²⁺ sensitivity of the myofilaments. Re-induction of the fetal gene program that includes atrial natriuretic peptide (ANP) and brain natriuretic peptide (BNP) attenuate pathological remodelling via PKG. PKG is also activated through increased bioavailability of nitric oxide (NO). Endothelial NO synthase (eNOS) can be activated by exercise or the PI3K.Akt pathway that also directly promotes physical hypertrophy. Peroxisome proliferation-activated receptors (PPARs) control the cardiac metabolic switch from fatty acid oxidation to a more glycolytic metabolism and consequently regulate the myocardial energy metabolism. Finally, many of these pathological pathways stimulate the formation of reactive oxygen specie (ROS) that induce cellular and genetic damage contributing to cardiac fibrosis and apoptosis. Green arrows represent the beneficial effects of physical exercise training.

In addition, several animal studies indicate that concentric and eccentric hypertrophy, besides a common response, are associated with distinct signaling pathways that contribute to the development of the corresponding phenotype. Expression levels of the pathological hypertrophy markers α-skeletal muscle actin and β-myosin heavy chain are elevated in response to pressure-overload and MI but less evidently increased in volume-overloading.⁴³⁻⁴⁶ Additionally, specific regulation of members of the mitogen-activated

protein kinase (MAPK) family appears to occur in pressure and volume-overload^{44,47} and different hemodynamic loading also differentially affects expression of peptide growth factors, with an up regulation of transforming growth factor beta (TGF β) and insulin-like growth factor 1 in pressure-overload and down regulation of acidic fibroblast growth factor in the volume-overloaded heart.⁴³ Apparently, the development of pathological hypertrophy is not completely similar in the different etiologies.

Another contributor to the development of pathological remodeling and HF is a reduction in bioavailability of protective molecules like nitric oxide (NO).⁴⁸ The biosynthesis of NO depends on the enzymatic activity of NO synthase (NOS) which catalyses the reaction between L-arginine and oxygen to form L-citrulline and NO and requires co-factors like tetrahydrobiopterin (BH4).⁴⁹⁻⁵⁰ Part of the cardioprotection by NO is mediated through NO protein S-nitrosylation.⁵¹ Protein S-nitrosylation not only leads to changes in protein structure and function but also prevents further oxidative protein modification. Consistent with a protective role for NO, cardioprotection has also been shown to involve an increase in NOS. In the heart, NO is produced by three NOS isoforms: neuronal NOS (nNOS), inducible NOS (iNOS) and endothelial NOS (eNOS).⁵² The cardioprotective effects of NO are predominantly induced through NO production by nNOS and eNOS that are constitutively present in the heart. nNOS is involved in the regulation of Ca²⁺ storage and stimulates cardiomyocyte contractile function by influencing the activities of Ca²⁺-handling genes and inhibiting Ca²⁺ entry through the L-type Ca²⁺ channels.⁵³ Beneficial properties of eNOS include vasodilation,⁵⁴ inhibition of leukocyte adhesion,⁵⁵ stimulation of cardiac function⁵⁶ and attenuation of pathological remodeling.⁵⁷⁻⁵⁸ However, under pathological conditions, oxidation or reduction of the eNOS cofactor BH4 causes eNOS to uncouple from a dimeric to a monomeric form that no longer produces NO but forms superoxide (O₂⁻) instead.⁵⁰ O₂⁻ by itself is capable of inducing severe cellular damage and additional eNOS uncoupling. Furthermore, O₂⁻ can react with NO to form the powerful oxidant peroxynitrite.⁵⁹ Consequently, eNOS mediated O₂⁻ production not only results in formation of damaging oxygen radicals but also reduces the bioavailability of NO. Likewise, iNOS is known for its role in pathology and constitutes an important component of the immune defence mechanism by producing large toxic amounts of NO.⁶⁰ Additionally potential iNOS uncoupling would contribute to adverse remodeling and dysfunction. On the other hand, iNOS induced NO production can also be cardioprotective in heart failure. Hence whether observed upregulation of iNOS in the pathological remodeled heart⁶¹ is an adaptive or maladaptive response remains the subject of debate. Consequently, the role and potential of NOS in cardiovascular diseases is complex and not yet completely understood.

In pathological remodeling elevated levels of O₂⁻ and other ROS not only result from NOS-uncoupling but initially involve excessive ROS production by mitochondria and ROS producing enzymes.⁶² Under healthy physiological conditions endogenous enzymatic and nonenzymatic antioxidants systems balance the formation of ROS to ensure proper cell functionality and allow small amounts of ROS to act as signaling molecules in many physiological processes.⁶³ However, under pathological conditions ROS production overwhelms the antioxidant defense mechanism, resulting in oxidative stress that induces

1

oxidation and damage to DNA, membranes, proteins and other macromolecules.^{62,64} Consequently oxidative stress influences different aspects of progressive heart failure such as cellular hypertrophy and dysfunction, altered gene expression, cell death, fibrosis and altered Ca^{2+} handling.⁶²⁻⁶³ Well characterized enzymatic antioxidants are superoxide dismutases (SODs) that catalyze the formation of hydrogen peroxide from superoxide⁶⁵⁻⁶⁶ and glutathione peroxidase and catalase that facilitate the conversion of hydrogen peroxide to water.^{48,65} In humans three forms of superoxide dismutase are present: cytosolic-SOD, mitochondrial-SOD and extracellular-SOD (EC-SOD) that resides in the interstitial space of tissues and in extracellular fluids.^{48,65} The antioxidant enzyme EC-SOD is particularly interesting because its potential role in maintaining the balance between NO and ROS: the nitroso-redox balance. A functional correlation between EC-SOD and eNOS is suggested by colocalization between EC-SOD and eNOS in the myocardium,⁶⁷ EC-SOD-increased NO bioavailability by preventing scavenging of endothelium-derived NO⁶⁸ and stimulation of EC-SOD expression by NO.⁶⁹ Hence EC-SOD could be a potent inhibitor of eNOS-uncoupling and accordingly play an important role in the defense against cardiac remodeling and dysfunction.

As mentioned above the detrimental effects of ROS in HF are partly caused by ROS induced DNA damage that results in gene transcriptional defects and consequent cellular dysfunction as well as increased vulnerability to pathological stimuli. Cumulated DNA damage is also linked to aging.⁷⁰ Interestingly, the aged heart shares many characteristics with the failing heart.⁷¹ First the total number of cardiomyocytes declines with age. This in turn leads to replacement hypertrophy of the remaining cardiomyocytes and deposition of collagen (i.e. cardiac fibrosis).⁷²⁻⁷³ Additionally, aging results in impaired Ca^{2+} handling and decreased cardiac responsiveness to β -adrenergic stimulation.⁷²⁻⁷³ These changes may affect cardiac function only minimally under non pathological conditions but likely result in reduced cardiac reserve and increased vulnerability of the heart to develop cardiac failure. Accordingly, clinical trials have shown that age is an important predictor for mortality in heart failure patients.^{3,74} To investigate the influence of cumulative DNA damage and concomitant accelerated aging, several genetic mouse models have been created that develop cumulative DNA damage by a defect in a DNA repair mechanism.⁷⁵ Among these mouse models, mice with a mutation of the XPD gene of the nucleotide excision repair mechanism, that consequently develop cumulative DNA damage and impaired DNA transcription, show prominent symptoms of accelerated aging resembling the human heritable disorder trichothiodystrophy (TTD).⁷⁶ These Xpd^{TTD} mice display many symptoms of premature aging, including cachexia, brittle hair and osteoporosis but no cardiac dysfunction.⁷⁷ Consequently this mouse model represents a very useful tool to further elucidate the effects of DNA damage on cardiac remodeling in response to pathological overload and could potentially contribute to a better understanding of the mechanism behind increased cardiac vulnerability with aging.

In summary pathological cardiac remodeling is induced by persistent overloading of the myocardium that initiates altered cellular signaling and gene expression. Subsequently, these alterations provoke LV hypertrophy and dilation as well as concomitant fibrosis, apoptosis and impaired Ca^{2+} handling that collectively promote the progression of HF.

Physiological cardiac remodeling

Interestingly, in contrast to pathological cardiac remodeling, exercise induces physiological remodeling in which cardiac hypertrophy occurs without maladaptive alterations and normal or even enhanced cardiac function. Exercise training is associated with cardiovascular adaptations that improve cardiac performance by enhancing oxygen extraction and reducing cardiac afterload.⁷⁸⁻⁸¹ Consequently, LV stroke volume is increased which facilitates elevation of cardiac output during exercise and thus improves exercise capacity. Additionally, exercise training induces reversible physiological cardiac hypertrophy that, unlike pathological remodeling, is characterized by increased chamber volume accompanied by proportional increased wall thickness (Figure 1) and appropriate structural and functional changes of the coronary vasculature that improve oxygen delivery to the myocardium.⁸²⁻⁸⁴ These adaptations are mediated by specific growth factors that activate the phosphoinositide-3 kinase (PI3K)/Akt pathway.⁸⁵⁻⁸⁶ Unlike in pathological hypertrophy, physiological hypertrophy is not accompanied by fibrosis or apoptosis and protects against the development of HF. Additionally, intensive physical activity potentially enhances cardiac function through several mechanisms including elevated peroxisome proliferator-activated receptor expression which improves lipid metabolism,³⁶ enhanced Ca^{2+} handling in the cardiomyocyte by increased Ca^{2+} sensitivity of the myofilaments, improved length-dependent activation of the sarcomeres⁷⁹ and elevated myosin ATPase activity.³⁷

The beneficial effects of exercise on physiological cardiac remodeling are critically regulated by eNOS.⁸⁷⁻⁸⁸ Physical exercise enhances eNOS and NO bio-availability through enhanced shear stress and mechanical stretch.⁵⁷ Increased shear stress stimulates endothelial NO production in the vasculature⁸⁹ that, by means of vasodilation, acutely increases blood flow to the heart and skeletal muscles to increase oxygen supply. In addition, shear stress induced endothelial NO also forms a significant source of NO for cardiomyocytes.⁹⁰ Repeated exercise training also induces chronic structural and functional coronary vascular adaptations that further aid to improve oxygen delivery to the myocardium.⁸² Additionally, exercise increases cardiomyocyte eNOS levels in response to cyclic stretch through stretch-activated channels⁵⁷ and growth factor activation of the PI3K/Akt pathway.⁵⁷ Hence, increased eNOS activation and expression affects the myocardium by elevating paracrine NO from nearby endothelial cells as well as autocrine NO production within the cardiomyocytes. Furthermore, NO promotes cardiac relaxation and filling by cGMP-PKG mediated desensitization of cardiac myofillaments,⁵⁶ increases Troponin I phosphorylation⁹¹ and decreases duration of contraction.⁹² Simultaneously, stretch-activated eNOS, independent of cGMP, increases contractile force by influencing Ca^{2+} release and uptake of the SR by regulating the SR-calcium release channel (RyR) and the SR-calcium ATPase channel.⁵⁷⁻⁹³ Additionally, eNOS inhibits pathological hypertrophy by activation of PKG. Finally, exercise elevates antioxidant enzymes levels⁹⁴ that by reducing ROS further enhance NO bioavailability and improve cardiovascular health.⁹⁵⁻⁹⁶ Indeed, in spite of safety concerns that exercise may provide additional hemodynamic overload to the diseased heart, both clinical and experimental studies showed that regular exercise training is safe for heart failure patients and not only induces numerous protective cardiovascular effects but also induces beneficial pulmonary and skeletal

muscle adaptations and increases quality of life.⁹⁷⁻¹⁰¹ Therefore, exercise training is currently an important aspect of cardiac rehabilitation programs for HF patients.⁹⁸ Accordingly, we previously demonstrated that exercise training³⁹ as well as eNOS overexpression¹⁰² attenuated cardiac dysfunction following MI. However, whether these cardioprotective effects of eNOS upregulation equally benefit heart failure induced by other etiologies is unclear. Additionally, pharmacological stimulation eNOS-mediated NO production without detrimental effects of exercise-induced systolic overload, could potentially be more effective than exercise training alone.

Aim and outline of this thesis

The general aim of this thesis is to study the role of alterations in the balance between NO and oxidative stress in pathological LV remodeling and dysfunction secondary to pressure-overload or MI in genetic mouse models and by investigating the effect of physical exercise training. Additionally, the influence of ROS induced cumulative DNA damage on adverse cardiac remodeling and dysfunction are investigated (Figure 3).

NO is an important regulator of cardiovascular function.⁵⁶ However the role of NOS remains controversial since NOS exhibits cardiac protective effects by producing NO as well as destructive properties when uncoupled and producing O_2^- .⁵⁷ Particularly the NOS isoform iNOS is well known for its detrimental properties of producing high toxic amounts of NO or generating ROS when uncoupled. In **chapter 2** we tested the hypothesis that iNOS-related ROS production contributes to cardiac hypertrophy and dysfunction in the pressure-overload heart by subjecting iNOS deficient mice to a transverse aortic constriction (TAC). The results showed that iNOS deficiency protects the heart from pressure-overload induced hypertrophy and attenuates cardiac dysfunction and pulmonary congestion by abrogation of iNOS uncoupling. In contrast to iNOS, eNOS has been proposed to improve cardiac health. To elucidate the influence of eNOS on cardiac pathology we first studied the in vivo effects of increased eNOS expression on the cardiovascular system in health, atherosclerosis (**chapter 3**) and in more detail in the regulation of vascular tone (**chapter 4**). The result showed that the 10-fold elevated gene expression was partly compensated by attenuation of eNOS-mediated vasodilation through blunted NO responsiveness of guanylyl cyclase. Because the beneficial cardiac effects of physical exercise training are thought to be principally mediated by eNOS,⁸⁸ we investigated in **chapter 5** the potentially protective effects of exercise training in pressure-overload. In contrast to previous reported beneficial effects of exercise on LV function after MI,³⁹ exercise training did not improve but instead tended to aggravate cardiac hypertrophy and dysfunction following TAC. Consequently, the beneficial effect of exercise training on cardiac hypertrophy and dysfunction, critically depend on the underlying cause. The absence of positive exercise effects in TAC may be explained by exacerbated systolic loading during exercise in this mouse model with a fixed aorta stenosis. Therefore, in **chapter 6**, we examine the mechanisms of exercise training without deleterious exacerbated hemodynamic loading by examining the influence of eNOS (as a mediator of exercise induced cardiac protection) on pressure-overload induced cardiac remodeling and dysfunction. To study the complete spectrum of eNOS

levels and elucidate the influence of reduced as well as elevated eNOS content, we used eNOS deficient mice and eNOS overexpressing mice.

To investigate the potential benefit of preventing oxidative stress, we studied in **chapter 7** the role of the antioxidant EC-SOD on pressure-overload induced LV hypertrophy and dysfunction in EC-SOD deficient mice. Given its co-localisation with eNOS and NO regulated expression, EC-SOD not only scavenges O_2^- in general but also presents a potential inhibitor of eNOS-uncoupling induced aggravation of cardiac failure. Indeed the results obtained in this research demonstrate that loss of EC-SOD deteriorates cardiac remodeling and dysfunction from TAC. Because different etiologies involve distinct patterns for cardiac remodeling and consequently ROS production is particularly increased in pressure-overload compared to other causes of HF, we investigated in **chapter 8** whether EC-SOD was also important in MI. Similar to results in pressure-overload (**chapter 7**) EC-SOD also proved to protect the heart against oxidative stress and hypertrophy following MI. ROS induced DNA damage not only evokes cardiac pathology but is also closely linked to aging.⁷⁰ Gene transcription and regulation defects endanger proper cellular function and increase the susceptibility to pathology. To investigate whether DNA damage contributes to increased vulnerability of the heart to pathological stimuli, we studied in **chapter 9** cardiac hypertrophy and dysfunction following TAC and MI in DNA-repair deficient mice that consequently age prematurely. In **chapter 10** a discussion of the major findings of the studies presented in this thesis and future perspectives are presented. Finally a summary of the research described in this thesis is given in **chapter 11**.

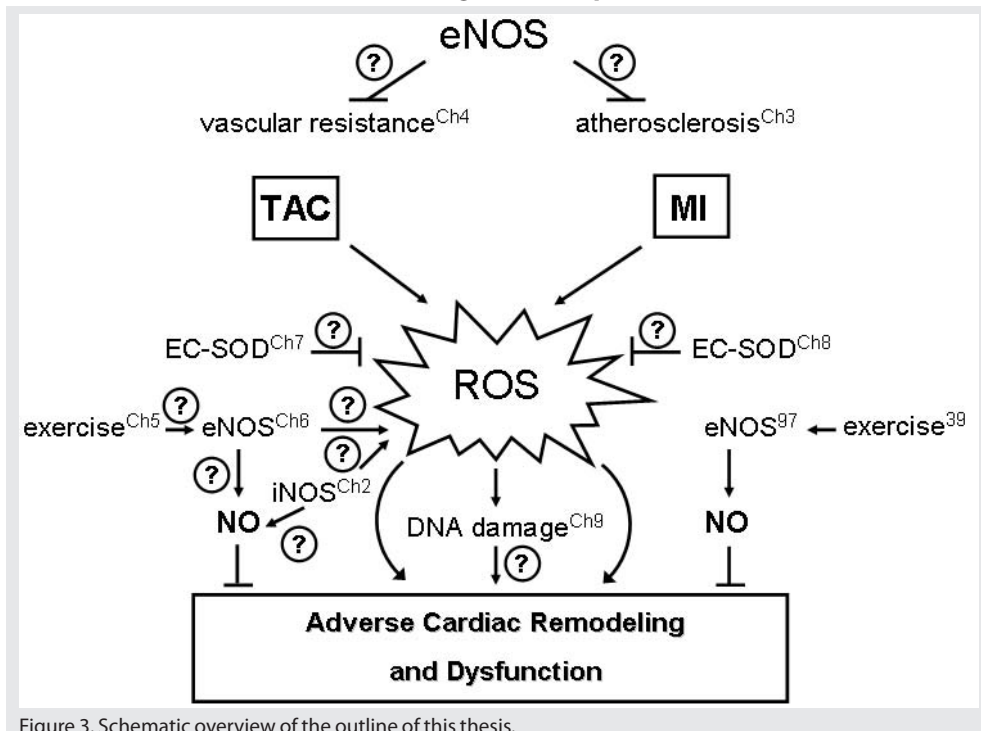


Figure 3. Schematic overview of the outline of this thesis.

References

1. World-Health-Organization, *The Global Burden of Disease: 2004 Update*. 2008: Geneva, Switzerland.
2. Netherlands-Heart-Foundation, *Hart- en vaatziekten in Nederland 2010, Cijfers over leefstijl- en risicofactoren, ziekte en sterfte*. 2010: Den Haag, The Netherlands.
3. Curtis, L.H., et al., *Incidence and prevalence of heart failure in elderly persons, 1994-2003*. Arch Intern Med, 2008. **168**(4): p. 418-24.
4. McCullough, P.A., et al., *Confirmation of a heart failure epidemic: findings from the Resource Utilization Among Congestive Heart Failure (REACH) study*. J Am Coll Cardiol, 2002. **39**(1): p. 60-9.
5. Bui, A.L., T.B. Horwich, and G.C. Fonarow, *Epidemiology and risk profile of heart failure*. Nat Rev Cardiol, 2011. **8**(1): p. 30-41.
6. Mosterd, A., et al., *Prevalence of heart failure and left ventricular dysfunction in the general population; The Rotterdam Study*. Eur Heart J, 1999. **20**(6): p. 447-55.
7. Redfield, M.M., et al., *Burden of systolic and diastolic ventricular dysfunction in the community: appreciating the scope of the heart failure epidemic*. JAMA, 2003. **289**(2): p. 194-202.
8. Roger, V.L., et al., *Heart disease and stroke statistics--2011 update: a report from the American Heart Association*. Circulation, 2011. **123**(4): p. e18-e209.
9. Levy, D., et al., *Long-term trends in the incidence of and survival with heart failure*. N Engl J Med, 2002. **347**(18): p. 1397-402.
10. Lloyd-Jones, D.M., et al., *Lifetime risk for developing congestive heart failure: the Framingham Heart Study*. Circulation, 2002. **106**(24): p. 3068-72.
11. Loefer, L.R., et al., *Heart failure incidence and survival (from the Atherosclerosis Risk in Communities study)*. Am J Cardiol, 2008. **101**(7): p. 1016-22.
12. Van de Werf, F., et al., *Management of acute myocardial infarction in patients presenting with persistent ST-segment elevation: the Task Force on the Management of ST-Segment Elevation Acute Myocardial Infarction of the European Society of Cardiology*. Eur Heart J, 2008. **29**(23): p. 2909-45.
13. Velagaleti, R.S., et al., *Long-term trends in the incidence of heart failure after myocardial infarction*. Circulation, 2008. **118**(20): p. 2057-62.
14. Mosterd, A. and A.W. Hoes, *Clinical epidemiology of heart failure*. Heart, 2007. **93**(9): p. 1137-46.
15. Chambers, J., *The left ventricle in aortic stenosis: evidence for the use of ACE inhibitors*. Heart, 2006. **92**(3): p. 420-3.
16. Opie, L.H., et al., *Controversies in ventricular remodelling*. Lancet, 2006. **367**(9507): p. 356-67.
17. Baliga, V. and R. Sapsford, *Review article: Diabetes mellitus and heart failure--an overview of epidemiology and management*. Diab Vasc Dis Res, 2009. **6**(3): p. 164-71.
18. Cohen-Solal, A., F. Beauvais, and D. Logeart, *Heart failure and diabetes mellitus: epidemiology and management of an alarming association*. J Card Fail, 2008. **14**(7): p. 615-25.
19. Kannel, W.B. and D.L. McGee, *Diabetes and cardiovascular risk factors: the Framingham study*. Circulation, 1979. **59**(1): p. 8-13.
20. Creemers, E.E., A.A. Wilde, and Y.M. Pinto, *Heart failure: advances through genomics*. Nat Rev Genet, 2011. **12**(5): p. 357-62.
21. Chatterjee, K. and J.E. Rame, *Systolic heart failure: chronic and acute syndromes*. Crit Care Med, 2008. **36**(1 Suppl): p. S44-51.
22. Paulus, W.J., *Novel strategies in diastolic heart failure*. Heart, 2010. **96**(14): p. 1147-53.
23. van der Velden, J., *Diastolic myofilament dysfunction in the failing human heart*. Pflugers Arch, 2011. **462**(1): p. 155-63.
24. Heineke, J. and J.D. Molkentin, *Regulation of cardiac hypertrophy by intracellular signalling pathways*. Nat Rev Mol Cell Biol, 2006. **7**(8): p. 589-600.
25. Picano, E., L. Gargani, and M. Gheorghide, *Why, when, and how to assess pulmonary congestion in heart failure: pathophysiological, clinical, and methodological implications*. Heart Fail Rev, 2010. **15**(1): p. 63-72.
26. Linzbach, A.J., *Heart failure from the point of view of quantitative anatomy*. Am J Cardiol, 1960. **5**: p. 370-82.
27. van Heerebeek, L., et al., *Myocardial structure and function differ in systolic and diastolic heart failure*. Circulation, 2006. **113**(16): p. 1966-73.
28. Kehat, I. and J.D. Molkentin, *Molecular pathways underlying cardiac remodeling during pathophysiological stimulation*. Circulation, 2010. **122**(25): p. 2727-35.
29. Berenji, K., et al., *Does load-induced ventricular hypertrophy progress to systolic heart failure? Am J Physiol Heart Circ Physiol*, 2005. **289**(1): p. H8-H16.

30. Frey, N., et al., *Hypertrophy of the heart: a new therapeutic target?* Circulation, 2004. **109**(13): p. 1580-9.
31. Duncker, D.J., V.J. de Beer, and D. Merkus, *Alterations in vasomotor control of coronary resistance vessels in remodelled myocardium of swine with a recent myocardial infarction.* Med Biol Eng Comput, 2008. **46**(5): p. 485-97.
32. Duncker, D.J., Y. Ishibashi, and R.J. Bache, *Effect of treadmill exercise on transmural distribution of blood flow in hypertrophied left ventricle.* Am J Physiol, 1998. **275**(4 Pt 2): p. H1274-82.
33. Kuster, D.W., et al., *'Integrative Physiology 2.0': integration of systems biology into physiology and its application to cardiovascular homeostasis.* J Physiol, 2011. **589**(Pt 5): p. 1037-45.
34. Mudd, J.O. and D.A. Kass, *Tackling heart failure in the twenty-first century.* Nature, 2008. **451**(7181): p. 919-28.
35. Schluter, K.D. and S. Wenzel, *Angiotensin II: a hormone involved in and contributing to pro-hypertrophic cardiac networks and target of anti-hypertrophic cross-talks.* Pharmacol Ther, 2008. **119**(3): p. 311-25.
36. Robinson, E. and D.J. Grieve, *Significance of peroxisome proliferator-activated receptors in the cardiovascular system in health and disease.* Pharmacol Ther, 2009. **122**(3): p. 246-63.
37. Wikman-Coffelt, J., W.W. Parmley, and D.T. Mason, *The cardiac hypertrophy process. Analyses of factors determining pathological vs. physiological development.* Circ Res, 1979. **45**(6): p. 697-707.
38. Diaz, M.E., et al., *The control of sarcoplasmic reticulum Ca content in cardiac muscle.* Cell Calcium, 2005. **38**(3-4): p. 391-6.
39. de Waard, M.C., et al., *Early exercise training normalizes myofilament function and attenuates left ventricular pump dysfunction in mice with a large myocardial infarction.* Circ Res, 2007. **100**(7): p. 1079-88.
40. Hashida, H., M. Hamada, and K. Hiwada, *Serial changes in sarcoplasmic reticulum gene expression in volume-overloaded cardiac hypertrophy in the rat: effect of an angiotensin II receptor antagonist.* Clin Sci (Lond), 1999. **96**(4): p. 387-95.
41. Schwinger, R.H., et al., *Reduced Ca(2+)-sensitivity of SERCA 2a in failing human myocardium due to reduced serin-16 phospholamban phosphorylation.* J Mol Cell Cardiol, 1999. **31**(3): p. 479-91.
42. van der Velden, J., et al., *Alterations in myofilament function contribute to left ventricular dysfunction in pigs early after myocardial infarction.* Circ Res, 2004. **95**(11): p. e85-95.
43. Calderone, A., et al., *Pressure- and volume-induced left ventricular hypertrophies are associated with distinct myocyte phenotypes and differential induction of peptide growth factor mRNAs.* Circulation, 1995. **92**(9): p. 2385-90.
44. Sopontammarak, S., et al., *Mitogen-activated protein kinases (p38 and c-Jun NH2-terminal kinase) are differentially regulated during cardiac volume and pressure overload hypertrophy.* Cell Biochem Biophys, 2005. **43**(1): p. 61-76.
45. Young, R.L., A.L. Gundlach, and W.J. Louis, *Altered cardiac hormone and contractile protein messenger RNA levels following left ventricular myocardial infarction in the rat: an in situ hybridization histochemical study.* Cardiovasc Res, 1998. **37**(1): p. 187-201.
46. Yue, P., et al., *Post-infarction heart failure in the rat is associated with distinct alterations in cardiac myocyte molecular phenotype.* J Mol Cell Cardiol, 1998. **30**(8): p. 1615-30.
47. Miyamoto, T., et al., *Activation of distinct signal transduction pathways in hypertrophied hearts by pressure and volume overload.* Basic Res Cardiol, 2004. **99**(5): p. 328-37.
48. Nediani, C., et al., *Nitric oxide/reactive oxygen species generation and nitroso/redox imbalance in heart failure: from molecular mechanisms to therapeutic implications.* Antioxid Redox Signal, 2011. **14**(2): p. 289-331.
49. Forstermann, U. and W.C. Sessa, *Nitric oxide synthases: regulation and function.* Eur Heart J, 2011.
50. Moens, A.L. and D.A. Kass, *Tetrahydrobiopterin and cardiovascular disease.* Arterioscler Thromb Vasc Biol, 2006. **26**(11): p. 2439-44.
51. Sun, J. and E. Murphy, *Protein S-nitrosylation and cardioprotection.* Circ Res, 2010. **106**(2): p. 285-96.
52. Umar, S. and A. van der Laarse, *Nitric oxide and nitric oxide synthase isoforms in the normal, hypertrophic, and failing heart.* Mol Cell Biochem, 2010. **333**(1-2): p. 191-201.
53. Sears, C.E., et al., *Cardiac neuronal nitric oxide synthase isoform regulates myocardial contraction and calcium handling.* Circ Res, 2003. **92**(5): p. e52-9.
54. Rapoport, R.M., M.B. Draznin, and F. Murad, *Endothelium-dependent relaxation in rat aorta may be mediated through cyclic GMP-dependent protein phosphorylation.* Nature, 1983. **306**(5939): p. 174-6.
55. Kubes, P., M. Suzuki, and D.N. Granger, *Nitric oxide: an endogenous modulator of leukocyte adhesion.* Proc Natl Acad Sci U S A, 1991. **88**(11): p. 4651-5.
56. Massion, P.B., et al., *Nitric oxide and cardiac function: ten years after, and continuing.* Circ Res, 2003. **93**(5): p. 388-98.
57. Balligand, J.L., O. Feron, and C. Dessy, *eNOS activation by physical forces: from short-term regulation of*

- contraction to chronic remodeling of cardiovascular tissues. *Physiol Rev*, 2009. **89**(2): p. 481-534.
58. Takimoto, E., et al., *Chronic inhibition of cyclic GMP phosphodiesterase 5A prevents and reverses cardiac hypertrophy*. *Nat Med*, 2005. **11**(2): p. 214-22.
 59. Otani, H., *The role of nitric oxide in myocardial repair and remodeling*. *Antioxid Redox Signal*, 2009. **11**(8): p. 1913-28.
 60. Lowenstein, C.J. and E. Padalko, *iNOS (NOS2) at a glance*. *J Cell Sci*, 2004. **117**(Pt 14): p. 2865-7.
 61. Haywood, G.A., et al., *Expression of inducible nitric oxide synthase in human heart failure*. *Circulation*, 1996. **93**(6): p. 1087-94.
 62. Seddon, M., Y.H. Looi, and A.M. Shah, *Oxidative stress and redox signalling in cardiac hypertrophy and heart failure*. *Heart*, 2007. **93**(8): p. 903-7.
 63. Sawyer, D.B., *Oxidative stress in heart failure: what are we missing?* *Am J Med Sci*, 2011. **342**(2): p. 120-4.
 64. Thannickal, V.J. and B.L. Fanburg, *Reactive oxygen species in cell signaling*. *Am J Physiol Lung Cell Mol Physiol*, 2000. **279**(6): p. L1005-28.
 65. Mates, J.M., *Effects of antioxidant enzymes in the molecular control of reactive oxygen species toxicology*. *Toxicology*, 2000. **153**(1-3): p. 83-104.
 66. Zelko, I.N., T.J. Mariani, and R.J. Folz, *Superoxide dismutase multigene family: a comparison of the CuZn-SOD (SOD1), Mn-SOD (SOD2), and EC-SOD (SOD3) gene structures, evolution, and expression*. *Free Radic Biol Med*, 2002. **33**(3): p. 337-49.
 67. Brahmajothi, M.V. and D.L. Campbell, *Heterogeneous basal expression of nitric oxide synthase and superoxide dismutase isoforms in mammalian heart : implications for mechanisms governing indirect and direct nitric oxide-related effects*. *Circ Res*, 1999. **85**(7): p. 575-87.
 68. Jung, O., et al., *Extracellular superoxide dismutase is a major determinant of nitric oxide bioavailability: in vivo and ex vivo evidence from ecSOD-deficient mice*. *Circ Res*, 2003. **93**(7): p. 622-9.
 69. Fukui, T., et al., *Regulation of the vascular extracellular superoxide dismutase by nitric oxide and exercise training*. *J Clin Invest*, 2000. **105**(11): p. 1631-9.
 70. Harman, D., *Aging: a theory based on free radical and radiation chemistry*. *J Gerontol*, 1956. **11**(3): p. 298-300.
 71. Oxenham, H. and N. Sharpe, *Cardiovascular aging and heart failure*. *Eur J Heart Fail*, 2003. **5**(4): p. 427-34.
 72. Bernhard, D. and G. Laufer, *The aging cardiomyocyte: a mini-review*. *Gerontology*, 2008. **54**(1): p. 24-31.
 73. Lakatta, E.G. and D. Levy, *Arterial and cardiac aging: major shareholders in cardiovascular disease enterprises: Part II: the aging heart in health: links to heart disease*. *Circulation*, 2003. **107**(2): p. 346-54.
 74. Lee, D.S., et al., *Predicting mortality among patients hospitalized for heart failure: derivation and validation of a clinical model*. *JAMA*, 2003. **290**(19): p. 2581-7.
 75. Hasty, P., et al., *Aging and genome maintenance: lessons from the mouse?* *Science*, 2003. **299**(5611): p. 1355-9.
 76. de Boer, J., et al., *Premature aging in mice deficient in DNA repair and transcription*. *Science*, 2002. **296**(5571): p. 1276-9.
 77. Wijnhoven, S.W., et al., *Accelerated aging pathology in ad libitum fed Xpd(Trp53) mice is accompanied by features suggestive of caloric restriction*. *DNA Repair (Amst)*, 2005. **4**(11): p. 1314-24.
 78. Cox, M.L., J.B. Bennett, 3rd, and G.A. Dudley, *Exercise training-induced alterations of cardiac morphology*. *J Appl Physiol*, 1986. **61**(3): p. 926-31.
 79. Diffie, G.M., *Adaptation of cardiac myocyte contractile properties to exercise training*. *Exerc Sport Sci Rev*, 2004. **32**(3): p. 112-9.
 80. Rawlins, J., A. Bhan, and S. Sharma, *Left ventricular hypertrophy in athletes*. *Eur J Echocardiogr*, 2009. **10**(3): p. 350-6.
 81. Weiner, R.B., et al., *The impact of endurance exercise training on left ventricular torsion*. *JACC Cardiovasc Imaging*, 2010. **3**(10): p. 1001-9.
 82. Duncker, D.J. and R.J. Bache, *Regulation of coronary blood flow during exercise*. *Physiol Rev*, 2008. **88**(3): p. 1009-86.
 83. Laughlin, M.H. and R.M. McAllister, *Exercise training-induced coronary vascular adaptation*. *J Appl Physiol*, 1992. **73**(6): p. 2209-25.
 84. Ellison, G.M., et al., *Physiological cardiac remodelling in response to endurance exercise training: cellular and molecular mechanisms*. *Heart*, 2011.
 85. McMullen, J.R. and G.L. Jennings, *Differences between pathological and physiological cardiac hypertrophy: novel therapeutic strategies to treat heart failure*. *Clin Exp Pharmacol Physiol*, 2007. **34**(4): p. 255-62.
 86. Owen, K.L., L. Pretorius, and J.R. McMullen, *The protective effects of exercise and phosphoinositide 3-kinase (p110alpha) in the failing heart*. *Clin Sci (Lond)*, 2009. **116**(5): p. 365-75.
 87. Green, D.J., et al., *Effect of exercise training on endothelium-derived nitric oxide function in humans*. *J Physiol*,

2004. **561**(Pt 1): p. 1-25.
88. de Waard, M.C., et al., *Beneficial effects of exercise training after myocardial infarction require full eNOS expression*. J Mol Cell Cardiol, 2010. **48**(6): p. 1041-9.
 89. Gielen, S., G. Schuler, and V. Adams, *Cardiovascular effects of exercise training: molecular mechanisms*. Circulation, 2010. **122**(12): p. 1221-38.
 90. Brutsaert, D.L., *Cardiac endothelial-myocardial signaling: its role in cardiac growth, contractile performance, and rhythmicity*. Physiol Rev, 2003. **83**(1): p. 59-115.
 91. Shah, A.M., et al., *8-bromo-cGMP reduces the myofilament response to Ca²⁺ in intact cardiac myocytes*. Circ Res, 1994. **74**(5): p. 970-8.
 92. Feron, O., et al., *Modulation of the endothelial nitric-oxide synthase-caveolin interaction in cardiac myocytes. Implications for the autonomic regulation of heart rate*. J Biol Chem, 1998. **273**(46): p. 30249-54.
 93. Seddon, M., A.M. Shah, and B. Casadei, *Cardiomyocytes as effectors of nitric oxide signalling*. Cardiovasc Res, 2007. **75**(2): p. 315-26.
 94. Powers, S.K. and M.J. Jackson, *Exercise-induced oxidative stress: cellular mechanisms and impact on muscle force production*. Physiol Rev, 2008. **88**(4): p. 1243-76.
 95. Ennezat, P.V., et al., *Physical training in patients with chronic heart failure enhances the expression of genes encoding antioxidative enzymes*. J Am Coll Cardiol, 2001. **38**(1): p. 194-8.
 96. Rush, J.W., J.R. Turk, and M.H. Laughlin, *Exercise training regulates SOD-1 and oxidative stress in porcine aortic endothelium*. Am J Physiol Heart Circ Physiol, 2003. **284**(4): p. H1378-87.
 97. Crimi, E., et al., *Mechanisms by which exercise training benefits patients with heart failure*. Nat Rev Cardiol, 2009. **6**(4): p. 292-300.
 98. Downing, J. and G.J. Balady, *The role of exercise training in heart failure*. J Am Coll Cardiol, 2011. **58**(6): p. 561-9.
 99. Letac, B., A. Cribier, and J.F. Desplanches, *A study of left ventricular function in coronary patients before and after physical training*. Circulation, 1977. **56**(3): p. 375-8.
 100. O'Connor, C.M., et al., *Efficacy and safety of exercise training in patients with chronic heart failure: HF-ACTION randomized controlled trial*. JAMA, 2009. **301**(14): p. 1439-50.
 101. Sullivan, M.J., M.B. Higginbotham, and F.R. Cobb, *Exercise training in patients with severe left ventricular dysfunction. Hemodynamic and metabolic effects*. Circulation, 1988. **78**(3): p. 506-15.
 102. de Waard, M.C., et al., *Detrimental effect of combined exercise training and eNOS overexpression on cardiac function after myocardial infarction*. Am J Physiol Heart Circ Physiol, 2009. **296**(5): p. H1513-23.





iNOS Aggravates Pressure- Overload Hypertrophy

2

Ping Zhang*, Xin Xu*, Xinli Hu, Elza D. van Deel,
Guangshuo Zhu, Yingjie Chen

*both authors contributed equally to this work

Circulation Research 2007;100(7):1089-98

Abstract

2

Inducible nitric oxide synthase (iNOS) protein is expressed in cardiac myocytes of patients and experimental animals with congestive heart failure (CHF). Here we show that iNOS expression plays a role in pressure overload–induced myocardial chamber dilation and hypertrophy. In wild-type mice, chronic transverse aortic constriction (TAC) resulted in myocardial iNOS expression, cardiac hypertrophy, ventricular dilation and dysfunction, and fibrosis, whereas iNOS-deficient mice displayed much less hypertrophy, dilation, fibrosis, and dysfunction. Consistent with these findings, TAC resulted in marked increases of myocardial atrial natriuretic peptide 4-hydroxy-2-nonenal (a marker of lipid peroxidation) and nitrotyrosine (a marker for peroxynitrite) in wild-type mice but not in iNOS-deficient mice. In response to TAC, myocardial endothelial NO synthase and iNOS was expressed as both monomer and dimer in wild-type mice, and this was associated with increased reactive oxygen species production, suggesting that iNOS monomer was a source for the increased oxidative stress. Moreover, systolic overload–induced Akt, mammalian target of rapamycin, and ribosomal protein S6 activation was significantly attenuated in iNOS-deficient mice. Furthermore, selective iNOS inhibition with 1400W (6 mg/kg per hour) significantly attenuated TAC induced myocardial hypertrophy and pulmonary congestion. These data implicate iNOS in the maladaptative response to systolic overload and suggest that selective iNOS inhibition or attenuation of iNOS monomer content might be effective for treatment of systolic overload-induced cardiac dysfunction.

Introduction

Several investigators have demonstrated that inducible nitric oxide synthase (iNOS) protein is expressed in cardiac myocytes and endocardial endothelium of patients and animals with ventricular hypertrophy or congestive heart failure (CHF) regardless of cause.¹⁻⁴ Thus, iNOS was coexpressed with tumor necrosis factor- α in cardiac myocytes from patients with dilated cardiomyopathy² and increased in several animal models of ventricular hypertrophy or CHF.⁵ Although unregulated NO production by iNOS has been proposed to exert negative effects on cardiomyocyte function, the effect of iNOS expression on ventricular hypertrophy and CHF in the *in vivo* heart is controversial. Thus, Heger et al⁶ reported that overexpression of iNOS in cardiac myocytes increased myocardial NOS activity and NO production but had no effect on cardiac morphology or function. In contrast, Mungrue et al⁷ reported that cardiac-specific overexpression of iNOS resulted in inflammatory cell infiltrate, left ventricular (LV) hypertrophy, dilation, fibrosis, and contractile dysfunction. The level of iNOS expression in these transgenic mice would depend on the promoter activity, and the iNOS-related phenotypes might vary depending on the level of myocardial iNOS expression. Furthermore, the effects of stress-induced iNOS expression in normal hearts may be different from that in the transgenic mice. Therefore, the present study examined the role of iNOS in the ventricular hypertrophy and CHF that develops in response to sustained pressure overload produced by transverse aortic constriction (TAC) in mice with or without the iNOS gene. We provide the first evidence, to our knowledge, that iNOS deficiency (iNOS^{-/-}) attenuates TAC-induced ventricular hypertrophy and CHF and that iNOS expressed in response to systolic overload serves as a source for myocardial reactive oxygen species (ROS) that contribute to LV dilatation and hypertrophy.

Materials and Methods

Mice and TAC

Body weight and age-matched (2 to 3 months old) male iNOS^{-/-} (crossed back to C57BL/6J for 12 times) and wild-type controls (C57BL/6J) were purchased from The Jackson Laboratory. This study was approved by the Institutional Animal Care and Use Committee of University of Minnesota.

TAC-induced LV hypertrophy. TAC was performed using the minimally invasive suprasternal approach described by Hu et al.⁸

Selective iNOS inhibition with 1400W. To study the effect of selective iNOS inhibition on TAC-induced ventricular hypertrophy and dysfunction, adult male C57BL/6J mice were randomly divided into 2 groups immediately after TAC; 1 group was treated with the selective iNOS inhibitor 1400W, whereas the other group was treated with saline vehicle. 1400W was delivered at a constant dose of 6 mg/kg per hour via an osmotic minipump (Alzet Model 2002). This dose of 1400W resulted in plasma

1400W concentrations that were 2.4- to 4.9-fold higher than the EC50 for tissue iNOS and decreased plasma nitric oxide metabolites generated by iNOS by 63% to 83%.⁹ This dose of 1400W had no effect on hemodynamic variables in normal animals, indicating lack of effect on constitutive NOS. We have found that male C57B6J mice develop ventricular dysfunction and pulmonary congestion in 4 weeks after moderate TAC (using a 26-gauge needle) and develop ventricular dysfunction and pulmonary congestion in 2 weeks after severe TAC (using a 27-gauge needle). To induce ventricular dysfunction in the mice within 2 weeks, because the capacity of the minipump to deliver the required dose of 1400W was 2 weeks, we produced severe TAC in these animals by ligating the aorta over a 27-gauge needle.

Echocardiography was performed when mice were anesthetized with 1.5% isoflurane by inhalation. The left ventricular (LV) ejection fraction (EF) was calculated from the LV end diastolic diameter (EDD) and LV end systolic diameter (ESD) as follows: $EF = (EDD^3 - ESD^3) / EDD^3 * 100\%$.

Western Blots

NOS Protein content was analyzed using Western blots as previously described.¹⁰ Primary antibodies against iNOS, eNOS, neuronal NOS (nNOS), atrial natriuretic peptide (ANP), protein arginine methyltransferase 1 (PRMT1), 4-hydroxy-2-nonenal (4-HNE), nitrotyrosine, total mammalian target of rapamycin (mTOR), phospho-mTOR, Akt, phospho-Akt, phospho-S6, and total p70S6K were purchased from Transduction Laboratories, Santa Cruz Biotechnology, Sigma, Upstate, and Cell Signaling Technology, respectively. Dimethylarginine dimethylaminohydrolase 1 (DDAH1) antibody was a gift from Dr M. Kimoto (Okayama Prefectural University, Japan).¹⁰

Measurement of ROS

Relative ROS production was determined by chemiluminescence of coelenterazine (4 $\mu\text{mol/L}$; Molecular Probes)¹¹ and the red fluorescent dye dihydroethidium (DHE) (2 $\mu\text{mol/L}$; Invitrogen). To assess ROS production with chemiluminescence of coelenterazine, flash-frozen myocardium (~40mg) was cut into fine pieces (about ~1mm³) on ice, and added to 500 μl ice cold Krebs bicarbonate buffer containing the following reagents, in mmol/l: NaCl, 118; KCl, 4.7; CaCl₂, 1.5; MgSO₄, 1.1; KH₂PO₄, 1.2; glucose, 5.6; and NaHCO₃, 25. Coelenterazine (4 μM) was added to the tissue suspension and chemiluminescence was assessed for 60 seconds at 5 min intervals over 60 min at room temperature in a Lumat LB 9507 tube luminometer. Data were normalized by sample weight. The superoxide anion production was also determined after nonselective NOS inhibition with LNME (1 mmol added 20 minutes before the assay) as previously described,¹² or selective iNOS inhibition with 1400W (100 μmol added 20 minutes before the assay).¹³ 1400W at a concentration of 100 μmol had no effect on NO production in cultured endothelial cells but attenuated iNOS activity, indicating that this concentration of 1400W does not inhibit eNOS activity.⁴ In addition, fresh frozen LV myocardium (8 μm slices) was incubated for 1 hour at 37°C with the red fluorescent dye DHE (2 μM ; Invitrogen) to assess O₂-formation (typically nuclear localization). Imaging was performed on a Zeiss microscope (Carl Zeiss Inc.).

Matrix Metalloproteinase Activity

In vitro gelatin lysis by matrix metalloproteinase (MMP)-2 and MMP-9 was assessed by zymography.¹⁴ Briefly, LV tissue was homogenized in modified buffer containing 20mM Tris-HCl pH7.4, 0.3% Triton-X100, and spun down at 1000 X g for 10 min at 4°C. Modified Laemmli buffer without mercaptoethanol was added to 25 µg of the protein samples and incubated for 10 min before loading on 10% SDS-PAGE with 1mg/ml gelatin. 1ng of collagenase type 2 was loaded as a positive control. After electrophoresis, gels were washed twice with renaturing buffer, followed by developing buffer and stained with SimplyBlue (Invitrogen).

Histological staining and measurement of myocardial fibrosis

Tissue sections (8µm) from the central portion of the LV were stained with H&E (Sigma) for overall morphology, Masson's Trichrome (Sigma) or Sirius Red (Sigma) for detection of fibrosis, and FITCconjugated wheat germ agglutinin (AF488, Invitrogen) to evaluate myocyte size. For mean myocyte size, the short diameter and cross sectional area of at least 120 cells/sample (from 4 areas) and at least 4 samples of each group were averaged. Relative myocardial fibrosis was expressed as the percent volume fibrosis determined with a method described in Unbiased Stereology.

For eNOS or iNOS staining, the sections were first fixed with 3.7% paraformaldehyde for 20 minutes, rinsed with PBS, followed by permeabilization with 0.2% Triton X100 for 10 minutes. The sections were incubated with 0.3% H₂O₂ in PBS for 1 hour followed by 1% BSA solution for 1 hour. Sections were then incubated with primary antibodies (1:100) against iNOS or eNOS (Transduction Labs) (or nonselective IgG as a negative control) for 1 hour. iNOS staining was done using Tyramide Signal Amplification Kits (Molecular Probes). AF555 - labelled secondary anti mouse-IgG (1:1000) was used for eNOS staining. All sections were incubated with DAPI for nucleus staining and wheat germ-AF555 (during iNOS stain) or wheat germ-AF488 (during eNOS stain) for cell membrane and connective tissue staining, before mounting with Anti-Fade Gold (Molecular Probes). The slides were examined using single photon confocal microscopes (FluoView 1000 Olympus).

Results

iNOS^{-/-} Attenuates Moderate TAC-Induced Ventricular Hypertrophy and Dysfunction
Ventricular mass, lung weight, the ratio of ventricular weight to body weight, and the ratio of lung weight to body weight in iNOS^{-/-} and wild-type mice in response to TAC are shown in (Figure 1 and Table 1). Under control conditions, ventricular weight, lung weight, and the ratio of organ weight to body weight were not different between iNOS^{-/-} and wild-type mice (Figure 1). Although TAC for 28 days resulted in ventricular hypertrophy in both wild-type and iNOS^{-/-} mice, iNOS^{-/-} significantly attenuated the TAC-induced increase of ventricular weight and the ratio of ventricular weight to body weight (Figure 1). As compared with wild-type mice, a significantly attenuated increase of ventricular weight and the ratio of ventricular weight to body weight was also observed in iNOS^{-/-} mice

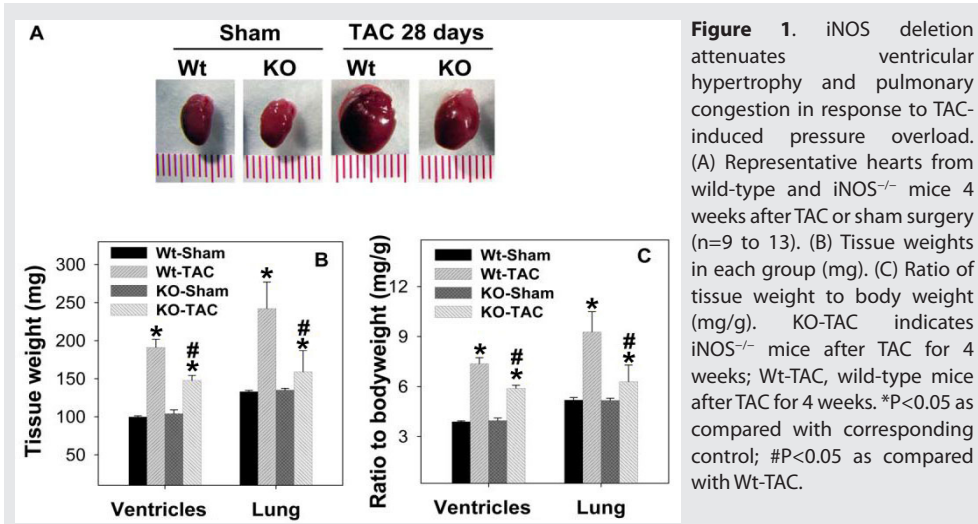


Figure 1. iNOS deletion attenuates ventricular hypertrophy and pulmonary congestion in response to TAC-induced pressure overload. (A) Representative hearts from wild-type and iNOS^{-/-} mice 4 weeks after TAC or sham surgery (n=9 to 13). (B) Tissue weights in each group (mg). (C) Ratio of tissue weight to body weight (mg/g). KO-TAC indicates iNOS^{-/-} mice after TAC for 4 weeks; Wt-TAC, wild-type mice after TAC for 4 weeks. *P<0.05 as compared with corresponding control; #P<0.05 as compared with Wt-TAC.

Table 1. Effect of iNOS deletion on left ventricular function and dimensions by 2-D guided M-mode echocardiography.

	Wt-sham	iNOS ^{-/-} -sham	Wt-TAC	iNOS ^{-/-} -TAC
Body weight (g)	25.6 ± 0.5	26.2 ± 0.8	25.7 ± 0.5	25.0 ± 0.4
AWTD (µm)	69.8 ± 0.9	74.7 ± 0.2	110 ± 3.3*	96.0 ± 3.2*#
PWTD (µm)	70.6 ± 0.7	74.7 ± 0.1	109 ± 2.7*	95.3 ± 2.9*#
AWTS (µm)	102 ± 4.5	110 ± 3.0	134 ± 4.3*	120 ± 2.8*#
PWTS (µm)	102 ± 4.5	109 ± 2.9	132 ± 4.2*	115 ± 2.2*#

Data are Mean ± SE from 9 to 14 mice per group. AWTD: anterior wall thickness at end diastole. PWTD: posterior wall thickness at end diastole. AWTS: anterior wall thickness at end systole. PWTS: posterior wall thickness at end systole. *P<0.05 as compared to the corresponding sham group. #P<0.05 as compared to Wt-TAC group.

8days after TAC (data not shown). In addition, lung weight and the ratio of lung weight to body weight were significantly greater in wild-type mice as compared with iNOS^{-/-} mice 28 days after TAC, indicating increased pulmonary congestion in the wild-type mice (Figure1). There was no difference in mortality rate between iNOS^{-/-} and wild-type mice following TAC. To determine the degree of pressure overload produced by the TAC, systolic pressure proximal to the TAC site and the pressure gradient across the TAC site were determined in a group of wild-type mice and knockout mice immediately after the TAC procedure. The results showed that TAC produced a similar increase of LV systolic pressure and the pressure gradient across the aortic constriction (Figure 2).

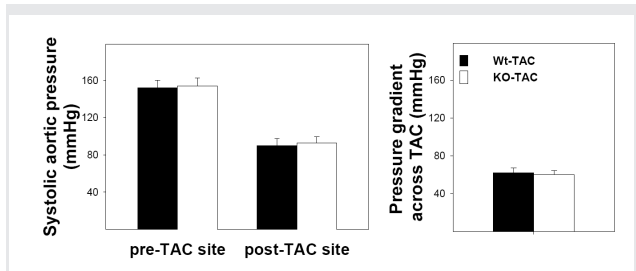
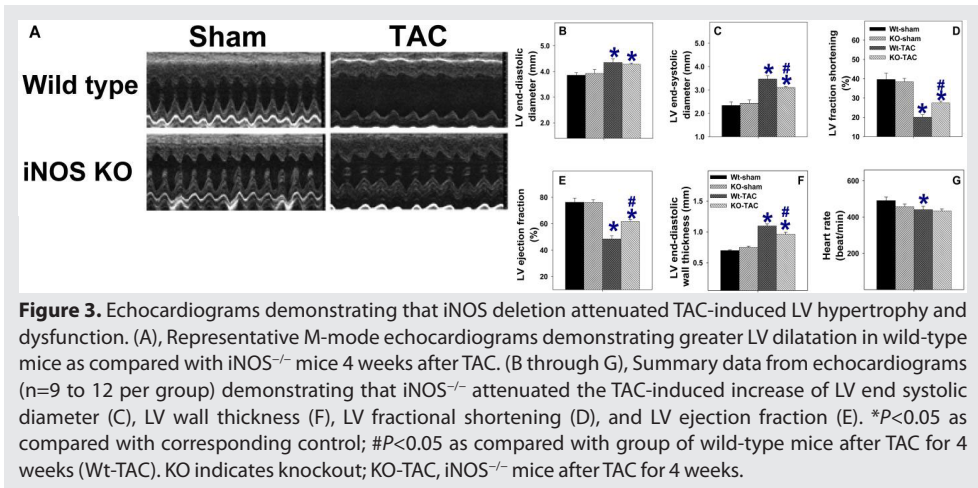


Figure 2. Systolic aortic pressure and pressure gradient across TAC site were not different between iNOS KO and wild type mice immediately after moderated TAC.



Echocardiographic imaging of the heart 28 days after TAC demonstrated significant increases of LV wall thickness, LV end systolic diameter and LV end diastolic diameter in both *iNOS*^{-/-} and wild-type mice in comparison with mice of similar body weight without TAC (Figure 3 and Table 1). However, TAC resulted in a significantly greater decrease of the LV systolic shortening fraction and ejection fraction in wild-type mice than in *iNOS*^{-/-} mice (Figure 3 and Table 1).

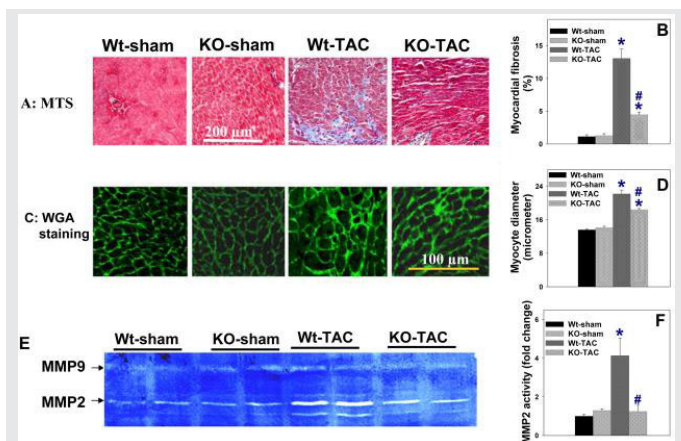


Figure 4. Histological staining demonstrating that *iNOS* deletion attenuated TAC-induced myocardial fibrosis (A and B), cardiac myocyte hypertrophy (C and D), and the increase of myocardial MMP-2 activity (E and F). MTS indicates Masson's trichrome staining; blue staining, fibrosis; WGA, staining for wheat germ agglutinin with fluorescein isothiocyanate-conjugated Fluor-488 (Invitrogen); bright green staining, the area of the matrix and cell membrane. Summarized average data are from 4 representative mice per group. * $P < 0.05$ compared with the corresponding control; # $P < 0.05$ as compared with wild-type mice after TAC for 4 weeks (Wt-TAC). KO indicates knockout; KO-TAC, *iNOS*^{-/-} mice after TAC for 4 weeks; Wt, wild type.

iNOS^{-/-} Attenuates TAC-Induced Ventricular Fibrosis

Histological staining of LV tissue at 28 days after TAC demonstrated more interstitial fibrosis in wild-type mice as compared with *iNOS*^{-/-} mice (Figure 4A and 4B). Under control conditions, the cross-sectional area of the cardiac myocytes was not different between wild-type mice ($227 \pm 10 \mu\text{mol/L}^2$) and *iNOS*^{-/-} mice ($206 \pm 13 \mu\text{mol/L}^2$). Myocyte hypertrophy occurred in both groups of animals in response to TAC, but the increase in myocyte cross-sectional

area was significantly less in *iNOS*^{-/-} mice ($395 \pm 20 \mu\text{mol/L}^2$) than in wild-type mice (wild type, $464 \pm 31 \mu\text{mol/L}^2$; $P < 0.05$) (Figure 4C and 4D).

TAC-Induced Alterations of eNOS, iNOS, nNOS, and ANP

Western blots demonstrated that iNOS protein was expressed in wild-type mice at both 8 and 28 days after TAC (Figure 5). eNOS protein content was significantly increased 28 days after TAC in wild-type mice, and *iNOS*^{-/-} attenuated the TAC-induced induction of eNOS. Myocardial nNOS was unchanged after TAC.

DDAH1 and protein arginine methyltransferase (PRMT1) regulate NO availability by either degrading or synthesizing the endogenous NOS inhibitor asymmetric dimethylarginine (ADMA). Therefore, the protein contents of DDAH1 and PRMT1 were determined. Interestingly, both DDAH1 and PRMT1 were increased in wild-type mice after TAC (Figure 5), whereas *iNOS*^{-/-} attenuated the TAC-induced induction of DDAH1.

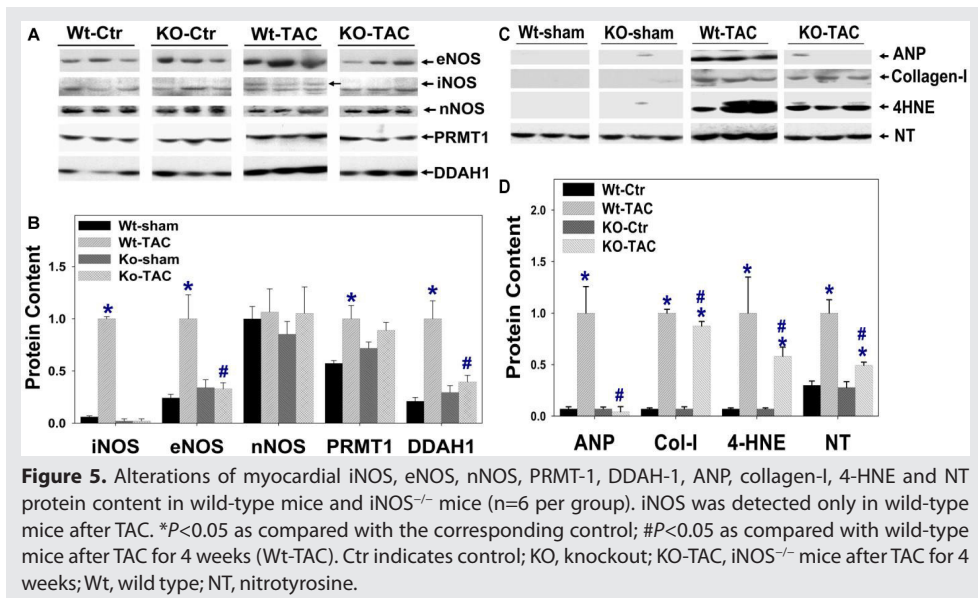


Figure 5. Alterations of myocardial iNOS, eNOS, nNOS, PRMT-1, DDAH-1, ANP, collagen-I, 4-HNE and NT protein content in wild-type mice and *iNOS*^{-/-} mice ($n=6$ per group). iNOS was detected only in wild-type mice after TAC. * $P < 0.05$ as compared with the corresponding control; # $P < 0.05$ as compared with wild-type mice after TAC for 4 weeks (Wt-TAC). Ctr indicates control; KO, knockout; KO-TAC, *iNOS*^{-/-} mice after TAC for 4 weeks; Wt, wild type; NT, nitrotyrosine.

In addition, *iNOS*^{-/-} attenuated TAC-induced increase of myocardial ANP (Figure 5), consistent with the finding of less ventricular hypertrophy and CHF in the *iNOS*^{-/-} mice. Myocardial nitrotyrosine and 4-hydroxy-2-nonenal (4HNE) were increased in both wild-type and *iNOS*^{-/-} mice after TAC (Figure 5), but the increases were significantly less in *iNOS*^{-/-} mice than in wild-type mice, implying lower oxidative stress in the *iNOS*^{-/-} mice.

Myocardial Fibrosis and MMP Activity

After TAC, *iNOS*^{-/-} hearts developed less fibrosis as compared with wild-type mice (Figure 4). Furthermore, *iNOS*^{-/-} mice had significantly lower myocardial MMP-2 activity as demonstrated by zymography (Figure 4). Although myocardial collagen-1 was increased in both wild-type and *iNOS*^{-/-} mice 28 days after TAC, the TAC-induced increase of

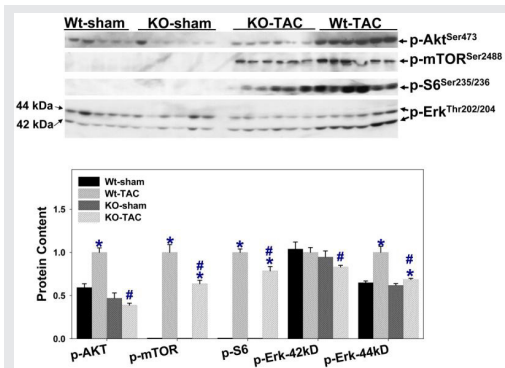


Figure 6. iNOS deletion attenuated the TAC-induced increases of phospho-Akt^{Ser473}, phospho-mTOR^{Ser2488}, phospho-S6^{Ser235/236}, and phospho-Erk^{Thr202/204}. * $P < 0.05$ as compared with the corresponding control; # $P < 0.05$ as compared with wild-type mice after TAC for 4 weeks (Wt-TAC). KO indicates knockout; KO-TAC, iNOS^{-/-} mice after TAC for 4 weeks; Wt, wild type.

collagen-I expression was significantly less in the iNOS^{-/-} mice (Figure 5).

iNOS^{-/-} Attenuates TAC-Induced Akt-mTOR-S6 Activation

As increased oxidative stress can activate Akt, and activation of mTOR and ribosomal protein S6 (S6) regulates cell growth, total and activated Akt, mTOR, and S6 were determined. TAC caused significant increases of phospho-Akt^{Ser473}, phospho-mTOR^{Ser2488}, phospho-S6^{Ser235/236}, and phospho-Erk^{Thr202/204}, whereas total Akt was unchanged (Figure 6). iNOS deletion attenuated the TAC-induced increases of Akt^{Ser473}, mTOR^{Ser2488}, S6^{Ser235/236}, and Erk^{Thr202/204} (Figure 6).

Expression of eNOS and iNOS Monomer and Dimer

NOS monomer produces superoxide anion, whereas NOS dimer generates NO. Because evidence of increased myocardial oxidative stress was observed in the wild-type mice after TAC, and iNOS was robustly expressed in the wild-type mice early after TAC, relative myocardial iNOS and eNOS monomer and dimer were determined in wild-type mice 8 days after TAC by using nondenatured gel. As shown in Figure 7, iNOS was present as both monomer and dimer in the wild-type mice after TAC (18±2% monomer). Myocardial eNOS monomer was undetectable in sham mice but was present in the iNOS^{-/-} mice (39±1% monomer) and wild-type mice (38±3% monomer) after TAC.

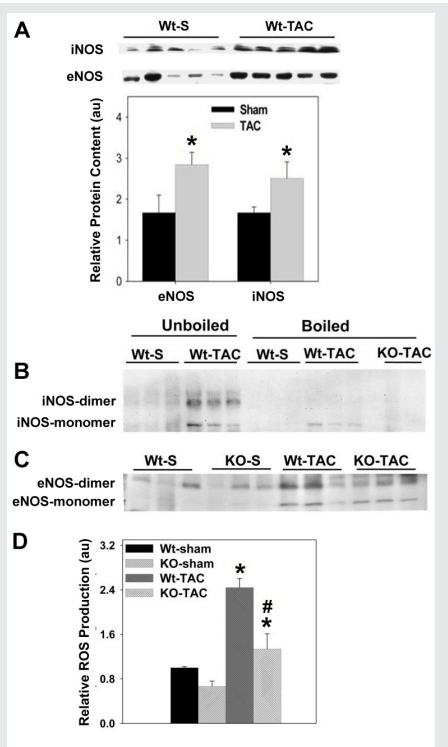


Figure 7. (A) Western blot showing increased myocardial eNOS and iNOS expression in wild-type mice in response to 8 days of severe TAC. (B) Both iNOS monomer and iNOS dimer were detected in wild-type mice 8 days after TAC in nonboiling conditions, whereas iNOS dimer was diminished after boiling the sample for 15 minutes. (C) eNOS expressed as both monomer and dimer in wild-type mice and iNOS^{-/-} mice 8 days after TAC in nonboiling conditions. (D) Attenuated ROS production in iNOS^{-/-} mice. # $P < 0.05$ as compared with wild-type mice after TAC for 4 weeks (Wt-TAC). KO indicates knockout; KO-TAC, iNOS^{-/-} mice after TAC for 4 weeks; Wt, wild type; Wt-S, wild-type sham.

iNOS^{-/-} Attenuates the TAC-Induced Increase of ROS

To determine whether the finding of NOS monomer was associated with increased ROS generation, superoxide anion content was determined with a chemiluminescence assay in myocardial tissue extracts. TAC resulted in increases of superoxide anion in both wild-type and iNOS-deficient mice (Figure 6D), but iNOS^{-/-} partially attenuated TAC-induced myocardial superoxide anion production (Figure 6D). In separate samples obtained from wild-type mice after TAC, both the selective iNOS inhibitor 1400W (decreased to

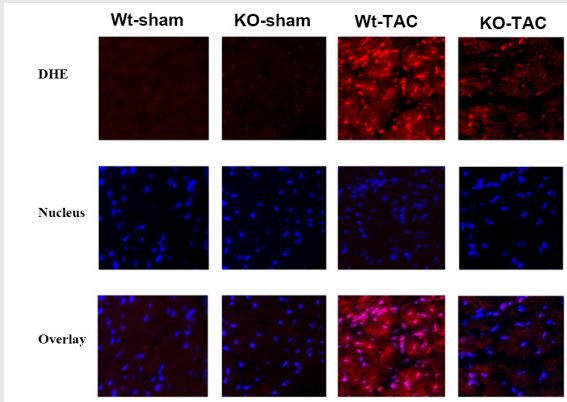


Figure 8. DHE staining shows that TAC resulted in an increase of ROS production in wild type mice, while iNOS deficiency attenuated the TAC-induced ROS production.

75±10% after 1400W treatment) or the nonselective NOS inhibitor L-NAME (decreased to 62±13% after L-NAME treatment) attenuated myocardial superoxide production. These findings support the notion that NOS uncoupling contributed to myocardial superoxide production. Intracellular ROS generation was also estimated with red DHE (typically nuclear localization) staining in frozen sections; the results demonstrated that TAC caused an increase of ROS production

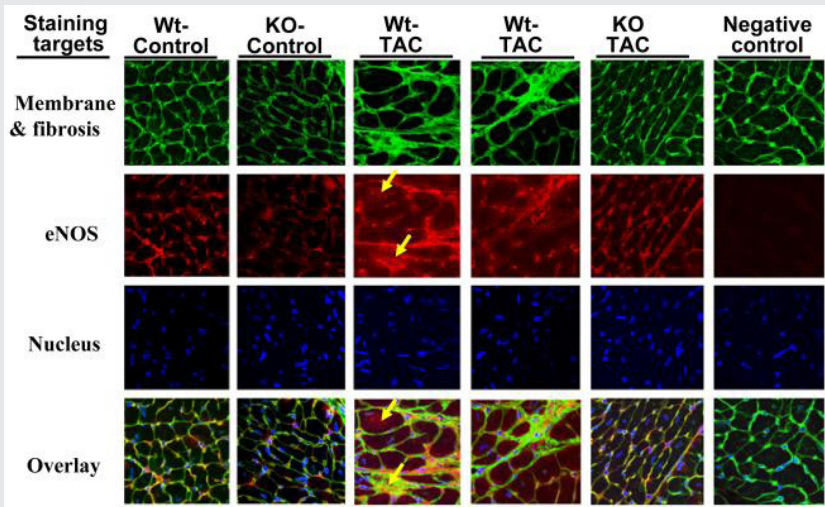
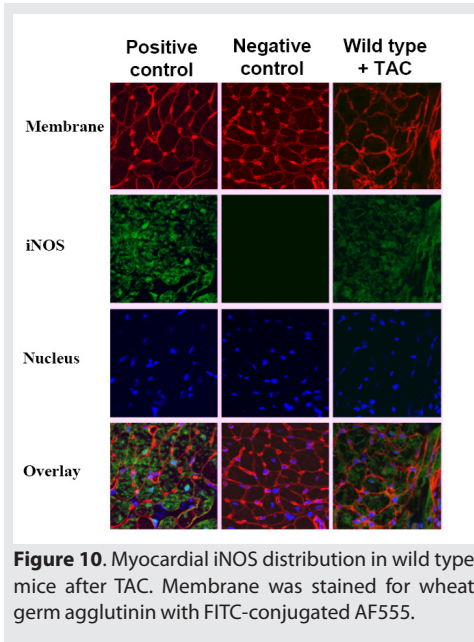


Figure 9. Myocardial eNOS was predominantly expressed in vascular endothelial cells in normal heart, and TAC increased eNOS expression in myocardial area with fibrosis and some adjacent cardiac myocytes in Wt mice. Wheat germ agglutinin staining (green) indicates areas of matrix, blood vessels, and cell membrane. Blue staining indicates the cell nuclei; red staining, eNOS. Samples used for staining were obtained 8 days after TAC or sham surgery. KO indicates knockout; KO-TAC, iNOS^{-/-} mice after TAC for 4 weeks; Wt, wild type; Wt-TAC, wild-type mice after TAC for 4 weeks.



after TAC (Figure 10). The TAC-induced myocardial iNOS expression pattern in wild-type mice was similar to the pattern of iNOS expression in mice following LPS stimulation.

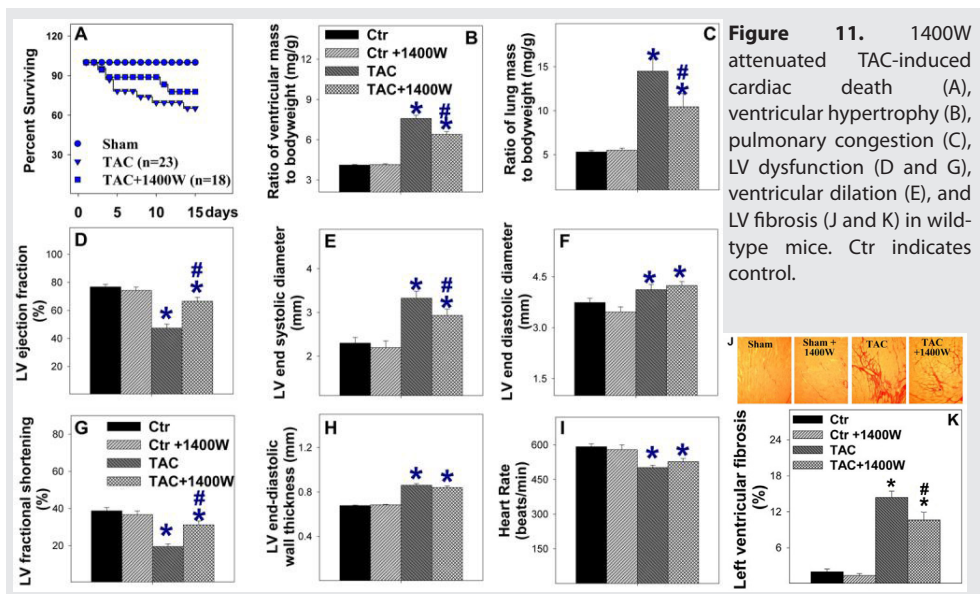
and that iNOS^{-/-} partially attenuated the TAC-induced superoxide production (Figure 8).

Myocardial eNOS and iNOS Distribution

Under control conditions, eNOS was mainly distributed in capillaries and endothelial cells of larger blood vessels, with a similar expression pattern in wild-type and iNOS^{-/-} mice (Figure 9). Interestingly, although eNOS was still highly expressed in endothelial cells of blood vessels after TAC, an apparent increase of eNOS expression was observed in areas of fibrosis and in cardiac myocytes around the fibrotic areas (Figure 9). This TAC-induced eNOS induction was attenuated in iNOS^{-/-} mice (Figure 9). Immunostaining demonstrated that iNOS was broadly expressed in cardiac myocytes and connective tissue in wild-type mice

1400W Attenuates TAC-Induced Ventricular Hypertrophy and Dysfunction

Because iNOS deficiency attenuated the TAC-induced ventricular hypertrophy and dysfunction, we examined whether selective iNOS inhibition with 1400W would have



similar protective effects on TAC-induced ventricular hypertrophy in wild-type mice. 1400W significantly attenuated the TAC-induced ventricular hypertrophy (Figure 11B), pulmonary congestion (Figure 11B), and ventricular dysfunction (Figure 11E and 11F). 1400W also significantly attenuated the TAC-induced myocardial fibrosis (Figure 11J and 11K). 1400W did not affect heart rate or LV wall thickness (Figure 11) and had no effect on mean aortic pressure (86 ± 3 mm Hg in mice treated with 1400W versus 83 ± 5 mm Hg in mice without 1400W) or LV systolic pressure (98 ± 3.7 in 1400W treated mice versus 102 ± 3.6 mm Hg in untreated mice). 1400W had no effect on ventricular function and fibrosis in sham mice.

Discussion

The major new findings of this study are that chronic systolic overload resulted in expression of myocardial iNOS as both monomer and dimer in wild-type mice, and this was associated with greater ventricular hypertrophy, dilation, fibrosis, and dysfunction as compared with iNOS^{-/-} mice. Consistent with these findings, selective iNOS inhibition with 1400W significantly attenuated the TAC-induced ventricular hypertrophy and dysfunction in wild-type mice. Expression of iNOS after TAC was associated with greater increases of myocardial nitrotyrosine, 4HNE, ANP, and phosphorylation of Akt, mTOR, S6 in wild-type mice as compared with iNOS^{-/-} mice. The finding of myocardial iNOS monomer, a structural unit that generates superoxide anion, suggests that iNOS is a significant source of superoxide anion in the overloaded or failing heart. The finding that iNOS deletion protected against TAC-induced ventricular hypertrophy and CHF, in association with decreased myocardial nitrotyrosine and 4HNE, suggests that selective iNOS inhibition might potentially be an effective strategy for treatment of myocardial dysfunction and CHF in the chronically overloaded heart.

iNOS Effects on Ventricular Remodeling/Fibrosis and CHF

Although no previous reports have directly examined the effect of iNOS deletion on pressure overload-induced ventricular hypertrophy and CHF, several investigators have studied the effect of iNOS deficiency on ventricular remodeling after myocardial infarction.^{5,15-17} Studies from 3 different groups have demonstrated that iNOS deficiency caused mildly or moderately decreased infarct-induced mortality, improved ventricular function, reduced myocardial nitrotyrosine content, reduced plasma nitrate, and decreased programmed cell death during both the acute and chronic phases of myocardial infarction,^{5,16-17} suggesting a detrimental effect of iNOS expression. In addition, using conditional cardiac specific transgenic mice, Mungro et al found that overexpression of human iNOS in cardiac myocytes resulted in increased myocardial peroxynitrite, myocardial fibrosis, ventricular hypertrophy, CHF and cardiac sudden death,⁷ indicating that high level overexpression of iNOS can induce ventricular hypertrophy and CHF. A recent study from our laboratory demonstrated that selective pharmacological iNOS inhibition significantly improved LV contractility and myocardial oxygen consumption in end-stage pacing-induced canine heart failure,³ indicating that iNOS inhibition can acutely improve ventricular function in failing hearts. It should be noted, however, that there are conflicting reports in which iNOS deficiency failed to reduce myocardial infarct-induced ventricular dysfunction or

mortality.¹⁵ The differing results regarding the role of iNOS in ventricular remodeling may be related to variations in infarct size, the stage of heart failure and different genetic backgrounds of the mice.^{5,15-17} The differing results obtained from two cardiac specific transgenic lines of iNOS overexpression may be attributable to variations of promoter efficiency in these transgenic lines.⁶⁻⁷

The TAC-induced iNOS expression in the wild-type mice in the present study, in conjunction with less severe ventricular hypertrophy, dilation, fibrosis and dysfunction in the iNOS^{-/-} mice in response to systolic overload, is consistent with previous reports that iNOS can exert detrimental effects on the heart. The finding that iNOS^{-/-} only partially attenuated the TAC-induced myocardial ROS production and ventricular dysfunction is not unexpected, because previous reports have demonstrated that other factors such as eNOS uncoupling,¹² and increases of NADPH oxidase¹⁸ and xanthine oxidase¹⁹ can contribute to increased oxidative stress in the failing heart. The finding that iNOS deficiency and selective iNOS inhibition with 1400W attenuated LV remodeling and dysfunction suggests that selective iNOS inhibition might be a useful approach for treating systolic overload-induced ventricular hypertrophy and CHF.

eNOS and iNOS expression in hypertrophied or failing hearts. Increased iNOS expression and activity have been documented in myocardial specimens from patients and animals with ventricular hypertrophy¹ and CHF.¹⁻⁴ In the present study, the finding of a faint iNOS band in the wild-type hearts 8 days after sham surgery was likely the result of tissue trauma from the sham surgery. The expression of myocardial iNOS protein in hearts of wild-type mice both 8 days and 28 days after TAC is consistent with previous reports of iNOS expression in hypertrophied and failing hearts,^{1-2,4} although the mechanism for upregulation of iNOS expression after TAC is not totally clear. The relatively higher expression of iNOS and eNOS protein early after TAC is consistent with a previous report in which iNOS and eNOS expression peaked 3 to 5 days after TAC.⁴ The increased expression of eNOS after TAC is consistent with previous reports that eNOS protein was increased in hearts with CHF^{4,10} or ventricular hypertrophy in response to pressure overload.^{4,20} The increased eNOS expression in cardiac myocytes near the area with fibrosis is consistent with a previous report in cardiomyopathy samples obtained from mice with mutations of γ -sarcoglycan or δ -sarcoglycan.²¹ In the context of a recent study demonstrating that eNOS uncoupling contributes to TAC-induced myocardial oxidative stress and ventricular remodeling,¹² and the fact that myocardial eNOS monomer was present after TAC, the protective effect of iNOS^{-/-} on TAC-induced ventricular remodeling may relate to an attenuation of eNOS induction. It should be noted that the effect of eNOS on TAC-induced cardiomyopathy is controversial; although 1 study demonstrated that eNOS deficiency profoundly attenuated TAC-induced ventricular hypertrophy and CHF, 2 other studies reported that eNOS deficiency exacerbated ventricular hypertrophy produced by mild TAC.^{20,22}

DDAH1 is an enzyme that degrades the endogenous NOS inhibitor ADMA, whereas PRMT1 is an enzyme that regulates ADMA production. In a canine model of pacing-induced heart failure, we recently found that myocardial DDAH activity was decreased,

whereas myocardial PRMT1 and DDAH1 protein contents were unchanged, after the development of CHF.¹⁰ Interestingly, in the present study TAC resulted in significant increases of both PRMT1 and DDAH1 in the wild-type mice, suggesting model- or strain-dependent responses of these proteins.

2

Contribution of iNOS to oxidative stress in hypertrophied and failing hearts. Myocardial hypertrophy and failure are associated with increased superoxide anion ($O_2^{\cdot-}$) production,²³ and accumulation of oxidized lipid and protein products such as nitrotyrosine and 4-HNE.⁵ We recently found that the SOD mimetic M40401 enhanced endothelium-dependent coronary vasodilation and increased LV dP/dt_{max} in dogs with pacing-induced CHF,¹⁰ implying that increased $O_2^{\cdot-}$ production is partially responsible for coronary endothelial dysfunction and ventricular dysfunction in the failing heart. Oxygen free radicals are linked to fibrosis and matrix turnover involving the activation of MMPs.²⁴ Overexpressing glutathione peroxidase,²⁵ or administering tetrahydrobiopterin (BH4) to decrease myocardial $O_2^{\cdot-}$ production¹² decreased myocardial MMP abundance. In the present study, the decreased myocardial oxidative stress in the iNOS-deficient mice was associated with decreased MMP-2 activity, supporting the notion that oxidative stress affects myocardial matrix turnover.

NOS Uncoupling

NOS can produce NO, $O_2^{\cdot-}$, or peroxynitrite. This unique property is a consequence of the dimeric nature of the enzyme, in which the 2 subunits are able to function independently.²⁶ NOS optimally exists as a homodimer that generates NO and L-citrulline from L-arginine. However, when exposed to oxidant stress, or when deprived of its reducing cofactor BH4 or substrate L-arginine, NOS can uncouple to the monomeric form that generates $O_2^{\cdot-}$ rather than NO.^{12,27-29} BH4 is required for iNOS dimerization³⁰ and also stabilizes nNOS and eNOS dimers. Thus, a decrease of BH4 or unregulated NO production by iNOS to decrease L-arginine availability can cause NOS uncoupling.^{26,31} Using purified iNOS protein, several studies have demonstrated that iNOS can produce both NO and $O_2^{\cdot-}$ and that deficiency of L-arginine or BH4 will induce iNOS to produce $O_2^{\cdot-}$,^{28,31} indicating that iNOS can be uncoupled. In addition, in cultured macrophages, depletion of cytosolic L-arginine triggered $O_2^{\cdot-}$ production by iNOS that was blocked by a NOS inhibitor, suggesting that iNOS uncoupling was responsible for the $O_2^{\cdot-}$ production.²⁷

In the cardiovascular system, most studies of NOS uncoupling have focused on eNOS. Thus, uncoupled eNOS produces $O_2^{\cdot-}$.³² in apoE-deficient mice, and BH4 improves the endothelial dysfunction associated with hypercholesterolemia, atherosclerosis, or hypertension.³³⁻³⁴ Takimoto et al recently demonstrated that TAC resulted in a decrease of plasma BH4, an increase of myocardial eNOS monomer content, and increased $O_2^{\cdot-}$ production.¹² Moreover, administration of BH4 reduced the eNOS monomer content and decreased myocardial $O_2^{\cdot-}$ production and TAC-induced cardiomyopathy, indicating that eNOS uncoupling contributed to the TAC-induced ventricular dysfunction.¹² In the present study, iNOS deletion reduced the evidence of TAC-induced myocardial oxidative stress, indicating that iNOS contributed to oxidative stress in the wild-type mice, either directly through iNOS uncoupling or by iNOS-dependent eNOS uncoupling. Based on

the finding that myocardial iNOS was expressed as both monomer and dimer, and that iNOS deletion attenuated the evidence of oxidative stress in animals exposed to TAC, it can be concluded that iNOS uncoupling contributed to the increased oxidative stress in the wild-type mice. However, iNOS might also decrease intracellular BH4 and L-arginine availability to eNOS and thereby induce eNOS uncoupling. The relative contributions of iNOS uncoupling versus iNOS-dependent eNOS uncoupling in the TAC-induced increase of myocardial oxidative stress merit further investigation.

Akt, mTOR, and S6 Activation in Response to Oxidative Stress

Akt phosphorylation can regulate ventricular hypertrophy,³⁵ and oxidative stress has been reported to activate Akt³⁶ by regulating PTEN. Akt was reported to cause downstream activation of mTOR and p70S6K, and previous reports have demonstrated that inhibition of mTOR signaling with rapamycin attenuated TAC-induced ventricular hypertrophy³⁷⁻³⁸ and caused regression of cardiac hypertrophy produced by TAC.³⁹ Interestingly, a recently study reported that activation of Akt-mTOR and nuclear factor κ B participate in the development of ventricular hypertrophy, whereas the antioxidant pyrrolidine dithiocarbamate attenuated nuclear factor κ B, Akt, and p70S6K activation and TAC-induced ventricular hypertrophy.³⁸ Ribosomal protein S6 is a downstream target of p70S6K, and S6 phosphorylation increases the translation of a subset of mRNAs that promote protein synthesis. The finding of increased phospho-Akt and phospho-S6 in our study is consistent with the previous reports.^{12,38} Our finding that iNOS deletion attenuated TAC-induced myocardial oxidative stress, phospho-Akt, phospho-mTOR, phospho-S6, and ventricular hypertrophy supports the notion that oxidative stress exacerbates systolic overload-induced Akt-mTOR activation and ventricular hypertrophy.

Limitations

The pressure gradient across the aortic constriction was not measured in the present study. However, care was taken to ensure that the identical TAC procedure was performed by the same surgeon who was blinded to the genotype of the mice. Because iNOS^{-/-} attenuated the TAC-induced increase of eNOS expression, and eNOS monomer was present in wild-type mice exposed to TAC, we were unable to determine whether the protective effect of iNOS^{-/-} was directly caused by the absence of iNOS or secondary to an attenuation of TAC-induced eNOS induction. We did not measure plasma BH4 levels in the present study. However, using an almost identical TAC model, a recent study reported that TAC resulted in a significant decrease of plasma BH4 in C57/B6J mice, and that administration of BH4 attenuated TAC-induced myocardial eNOS monomer formation and oxidative stress, suggesting that a decrease of BH4 after TAC may contribute to NOS monomer formation.¹² An additional limitation is that the iNOS^{-/-} and wild-type mice were not littermates. Finally, because of the relatively large amount of tissue required for assay of myocardial NOS activity, this determination was not performed in the present study.

Acknowledgments

We acknowledge the guidance, support, and encouragement of Dr Robert J. Bache, who contributed importantly to the successful completion of this study.

Sources of Funding

This study was supported by NIH/National Heart, Lung, and Blood Institute grants HL71790 and HL21872. P.Z. is supported by a Scientist Development Award from the American Heart Association.

2

Disclosures

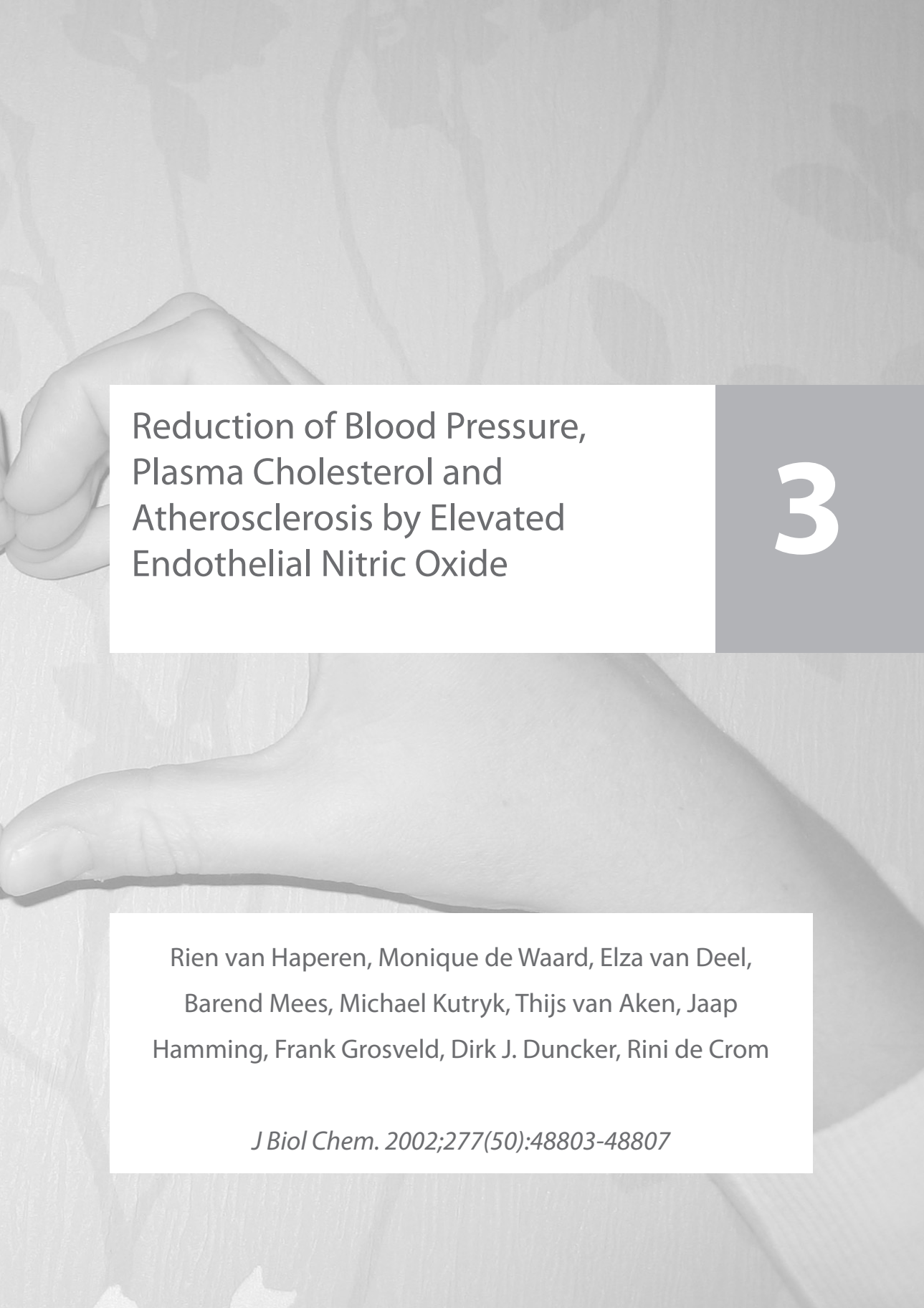
None.

References

1. Haywood GA, Tsao PS, von der Leyen HE, Mann MJ, Keeling PJ, Trindade PT, Lewis NP, Byrne CD, Rickenbacher PR, Bishopric NH, Cooke JP, McKenna WJ, Fowler MB. *Expression of inducible nitric oxide synthase in human heart failure*. *Circulation*. 1996; 93: 1087–1094.
2. Habib FM, Springall DR, Davies GJ, Oakley CM, Yacoub MH, Polak JM. *Tumour necrosis factor and in dilated cardiomyopathy*. *Lancet*. 1996; 347: 1151–1155.
3. Chen Y, Traverse JH, Du R, Hou M, Bache RJ. *Nitric oxide modulates myocardial oxygen consumption in the failing heart*. *Circulation*. 2002; 106: 273–279.
4. Nadruz W Jr, Lagosta VJ, Moreno H Jr, Coelho OR, Franchini KG. *Simvastatin prevents load-induced protein tyrosine nitration in overloaded hearts*. *Hypertension*. 2004; 43: 1060–1066.
5. Liu YH, Carretero OA, Cingolani OH, Liao TD, Sun Y, Xu J, Li LY, Pagano PJ, Yang JJ, Yang XP. *Role of inducible nitric oxide synthase in cardiac function and remodeling in mice with heart failure due to myocardial infarction*. *Am J Physiol Heart Circ Physiol*. 2005; 289: H2616–H2623.
6. Heger J, Godecke A, Flögel U, Merx MW, Molojavci A, Kuhn-Velten WN, Schrader J. *Cardiac-specific overexpression of inducible nitric oxide synthase does not result in severe cardiac dysfunction*. *Circ Res*. 2002; 90: 93–99.
7. Mungro IN, Gros R, You X, Pirani A, Azad A, Csont T, Schulz R, Butany J, Stewart DJ, Husain M. *Cardiomyocyte overexpression of iNOS in mice results in peroxynitrite generation, heart block, and sudden death*. *J Clin Invest*. 2002; 109: 735–743.
8. Hu P, Zhang D, Swenson L, Chakrabarti G, Abel ED, Litwin SE. *Minimally invasive aortic banding in mice: effects of altered cardiomyocyte insulin signaling during pressure overload*. *Am J Physiol Heart Circ Physiol*. 2003; 285: H1261–H1269.
9. Thomsen LL, Scott JM, Topley P, Knowles RG, Keerie AJ, Friend AJ. *Selective inhibition of inducible nitric oxide synthase inhibits tumor growth in vivo: studies with 1400W, a novel inhibitor*. *Cancer Res*. 1997; 57: 3300–3304.
10. Chen Y, Li Y, Zhang P, Traverse JH, Hou M, Xu X, Kimoto M, Bache RJ. *Dimethylarginine dimethylaminohydrolase and endothelial dysfunction in failing hearts*. *Am J Physiol Heart Circ Physiol*. 2005; 289: H2212–H2219.
11. Takemoto M, Node K, Nakagami H, Liao Y, Grimm M, Takemoto Y, Kitakaze M, Liao JK. *Statins as antioxidant therapy for preventing cardiac myocyte hypertrophy*. *J Clin Invest*. 2001; 108: 1429–1437.
12. Takimoto E, Champion HC, Li M, Ren S, Rodriguez ER, Tavazzi B, Lazzarino G, Paolucci N, Gabrielson KL, Wang Y, Kass DA. *Oxidant stress from nitric oxide synthase-3 uncoupling stimulates cardiac pathologic remodeling from chronic pressure load*. *J Clin Invest*. 2005; 115: 1221–1231.
13. Kalinowski L, Dobrucki LW, Brovkovich V, Malinski T. *Increased nitric oxide bioavailability in endothelial cells contributes to the pleiotropic effect of cerivastatin*. *Circulation*. 2002; 105: 933–8.
14. Vellaichamy E, Khurana ML, Fink J, Pandey KN. *Involvement of the NF-kappa B/matrix metalloproteinase pathway in cardiac fibrosis of mice lacking guanylyl cyclase/natriuretic peptide receptor A*. *J Biol Chem*. 2005; 280: 19230–19242.
15. Jones SP, Greer JJ, Ware PD, Yang J, Walsh K, Lefer DJ. *Deficiency of iNOS does not attenuate severe congestive heart failure in mice*. *Am J Physiol Heart Circ Physiol*. 2005; 288: H365–H370.
16. Feng Q, Lu X, Jones DL, Shen J, Arnold JMO. *Increased inducible nitric oxide synthase expression contributes to myocardial dysfunction and higher mortality after myocardial infarction in mice*. *Circulation*. 2001; 104: 700–704.
17. Sam F, Sawyer DB, Xie Z, Chang DLF, Ngoy S, Brenner DA, Siwik DA, Singh K, Apstein CS, Colucci WS. *Mice lacking inducible nitric oxide synthase have improved left ventricular contractile function and reduced apoptotic cell death late after myocardial infarction*. *Circ Res*. 2001; 89: 351–356.
18. Cave A, Grieve D, Johar S, Zhang M, Shah AM. *NADPH oxidase-derived reactive oxygen species in cardiac pathophysiology*. *Philos Trans R Soc Lond B Biol Sci*. 2005; 360: 2327–2334.
19. Berry CE, Hare JM. *Xanthine oxidoreductase and cardiovascular disease: molecular mechanisms and pathophysiological implications*. *J Physiol*. 2004; 555: 589–606.
20. Ruetten H, Dimmeler S, Gehring D, Ihling C, Zeiher AM. *Concentric left ventricular remodeling in endothelial nitric oxide synthase knockout mice by chronic pressure overload*. *Cardiovasc Res*. 2005; 66: 444–453.
21. Heydemann A, Huber JM, Kakkar R, Wheeler MT, McNally EM. *Functional nitric oxide synthase mislocalization in cardiomyopathy*. *J Mol Cell Cardiol*. 2004; 36: 213–223.
22. Ichinose F, Bloch KD, Wu JC, Hataishi R, Aretz HT, Picard MH, Scherrer-Crosbie M. *Pressure overload-induced LV hypertrophy and dysfunction in mice are exacerbated by congenital NOS3 deficiency*. *Am J Physiol Heart Circ Physiol*. 2004; 286: H1070–H1075.

23. Ide T, Tsutsui H, Kinugawa S, Suematsu N, Hayashidani S, Ichikawa K, Utsumi H, Machida Y, Egashira K, Takeshita A. *Direct evidence for increased hydroxyl radicals originating from superoxide in the failing myocardium.* *Circ Res.* 2000; 86: 152–157.
24. Siwik DA, Pagano PJ, Colucci WS. *Oxidative stress regulates collagen synthesis and matrix metalloproteinase activity in cardiac fibroblasts.* *Am J Physiol Cell Physiol.* 2001; 280: C53–C60.
25. Shiomi T, Tsutsui H, Matsusaka H, Murakami K, Hayashidani S, Ikeuchi M, Wen J, Kubota T, Utsumi H, Takeshita A. *Overexpression of glutathione peroxidase prevents left ventricular remodeling and failure after myocardial infarction in mice.* *Circulation.* 2004; 109: 544–549.
26. Andrew PJ, Mayer B. *Enzymatic function of nitric oxide synthases.* *Cardiovasc Res.* 1999; 43: 521–531.
27. Xia Y, Zweier JL. *Direct measurement of nitric oxide generation from nitric oxide synthase.* *Proc Natl Acad Sci U S A.* 1997; 94: 12705–12710.
28. Xia Y, Dawson VL, Dawson TM, Snyder SH, Zweier JL. *Nitric oxide synthase generates superoxide and nitric oxide in arginine-depleted cells leading to peroxynitrite-mediated cellular injury.* *Proc Natl Acad Sci U S A.* 1996; 93: 6770–6774.
29. Kuzkaya N, Weissmann N, Harrison DG, Dikalov S. *Interactions of peroxynitrite, tetrahydrobiopterin, ascorbic acid, and thiols: implications for uncoupling endothelial nitric-oxide synthase.* *J Biol Chem.* 2003; 278: 22546–22554.
30. Crane BR, Arvai AS, Ghosh DK, Wu C, Getzoff ED, Stuehr DJ, Tainer JA. *Structure of nitric oxide synthase oxygenase dimer with pterin and substrate.* *Science.* 1998; 279: 2121–2126.
31. Xia Y, Roman LJ, Masters BS, Zweier JL. *Inducible nitric-oxide synthase generates superoxide from the reductase domain.* *J Biol Chem.* 1998; 273: 22635–22639.
32. Laursen JB, Somers M, Kurz S, McCann L, Warnholtz A, Freeman BA, Tarpey M, Fukai T, Harrison DG. *Endothelial regulation of vasomotion in apoE-deficient mice: implications for interactions between peroxynitrite and tetrahydrobiopterin.* *Circulation.* 2001; 103: 1282–1288.
33. Cosentino F, Patton S, d'Uscio LV, Werner ER, Werner-Felmayer G, Moreau P, Malinski T, Luscher TF. *Tetrahydrobiopterin alters superoxide and nitric oxide release in prehypertensive rats.* *J Clin Invest.* 1998; 101: 1530–1537.
34. Stroes E, Kastelein J, Cosentino F, Erkelens W, Wever R, Koomans H, Luscher T, Rabelink T. *Tetrahydrobiopterin restores endothelial function in hypercholesterolemia.* *J Clin Invest.* 1997; 99: 41–46.
35. Matsui T, Li L, Wu JC, Cook SA, Nagoshi T, Picard MH, Liao R, Rosenzweig A. *Phenotypic spectrum caused by transgenic overexpression of activated Akt in the heart.* *J Biol Chem.* 2002; 277: 22896–22901.
36. Leslie NR, Bennett D, Lindsay YE, Stewart H, Gray A, Downes CP. *Redox regulation of PI 3-kinase signalling via inactivation of PTEN.* *EMBO J.* 2003; 22: 5501–5510.
37. Shioi T, McMullen JR, Tarnavski O, Converso K, Sherwood MC, Manning WJ, Izumo S. *Rapamycin attenuates load-induced cardiac hypertrophy in mice.* *Circulation.* 2003; 107: 1664–1670.
38. Ha T, Li Y, Gao X, McMullen JR, Shioi T, Izumo S, Kelley JL, Zhao A, Haddad GE, Williams DL, Browder IW, Kao RL, Li C. *Attenuation of cardiac hypertrophy by inhibiting both mTOR and NFkappaB activation in vivo.* *Free Radic Biol Med.* 2005; 39: 1570–1580.
39. McMullen JR, Sherwood MC, Tarnavski O, Zhang L, Dorfman AL, Shioi T, Izumo S. *Inhibition of mTOR signaling with rapamycin regresses established cardiac hypertrophy induced by pressure overload.* *Circulation.* 2004; 109: 3050–3055.





Reduction of Blood Pressure,
Plasma Cholesterol and
Atherosclerosis by Elevated
Endothelial Nitric Oxide

3

Rien van Haperen, Monique de Waard, Elza van Deel,
Barend Mees, Michael Kutryk, Thijs van Aken, Jaap
Hamming, Frank Grosveld, Dirk J. Duncker, Rini de Crom

J Biol Chem. 2002;277(50):48803-48807

Abstract

3 In the vascular system, nitric oxide is generated by endothelial NO synthase (eNOS). NO has pleiotropic effects, most of which are believed to be atheroprotective. Therefore, it has been argued that patients suffering from cardiovascular disease could benefit from an increase in eNOS activity. However, increased NO production can cause oxidative damage, cell toxicity and apoptosis, and hence could be atherogenic rather than beneficial. In order to study the in vivo effects of increased eNOS activity, we created transgenic mice overexpressing human eNOS. Aortic blood pressure was ~20 mm Hg lower in the transgenic mice compared to control mice due to a lower systemic vascular resistance. The effects of eNOS overexpression on diet-induced atherosclerosis were studied in apolipoprotein E deficient mice. Elevation of eNOS activity decreased blood pressure (~20 mm Hg) and plasma levels of cholesterol (~17%), resulting in a reduction in atherosclerotic lesions by 40%. We conclude that an increase in eNOS activity is beneficial and provides protection against atherosclerosis.

Introduction

Endothelial nitric oxide synthase (eNOS) plays an important role in the regulation of vascular tone, vascular biology and haemostasis. For example, NO produced by eNOS causes vasodilation. Thus, eNOS knock out mice are hypertensive,¹ while eNOS transgenic mice have hypotension.² In addition, NO reduces the activation and aggregation of platelets,^{3,4} attenuates adhesion of leukocytes to the endothelium,⁵⁻⁷ reduces the permeability of the endothelium and inhibits proliferation and migration of vascular smooth muscle cells.⁸ Impaired activity of eNOS is associated with endothelial cell dysfunction.⁹ For these reasons eNOS has been proposed to modulate atherosclerotic disease.¹⁰⁻¹² Indeed, impairment or deficiency of eNOS gives rise to accelerated atherosclerosis in animal models,^{10,12-14} indicating that physiological levels of eNOS are anti-atherogenic. This suggests that patients at increased risk of atherosclerotic vascular disease could possibly benefit from an increase of eNOS activity by pharmacological means or (local) gene therapy. However, eNOS derived NO also has detrimental effects,¹⁵ like the generation of superoxides,¹⁶ making it difficult to predict whether increased eNOS activity is beneficial or harmful.¹⁷ In order to determine whether increased eNOS activity may be beneficial, we created transgenic mice that express the human eNOS gene. These mice were crossbred to apolipoprotein E deficient (apoE0) mice in order to evaluate the effects of a constitutive increase in eNOS activity on the development of atherosclerosis.

Materials and Methods

Mice

A DNA fragment containing the human eNOS gene was isolated from a home made human genomic cosmid library¹⁸ using eNOS cDNA (kindly donated by Dr. S. Janssens, Leuven, Belgium¹⁹) as a probe. In addition, the DNA fragment contained ~6kb of 5' natural flanking sequence, including the native eNOS promoter, and ~3kb of 3' sequence to the gene. Vector sequences were removed by restriction endonucleases. A solution of 1-2 µg/ml of DNA was used for microinjection of fertilized oocytes from FVB donor mice and transplanted into the oviducts of pseudopregnant B10xCBA mice. Founder mice and offspring were genotyped by PCR on DNA isolated from tail biopsies. Primers used were: 5'-GTC CTG CAG ACC GTG CAG C-3' (sense) and 5'-GGC TGT TGG TGT CTG AGC CG-3' (antisense). Mice were backcrossed to C57Bl6 for at least 5 generations (>96% C57Bl6). All eNOS transgenic mice were hemizygous. ApoE0 mice were obtained from the The Jackson Laboratory, Bar Harbor, ME. Male mice were used in all experiments. All animal experiments were performed in compliance with institutional (Erasmus MC, Rotterdam, The Netherlands) and national (Ministry of Health, Welfare and Sport, The Hague, The Netherlands) guidelines.

Western blotting and immuno-histochemistry

Aortas were collected and homogenized in 50 mM Tris-HCl, pH7.4 containing 1 mM EDTA, 0.25 M sucrose and 20 mM CHAPS. Western blotting was performed as described

previously.²⁰ 25 µg of protein (BCA protein assay kit; Pierce Chemical Company, Rockford, IL) was applied to each lane. Anti-eNOS was obtained from Santa Cruz Biotechnology Inc., Santa Cruz, CA. This antibody was also used for immuno-histochemistry experiments, which were performed according to Bakker et al.²¹

Hemodynamic measurements

Baseline blood pressure measurements.

Mice were weighed, anesthetized with ketamine (100 mg/kg ip) and xylazine (20 mg/kg ip), intubated and ventilated with a mixture of O₂ and N₂ (1/2 vol/vol) with a pressure controlled ventilator (Servo ventilator 900C, Siemens-Elema, Sweden). The ventilation rate was set at 100 strokes/min with a peak inspiration pressure of 18 cmH₂O and a positive end expiration pressure (PEEP) of 6 cmH₂O. After intubation the mice were placed on a heating pad to maintain body temperature at 37°C and a polyethylene catheter (PE 10) was inserted into the right carotid artery and advanced into the aortic arch, for the measurement of aortic pressure. In the first part of the study we used 12 eNOS-Tg2 and 5 eNOS-Tg3 mice for screening of eNOS expression, and compared them to 33 wild type mice. Ten min after a second intraperitoneal bolus of anesthetics (100 mg/kg ketamine and 20 mg/kg xylazine) baseline blood pressure recordings were obtained.

Effect of L-NAME on systemic vascular resistance.

Subsequently, we chose the eNOS-Tg2 line to determine whether the lower aortic blood pressure was the result of an NO-mediated decrease in systemic vascular resistance. For this purpose, in 17 eNOS-Tg2 mice and 17 wild type mice a polyethylene catheter (PE 10) was inserted into the right carotid artery and advanced into the aortic arch, for the measurement of aortic pressure, while another PE 10 catheter was introduced into the right external jugular vein and advanced into the superior caval vein for infusion of L-NAME. After thoracotomy through the second right intercostal space, the ascending aorta was exposed and a transit-time flow probe (ID 1.5 mm; Transonics systems Inc. T206) was placed around the aorta for measuring aorta flow. Ten min after a second intraperitoneal bolus of 100 mg/kg ketamine and 20 mg/kg xylazine, baseline recordings were obtained. Then, a continuous 10 min intravenous infusion of L-NAME (100 mg/kg) was started and 10 min after completion of the infusion, measurements were repeated.

Effects of dietary supplementation of L-arginine on baseline hemodynamics.

In the eNOS-Tg2 line we studied whether L-arginine deficiency contributed to the modest effects of eNOS overexpression on systemic vascular resistance. For this purpose, in 6 eNOS-Tg2 male mice and 7 wild type male mice, L-arginine was supplemented in their drinking water (2.5% w/v). One week later, animals were instrumented as described above and hemodynamic measurements were performed under baseline conditions.

Data analysis

Hemodynamic data were recorded and digitized using an on-line 4 channel data acquisition program (ATCODAS, Dataq Instruments, Akron, OH), for later analysis with a program written in MatLab (Mathworks Inc, Natick, MA). Fifteen consecutive beats were selected for determination of heart rate, aortic pressure, and aorta blood flow.

eNOS activity assay

Aortas were collected and homogenized in 50 mM Tris-HCl, pH7.4 containing 1 mM EDTA, 0.25 M sucrose and 20 mM CHAPS. eNOS activity assays were performed by measuring L-arginine to L-citrulline conversion using a nitric oxide synthase assay kit (Calbiochem, La Jolla, CA; cat.no. 482700) according to the manufacturers instructions. Protein content was measured by the BCA protein assay kit (Pierce Chemical Company, Rockford, IL).

Lipid measurements

Blood was collected via orbital puncture after an overnight fasting period. Plasma was frozen freshly or subjected to ultracentrifugation in a Beckman 42.2 Ti rotor (42000 rpm, 3 h, 12 °C) at $d = 1.063$ g/ml. Tubes were sliced and two fractions were collected: VLDL + LDL: $d < 1.063$ g/ml, and HDL: $d > 1.063$ g/ml. Cholesterol was measured with the F-chol kit (Boehringer Mannheim, Germany) after hydrolysis of cholesteryl esters with cholesterol esterase from *Candida cylindracea* (Boehringer Mannheim).

Atherosclerosis

Atherosclerosis experiments were performed in age and sex matched mice. Male mice of 8 weeks were fed a Western type diet, containing 15% (w/w) cocoa butter and 0.25% (w/w) cholesterol (diet W, Hope Farms, Woerden, The Netherlands) for 6 weeks, which leads to appreciable atherosclerosis.²²⁻²⁴ Animals were anesthetized using isoflurane and in situ fixation was performed via the left ventricle of the heart using phosphate buffered formalin (4%, v/v). A Sony digital camera was used to obtain images of sections of the aortic root. These were analyzed by Scion Image processing and analyzing software (available from www.scioncorp.com). Atherosclerosis was quantified in five sections per mouse with 80 μ m intervals using the method of Paigen et al.²⁵

Data analysis

Analysis of data was performed using two-way or one-way analysis of variance followed by Scheffé's test, as appropriate. Statistical significance was accepted when $P < 0.05$ (two-tailed). Data are presented as mean \pm SEM.

Results and Discussion

For the generation of eNOS transgenic mice, we used a DNA fragment that comprised the complete human eNOS genomic sequence, including all exons and introns as well its natural flanking sequences. Therefore, our mice are different from those described by Ohashi *et al.* which overexpressed bovine eNOS cDNA, driven by the murine preproendothelin-1 promoter.² Our approach was chosen in order to preserve the natural regulation of the gene and to prevent ectopic expression. For example, the endothelium enhancer element that is located 4.9 kilobases upstream from the transcription start site of the eNOS gene²⁶ is included in this construct. By using this construct we mimic the human situation in terms of regulation and tissue distribution of eNOS as much as possible.

Two independent lines with appreciable overexpression of the transgene, as measured by RT-PCR (not shown), were selected and arbitrarily designated eNOS_{Tg2} and eNOS_{Tg3}. Production of human eNOS protein was demonstrated by Western blotting of aorta homogenates (Fig. 1A). Subsequently, eNOS activity in aortas from control (wild type) and eNOS overexpressing mice was measured, using the L-arginine to L-citrulline conversion assay.²⁷ In aorta, the level of active eNOS enzyme was 10-fold increased in eNOS_{Tg2} mice and 7.5-fold in eNOS_{Tg3} mice, respectively, when compared to wild type animals (Fig 1B). Expression of human eNOS was also investigated by immunohistochemistry. There was no human eNOS staining of aortas of wild type mice, whereas the endothelial layer of the aorta was clearly stained in both human eNOS transgenic lines (Fig 1C).

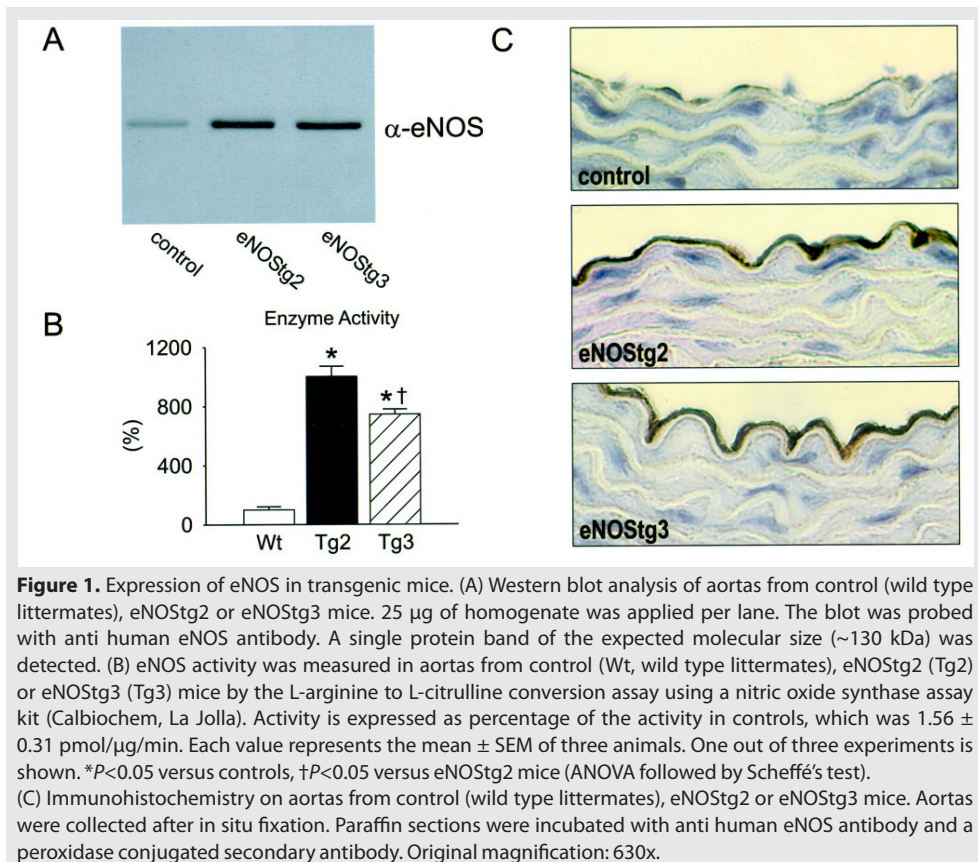


Figure 1. Expression of eNOS in transgenic mice. (A) Western blot analysis of aortas from control (wild type littermates), eNOS_{Tg2} or eNOS_{Tg3} mice. 25 μ g of homogenate was applied per lane. The blot was probed with anti human eNOS antibody. A single protein band of the expected molecular size (~130 kDa) was detected. (B) eNOS activity was measured in aortas from control (Wt, wild type littermates), eNOS_{Tg2} (Tg2) or eNOS_{Tg3} (Tg3) mice by the L-arginine to L-citrulline conversion assay using a nitric oxide synthase assay kit (Calbiochem, La Jolla). Activity is expressed as percentage of the activity in controls, which was 1.56 ± 0.31 pmol/ μ g/min. Each value represents the mean \pm SEM of three animals. One out of three experiments is shown. * $P < 0.05$ versus controls, † $P < 0.05$ versus eNOS_{Tg2} mice (ANOVA followed by Scheffé's test). (C) Immunohistochemistry on aortas from control (wild type littermates), eNOS_{Tg2} or eNOS_{Tg3} mice. Aortas were collected after in situ fixation. Paraffin sections were incubated with anti human eNOS antibody and a peroxidase conjugated secondary antibody. Original magnification: 630x.

The expression pattern of the the human eNOS transgene was investigated by immunohistochemistry in heart (Fig. 2A), liver (Fig. 2B), kidney (Fig. 2C), adrenal (Fig. 2D) and testis (Fig. 2E). Sections from wild type controls show virtually no immuno-staining (not shown). The lining of the larger vessels is clearly stained (Fig. 2A, Fig. 2D and 2E). Staining of capillaries is visible in the heart, between the cardiomyocytes. Immunoreactivity is observed in the sinusoids in the liver, and, in the kidney, in the peritubular capillaries as well as in the capillaries from the glomeruli. In the adrenal, the cortical capillaries as well

as medullary capillary sinusoids and veins are stained. In the testis, only blood vessels between the seminiferous tubules are stained. The parenchyma cells of none of these organs show appreciable immunoreactivity. Similar results were found with sections from eNOSTg3 mice (not shown).

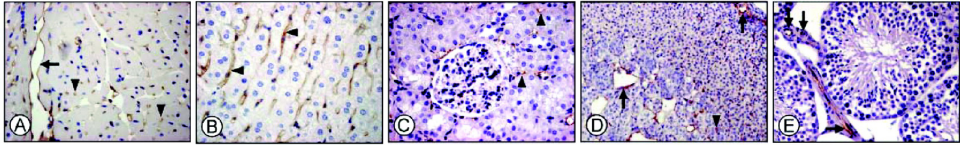


Figure 2. Expression pattern of human eNOS in transgenic mice. Organs from eNOSTg2 mice were collected after in situ fixation. Paraffin sections were incubated with anti human eNOS antibody and a peroxidase conjugated secondary antibody. (A) heart, (B) liver, (C) kidney, (D) adrenal, (E) testis tissue. Arrowheads indicate representative immunoreactive capillaries; arrows indicate larger blood vessels. Original magnification: 400x.

Our results show that the genomic sequences included in the DNA fragment we used are sufficient for expression in endothelial cells. Although eNOS activity is tightly regulated at the post-translational level,^{28,29} there is also extensive regulation at the transcriptional level.^{30,31} The present study shows that our construct results in high level expression of human eNOS which is not prevented by a feedback mechanism.

To study the effect of increased eNOS activity on blood pressure and vascular tone, we performed hemodynamic studies.³² Heart rates were similar for wild-type controls and eNOS transgenic lines, whereas both eNOS transgenic lines each exhibited a 20-25 mmHg lower mean aortic blood pressure compared to littermate controls (Fig. 3A). Subsequent hemodynamic studies were performed in the transgenic mouse line with the highest expression, eNOSTg2. These experiments showed that the lower aortic blood pressure was the result of a 30% lower systemic vascular resistance, as mean aortic blood flow and heart rate were similar in both groups (Fig. 3B). Subsequent infusion of the NOS inhibitor N⁶-nitro-L-arginine methyl ester (L-NAME) increased systemic vascular resistance and abolished the difference between control and eNOSTg2 mice. We therefore conclude that the lower basal systemic vascular resistance in eNOSTg2 mice is the result of increased NO production (Fig. 3B). This is corroborated by the significantly larger increase in blood pressure in response to L-NAME in the transgenic mice. Suppletion of L-arginine had no effect on the already lower mean aortic blood pressure and heart rate in the transgenic mice (Fig. 3C). We therefore also conclude that the blood pressure lowering effect of eNOS overexpression was not limited by a shortage of substrate.

The present study shows that the lower blood pressure associated with eNOS overexpression (as reported before²) is the result of a lower systemic vascular resistance. Thus eNOS activity was not only increased in the larger blood vessels but also in the microcirculation. Although eNOSTg2 and eNOSTg3 mice showed a slight variation in eNOS activity (Fig. 1B), the degree to which blood pressure was lowered was not different. This suggests that another rate-limiting factor, or one or more compensatory mechanisms prevented a further decrease in blood pressure in the eNOSTg2 mice.

3

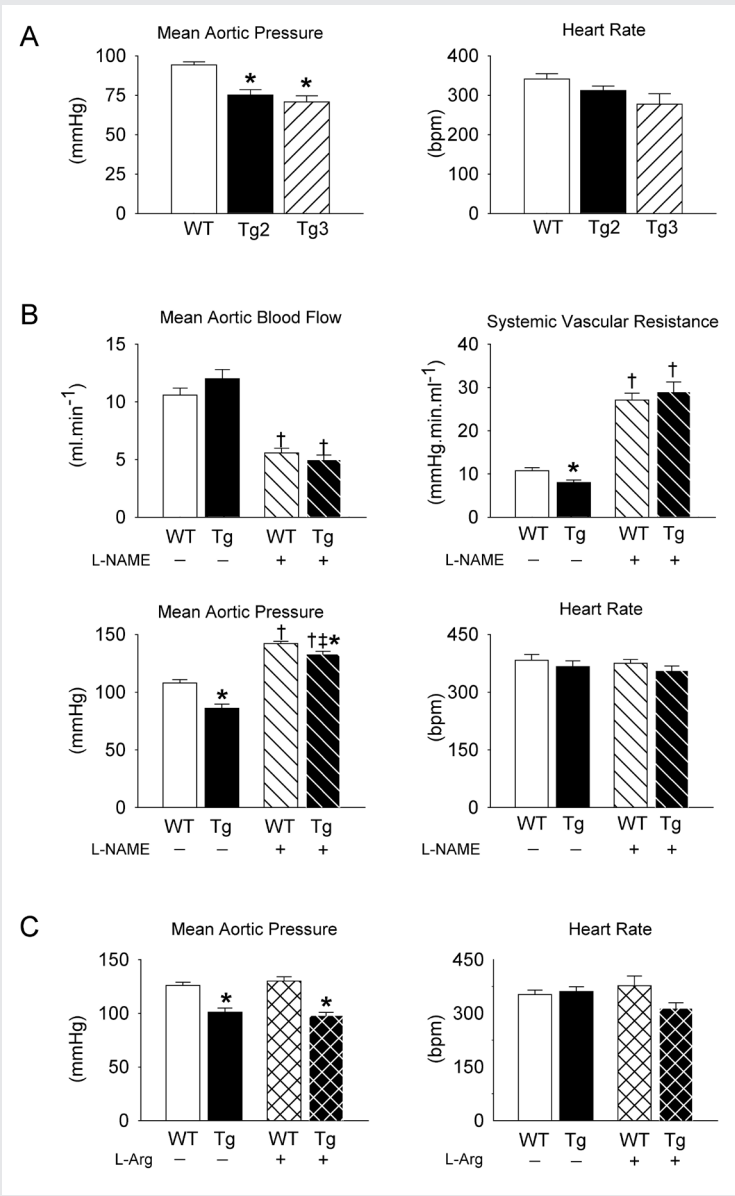


Figure 3. Hemodynamic measurements. (A) Mean aortic pressure and heart rate were measured in anesthetized control (Wt, wild type littermates), eNOS^{Tg2} (Tg2) or eNOS^{Tg3} (Tg3) mice. (B) Mean aortic pressure, heart rate, mean aortic blood flow and systemic vascular resistance were analyzed in control (Wt, wild type littermates) or eNOS^{Tg2} (Tg) mice before and following infusion of L-NAME. (C) Mean aortic pressure and heart rate were measured in anesthetized control (Wt, wild type littermates), or eNOS^{Tg2} (Tg) mice following one week of drinking water with or without L-arginine supplementation (L-Arg, 2.5% w/v). Each value represents the mean ± SEM of 5 five animals. **P*<0.05 versus controls (Wt), †*P*<0.05 versus baseline (before infusion of L-NAME), ‡*P*<0.05 versus controls (Wt) after infusion of L-NAME (ANOVA followed by Scheffé’s test).

To study whether increased expression of eNOS protects the mice against the development of diet-induced atherosclerosis, eNOS transgenic mice were cross-bred to apoE0 mice, which represent a well-known mouse model for studying atherosclerosis.^{33,34} The animals were fed a Western type diet for 6 weeks. As shown in Fig. 4A, overexpression of eNOS also caused a decrease in systemic blood pressure under these conditions, while heart rates were similar. Plasma cholesterol levels were measured before the start of the atherogenic diet (i.e. on normal chow diet) and at the end of the experiment (Table 1). Both eNOS transgenic lines showed a decrease in plasma cholesterol of approximately 15% when compared to apoE0 mice when fed a normal chow diet. As expected, the Western diet resulted in a dramatic increase (~3-fold) in plasma cholesterol levels, while the total cholesterol concentration remained lower in the eNOS transgenic animals when compared to apoE0 controls (approximately -16%). This difference was due to variations in the very low density (VLDL) and low density lipoproteins (LDL), which contain the bulk of the plasma cholesterol under these conditions: HDL-cholesterol concentration in plasma was 0.4 mM and did not differ between the groups (Table 1). These findings indicate that elevated eNOS activity results in a slightly more favorable (i.e. less atherogenic) lipoprotein profile, because VLDL and LDL contain the atherogenic portion of plasma cholesterol,³⁵ while HDL is protective against the development of atherosclerosis.^{36,37}

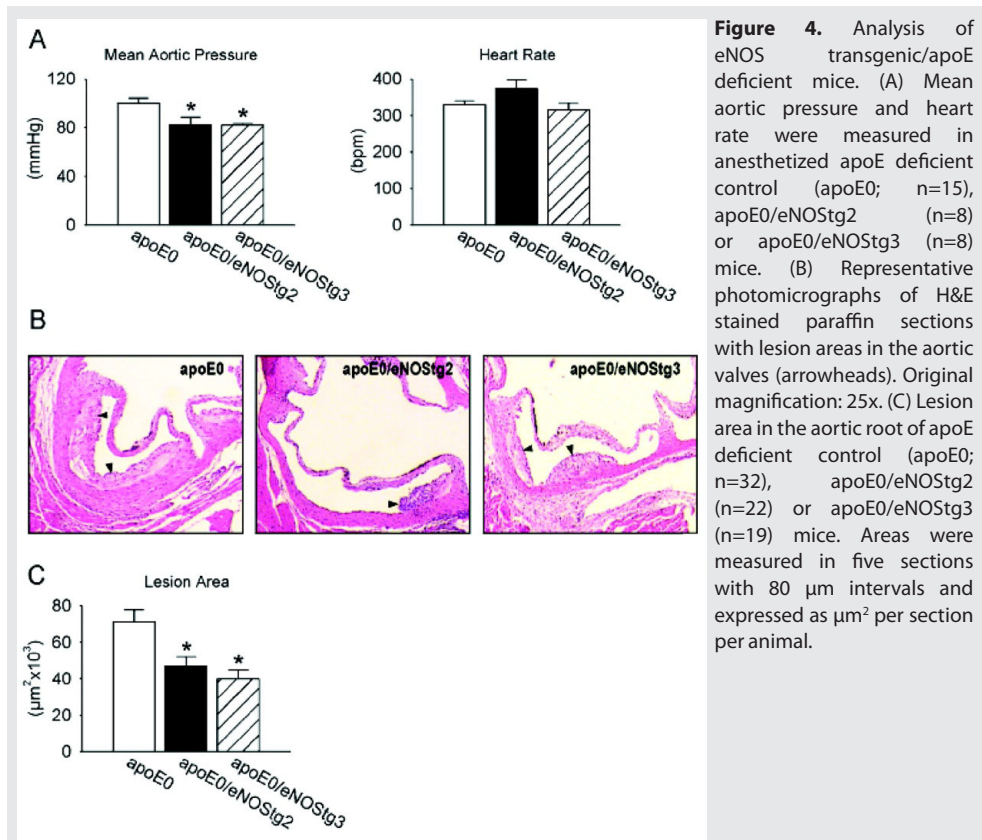


Figure 4. Analysis of eNOS transgenic/apoE deficient mice. (A) Mean aortic pressure and heart rate were measured in anesthetized apoE deficient control (apoE0; n=15), apoE0/eNOSlg2 (n=8) or apoE0/eNOSlg3 (n=8) mice. (B) Representative photomicrographs of H&E stained paraffin sections with lesion areas in the aortic valves (arrowheads). Original magnification: 25x. (C) Lesion area in the aortic root of apoE deficient control (apoE0; n=32), apoE0/eNOSlg2 (n=22) or apoE0/eNOSlg3 (n=19) mice. Areas were measured in five sections with 80 μm intervals and expressed as μm^2 per section per animal.

Table 1. Plasma lipid and lipoprotein analysis

Total cholesterol concentrations in plasma from apoE deficient control (apoE0), apoE0/eNOS_{tg2} or apoE0/eNOS_{tg3} mice after feeding a normal chow diet or an atherogenic diet. Cholesterol concentrations were determined by enzymatic methods. VLDL+LDL and HDL fractions were isolated by ultracentrifugation. TC: total cholesterol (mM); VLDL+LDL: cholesterol in VLDL and LDL (mM); HDL: cholesterol in HDL (mM).

	n	Chow TC	Atherogenic diet		
			TC	VLDL+LDL	HDL
apoE0	32	10.9 ± 0.3	28.4 ± 0.9	27.3 ± 0.8	0.4 ± 0.02
apoE0/eNOS _{tg2}	22	9.2 ± 0.4 ^a	23.3 ± 1.1 ^a	21.9 ± 1.1 ^b	0.4 ± 0.02
apoE0/eNOS _{tg3}	19	9.0 ± 0.2 ^b	24.4 ± 1.1 ^c	24.3 ± 1.1 ^c	0.4 ± 0.02

^a p < 0.01 ^b p < 0.001 ^c p < 0.05

To study the effect of eNOS overexpression on atherosclerosis, the atherosclerotic lesion areas in the aortic roots were measured. Fig. 4B shows representative examples of histological sections. Compared with apoE0 mice, we observed a decrease in atherosclerosis in both lines of eNOS transgenic mice studied (Fig. 4C).

Several studies have described a relation between plasma cholesterol and eNOS activity.³⁸⁻⁴⁰ However, these investigations exclusively focussed on the effects of changes in plasma cholesterol levels on eNOS activity. Hypercholesterolemia is associated with decreased eNOS activity, probably via an interaction of oxidized LDL with caveolae, the plasma membrane domains in which eNOS resides.⁴¹ Cholesterol synthesis inhibitors (statins) have been reported to increase eNOS activity in addition to their cholesterol lowering effects, but these actions appear to be independent.³⁸ In the present study we see an inverse correlation, i.e. the level of eNOS-expression affects the level of plasma cholesterol: plasma levels of cholesterol were about 15% lower in eNOS_{tg}/apoE0 mice as compared to apoE0 controls. A similar difference in plasma cholesterol levels was found after feeding the mice a Western type diet for 6 weeks, indicating that eNOS overexpression alleviates diet-induced hypercholesterolemia. This effect is not caused by ectopic expression in organs involved in lipid metabolism, e.g. the liver, as the expression pattern is restricted to endothelial cells in all organs that were examined (Fig. 2). Recently it was shown that hypercholesterolemia in mice results in CD36-mediated cholesterol depletion of caveolae, followed by translocation of eNOS from caveolae and subsequent inactivation of the enzyme.⁴² Thus, eNOS activity is directly related to the cholesterol content of caveolae. Possibly, the moderate decrease in plasma cholesterol that we observed in our eNOS transgenic mice is caused by a recruitment of plasma cholesterol by the endothelial cells in order to handle the increased level of eNOS protein. This small decrease in plasma cholesterol likely contributed, at least in part, to the observed lower susceptibility to diet-induced atherosclerosis.

Although it has been proposed that elevation of eNOS activity would attenuate atherosclerosis,¹¹ serious doubts have also been expressed as to whether an increase in eNOS activity *in vivo* would have beneficial effects, because high levels of NO (e.g. as produced by inducible NO synthase) have been implicated in cell toxicity and apoptosis.^{15,43} During the preparation of our manuscript, Ozaki et al.⁴⁴ reported the unexpected observation that relatively modest overexpression of eNOS resulted in

increased atherosclerosis. Based on our findings, we conclude that this conclusion cannot be generalized, taking into account the following considerations: (1) As enzyme activity is ± 1.5 fold increased, the level of eNOS overexpression in the mice used by Ozaki et al. is relatively low, when compared with the much higher NO production levels by activated iNOS (inducible NO synthase). A 1.5 fold increase is also rather low in terms of possible drug or gene therapy applications; (2) The observed increase in atherosclerosis is explained by measurements indicating that the overexpressed eNOS enzyme is dysfunctional in the mouse model used by Ozaki et al. This finding is not unexpected, given the moderate level of overexpression in their mice, as it has been previously reported that endogenous eNOS is indeed dysfunctional in terms of NO production in apoE0 mice fed a Western type diet.⁴⁵ The results from the study by Ozaki et al. are probably (at least in part) explained by the construct used by the authors, which consists of cDNA (often leading to low expression levels) and a heterologous promoter. In contrast, Our results demonstrate that overexpression of human eNOS in endothelial cells indeed results in decreased atherosclerosis, most likely via lowering blood pressure and plasma cholesterol. Our study therefore suggests that elevation of eNOS activity could be beneficial for patients at risk of developing atherosclerotic disease.

References

1. Huang, P. L., Huang, Z., Mashimo, H., Bloch, K. D., Moskowitz, M. A., Bevan, J. A., and Fishman, M. C. (1995) *Nature* **377**, 239-242.
2. Ohashi, Y., Kawashima, S., Hirata, K., Yamashita, T., Ishida, T., Inoue, N., Sakoda, T., Kurihara, H., Yazaki, Y., and Yokoyama, M. (1998) *J. Clin. Invest.* **102**, 2061-2071.
3. Riddell, D. R., and Owen, J. S. (1999) *Vitam. Horm.* **57**, 25-48
4. Loscalzo, J. (2001) *Circ. Res.* **88**, 756-762.
5. Lefer, A. M. (1997) *Circulation* **95**, 553-554.
6. Qian, H., Neplioueva, V., Shetty, G. A., Channon, K. M., and George, S. E. (1999) *Circulation* **99**, 2979-2982.
7. Niebauer, J., Dulak, J., Chan, J. R., Tsao, P. S., and Cooke, J. P. (1999) *J. Am. Coll. Cardiol.* **34**, 1201-1207.
8. Li, H., and Forstermann, U. (2000) *J. Pathol.* **190**, 244-254.
9. Harrison, D. G. (1997) *J. Clin. Invest.* **100**, 2153-2157.
10. Barton, M., Haudenschild, C. C., d'Uscio, L. V., Shaw, S., Munter, K., and Luscher, T. F. (1998) *Proc. Natl. Acad. Sci. U. S. A.* **95**, 14367-14372.
11. Drummond, G. R., and Harrison, D. G. (1998) *J. Clin. Invest.* **102**, 2033-2034.
12. Kano, H., Hayashi, T., Sumi, D., Esaki, T., Asai, Y., Thakur, N. K., Jayachandran, M., and Iguchi, A. (1999) *Biochem. Biophys. Res. Commun.* **259**, 414-419.
13. Knowles, J. W., Reddick, R. L., Jennette, J. C., Shesely, E. G., Smithies, O., and Maeda, N. (2000) *J. Clin. Invest.* **105**, 451-458.
14. Kuhlencordt, P. J., Gyurko, R., Han, F., Scherrer-Crosbie, M., Aretz, T. H., Hajjar, R., Picard, M. H., and Huang, P. L. (2001) *Circulation* **104**, 448-454.
15. Wever, R. M., Luscher, T. F., Cosentino, F., and Rabelink, T. J. (1998) *Circulation* **97**, 108-112.
16. Xia, Y., Tsai, A. L., Berka, V., and Zweier, J. L. (1998) *J. Biol. Chem.* **273**, 25804-25808
17. O'Donnell, V. B., and Freeman, B. A. (2001) *Circ. Res.* **88**, 12-21
18. van Haperen, R., van Tol, A., Vermeulen, P., Jauhainen, M., van Gent, T., van den Berg, P., Ehnholm, S., Grosveld, F., van der Kamp, A., and de Crom, R. (2000) *Arterioscler. Thromb. Vasc. Biol.* **20**, 1082-1088.
19. Janssens, S. P., Shimouchi, A., Quertermous, T., Bloch, D. B., and Bloch, K. D. (1992) *J. Biol. Chem.* **267**, 14519-14522
20. de Crom, R., van Haperen, R., Janssens, R., Visser, P., Willemsen, R., Grosveld, F., and van der Kamp, A. (1999) *Biochim. Biophys. Acta* **1437**, 378-392
21. Bakker, C. E., de Diego Otero, Y., Bontekoe, C., Raghoe, P., Luteijn, T., Hoogeveen, A. T., Oostra, B. A., and Willemsen, R. (2000) *Exp. Cell Res.* **258**, 162-170
22. Nakashima, Y., Plump, A. S., Raines, E. W., Breslow, J. L., and Ross, R. (1994) *Arterioscler. Thromb.* **14**, 133-140
23. Murayama, T., Yokode, M., Kataoka, H., Imabayashi, T., Yoshida, H., Sano, H., Nishikawa, S., and Kita, T. (1999) *Circulation* **99**, 1740-1746
24. Sjolund, H., Eitzman, D. T., Gordon, D., Westrick, R., Nabel, E. G., and Ginsburg, D. (2000) *Arterioscler. Thromb. Vasc. Biol.* **20**, 846-852
25. Paigen, B., Morrow, A., Holmes, P. A., Mitchell, D., and Williams, R. A. (1987) *Atherosclerosis* **68**, 231-240.
26. Laumonier, Y., Nadaud, S., Agrapart, M., and Soubrier, F. (2000) *J. Biol. Chem.* **275**, 40732-40741.
27. Garcia-Cardena, G., Fan, R., Stern, D. F., Liu, J., and Sessa, W. C. (1996) *J. Biol. Chem.* **271**, 27237-27240
28. Marletta, M. A. (2001) *Trends Biochem. Sci.* **26**, 519-521.
29. Fulton, D., Gratton, J. P., and Sessa, W. C. (2001) *J. Pharmacol. Exp. Ther.* **299**, 818-824.
30. Forstermann, U., Boissel, J. P., and Kleinert, H. (1998) *Faseb J.* **12**, 773-790.
31. Govers, R., and Rabelink, T. J. (2001) *Am. J. Physiol. Renal Physiol.* **280**, F193-206.
32. Kamphoven, J. H., Stubenitsky, R., Reuser, A. J., Van Der Ploeg, A. T., Verdouw, P. D., and Duncker, D. J. (2001) *Physiol. Genomics* **5**, 171-179
33. Breslow, J. L. (1996) *Science* **272**, 685-688.
34. Daugherty, A. (2002) *Am J. Med. Sci.* **323**, 3-10.
35. Brown, M. S., and Goldstein, J. L. (1986) *Science* **232**, 34-47.
36. Gordon, D. J., and Rifkind, B. M. (1989) *N. Engl. J. Med.* **321**, 1311-1316.
37. Libby, P. (2001) *Am. J. Cardiol.* **88**, 3N-8N.
38. Sessa, W. C. (2001) *Trends Mol. Med.* **7**, 189-191.

39. Feron, O., Dessy, C., Moniotte, S., Desager, J. P., and Balligand, J. L. (1999) *J. Clin. Invest.* **103**, 897-905.
40. Feron, O., Dessy, C., Desager, J. P., and Balligand, J. L. (2001) *Circulation* **103**, 113-118
41. Everson, W. V., and Smart, E. J. (2001) *Trends Cardiovasc. Med.* **11**, 246-250.
42. Kincer, J. F., Uittenbogaard, A., Dressman, J., Guerin, T. M., Febbraio, M., Guo, L., and Smart, E. J. (2002) *J. Biol. Chem.* **277**, 23525-23533
43. Hoit, B. D. (2001) *Circ. Res.* **89**, 289-291.
44. Ozaki, M., Kawashima, S., Yamashita, T., Hirase, T., Namiki, M., Inoue, N., Hirata, K., Yasui, H., Sakurai, H., Yoshida, Y., Masada, M., and Yokoyama, M. (2002) *J. Clin. Invest.* **110**, 331-340
45. d'Uscio, L. V., Baker, T. A., Mantilla, C. B., Smith, L., Weiler, D., Sieck, G. C., and Katusic, Z. S. (2001) *Arterioscler. Thromb. Vasc. Biol.* **21**, 1017-1022





Vasomotor Control in Mice
Overexpressing Human
Endothelial Nitric Oxide Synthase

4

Elza D. van Deel, Daphne Merkus, Rien van Haperen,
Monique C. de Waard, Rini de Crom, and Dirk J. Duncker

*American Journal of Physiology - Heart and Circulatory
Physiology* 2007; 293(2):H1144-1153

Abstract

Nitric oxide (NO) plays a key role in regulating vascular tone. Mice overexpressing endothelial NO synthase [eNOS-transgenic (Tg)] have a 20% lower systemic vascular resistance (SVR) than wild-type (WT) mice. However, because eNOS enzyme activity is 10 times higher in tissue homogenates from eNOS-Tg mice, this *in vivo* effect is relatively small. We hypothesized that the effect of eNOS overexpression is attenuated by alterations in NO signaling and/or altered contribution of other vasoregulatory pathways. In isoflurane-anesthetized open-chest mice, eNOS inhibition produced a significantly greater increase in SVR in eNOS-Tg mice compared with WT mice, consistent with increased NO synthesis. Vasodilation to sodium nitroprusside (SNP) was reduced, whereas the vasodilator responses to phosphodiesterase-5 blockade and 8-bromo-cGMP (8-Br-cGMP) were maintained in eNOS-Tg compared with WT mice, indicating blunted responsiveness of guanylyl cyclase to NO, which was supported by reduced guanylyl cyclase activity. There was no evidence of eNOS uncoupling, because scavenging of reactive oxygen species (ROS) produced even less vasodilation in eNOS-Tg mice, whereas after eNOS inhibition the vasodilator response to ROS scavenging was similar in WT and eNOS-Tg mice. Interestingly, inhibition of other modulators of vascular tone [including cyclooxygenase, cytochrome P-450 2C9, endothelin, adenosine, and Ca-activated K⁺ channels] did not significantly affect SVR in either eNOS-Tg or WT mice, whereas the marked vasoconstrictor responses to ATP-sensitive K⁺ and voltage-dependent K⁺ channel blockade were similar in WT and eNOS-Tg mice. In conclusion, the vasodilator effects of eNOS overexpression are attenuated by a blunted NO responsiveness, likely at the level of guanylyl cyclase, without evidence of eNOS uncoupling or adaptations in other vasoregulatory pathways.

Introduction

Endothelial nitric oxide synthase (eNOS)-derived nitric oxide (NO) plays a key role in cardiovascular homeostasis.²³ Loss of NO bioavailability is implicated in the etiology and pathogenesis of ischemic heart disease,^{14,48} whereas an increase in NO bioavailability has been shown to ameliorate ischemic heart disease at its various stages, including atherosclerosis,⁴⁷ ischemia-reperfusion injury,²⁶ and heart failure.²⁷

To study the beneficial effects of increased eNOS activity, we have previously developed and described transgenic (Tg) mice that overexpress the human eNOS gene.^{46,47} In these eNOS-Tg mice, eNOS protein level is significantly increased as demonstrated by Western blot analysis and immunohistochemistry.^{27,46,47} Phosphorylated eNOS levels were highly increased in eNOS-Tg mice indicating that the overexpressed eNOS is active.⁴⁶ Furthermore, the overexpressed eNOS is localized exclusively in the endothelial cells of smaller and larger blood vessels of several organs such as the aorta, heart, and kidney, but not in myocardial cells or parenchymal cells of these organs.^{46,47} Within the endothelial cells, eNOS is expressed in the Golgi complex and at the plasma membrane, which exactly matches the sites where eNOS is known to be primarily located.⁴⁶ As a consequence of the eNOS overexpression, eNOS enzyme activity was increased 10-fold in eNOS-Tg mice.^{27,46,47} Accordingly, eNOS-Tg mice have a significantly lower aortic blood pressure compared with wild-type (WT) mice as a result of a lower systemic vascular resistance (SVR). After administration of the NOS inhibitor *N*^ω-nitro-L-arginine methyl ester (L-NAME), SVR increases more in Tg animals, indicating that in the eNOS-Tg mice an elevated eNOS activity is indeed responsible for the lower SVR.⁴⁷ However, from the 10-fold increase in vascular eNOS protein level and *in vitro* enzyme activity,⁴⁷ the 20% lower SVR appears rather modest when compared with the 150% increase in SVR observed in WT mice produced by inhibition of the endogenous murine eNOS with L-NAME.⁴⁷ These observations led us to hypothesize that the vasodilator influence of a 10-fold overexpression of eNOS is blunted through alterations in vasomotor control of the resistance vessels in the systemic bed of eNOS-Tg mice.

A variety of vasomotor control mechanisms could have contributed to the blunted vasodilator influence of eNOS overexpression. For example, a chronic increase in NO production has been shown to blunt the responsiveness of soluble guanylyl cyclase (sGC) and protein kinase G (PKG) in aortic rings obtained from mice overexpressing bovine eNOS.⁵¹ Alternatively, under conditions of oxidative stress and eNOS substrate and cofactor depletion, eNOS can become uncoupled and produce superoxide instead of NO.^{2,50} It is possible that high levels of eNOS expression result in simultaneous NO and superoxide production, thereby reducing the bioavailability of NO. Finally, control of vascular tone is characterized by cross-talk between redundant vasoregulatory pathways. Thus loss of eNOS activity can result in a compensatory increase in the vasodilator influence of cytochrome *P*-450 2C9 (CYP2C9),^{13,36} cyclooxygenase (COX),^{33,38} adenosine,²⁸ or ATP-sensitive K⁺ (K_{ATP}) channels,²⁴ and increase endothelin.²¹ Consequently, overexpression of eNOS may attenuate the vasodilator influence of other vasodilator pathways, thereby counteracting the NO-induced decrease in SVR.

From these considerations, the aim of the present study was to investigate *in vivo* the alterations in vasomotor control of SVR in mice overexpressing human eNOS. Specifically, we investigated whether alterations in vascular NO signaling and/or alterations in the vasomotor influence of other pathways blunted the vasodilator influence of eNOS overexpression.

Methods

All experiments were performed in accordance with the “Guiding Principles in the Care and Use of Animals” as approved by the Council of the American Physiological Society and with prior approval of the Animal Care Committee of the Erasmus MC.

4

A total of 178 eNOS-Tg mice and 179 WT littermates in C57BL/6 background of both sexes entered the study (19–35 g). The generation of eNOS-Tg mice has been previously described.^{46,47} Briefly, a DNA fragment, containing the human eNOS gene and ~6 kb of 5′-natural flanking sequence, including the native eNOS promoter, and ~3 kb of 3′-sequence to the gene, was used for microinjection of fertilized oocytes. Transgenic offspring was backcrossed to C57BL/6 for >10 generations.

Western Blot Analysis and Enzyme Activity Measurement

To determine the expression level and activity of guanylyl cyclase (GC), the aorta, kidney, and brain of WT and eNOS-Tg mice were homogenized in 50 mM Tris-HCl, pH 7.4, containing 1 mM EDTA, 0.25 M sucrose, and 20 mM CHAPS. Western blot analysis was performed as previously described.¹² Anti-GC was obtained from Sigma-Aldrich. GC activity was determined with an immunoassay for the quantification of total cGMP (Sigma-Aldrich).

Surgical Instrumentation

Mice were weighed, sedated with 4% isoflurane, intubated, and connected to a pressure-controlled ventilator (SAR-830/P; CWE). Respiration rate was set at 90 breaths/min with a peak inspiratory pressure of 18 cmH₂O and a positive end-expiratory pressure of 4 cmH₂O. All animals were ventilated with a gas mixture of O₂-N₂O (1:2 vol/vol) containing 2.5% isoflurane to maintain anesthesia while placed on a temperature-controlled heating pad to maintain body temperature at 37°C. A polyethylene catheter (PE-10) was inserted in the right carotid artery and advanced into the aortic arch to measure aortic pressure and heart rate. A flame-stretched PE-50 catheter was inserted in the jugular vein to allow infusion of drugs. After thoracotomy through the first right intercostal space was performed, the ascending aorta was exposed and a transit time flow probe (ID 1.5 mm; T206, Transonic systems) was placed around the aorta for measurement of aortic blood flow.

Experimental Protocols

After a 10-min stabilization period, baseline hemodynamics (heart rate, aortic pressure, and aortic blood flow) were measured, followed by intravenous infusion of various drugs or intravenous infusion of an equal volume of vehicle (0.5 ml saline). All drugs

were purchased from Sigma-Aldrich (except the PDE5 inhibitor EMD-360527 and the ET_A/ET_B receptor antagonist tezosentan, which were generous gifts from Prof. Schelling, Merck kGaA, and Dr. M. Clozel, Actelion, respectively) and were dissolved in saline and administered intravenously. Unless otherwise stated, each mouse was subjected to single drug treatment. Hemodynamics were recorded continuously throughout the 10-min infusion period and subsequent 10-min washout period. Fifteen WT and 15 eNOS-Tg mice were infused with saline to determine the effect of the vehicle on SVR.

Alterations in systemic vascular NO signaling

To confirm previous observations^{46,47} that eNOS contributes to the lower vascular tone in the systemic bed of eNOS-Tg mice, we first studied the effect of the eNOS inhibitor L-NAME (100 mg/kg) in 10 WT and 10 eNOS-Tg mice. Subsequently, to study alterations in the NO signal transduction pathway, we determined the systemic vasodilator responses to the eNOS-dependent vasodilator acetylcholine (ACh, 200 µg/kg) (10 WT and 10 eNOS-Tg mice), the NO donor sodium nitroprusside (SNP, 300 µg/kg) (15 WT and 15 eNOS-Tg mice), the PDE5 inhibitor EMD-360527 (EMD, 30 mg/kg) (10 WT and 10 eNOS-Tg mice), or the PKG activator 8-bromo-cGMP (8-Br-cGMP, 10 mg/kg) (10 WT and 10 eNOS-Tg mice). Higher NO background concentrations in eNOS-Tg mice might blunt the effect of exogenous NO (via SNP infusion), because the relative amount of extra NO would be lower. To circumvent this issue, we additionally studied the effects of SNP (300 µg/kg) after pretreatment with L-NAME (100 mg/kg) (15 WT and 15 eNOS-Tg mice). Furthermore, to determine whether the difference in vasodilator response to SNP in WT and eNOS-Tg mice was nonspecific to the NO pathway and not a general blunting of the vascular smooth muscle responsiveness, we also studied the vasodilator response to the NO independent K channel opener bimakalim (0.5 mg/kg), both in the presence (6 WT and 6 eNOS-Tg mice) and the absence (10 WT and 10 eNOS-Tg mice) of L-NAME (100 mg/kg).

To investigate whether eNOS uncoupling [due to either substrate or cofactor tetrahydrobiopterin (BH₄) deficiency] resulted in reduced NO bioavailability and increased superoxide formation, thereby reducing the effects of eNOS overexpression, we determined the systemic vascular effects of the ROS scavenger *N*-acetyl cysteine (NAC, 500 mg/kg) and the superoxide dismutase (SOD) mimetic 4-hydroxy-2,2,6,6-tetramethylpiperidin-1-oxyl (TEMPOL, 100 mg/kg) in 10 WT and 10 eNOS-Tg mice. To determine the NO independent effect of ROS scavenging on SVR, the effects of NAC were also studied in the presence of L-NAME (100 mg/kg) (10 WT and 10 eNOS-Tg mice). Additionally, superoxide potentially increases endothelin levels either through a direct effect⁴⁴ or by upregulation of gene expression.¹⁰ In this way eNOS uncoupling could increase the vasoconstrictor effect of endothelin and counterbalance eNOS overexpression. To establish whether the vasomotor influence of endothelin was indeed higher in eNOS-Tg mice, 6 WT and 6 eNOS-Tg mice received the mixed ET_A/ET_B receptor antagonist tezosentan (50 mg/kg) in both the absence and presence of L-NAME (100 mg/kg).

Alterations in vasomotor control by of other mediators of vasodilation and their end effectors

To determine alterations in vasomotor influence of other endothelial vasodilator systems

in eNOS-Tg mice, 6 WT and 6 eNOS-Tg mice received the COX inhibitor indomethacin (100 mg/kg), or CYP2C9 inhibitor sulfaphenazole (10 mg/kg). To investigate alterations in adenosine-mediated vasomotor control, we infused the adenosine receptor antagonist 8-S-phenyltheophylline (8SPT, 50 mg/kg) to 6 WT and 6 eNOS-Tg mice. To study alterations in the vasomotor influence of ATP-sensitive K^+ (K_{ATP}^+), Ca-activated K^+ (K_{Ca}^+), and voltage-dependent K^+ (K_V^+) channels, 15 WT and 15 eNOS-Tg mice were given the K_{ATP}^+ channel blocker glibenclamide (10 mg/kg). The K_{Ca}^+ channel blocker tetraethylammonium chloride (TEA, 100 mg/kg) and the K_V^+ channel blocker 4-aminopyridin (4-AP, 16 mg/kg) were administered to 6 WT and 6 eNOS-Tg mice.

Data Analysis

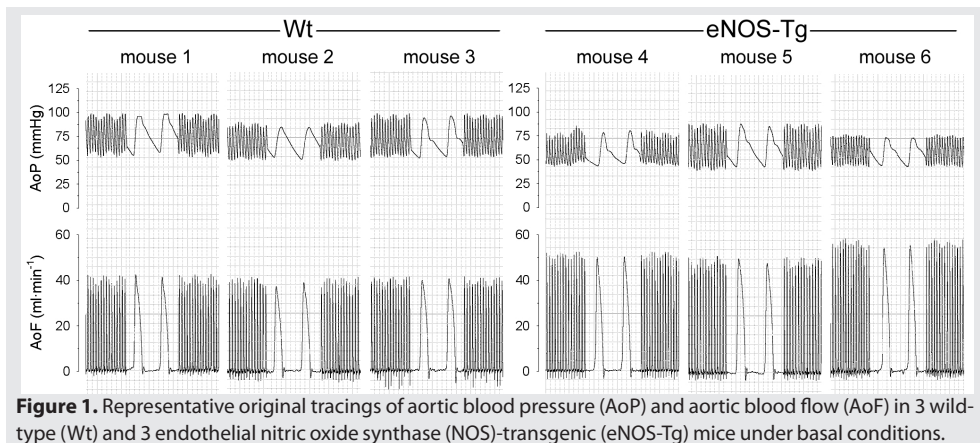
All hemodynamic data were recorded and digitized (400 Hz/channel) on-line using an eight-channel data-acquisition program (ATCODAS, Dataq Instruments, Akron, OH) and stored on a computer for off-line analysis. Data were analyzed at baseline and at various time points during drug infusion. A minimum of 10 consecutive beats was selected for analysis of each time point, from which heart rate, mean aortic pressure, and mean aortic blood flow were determined. SVR was subsequently computed as the ratio of mean aortic pressure and mean aortic blood flow at each time point. From these values, absolute changes from baseline were determined for heart rate, aortic blood flow, aortic blood pressure, and SVR.

Statistics

All hemodynamic data were tested using two-way (genotype x effect of drug) analysis of variance followed by post hoc testing with Student-Newman-Keuls test. A value of $P \leq 0.05$ was considered statistically significant. All data are presented as means \pm SE.

Results

eNOS overexpression had no effect on heart rate but resulted in a lower aorta pressure, despite a higher aorta flow (Figures 1 and 2 and Table 1), implying that the lower aorta



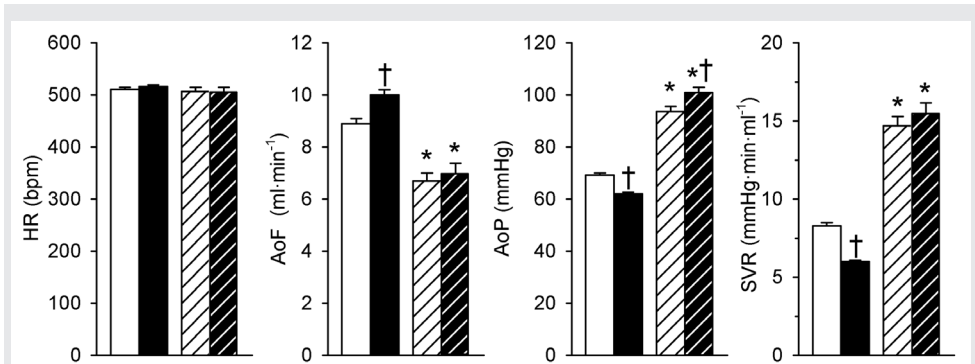


Figure 2. Absolute baseline measurements of heart rate (HR), AoP, AoF, and systemic vascular resistance (SVR) before (nonhatched bars) and after *N*^ω-nitro-L-arginine methyl ester (L-NAME) infusion (hatched bars) in Wt (open bars) and eNOS-Tg mice (solid bars). **P* ≤ 0.05 vs. before L-NAME infusion; † *P* ≤ 0.05 vs. Wt.

Table 1. Hemodynamic changes in Wt and eNOS-Tg mice produced by 10 min infusion of various vasoactive drugs

	number		AoP, mmHg		AoF, ml/min		SVR, mmHg·min·ml ⁻¹	
	Wt	eNOS-Tg	Wt	eNOS-Tg	Wt	eNOS-Tg	Wt	eNOS-Tg
Control								
Saline (vehicle)	15	15	1 ± 2	2 ± 2	-0.7 ± 0.4	-0.3 ± 0.3	0.6 ± 0.3	0.3 ± 0.3
L-NAME	10	10	24 ± 3	37 ± 2 [†]	-3.9 ± 0.6	-3.8 ± 0.7	7.8 ± 0.9	10.6 ± 0.9 [†]
ACh	10	10	-16 ± 2	-15 ± 2	-0.6 ± 0.3	-0.1 ± 0.6	-1.4 ± 0.3	-1.3 ± 0.2
Nitroprusside	15	15	-25 ± 3	-15 ± 1 [†]	-1.4 ± 0.5	-0.1 ± 0.3 [†]	-2.2 ± 0.3	-1.4 ± 0.2 [†]
EMD	10	10	-11 ± 2	-15 ± 3	0.5 ± 0.4	0.6 ± 0.2	-1.9 ± 0.5	-1.9 ± 0.3
8-Br-cGMP	10	10	-18 ± 2	-15 ± 3	-0.9 ± 0.3	-0.6 ± 0.4	-1.3 ± 0.2	-1.3 ± 0.2
Bimakalim	10	10	-29 ± 2	-23 ± 2 [†]	-0.9 ± 0.4	-0.6 ± 0.3	-2.9 ± 0.4	-2.5 ± 0.3
NAC	10	10	-9 ± 2	-7 ± 2	0.5 ± 0.4	0.3 ± 0.6	-1.7 ± 0.2	-0.8 ± 0.2 [†]
TEMPOL	10	10	-12 ± 1	-13 ± 2	-0.2 ± 0.3	-1.2 ± 0.6 [†]	-1.4 ± 0.4	-0.6 ± 0.2
Tezosentan	6	6	-8 ± 1	-2 ± 2 [†]	-1.4 ± 0.4	-1.8 ± 0.7	0.6 ± 0.4	0.8 ± 0.2
Indomethacin	6	6	-13 ± 3	-15 ± 3	-2.1 ± 0.6	-2.7 ± 0.6	0.3 ± 0.6	1.2 ± 0.5
Sulfaphenazole	6	6	-3 ± 2	-6 ± 1	-1.2 ± 0.5	-0.1 ± 0.3	0.7 ± 0.3	-0.5 ± 0.2
8-SPT	6	6	2 ± 2	2 ± 2	-1.5 ± 0.6	-0.8 ± 0.3	1.7 ± 0.5	0.8 ± 0.3
Glibenclamide	15	15	17 ± 2	14 ± 3	-1.8 ± 0.4	-3.5 ± 0.6 [†]	5.1 ± 0.8	6.5 ± 1.3
TEA	6	6	-6 ± 3	-5 ± 4	1.2 ± 0.4	0.0 ± 0.5	-1.2 ± 0.4	-0.3 ± 0.5
4-AP	6	6	16 ± 6	16 ± 1	-0.6 ± 0.8	-1.5 ± 0.2	4.2 ± 0.9	3.5 ± 0.8
Post-L-NAME								
Nitroprusside	15	15	-50 ± 3	-33 ± 3 [†]	1.4 ± 0.5	1.9 ± 0.4	-9.1 ± 0.7	-6.7 ± 0.7 [†]
Bimakalim	6	6	-43 ± 3	-49 ± 4	0.4 ± 0.5	1.0 ± 0.4	-7.7 ± 1.2	-8.6 ± 1.1
NAC	10	11	2 ± 2	-9 ± 3 [†]	1.3 ± 0.5	0.2 ± 0.4	-1.7 ± 0.6	-2.1 ± 1.1
Tezosentan	6	6	-4 ± 4	-4 ± 4	-0.1 ± 0.2	0.0 ± 0.3	-1.1 ± 0.9	-1.5 ± 1.2

Values are means ± SE. AoP, mean aortic blood pressure; AoF, mean aortic blood flow; SVR, mean systemic vascular resistance; Wt, wild-type; eNOS-Tg, endothelial nitric oxide synthase transgenic; L-NAME, *N*^ω-nitro-L-arginine methyl ester. Data are presented as absolute change from corresponding baseline either under Control conditions (Control) or in the presence of L-NAME (Post-L-NAME); 8-SPT, 8-*S*-phenyltheophylline; Glib, Glibenclamide; TEA, tetraethylammonium chloride; ACh, acetylcholine; EMD, PDE5 inhibitor EMD-360527; 8-Br-cGMP, 8-bromo-cGMP; NAC, *N*-acetyl cysteine.

* *P* ≤ 0.05 vs. corresponding saline; † *P* ≤ 0.05 eNOS-Tg vs. Wt.

pressure was caused by a reduction in SVR. The difference in SVR between WT and eNOS-Tg mice was abolished after eNOS inhibition with L-NAME, indicating that increased eNOS activity indeed underlies the lower SVR in eNOS-Tg mice (Figure 2). Consequently, eNOS inhibition induced a significantly larger increase in SVR in eNOS-Tg than that in WT animals (Figure 3). Infusion of the vehicle saline (0.5 ml) had no effect on SVR in either WT or eNOS-Tg mice (Figure 3).

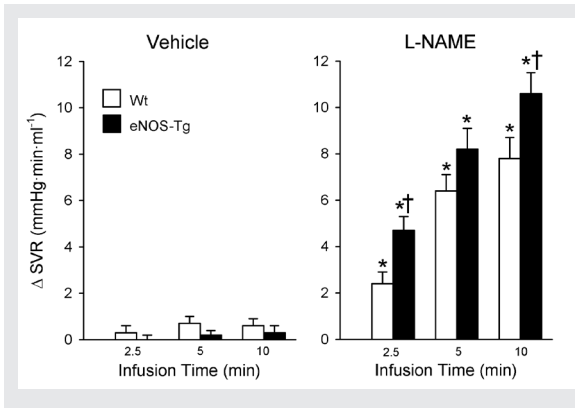
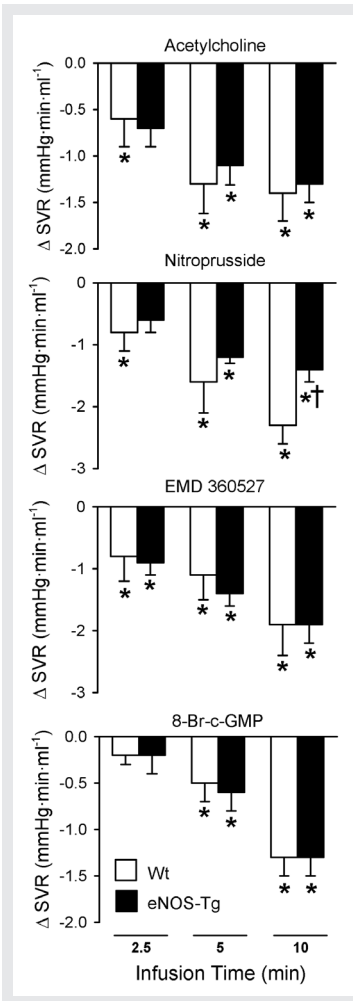


Figure 3. Changes in SVR (Δ SVR) from baseline produced by infusion of saline (Vehicle) and L-NAME in Wt (open bars) and eNOS-Tg mice (solid bars). * $P \leq 0.05$ vs. corresponding saline; † $P \leq 0.05$ vs. change in corresponding Wt.

Alterations in Systemic Vascular NO Signaling

Infusion of the eNOS-dependent vasodilator ACh produced similar degrees of vasodilation in WT and eNOS-Tg animals, whereas the systemic vasodilation by the endothelium-independent NO-donor SNP was blunted in eNOS-Tg animals (Figure 4). Inhibition of PDE5 with EMD-360527 and stimulation of PKG with 8-Br-cGMP resulted in similar vasodilator responses in both genotypes (Figure 4). Western blot analyses of aorta, kidney, and brain homogenates of WT and eNOS-Tg mice, showing a protein band of the expected molecular size (~70 kDa), demonstrated a trend toward a reduced expression of the GC protein, although this difference was not statistically significant after densitometric analysis (Figure 5). However, subsequent enzymatic activity measurements clearly showed a decreased GC activity in eNOS-Tg mice compared with WT mice in organs that are of importance in controlling SVR, but not in the aorta (Figure 5).



The blunted vasodilator response to SNP in eNOS-Tg mice was not merely due to a dilution of the effect of a dose of exogenous NO in eNOS-Tg mice (caused by higher NO background levels), because the vasodilator response to SNP in the presence of L-NAME was similarly blunted in eNOS-Tg compared

Figure 4. Δ SVR from baseline produced by infusion of acetylcholine, sodium nitroprusside, PDE5 inhibitor EMD-360527, and 8-Br-cGMP. * $P \leq 0.05$ vs. corresponding saline (presented in Figure 3); † $P \leq 0.05$ vs. change in corresponding Wt.

with that of WT mice (Figure 6). Furthermore, the blunted vasodilation to SNP could not be ascribed to a nonspecific decrease in vascular smooth muscle responsiveness, because the vasodilation produced by the K_{ATP} channel opener bimakalim was identical in eNOS-Tg and WT mice both in the absence and in the presence of L-NAME (Figure 6).

The ROS scavenger NAC elicited modest vasodilation in both WT and eNOS-Tg mice. However, the vasodilation was significantly less in eNOS-Tg mice (Figure 6). Similar observations were made with the SOD mimetic TEMPOL (Table), which indicates that superoxide levels are initially lower in eNOS-Tg mice. After infusion of L-NAME, the vasodilation by NAC was the same in WT and eNOS-Tg mice. ET_A/ET_B blockade with tezosentan had minimal effects on SVR in WT and eNOS-Tg mice, either in the absence or in the presence of L-NAME (Figure 6).

Alterations in vasomotor control by other mediators of vasodilation and their end effectors

Blockade of COX with indomethacin or of CYP2C9 with sulfaphenazole had no significant effect on SVR in either WT or eNOS-Tg mice. Adenosine receptor blockade with 8-SPT had no significant effect on SVR (Figure 7). K_{ATP}^+ channel blockade with glibenclamide and K_V^+ channel blockade with 4-AP resulted in marked, but identical, vasoconstriction in WT and eNOS-Tg mice (Figures 7 and 8). In contrast, K_{CA}^+ channel blockade with TEA had no effect in either WT or eNOS-Tg mice (Figure 7).

Discussion

The present study is the first to investigate in detail the regulation of systemic vasomotor control in mice *in vivo* and was designed to investigate alterations in vasomotor control of systemic resistance vessels in mice overexpressing human eNOS.⁴⁷ In these eNOS-Tg mice, eNOS protein expression as well as *in vitro* eNOS activity, were markedly elevated,

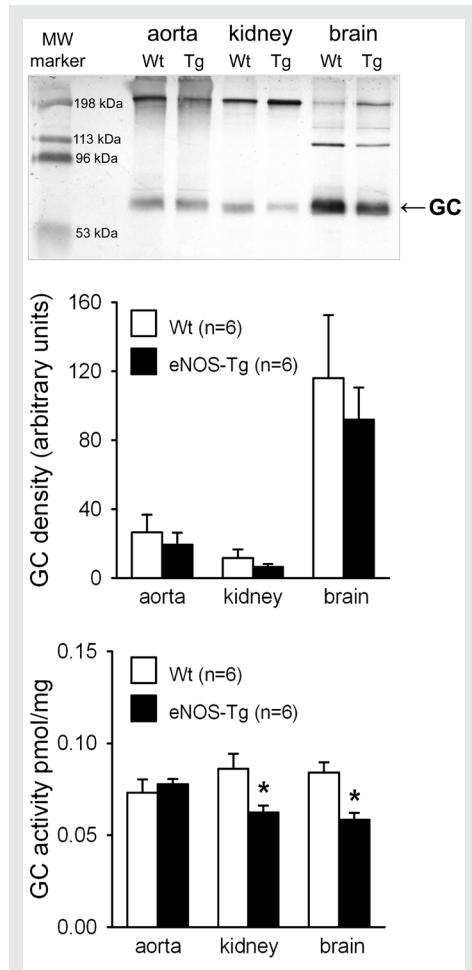


Figure 5. Representative Western blot analysis (top) and densitometry (middle) and enzyme activity measurements (bottom) of guanylyl cyclase (GC) in aorta, kidney, and brain homogenates of WT and eNOS-Tg mice. MW, Molecular weight. * $P \leq 0.05$ vs. corresponding Wt.

Figure 5. Representative Western blot analysis (top) and densitometry (middle) and enzyme activity measurements (bottom) of guanylyl cyclase (GC) in aorta, kidney, and brain homogenates of WT and eNOS-Tg mice (Figure 7).

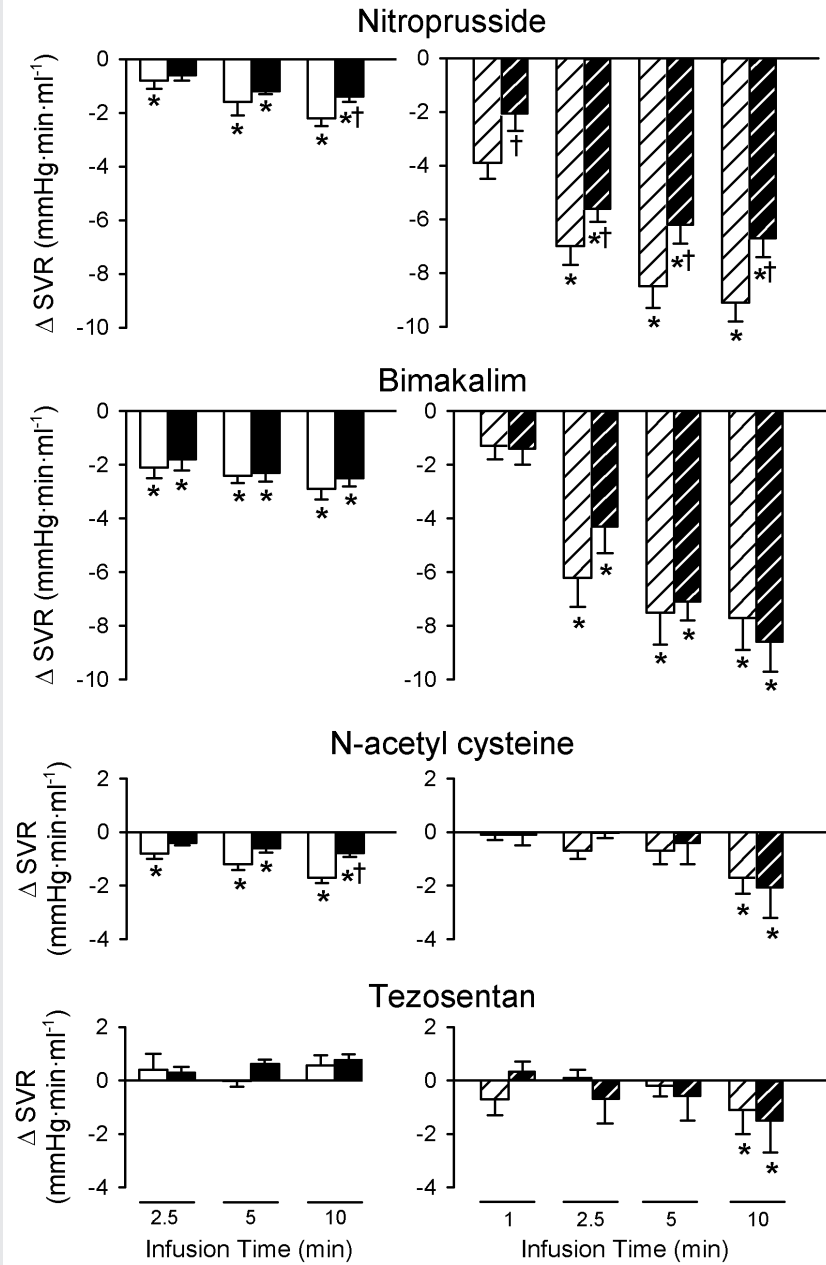


Figure 6. Δ SVR from baseline produced by sodium nitroprusside (SNP), bimakalim, *N*-acetyl cysteine (NAC), and tezosentan in Wt (open bars) and eNOS-Tg mice (solid bars) without L-NAME (nonhatched) and after L-NAME infusion (hatched). * $P \leq 0.05$ vs. corresponding saline (presented in Figure3); † $P \leq 0.05$ vs. change in corresponding Wt.

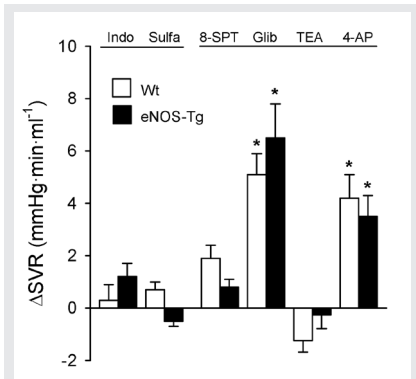


Figure 7. Δ SVR from baseline produced by indomethacin (Indo), sulfaphenazole (Sulfa), 8-5-phenyltheophylline (8-SPT), glibenclamide (Glib), tetraethylammonium chloride (TEA), and 4-aminopyridin (4-AP) in Wt (open bars) and eNOS-Tg mice (solid bars). * $P \leq 0.05$ vs. corresponding saline (presented in Figure 3); no statistically significant differences were found between the effects of the drugs in Wt vs. eNOS-Tg mice.

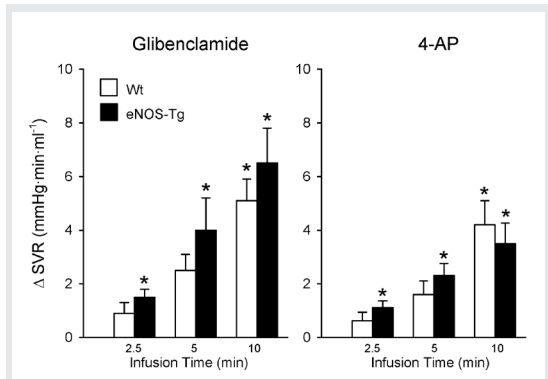


Figure 8. Δ SVR from baseline produced by Glib and 4-AP in Wt (open bars) and eNOS-Tg mice (solid bars). * $P \leq 0.05$ vs. corresponding saline (presented in Figure 3); no statistically significant differences were found between the effects of the drugs in Wt vs. eNOS-Tg mice.

resulting in an eNOS-dependent ~20% decrease in SVR in eNOS-Tg mice. The main findings are that¹ the vasodilator response to exogenous NO was blunted in eNOS-Tg mice, which appeared to occur at the level of GC, and which was corroborated by reduced activity of GC and a trend toward lower GC protein expression;² there was no evidence for increased ROS production [e.g., due to eNOS uncoupling];^{2,3} finally, there were no apparent adaptations in other vasomotor control pathways. The implications of these findings will be discussed below.

Methodological Limitations

The present study was performed in open-chest, isoflurane-anesthetized mice. Isoflurane anesthesia results in heart rate values that approximate values observed in the awake state, suggesting that sympathetic activity under isoflurane anesthesia is similar to that in the awake state.^{6,25,29,52} Conversely, blood pressures in isoflurane-anesthetized, open-chest mice are lower than values typically observed in awake mice.^{6,25,29,52} The latter may have resulted in activation of the renin-angiotensin system,³² thereby influencing systemic vasomotor control and potentially confounding interpretation of the results. However, we previously reported that blood pressure differences between WT and eNOS-Tg mice were present independently of the employed anesthetic regimen,¹⁵ suggesting that any alteration in renin-angiotensin system due to the lower blood pressure affected WT and eNOS-Tg mice in a similar fashion. Therefore, it is unlikely that the differences in vasomotor control between WT and eNOS-Tg mice, as observed in the present study, are due to the lower blood pressures associated with isoflurane anesthesia and open-chest conditions.

In the present study we observed an exaggerated increase of SVR in response to L-NAME in eNOS-Tg compared with WT mice. Although this finding [which confirms previous observations in our laboratory^{27,46,47}] is consistent with the overexpression of eNOS, we cannot entirely exclude that part of the effect of L-NAME is mediated by inhibition of other NOS isoforms. For example, L-NAME could have inhibited central neuronal NOS (nNOS). However, since we have previously shown that the eNOS transgene is selectively overexpressed in endothelial cells,^{46,47} it is unlikely that central nNOS would be different between WT and eNOS-Tg mice. Moreover, blockade of nNOS by L-NAME will result in sympathetic activation,⁴¹ thereby increasing heart rate. In contrast, heart rate did not increase after L-NAME infusion in the present study. Based on these observations, it is unlikely that the different effect of L-NAME on SVR in eNOS-Tg versus WT mice is due to inhibition of nNOS by L-NAME.

4

Alterations in Vasomotor Control by Other Mediators of Vasodilation and Their End Effectors

Control of resistance vessel tone is characterized by a high degree of redundancy. Thus when formation of a particular vasoactive compound is compromised, other vasodilator mechanisms assume greater importance in the regulation of vascular tone and act to compensate.^{11,43} Conversely, when a particular vasodilator influence is increased, other pathways may become downregulated to compensate. For example, NO has been shown to decrease the production of endothelium-derived hyperpolarizing factor⁴ and prostanoids.^{33,38,45} Sulfaphenazole had no effect on SVR in either WT or eNOS-Tg mice, indicating that CYP2C9 metabolites are not essential for the regulation of systemic vascular tone. Indomethacin produced a decrease in blood pressure, which was, however, solely the result of a decrease in aortic blood flow, whereas SVR remained unaffected over the entire infusion period. Although the mechanism of the decrease in aortic flow in the present study in mice remains uncertain, similar results have been reported with the COX inhibitor aspirin in rats.⁴²

Blocking the adenosine receptor or the K_{Ca}^+ channels had no effect on SVR in either WT or eNOS-Tg mice. In contrast, blockade of K_{ATP}^+ and K_V^+ channels demonstrated a robust but similar increase in SVR in WT and eNOS-Tg mice. Taken together, these observations indicate that eNOS overexpression is not compensated by blunted vasodilator influences of prostanoids, CYP2C9 metabolites, adenosine, or by altered K_{ATP}^+ , K_{Ca}^+ , or K_V^+ channel opening.

Alterations in Systemic Vascular NO Signaling

Infusion of the same dose of exogenous NO by administration of the NO donor SNP resulted in a vasodilator response that was smaller in eNOS-Tg mice indicating a reduced vascular sensitivity to NO. Because the effects of inhibiting cGMP breakdown and administering 8-Br-cGMP were similar in WT and eNOS-Tg mice, the signal transduction pathway downstream of cGMP was apparently unaffected by eNOS overexpression. A critical role for sGC in response to alterations in NO bioavailability is also suggested by studies in which pharmacological inhibition of eNOS or knocking out eNOS resulted in enhanced sensitivity to SNP but not to 8-Br-cGMP.^{8,16,22,34}

The reduced effect of SNP in eNOS-Tg mice did not result from the higher amount of NO already present in these mice as the same effect was observed after inhibition of eNOS. Therefore, the reduced responsiveness to NO within the NO pathway could be attributed exclusively to sGC. Indeed, the enzyme activity of GC was lower in eNOS-Tg mice compared with that of WT animals, and also the expression level of GC tended to be smaller in eNOS-Tg mice, which is evidently one of the mechanisms by which eNOS-Tg mice partly compensate for the eNOS overexpression. The observation that the vasodilator response to SNP and enzyme activity of GC was reduced are in partial agreement with the report by Yamashita et al.⁵¹, who described not only a reduced activity of sGC but also of PKG as well as decreased levels of PKG in eNOS-Tg mice. The difference between the outcome of their study and our observations could be explained by differences in experimental design. For example, in our eNOS-Tg mice, we used a cosmid with the human eNOS gene and the native eNOS promoter that contains all the regulatory sequences of eNOS. Yamashita et al.⁵¹ used a murine prepro-endothelin-1 promoter-bovine eNOS cDNA fusion construct that does not include any of the natural regulatory noncoding sequences of eNOS and has a heterologous promoter. Furthermore, some stimuli affect these promoters differently,^{7,31} and NO has been shown to inhibit the expression of the prepro-endothelin-1 gene.¹⁹

Consequently, the different promoters used in the mice of Yamashita et al. and our mice may result in different expression levels of eNOS. Indeed, NOS activity measured *in vitro* in the aorta demonstrated a 1.8-fold increase in enzyme activity in the mice of Yamashita et al.³⁷ and a 10-fold increase in our eNOS-Tg mice.⁴² Perhaps more important is the observation that the experiments by Yamashita et al. were performed *in vitro* on mouse aortic rings. Because the aorta does not contribute to the regulation of SVR, the vasodilator properties of the aorta may well be different from those of the integrated systemic resistance vessels.¹⁷

Interestingly, stimulation of endogenous NO production with ACh produced similar vasodilator responses in WT and eNOS-Tg animals. From the blunted vasodilator response in eNOS-Tg mice to exogenous NO via SNP infusion, it follows that the maintained ACh-induced vasodilation is likely the result of increased ACh-mediated NO production that is counteracted by a reduced sGC responsiveness to NO.

NO signaling is also influenced by the presence of ROS. eNOS overexpression could result in substrate and cofactor depletion, leading to uncoupling of eNOS and production of superoxide instead of NO.^{2,49,50} Superoxide rapidly reacts with NO to form peroxynitrite⁴⁰ thereby reducing NO bioavailability. Moreover, peroxynitrite oxidizes eNOS cofactor BH₄, resulting in further eNOS uncoupling.^{9,30} In addition, superoxide can also increase endothelin levels through either a direct effect⁴⁴ or by upregulation of gene expression,¹⁰ which could blunt the vasodilator effects of eNOS overexpression. Enhanced production of superoxide caused by uncoupling of eNOS has been described in nitrate tolerance³⁵ and could also occur in eNOS-Tg mice in which eNOS expression is increased 10-fold. However, we have previously shown that supplementation of L-arginine to eNOS-Tg mice did not affect aortic blood pressure and SVR,⁴⁷ suggesting that substrate availability is not limited. Furthermore, scavenging of ROS by NAC resulted in a smaller decrease in SVR in eNOS-Tg than in WT mice, suggesting that eNOS-Tg mice have lower rather than higher ROS levels,

possibly as a result of increased superoxide scavenging by NO. Although NAC is known to scavenge ROS other than superoxide,³ the effects of NAC on SVR are likely mediated through superoxide scavenging, because similar observations were made with the SOD mimetic TEMPOL. Finally, our hypothesis that superoxide could exert a vasoconstrictor influence via an increased endothelin vasoconstrictor influence was not supported by our data as the endothelin blocker tezosentan produced similar effects on SVR in eNOS-Tg or WT mice, in both the absence or presence of L-NAME. Taken together these findings fail to provide evidence for eNOS uncoupling and increased superoxide production.

4 There are several other potential mechanisms that could have counteracted the effects of eNOS overexpression. For example, in the endothelial cell, eNOS is targeted into the Golgi complex and the plasma membrane but the individual role of each pool of eNOS is incompletely understood. However, it has been shown that eNOS localized in the Golgi complex or in the plasma membrane is activated by different stimuli.¹⁸ It is therefore possible that the vasodilator effect of eNOS can be influenced by alterations in the subcellular targeting. NO itself can also inhibit NOS activity by forming a ferrous-nitrosyl complex with the heme iron in the NOS enzyme.^{1,20} It is likely that this negative feedback mechanism is increased in eNOS-Tg mice, which produce more NO. Therefore, the markedly elevated eNOS activity, as measured under optimal in vitro conditions, does not necessarily imply that all overexpressed eNOS is functionally active in vivo. Isolated aortas of eNOS transgenic mice showed only a 30% increase in NO release.⁴⁶ Measuring NO directly in the blood of mice in vivo is difficult with the currently available techniques. Alternatively, an indication of NO concentrations could be obtained by measuring the NO metabolite (nitrite and nitrate) levels.^{5,39} Such measurements should be the subject of future studies.

In conclusion, eNOS-overexpressing mice demonstrate a blunted responsiveness to NO, which appears to be, at least in part, due to a reduced responsiveness of sGC. Despite significant redundancy of pathways involved in the regulation of vascular tone, other vasodilator and constrictor pathways were not affected by eNOS overexpression. This feature makes the eNOS-Tg mouse model very reliable for studying the effect of eNOS on the physiology and pathophysiology of the cardiovascular system, without the confounding influence of alterations in other vasomotor control pathways.

Grants

This study was supported by grants from The Netherlands Heart Foundation [2000T038 (to D. J. Duncker) and 2000T042 (to D. Merkus)].

References

1. Abu-Soud HM, Wang J, Rousseau DL, Fukuto JM, Ignarro LJ, Stuehr DJ. *Neuronal nitric oxide synthase self-inactivates by forming a ferrous-nitrosyl complex during aerobic catalysis*. *J Biol Chem* 270: 22997–23006, 1995.
2. Alp NJ, Channon KM. *Regulation of endothelial nitric oxide synthase by tetrahydrobiopterin in vascular disease*. *Arterioscler Thromb Vasc Biol* 24: 413–420, 2004.
3. Aruoma OI, Halliwell B, Hoey BM, Butler J. *The antioxidant action of N-acetylcysteine: its reaction with hydrogen peroxide, hydroxyl radical, superoxide, and hypochlorous acid*. *Free Radic Biol Med* 6: 593–597, 1989.
4. Bauersachs J, Popp R, Hecker M, Sauer E, Fleming I, Busse R. *Nitric oxide attenuates the release of endothelium-derived hyperpolarizing factor*. *Circulation* 94: 3341–3347, 1996.
5. Baylis C, Vallance P. *Measurement of nitrite and nitrate levels in plasma and urine—what does this measure tell us about the activity of the endogenous nitric oxide system?* *Curr Opin Nephrol Hypertens* 7: 59–62, 1998.
6. Bernstein D. *Exercise assessment of transgenic models of human cardiovascular disease*. *Physiol Genomics* 13: 217–226, 2003.
7. Bitzan MM, Wang Y, Lin J, Marsden PA. *Verotoxin and ricin have novel effects on preproendothelin-1 expression but fail to modify nitric oxide synthase (ecNOS) expression and NO production in vascular endothelium*. *J Clin Invest* 101: 372–382, 1998.
8. Brandes RP, Kim D, Schmitz-Winnenthal FH, Amidi M, Godecke A, Mulsch A, Busse R. *Increased nitrovasodilator sensitivity in endothelial nitric oxide synthase knockout mice: role of soluble guanylyl cyclase*. *Hypertension* 35: 231–236, 2000.
9. Cai H, Harrison DG. *Endothelial dysfunction in cardiovascular diseases: the role of oxidant stress*. *Circ Res* 87: 840–844, 2000.
10. Cheng TH, Shih NL, Chen SY, Loh SH, Cheng PY, Tsai CS, Liu SH, Wang DL, Chen JJ. *Reactive oxygen species mediate cyclic strain-induced endothelin-1 gene expression via Ras/Raf/extracellular signal-regulated kinase pathway in endothelial cells*. *J Mol Cell Cardiol* 33: 1805–1814, 2001.
11. Clifford PS, Hellsten Y. *Vasodilatory mechanisms in contracting skeletal muscle*. *J Appl Physiol* 97: 393–403, 2004.
12. De Crom R, van Haperen R, Janssens R, Visser P, Willemsen R, Grosveld F, van der Kamp A. *Gp96/GRP94 is a putative high density lipoprotein-binding protein in liver*. *Biochim Biophys Acta* 1437: 378–392, 1999.
13. Ding Z, Godecke A, Schrader J. *Contribution of cytochrome P450 metabolites to bradykinin-induced vasodilation in endothelial NO synthase deficient mouse hearts*. *Br J Pharmacol* 135: 631–638, 2002.
14. Drummond GR, Harrison DG. *eNOS-overexpressing mice: too much NO makes the blood pressure low*. *J Clin Invest* 102: 2033–2034, 1998.
15. Duncker DJ, van Haperen R, van Deel E, de Waard M, Mees B, de Crom R. *Endothelial nitric oxide synthase in cardiovascular homeostasis and disease*. In: *The Physiological Genomics of the Critically Ill Mouse*, edited by Ince C. Dordrecht/Boston/London: Kluwer Academic, 2004, p. 291–310.
16. Faraci FM, Sigmund CD, Shesely EG, Maeda N, Heistad DD. *Responses of carotid artery in mice deficient in expression of the gene for endothelial NO synthase*. *Am J Physiol Heart Circ Physiol* 274: H564–H570, 1998.
17. Freitas MR, Schott C, Corriu C, Sassard J, Stoclet JC, Andriantsitohaina R. *Heterogeneity of endothelium-dependent vasorelaxation in conductance and resistance arteries from Lyon normotensive and hypertensive rats*. *J Hypertens* 21: 1505–1512, 2003.
18. Fulton D, Babbitt R, Zoellner S, Fontana J, Acevedo L, McCabe TJ, Iwakiri Y, Sessa WC. *Targeting of endothelial nitric-oxide synthase to the cytoplasmic face of the Golgi complex or plasma membrane regulates Akt- versus calcium-dependent mechanisms for nitric oxide release*. *J Biol Chem* 279: 30349–30357, 2004.
19. Galie N, Manes A, Branzi A. *The endothelin system in pulmonary arterial hypertension*. *Cardiovasc Res* 61: 227–237, 2004.
20. Griscavage JM, Fukuto JM, Komori Y, Ignarro LJ. *Nitric oxide inhibits neuronal nitric oxide synthase by interacting with the heme prosthetic group. Role of tetrahydrobiopterin in modulating the inhibitory action of nitric oxide*. *J Biol Chem* 269: 21644–21649, 1994.
21. Houweling B, Merkus D, Dekker MM, Duncker DJ. *Nitric oxide blunts the endothelin-mediated pulmonary vasoconstriction in exercising swine*. *J Physiol* 568: 629–638, 2005.
22. Hussain MB, Hobbs AJ, MacAllister RJ. *Autoregulation of nitric oxide-soluble guanylate cyclase-cyclic GMP*

- signalling in mouse thoracic aorta. *Br J Pharmacol* 128: 1082–1088, 1999.
23. Ignarro LJ, Cirino G, Casini A, Napoli C. *Nitric oxide as a signaling molecule in the vascular system: an overview.* *J Cardiovasc Pharmacol* 34: 879–886, 1999.
 24. Ishibashi Y, Duncker DJ, Zhang J, Bache RJ. *ATP-sensitive K⁺ channels, adenosine, and nitric oxide-mediated mechanisms account for coronary vasodilation during exercise.* *Circ Res* 82: 346–359, 1998.
 25. Janssen BJ, De Celle T, Debets JJ, Brouns AE, Callahan MF, Smith TL. *Effects of anesthetics on systemic hemodynamics in mice.* *Am J Physiol Heart Circ Physiol* 287: H1618–H1624, 2004.
 26. Jones SP, Greer JJ, Kakkar AK, Ware PD, Turnage RH, Hicks M, van Haperen R, de Crom R, Kawashima S, Yokoyama M, Lefer DJ. *Endothelial nitric oxide synthase overexpression attenuates myocardial reperfusion injury.* *Am J Physiol Heart Circ Physiol* 286: H276–H282, 2004.
 27. Jones SP, Greer JJ, van Haperen R, Duncker DJ, de Crom R, Lefer DJ. *Endothelial nitric oxide synthase overexpression attenuates congestive heart failure in mice.* *Proc Natl Acad Sci USA* 100: 4891–4896, 2003.
 28. Kostic MM, Schrader J. *Role of nitric oxide in reactive hyperemia of the guinea pig heart.* *Circ Res* 70: 208–212, 1992.
 29. Kramer K, Voss HP, Grimbergen JA, Mills PA, Huetteman D, Zwiers L, Brockway B. *Telemetric monitoring of blood pressure in freely moving mice: a preliminary study.* *Lab Anim Sci* 34: 272–280, 2000.
 30. Landmesser U, Dikalov S, Price SR, McCann L, Fukai T, Holland SM, Mitch WE, Harrison DG. *Oxidation of tetrahydrobiopterin leads to uncoupling of endothelial cell nitric oxide synthase in hypertension.* *J Clin Invest* 111: 1201–1209, 2003.
 31. Le Cras TD, Tyler RC, Horan MP, Morris KG, McMurty IF, Johns RA, Abman SH. *Effects of chronic hypoxia and altered hemodynamics on endothelial nitric oxide synthase and preendothelin-1 expression in the adult rat lung.* *Chest* 114: 355–365, 1998.
 32. Lum C, Shesely EG, Potter DL, Beierwaltes WH. *Cardiovascular and renal phenotype in mice with one or two renin genes.* *Hypertension* 43: 79–86, 2004.
 33. Merkus D, Houweling B, Zarbanoui A, Duncker DJ. *Interaction between prostanoids and nitric oxide in regulation of systemic, pulmonary, and coronary vascular tone in exercising swine.* *Am J Physiol Heart Circ Physiol* 286: H1114–H1123, 2004.
 34. Moncada S, Rees DD, Schulz R, Palmer RM. *Development and mechanism of a specific supersensitivity to nitrovasodilators after inhibition of vascular nitric oxide synthesis in vivo.* *Proc Natl Acad Sci USA* 88: 2166–2170, 1991.
 35. Munzel T, Li H, Mollnau H, Hink U, Matheis E, Hartmann M, Oelze M, Skatchkov M, Warnholtz A, Duncker L, Meinertz T, Forstermann U. *Effects of long-term nitroglycerin treatment on endothelial nitric oxide synthase (NOS III) gene expression, NOS III-mediated superoxide production, and vascular NO bioavailability.* *Circ Res* 86: E7–E12, 2000.
 36. Nishikawa Y, Stepp DW, Chilian WM. *Nitric oxide exerts feedback inhibition on EDHF-induced coronary arteriolar dilation in vivo.* *Am J Physiol Heart Circ Physiol* 279: H459–H465, 2000.
 37. Ozaki M, Kawashima S, Yamashita T, Hirase T, Namiki M, Inoue N, Hirata K, Yasui H, Sakurai H, Yoshida Y, Masada M, Yokoyama M. *Overexpression of endothelial nitric oxide synthase accelerates atherosclerotic lesion formation in apoE-deficient mice.* *J Clin Invest* 110: 331–340, 2002.
 38. Puybasset L, Bea ML, Ghaleh B, Giudicelli JF, Berdeaux A. *Coronary and systemic hemodynamic effects of sustained inhibition of nitric oxide synthesis in conscious dogs. Evidence for cross talk between nitric oxide and cyclooxygenase in coronary vessels.* *Circ Res* 79: 343–357, 1996.
 39. Rosselli M, Imthurn B, Keller PJ, Jackson EK, Dubey RK. *Circulating nitric oxide (nitrite/nitrate) levels in postmenopausal women substituted with 17 beta-estradiol and norethisterone acetate. A two-year follow-up study.* *Hypertension* 25: 848–853, 1995.
 40. Rubio AR, Morales-Segura MA. *Nitric oxide, an iceberg in cardiovascular physiology: far beyond vessel tone control.* *Arch Med Res* 35: 1–11, 2004.
 41. Sartori C, Lepori M, Scherrer U. *Interaction between nitric oxide and the cholinergic and sympathetic nervous system in cardiovascular control in humans.* *Pharmacol Ther* 106: 209–220, 2005.
 42. Schoemaker RG, Saxena PR, Kalkman EA. *Low-dose aspirin improves in vivo hemodynamics in conscious, chronically infarcted rats.* *Cardiovasc Res* 37: 108–114, 1998.
 43. Scotland RS, Madhani M, Chauhan S, Moncada S, Andresen J, Nilsson H, Hobbs AJ, Ahluwalia A. *Investigation of vascular responses in endothelial nitric oxide synthase/cyclooxygenase-1 double-knockout mice: key role for endothelium-derived hyperpolarizing factor in the regulation of blood pressure in vivo.*

- Circulation 111: 796–803, 2005.
44. Sethi AS, Lees DM, Douthwaite JA, Dawnay AB, Corder R. *Homocysteine-induced endothelin-1 release is dependent on hyperglycaemia and reactive oxygen species production in bovine aortic endothelial cells.* J Vasc Res 43: 175–183, 2006.
 45. Sun D, Huang A, Smith CJ, Stackpole CJ, Connetta JA, Shesely EG, Koller A, Kaley G. *Enhanced release of prostaglandins contributes to flow-induced arteriolar dilation in eNOS knockout mice.* Circ Res 85: 288–293, 1999.
 46. Van Haperen R, Cheng C, Mees BM, van Deel E, de Waard M, van Damme LC, van Gent T, van Aken T, Krams R, Duncker DJ, de Crom R. *Functional expression of endothelial nitric oxide synthase fused to green fluorescent protein in transgenic mice.* Am J Pathol 163: 1677–1686, 2003.
 47. Van Haperen R, De Waard M, Van Deel E, Mees B, Kutryk M, Van Aken T, Hamming J, Grosveld F, Duncker DJ, De Crom R. *Reduction of blood pressure, plasma cholesterol, and atherosclerosis by elevated endothelial nitric oxide.* J Biol Chem 277: 48803–48807, 2002.
 48. Vanhoutte PM. *Endothelial control of vasomotor function: from health to coronary disease.* Circulation 67: 572–575, 2003.
 49. Werner ER, Gorren AC, Heller R, Werner-Felmayer G, Mayer B. *Tetrahydrobiopterin and nitric oxide: mechanistic and pharmacological aspects.* Exp Biol Med (Maywood) 228: 1291–1302, 2003.
 50. Xia Y, Tsai AL, Berka V, Zweier JL. *Superoxide generation from endothelial nitric-oxide synthase. A Ca²⁺/calmodulin-dependent and tetrahydrobiopterin regulatory process.* J Biol Chem 273: 25804–25808, 1998.
 51. Yamashita T, Kawashima S, Ohashi Y, Ozaki M, Rikitake Y, Inoue N, Hirata K, Akita H, Yokoyama M. *Mechanisms of reduced nitric oxide/cGMP-mediated vasorelaxation in transgenic mice overexpressing endothelial nitric oxide synthase.* Hypertension 36: 97–102, 2000.
 52. Zuurbier CJ, Emons VM, Ince C. *Hemodynamics of anesthetized ventilated mouse models: aspects of anesthetics, fluid support, and strain.* Am J Physiol Heart Circ Physiol 282: H2099–H2105, 2002.



Exercise Training does not
Improve Cardiac Function in
Compensated or Decompensated
Left Ventricular Hypertrophy
Induced by Aortic Stenosis

5

Elza D. van Deel, Martine de Boer, Diederik W. Kuster,
Nicky M. Boontje, Patricia Holemans, Karin R. Sipido,
Jolanda van der Velden, Dirk J. Duncker

Journal of Molecular and Cellular Cardiology

2011; 50(6):1017-1025

Abstract

There is ample evidence that regular exercise exerts beneficial effects on left ventricular (LV) hypertrophy, remodeling and dysfunction produced by ischemic heart disease or systemic hypertension. In contrast, the effects of exercise on pathological LV hypertrophy and dysfunction produced by LV outflow obstruction have not been studied to date. Consequently, we evaluated the effects of 8 weeks of voluntary wheel running in mice (which mitigates post-infarct LV dysfunction) on LV hypertrophy and dysfunction produced by mild (mTAC) and severe (sTAC) transverse aortic constriction. mTAC produced ~40% LV hypertrophy and increased myocardial expression of hypertrophy marker genes but did not affect LV function, SERCA2a protein levels, apoptosis or capillary density. Exercise had no effect on global LV hypertrophy and function in mTAC but increased interstitial collagen, and ANP expression. sTAC produced ~ 80% LV hypertrophy and further increased ANP expression and interstitial fibrosis and, in contrast with mTAC, also produced LV dilation, systolic as well as diastolic dysfunction, pulmonary congestion, apoptosis and capillary rarefaction and decreased SERCA2a and ryanodine receptor (RyR) protein levels. LV diastolic dysfunction was likely aggravated by elevated passive isometric force and Ca²⁺-sensitivity of myofilaments. Exercise training failed to mitigate the sTAC-induced LV hypertrophy and capillary rarefaction or the decreases in SERCA2a and RyR. Exercise attenuated the sTAC-induced increase in passive isometric force but did not affect myofilament Ca²⁺-sensitivity and tended to aggravate interstitial fibrosis. In conclusion, exercise had no effect on LV function in compensated and decompensated cardiac hypertrophy produced by LV outflow obstruction, suggesting that the effect of exercise on pathologic LV hypertrophy and dysfunction depends critically on the underlying cause.

Introduction

Myocardial hypertrophy is a compensatory mechanism by which the left ventricle (LV) adapts to an increased systolic load, which serves to restore LV wall stress to normal levels and maintain cardiac pump function.^{1,2} Clinically, chronic systolic overload of the LV most commonly results from regional loss of myocardial tissue (myocardial infarction) or elevated impedance to LV outflow (hypertension and aortic stenosis).^{3,4} Despite the apparent appropriateness of hypertrophic remodeling in response to an increased systolic workload, LV hypertrophy has been shown to be an independent risk factor for the development of angina pectoris, congestive heart failure and sudden death.^{1,5} In contrast, hypertrophy produced by exercise training is not associated with the contractile dysfunction and perfusion abnormalities described for pressure-overload⁶ or post-infarction induced hypertrophy⁷ and reduces, rather than increases, the risk for developing heart failure.⁵

There is ample evidence from both clinical and experimental studies that aerobic exercise training has a beneficial effect on cardiac function and remodeling in case of ischemic cardiomyopathy.⁸⁻¹⁰ Similarly, the majority of experimental studies in genetic models of systemic hypertension¹¹⁻¹³ have shown a beneficial effect of regular exercise on cardiac remodeling and function, which is supported by recent clinical studies.^{14,15} In contrast, little is known about the effects of exercise on LV pressure-overload hypertrophy as a result of mechanical obstruction to outflow. This is important because there is an increasing number of patients with (congenital) aortic stenosis that are chronically exposed to LV pressure-overload and which will ultimately require surgery during their adult life.¹⁶ The effects of regular physical exercise in such patients may well be different from that in patients with cardiac hypertrophy due to systemic hypertension. Thus the presence of an aortic stenosis results in exaggerated LV pressure responses to exercise thereby producing aggravated increases in afterload during each exercise bout,⁶ which contrasts with the relatively normal LV hemodynamic responses to exercise in case of systemic hypertension.¹⁷ It is therefore possible that exercise training in case of a chronic aortic stenosis does not recapitulate the beneficial effects that are observed in ischemic heart disease or systemic hypertension.

In light of these considerations, we investigated the effects of dynamic exercise training on aortic stenosis induced LV hypertrophy and dysfunction. For this purpose, we employed 8 weeks of voluntary wheel running, an exercise protocol which we have previously shown to blunt LV dysfunction in mice with a myocardial infarction (MI).⁹ Since the effects of exercise training might depend on the severity of the aortic stenosis, we assessed the effects of exercise in mice subjected to either mild or severe aortic stenosis.

Methods

All experiments were performed in accordance with the "Guiding Principles in the Care

and Use of Animals” as approved by the Council of the American Physiological Society and with prior approval of the Animal Care Committee of the Erasmus MC Rotterdam. A total of 134 C57Bl/6 mice (26 ± 0.4 g) of 20 weeks of age entered the study.

Experimental procedure

All mice were weighed, sedated with 4% isoflurane, intubated and connected to a pressure-controlled ventilator (SAR-830/P; CWE), set at 90 breaths/min with a peak inspiratory pressure of 18 cm H₂O and a positive end expiratory pressure of 4 cm H₂O.^{9,18} A gas mixture of O₂/N₂ (v/v = 1/2) containing 2.5% isoflurane was used to maintain anesthesia. Body temperature was kept at 37 °C and buprenorphine (50 µg/kg) was injected s.c. for postsurgical analgesia. Thoracotomy was performed through the first intercostal space and the aorta was constricted with a 7-0 silk suture, between the truncus brachiocephalicus and the arteria carotis communis sinistra.¹⁹ A 25 G needle was used to induce mild TAC (mTAC) (n = 29) and a 27 G needle (n = 64) to induce severe TAC (sTAC). In pilot experiments we observed that mTAC (n = 7) and sTAC (n = 7) resulted in acute systolic pressure gradients of 37 ± 3 and 57 ± 4 mm Hg respectively. The sham (SH) procedure was performed identically but without the aortic ligation (n = 41). Immediately following surgery, 13 mTAC, 29 sTAC and 21 SH animals were exposed to voluntary wheel running.

Eight weeks after surgery, the mice were again anesthetized with isoflurane and ventilated as outlined above. Aortic pressure distal to the stenosis was measured through a PE10 catheter in the left carotid artery. A 1.4-Fr microtipped manometer (Millar Instruments; Houston, Texas, USA) was inserted in the right carotid artery to record aortic pressure proximal to the stenosis and subsequently advanced into the LV to measure LV pressure (LVP). 2-D guided M-mode echocardiography was performed with an Aloka SSD 4000 echo device (Aloka; Tokyo, Japan) using a 12-MHz probe.

Data analyses

Echocardiography data were stored for later analysis. LV end-diastolic diameter (LVEDD), LV end-systolic diameter (LVESD) and LV wall thickness were measured from the M-mode images.^{9,18} Fractional shortening was calculated from short axes M-mode images as $100\% \times (\text{LVEDD} - \text{LVESD}) / \text{LVEDD}$. Hemodynamic data were digitized (400 Hz/channel) on-line and processed using a data-acquisition program (ATCODAS, Dataq Instruments, Akron, OH) and stored on a computer for off-line analysis with a program written in MatLab (Mathworks, Natick, MA). Series of beats were collected to determine the mean and systolic aortic pressure, heart rate, LV end-diastolic pressure (LVEDP), LV peak systolic pressure, the maximum rate of rise (LV dP/dt_{\max}) and fall (LV dP/dt_{\min}) of LV pressure, and the rate of rise of LV pressure at a pressure of 40 mm Hg (LV dP/dt_{p40}). The time constant of LV pressure decay (tau), was computed from the equation $\text{LVP}(t) = \text{LVP}_0 \cdot e^{-t/\text{tau}}$ in which $\text{LVP}_0 = \text{LVP at } dP/dt_{\min}$, using data points between LVP_0 and $\text{LVP at LVEDP} + 5 \text{ mm Hg}$.²⁰ Pressure–diameter relations were constructed by synchronizing the echocardiography M-mode data and LV pressure, using ECG.^{9,18} LV stress was calculated as $(\text{LVP} \times 0.5 \text{ LV diameter}) / (2 \times \text{LV wall thickness})$ and diastolic elastance was determined by fitting LVP and LV diameter during the filling phase of the LV in between the minimal LVP and LVEDP. Data from several consecutive beats were averaged.

Tissue preparation

At the end of each experiment the heart was excised for histological and molecular biological analysis and LV, right ventricle (RV), wet and dry lung weights and tibia length (TL) were determined.

Histomorphometry

Paraffin embedded LV tissue was serially sectioned into 4- μ m slices. Masson's trichrome staining was performed to measure cardiomyocyte cross-sectional area (CSA). Apoptosis was determined via a TUNEL assay (Roche) and lectin staining was used to calculate capillary density. Collagen content was measured using Picro Sirius Red staining. Total collagen was determined from bright field images. Relative contents of type I and III collagens were determined using linear polarization microscopy.²¹ LV sections of 6 mice per group were analyzed with a quantitative image analysis system (Clemex Technologies).

RNA preparation and quantitative real-time PCR analysis

RNA was extracted from 6 frozen LV samples per group using a Qiagen fibrous tissue RNA kit. cDNA was synthesized from 100 ng of total RNA with iScript Reverse Transcriptase (Bio-Rad). Quantitative real-time PCR (MyIQ, Bio-Rad) was performed with SYBR Green (Bio-Rad). PCR primers for myocardial hypertrophy marker genes atrial natriuretic peptide (ANP), brain natriuretic peptide (BNP) and α -skeletal actin (α -SKA) were employed. Target gene mRNA levels were expressed relative to the housekeeping gene hypoxanthine guanine phosphoribosyl transferase (HPRT) as an endogenous control.

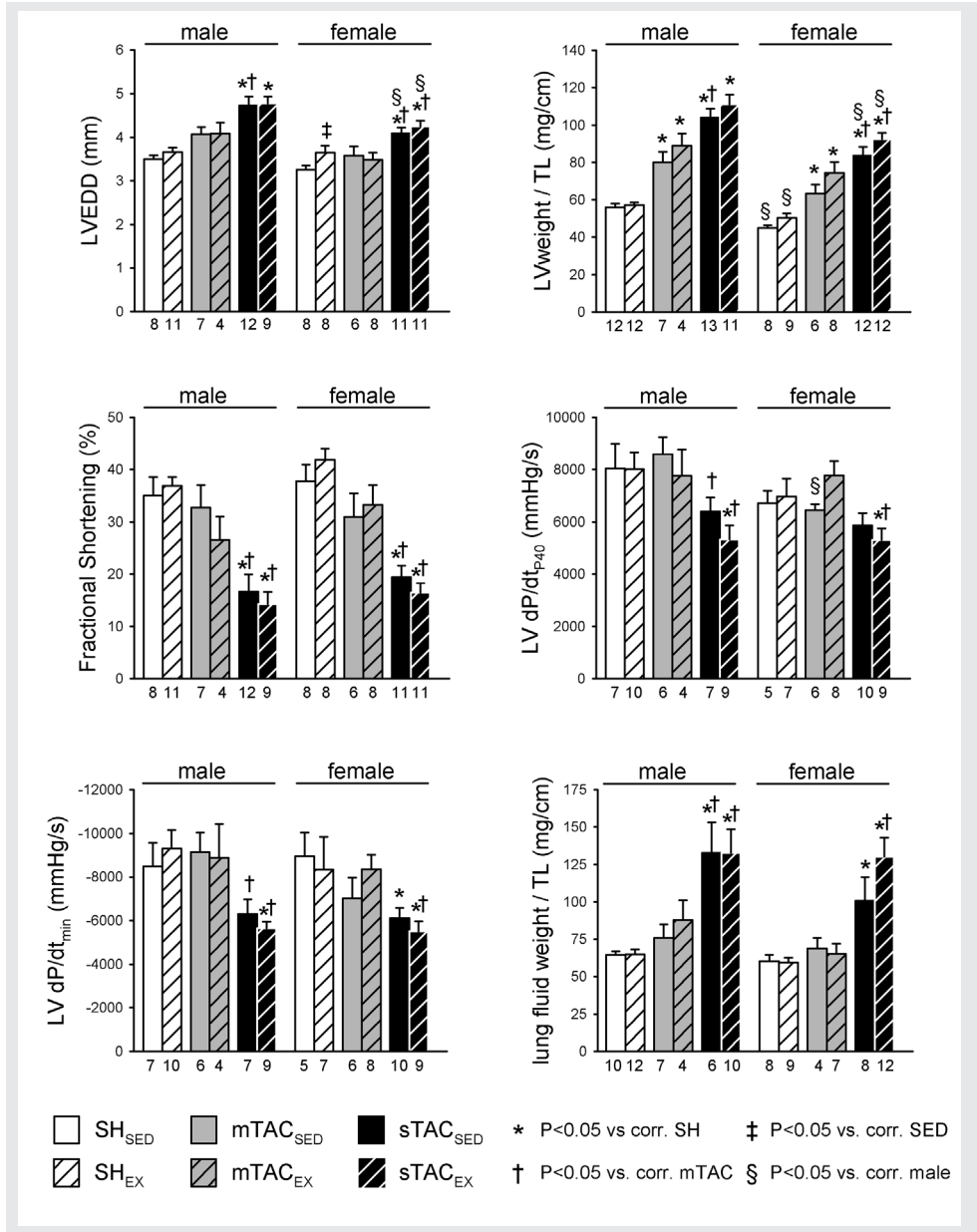
Western blotting

Four frozen LV tissue homogenates per group were used for immunoblotting of sarco-endoplasmic reticulum Ca^{2+} -ATPase (SERCA2a) and phospholamban (PLB) levels, as previously described⁹ and normalized to GAPDH. Immunoblotting for the $\text{Na}^+/\text{Ca}^{2+}$ exchanger (NCX) (1/1000, Swant, Bellinzona, Switzerland) and the ryanodine receptor (RyR) (1/500, Affinity BioReagents, Golden, USA) was performed in SH_{SED} , STAC_{SED} and STAC_{EX} mice in 6 frozen LV tissue samples per group.²²

Myofilament function

Cells from 6 LV sections per group (2–4 cells per section) were mechanically isolated and incubated for 5-min in relaxing solution supplemented with 0.5% Triton X-100 to remove all membranes. Thereafter, the cells were washed twice in the relaxing solution and a single cardiomyocyte was attached between a force transducer and a piezoelectric motor using silicone adhesive.^{9,23} All force values were normalized for cardiomyocyte CSA. On transfer of the cardiomyocyte from relaxing to activating solution, isometric force started to develop. Once a steady-state force level was reached, the cell was shortened within 1 ms to 80% of its original length to determine the baseline of the force transducer. The difference between the baseline and the steady force level represents the total isometric force (F_{total}). After 20 ms the cell was re-stretched and returned to the relaxing solution, in which a second slack-test of 10 second duration was performed to determine resting or passive force (F_{pas}). Maximal calcium activated tension (F_{max}) was calculated as the difference between F_{total} at saturating $[\text{Ca}^{2+}]$ ($\text{pCa}4.5$) and F_{pas} . Force measurements were

repeated after incubation with the catalytic subunit of protein kinase A (PKA) (100 U/ml, batch 12K7495; Sigma, Brooklyn, NY) and 6 mmol/L dithiothreitol (MP Biochemicals, Irvine, CA). Control incubations in relaxing solution with 6 mmol/L dithiothreitol, but without PKA, did not alter force characteristics of cardiomyocytes.



Statistical analysis

All data were tested using 2-way (exercise \times stenosis) ANOVA followed by post-hoc testing with a Student–Newman–Keuls test. A value of $P \leq 0.05$ was considered statistically significant (two-tailed). Data are presented as means \pm SEM.

All groups contained similar numbers of male and female mice. We tested for sex differences and consistently found across all groups that females were characterized by a $\sim 30\%$ lower body weight and a $\sim 3\%$ lower tibia length, while in SH mice the relative LV and RV weights were $\sim 20\%$ lower in female mice compared to males (all $P < 0.05$). Although sex differences are frequently reported in the literature,²⁴ using 3-way ANOVA (sex \cdot exercise \cdot stenosis) we did not observe an influence of sex on the effects of TAC and/or exercise on the survival, LV dysfunction (fractional shortening, LV dp/dt_{p40} , LV dp/dt_{min} and pulmonary congestion) or LV remodeling (LVEDD and LV weight/TL) (Figure 1). Similarly, no consistent sex influences were found with respect to the histological and biochemical markers or myofilament function. Consequently, we pooled male and female mice for final analysis.

Results

Exercise and survival

All mice in the exercise groups started to run on the first day after surgery with daily running distance progressively increasing over the first 2 weeks after surgery (Figure 2). $sTAC_{EX}$ mice ran a total distance (276 ± 38 km over 8-weeks) that was significantly less than that in SH_{EX} (432 ± 37 km) and $mTAC_{EX}$ (409 ± 42 km) mice. $mTAC_{SED}$ and $sTAC_{SED}$ were associated with mortality rates of 19% and 29%, respectively. Voluntary wheel running tended to improve survival but this failed to reach levels of statistical significance ($P = 0.08$ for $mTAC$).

Cardiac geometry and function

Eight weeks of $mTAC_{SED}$ or $sTAC_{SED}$ had no effect on body weight or tibia length, but produced stenosis severity dependent LV hypertrophy, reflected in an

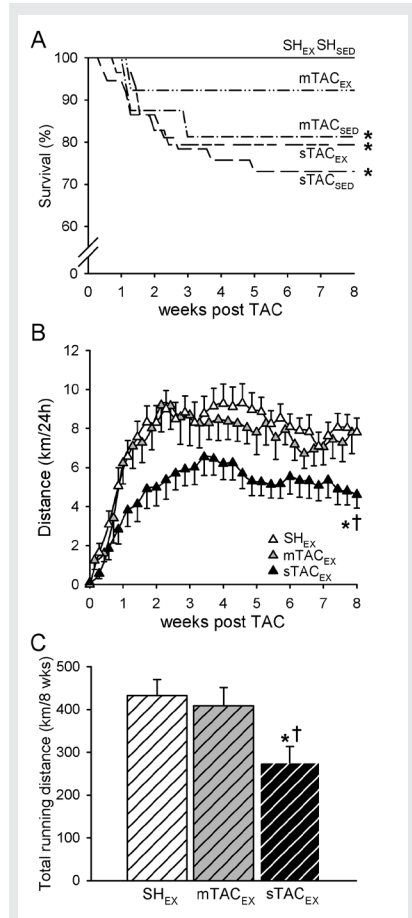


Figure 2. (A) Kaplan–Meier survival curve for all groups. (B) Daily running distance in TAC and SH mice that survived the entire 8-week follow-up period. (C) Total distance ran over 8 weeks. * $P < 0.05$ vs corresponding SH; † $P < 0.05$ vs corresponding $mTAC$.

Total number of sedentary and exercised animals entering the study: SH_{SED} ($n=20$), SH_{EX} ($n=21$), $mTAC_{SED}$ ($n=16$), $mTAC_{EX}$ ($n=13$), $sTAC_{SED}$ ($n=35$) and $sTAC_{EX}$ ($n=29$).

Table 1: Anatomical data

		Sedentary	Exercise
Body weight (g)	SH	27.3 ± 1.2	25.2 ± 0.9
	mTAC	25.5 ± 1.0	24.5 ± 1.2
	sTAC	26.3 ± 1.1	25.7 ± 0.8
Tibia length (cm)	SH	1.84 ± 0.01	1.83 ± 0.01
	mTAC	1.85 ± 0.01	1.83 ± 0.01
	sTAC	1.87 ± 0.02	1.84 ± 0.01
LV weight (mg)	SH	95 ± 4	100 ± 3
	mTAC	133 ± 8 *	146 ± 9 *
	sTAC	177 ± 7 *†	187 ± 7 *†
RV weight (mg)	SH	24 ± 1	22 ± 1
	mTAC	23 ± 1	25 ± 2
	sTAC	34 ± 2 *†	37 ± 2 *†
Lung fluid weight (mg)	SH	115 ± 5	115 ± 4
	mTAC	135 ± 12	134 ± 14
	sTAC	211 ± 24 *†	231 ± 20 *†
LV weight / tibia length (mg/cm)	SH	51.6 ± 1.8	54.2 ± 1.5
	mTAC	72.2 ± 4.4 *	79.4 ± 4.6 *
	sTAC	94.3 ± 3.8 *†	101.5 ± 3.5 *†
LV weight /body weight (mg/g)	SH	3.5 ± 0.1	4.0 ± 0.1 ‡
	mTAC	5.3 ± 0.3 *	6.0 ± 0.3 *
	sTAC	6.9 ± 0.4 *†	7.3 ± 0.2 *†

SH_{SED} (n=20), SH_{EX} (n=21), mTAC_{SED} (n=13), mTAC_{EX} (n=12), sTAC_{SED} (n=25), sTAC_{EX} (n=23). *P<0.05 vs corresponding SH; †P<0.05 vs corresponding mTAC; ‡P<0.05 vs corresponding SED.

increase in relative LV weight of 40% in mTAC and 86% in sTAC (Table 1, Figure 3). In mTAC_{SED} mice, indices of systolic function (fractional shortening and LV dP/dt_{p40}) and early (tau and LV dP/dt_{min}) as well as late (LVEDP and late diastolic elastance) diastolic function were well maintained but end systolic and end diastolic stress where both increased (Figure 3). Furthermore, there was no sign of pulmonary congestion or secondary RV hypertrophy (Figure 3). Conversely, sTAC_{SED} was associated with LV dilation, systolic and early as well as late diastolic dysfunction, severe pulmonary congestion and RV hypertrophy. Inspection of LV pressure-diameter relations in Figure 4 shows that sTAC_{SED} demonstrated significant outward remodeling and reduced capacity to generate high LV systolic pressures. This notion is supported by the observation that the peak systolic pressure gradient across the stenosis decreased from 57 ± 4 mm Hg immediately after sTAC to 49 ± 4 mm Hg after 8 weeks, which was no longer different from that observed in the mTAC_{SED} mice at 8 weeks (40 ± 5 mm Hg).

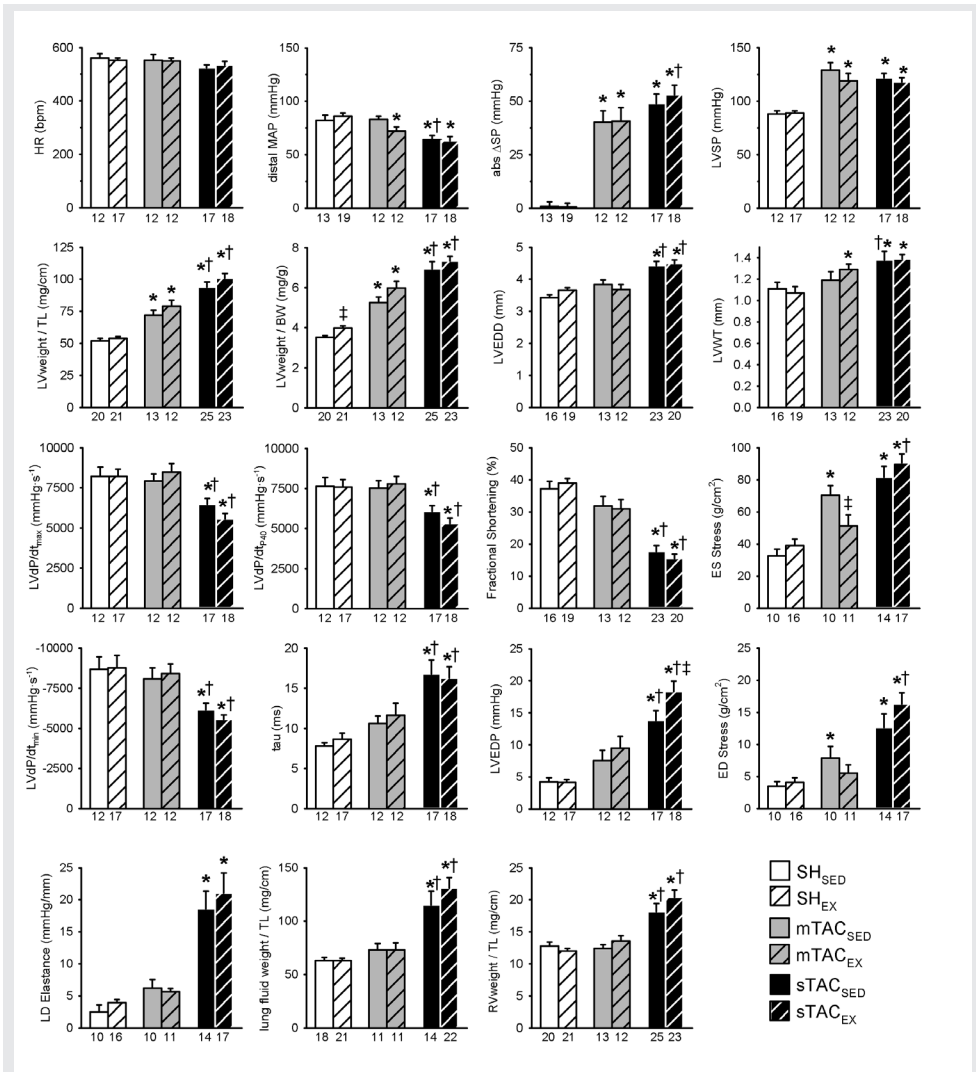


Figure 3. Effect of TAC and exercise on LV mass and geometry, hemodynamic parameters, RV mass and lung fluid weight (lung wet weight minus lung dry weight). HR, heart rate; MAP, mean aortic pressure; abs ΔSP, absolute systolic pressure gradient over the stenosis; LVSP, LV systolic pressure; BW, body weight; LVWT, LV wall thickness; ES, end systolic; ED, end diastolic; LD elastance, late diastolic elastance. *P < 0.05 vs corresponding SH; † P < 0.05 vs corresponding mTAC; ‡ P < 0.05 vs corresponding sedentary group. The number of animals is indicated below each bar.

Exercise in SH, mTAC or sTAC mice had no effect on absolute or relative LV weight, normalized to tibia length. Only when LV weight was normalized to body weight, were small increases observed, which reached statistical significance in SH mice. Global LV function was not affected by exercise in either SH or mTAC mice. Conversely, in sTAC mice exercise tended to aggravate LV dysfunction and pulmonary congestion, which reached statistical significance only for the further elevation of LVEDP (Figures 3 and 4).

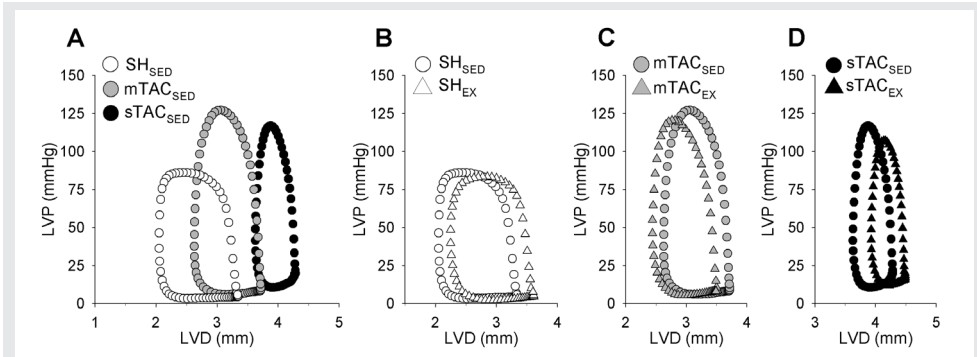


Figure 4. LV pressure–diameter relations of sedentary Sham, mTAC and sTAC mice (panel A) illustrating the progression of LV dilation and dysfunction with increased severity of stenosis and LV pressure–diameter relations comparing sedentary and exercised Sham animals (panel B), mTAC (panel C) and sTAC mice (panel D) demonstrating the effect of exercise. SH_{SED} n = 10, SH_{EX} n = 16, mTAC_{SED} n = 10, mTAC_{EX} n = 11, sTAC_{SED} n = 14, sTAC_{EX} n = 17.

5

Myocardial morphology

mTAC and sTAC produced load-dependent increases in cardiomyocyte CSA, apoptosis and fibrosis and decreases in capillary densities (Figure 5). The relative amount of type I vs type III collagen was higher in mTAC and sTAC (I/III ratio: 4.4 ± 0.8 in mTAC_{SED} and 6.9 ± 2.6 in sTAC_{SED}) than in SH_{SED} (1.7 ± 0.5 ; Figure 6).

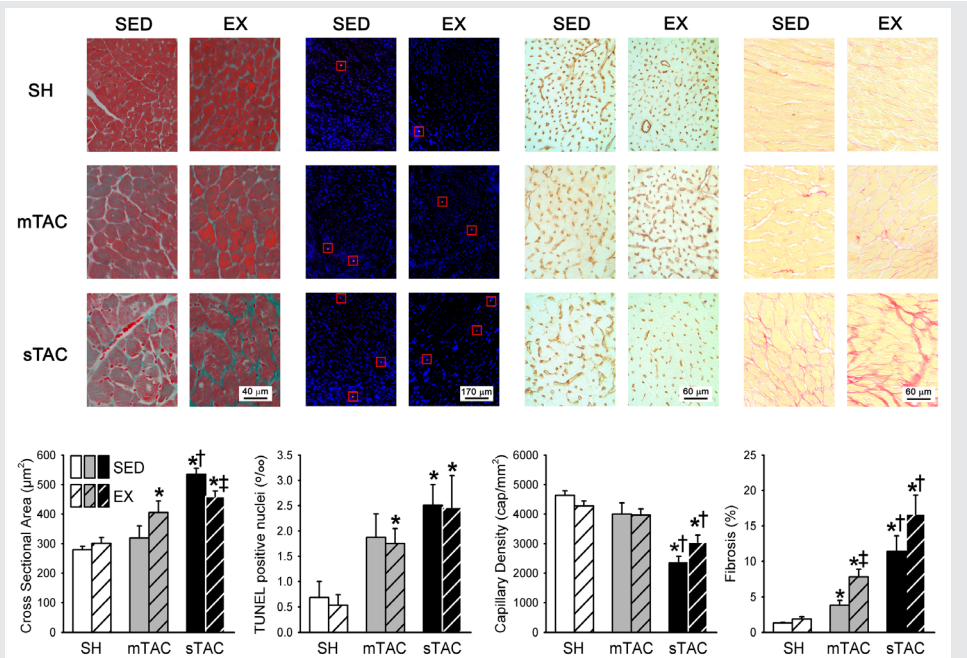
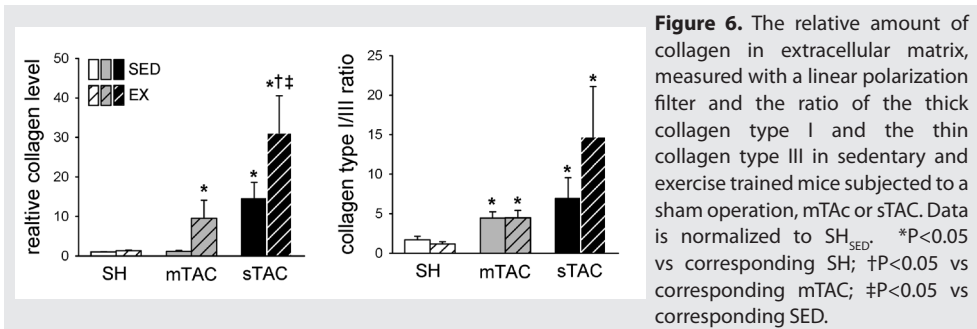


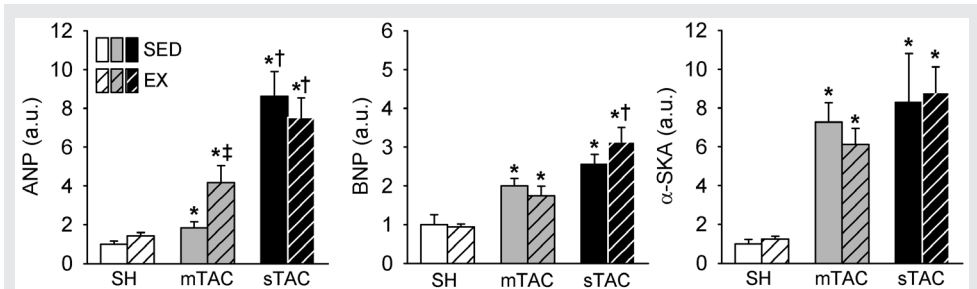
Figure 5. Histological analyses of the effect of TAC and exercise on cardiomyocyte cross sectional area, apoptosis, capillary density and fibrosis in sedentary and exercise trained mice. (n = 6 mice in all groups). *P < 0.05 vs corresponding SH; † P < 0.05 vs corresponding mTAC; ‡ P < 0.05 vs corresponding SED.



Exercise increased interstitial fibrosis in mTAC. In sTAC exercise blunted the increase in cardiomyocyte CSA but had no effect on apoptosis or capillary density. Although it did not reach statistical significance, there was a strong trend towards increased fibrosis with exercise in sTAC, which was predominantly due to higher levels of collagen type I vs type III in sTAC_{EX} (I/III ratio: 1.2 ± 0.3 in SH_{EX}, 4.5 ± 1.0 in mTAC_{EX} and 14.7 ± 6.4 in sTAC_{EX}).

Expression of hypertrophy markers

Expression of the hypertrophy markers ANP, BNP and α -SKA was elevated in mTAC_{SED} mice (Figure 7). sTAC resulted in a significant further increase in expression of ANP but not BNP or α -SKA. Exercise had no effect on expression of hypertrophy markers with the exception of ANP expression in mTAC mice which was slightly further increased by exercise.



SERCA2a, PLB, NCX and RyR protein expression

Protein levels of SERCA2a and PLB were not different in mTAC_{SED} compared to SH_{SED} mice, but were lower in sTAC_{SED} mice (Figure 8(A)). The ratio of SERCA2a and PLB was not significantly changed by TAC (data not shown). Because of the lack of significant dysfunction as well as the lack of effect on protein levels of SERCA2a and PLB in mTAC mice we elected to include only sTAC samples for the evaluation of NCX and RyR. sTAC reduced RyR protein content, compared to SH_{SED} but unexpectedly did not affect NCX protein levels (Figure 8(A)). Exercise had no effect on SERCA2a, PLB, NCX or RyR, in any of the experimental groups.

Cardiac myofilament function

Since there was no sign of contractile dysfunction in mTAC mice, we elected to explore alterations in myofilament function produced by TAC and the effects of exercise training thereupon in SH and sTAC mice only. Both F_{\max} and F_{pas} were elevated in sTAC_{SED} compared to SH_{SED} mice (Figure 8(B)). In addition, the force-pCa curves demonstrated a leftward shift in sTAC_{SED} animals, reflecting a higher myofilament Ca^{2+} -sensitivity (pCa_{50}). Interestingly, treatment with the catalytic subunit of PKA produced similar decreases in pCa_{50} in SH_{SED} and sTAC_{SED} mice.

Exercise in sTAC was associated with a slight reduction in F_{pas} , but had no effect on F_{\max} in either SH or sTAC mice (Figure 8(B)). Similarly, exercise did not affect myofilament Ca^{2+} -sensitivity.

PKA produced small increases in F_{\max} in all four groups (all $P < 0.05$ except SH_{SED}), but had no effect on F_{pas} in any group (data not shown).

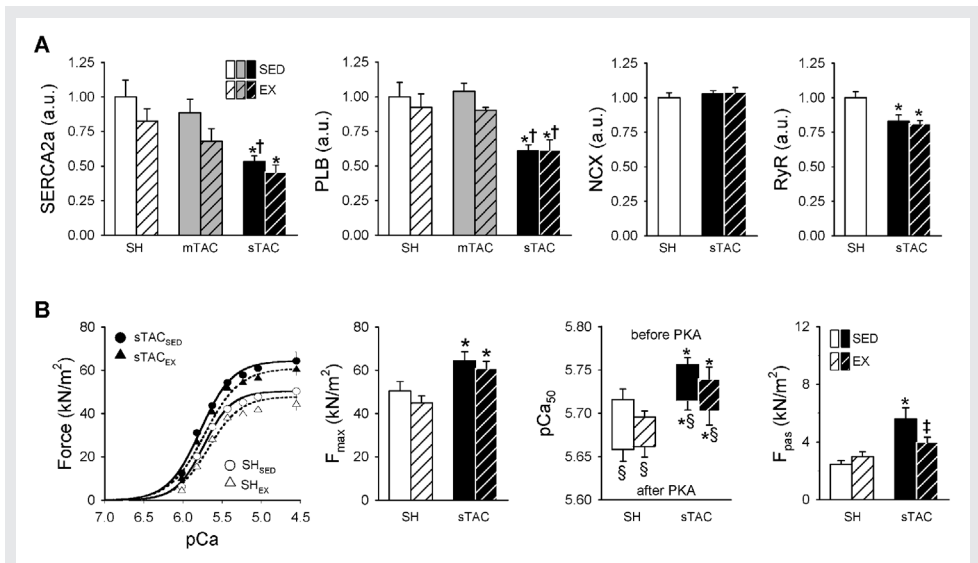


Figure 8. Calcium handling proteins and myofilament function. (A) Effect of TAC and exercise on protein levels of sarco-endoplasmic reticulum Ca^{2+} -ATPase (SERCA2a) ($n = 4$), its inhibitory protein phospholamban (PLB) ($n = 4$), the sodium calcium channel (NCX) ($n = 6$) and the ryanodine receptor (RyR) ($n = 6$). (B) Effect of TAC and exercise on myofilament force characteristics. Maximal force (F_{\max}), Ca^{2+} -sensitivity (pCa_{50}) of force before (top means) and after (bottom means) incubation with PKA and passive force (F_{pas}) were measured in 13–18 LV cardiomyocytes per group (6 mice per group; 2–4 LV cardiomyocytes per mouse). * $P < 0.05$ vs corresponding SH; † $P < 0.05$ vs corresponding mTAC; ‡ $P < 0.05$ vs corresponding SED; § $P < 0.05$ vs corresponding pCa_{50} before PKA.

Discussion

In this study we investigated the effect of 8 weeks of voluntary wheel running on pressure-overload-induced LV hypertrophy and dysfunction produced by two degrees

of TAC in mice. The main findings were that: (i) mTAC resulted in ~ 40% LV hypertrophy and elevated levels of hypertrophy marker genes and mild fibrosis, but did not result in LV dysfunction, reduced SERCA levels, or decreased capillary density; (ii) exercise had no effect on global LV dysfunction but increased interstitial fibrosis, and ANP levels in mTAC; (iii) sTAC resulted in ~ 80% LV hypertrophy and further increased myocardial fibrosis and expression levels of ANP compared to mTAC, but also produced LV systolic and diastolic dysfunction, LV dilation, pulmonary congestion, apoptosis and capillary rarefaction and reduced SERCA2a and RyR levels. Furthermore, sTAC altered myofilament function by increasing maximal and passive isometric force as well as myofilament Ca^{2+} -sensitivity; (iv) exercise training in sTAC failed to mitigate LV hypertrophy, dilation and dysfunction, restore SERCA2a and RyR levels, or normalize apoptosis, capillary density, fibrosis or myofilament Ca^{2+} -sensitivity.

Pressure-overload induced alterations

The mouse model of severe transverse aortic constriction has been extensively employed to study pressure-overload induced cardiac hypertrophy and dysfunction.^{19,25,26} In agreement with previous reports, we found that sTAC resulted in LV remodeling, characterized by marked LV hypertrophy, capillary rarefaction and interstitial fibrosis. In addition, we observed LV systolic dysfunction, characterized by a decrease in fractional shortening and LV $\text{dP}/\text{dt}_{\text{p40}}$ as well as LV diastolic dysfunction, characterized by reduced LV $\text{dP}/\text{dt}_{\text{min}}$ and increases in tau and LVEDP. The latter was associated with pulmonary congestion reflected in pulmonary edema and secondary RV hypertrophy. In contrast, mTAC resulted in only ~ 40% LV hypertrophy that was not associated with LV systolic or diastolic dysfunction, reflecting a state of compensated hypertrophy. Those observations are in good agreement with previous studies that reported minimal changes in LV systolic function up to 9 weeks after mTAC^{25,27} while sTAC showed marked loss of function already after 3 weeks.²⁷

Previously we showed in swine²⁸ and mice⁹ with a recent MI that myofilament dysfunction, characterized by a decrease in F_{max} and an increase in Ca^{2+} -sensitivity, of remote surviving myocardium, is a likely contributor to global LV dysfunction. To assess whether alterations in myofilament function similarly contribute to the LV systolic and diastolic dysfunction observed in sTAC mice, we analyzed steady state calcium-force relations in isolated cardiomyocytes. In contrast to the lower F_{max} in post-MI remodeled myocardium, sTAC-induced hypertrophied myocardium was characterized by a slightly elevated F_{max} , which would act to increase rather than decrease systolic force development. Similarly, the elevated pCa_{50} , which was not due to reduced PKA activity, would act to increase systolic function. These findings suggest that the increased myofilament F_{max} and pCa_{50} may actually represent adaptive responses to cope with increased systolic loading conditions, but also indicate that factors other than myofilament responsiveness to calcium are responsible for the observed LV systolic dysfunction. One such factor could be perturbed Ca^{2+} handling. A reduction in peak Ca^{2+} amplitude and Ca^{2+} transient decay velocity would be expected on the basis of the lower SERCA2a and RyR protein content in sTAC mice compared to sham, respectively. Indeed, experimental studies show a clear slowing of the Ca^{2+} transient decay in TAC,^{27,29,30} but only one study reported a decrease in peak Ca^{2+}

transient amplitude,²⁹ while transient amplitudes were reported to be maintained in two other studies^{27,30} The observation that end-systolic stress was markedly elevated in the sTAC mice suggests that elevated cardiomyocyte afterload may also have contributed to the systolic dysfunction observed in sTAC. The exact mechanism of LV systolic dysfunction in sTAC should be the subject of future studies.

Another prominent feature of sTAC was the presence of significant diastolic dysfunction, characterized by slowed relaxation (lower LV dP/dt_{min} and increased tau) and elevated LV filling pressures. The slower relaxation has been attributed to slowing of the Ca^{2+} transient decay^{27,29,30} likely as a result of the lower SERCA2a protein content²⁷ and the present study) or calcium leak from the sarcoplasmic reticulum through “leaky” RyR during diastole³¹ The present study shows for the first time that an increased myofilament Ca^{2+} -sensitivity may also contribute to the impaired LV relaxation in TAC mice. The present study also shows for the first time that besides interstitial fibrosis and increased LV wall thickness, an increase in F_{pas} possibly in conjunction with the increase in pCa_{50} , may contribute to the increased LV end-diastolic pressure in pressure-overload hypertrophy. This is also supported by previous observations in our laboratory in post-MI remodeled myocardium, in which F_{pas} levels were not elevated, coinciding with marginal elevations in LV end-diastolic pressure (Figure 9).⁹ In contrast to our observations in post-MI remodeled myocardium,⁹ PKA did not reduce Ca^{2+} -sensitivity in sTAC_{SED} to values observed in SH_{SED}. This implies that the increase in myofilament Ca^{2+} -sensitivity was not the result of reduced PKA-mediated phosphorylation of myofilament proteins, including cardiac troponin I (cTnI). Conversely, the expression of the β -isoform of protein kinase C is increased in heart failure,³² which can increase Ca^{2+} -sensitivity through phosphorylation of cTnI at the threonine-144 site.³³ Alternatively, an increase in protein phosphatase 1 expression³⁴ and re-expression of atrial light chain 1³⁵ and fetal troponin T³⁶ could also contribute to increase myofilament Ca^{2+} -

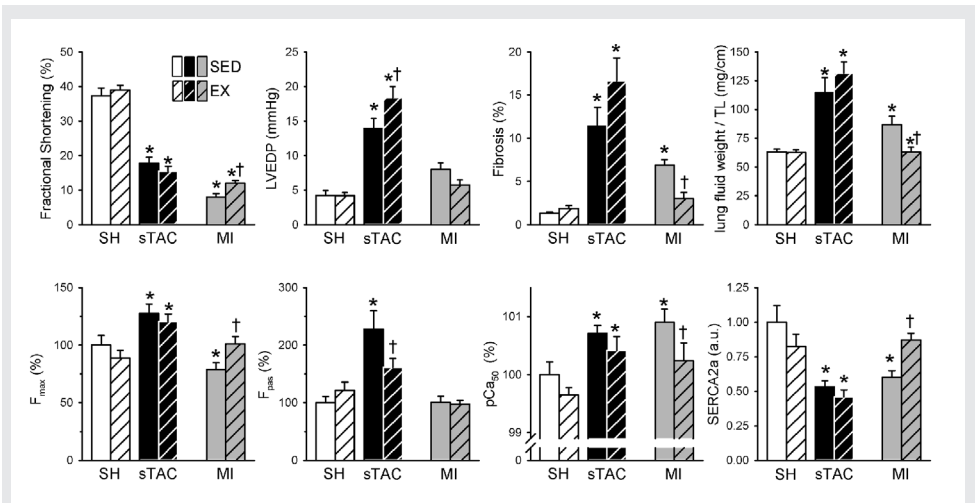


Figure 9. Comparative data on the effect of exercise on cardiac function and geometry after sTAC (present study) and MI (historical data from de Waard et al.)^{9,18} Data on myofilament function are normalized to corresponding SH_{SED}. *P < 0.05 vs corresponding SH; † P < 0.05 vs corresponding SED.

sensitivity in pressure-overloaded hearts. Increased myofilament Ca^{2+} -sensitivity is likely the resultant of several combined protein changes,^{23,36} and future studies are needed to unravel the molecular mechanisms underlying the increased myofilament Ca^{2+} -sensitivity in pressure-overload hypertrophy.

Effects of exercise on pressure-overload LV hypertrophy

Both clinical and experimental studies indicate that dynamic exercise training has a beneficial effect on function and remodeling of hearts with ischemic cardiomyopathy.⁸⁻¹⁰ Similarly, the majority of experimental studies in genetic models of systemic hypertension¹¹⁻¹³ as well as some recent clinical studies,^{14,15} generally point towards a beneficial effect of regular exercise on cardiac hypertrophy and function, although one study reported a negative effect of excessive long-term exercise in spontaneously hypertensive female rats.³⁷

Since life expectancy is increasing in the Western society and the prevalence of aortic stenosis increases with age, the number of patients suffering from pressure-overload-induced cardiac hypertrophy due to aortic stenosis is inevitably growing.³⁸ It is therefore imperative to investigate new therapies for the prevention and treatment of cardiac dysfunction in these patients. So far the potentially beneficial effects of exercise on cardiac function and hypertrophy have been insufficiently examined in this group of patients. Several studies recommended patients with pressure-overload hypertrophy to participate only in mild physical training^{39,40} to minimize the increase in workload to the heart during exercise, but solid clinical evidence for such guidelines is lacking. The present study is the first to investigate the effects of dynamic exercise on LV pressure-overload hypertrophy produced by mechanical obstruction to LV outflow. Since the effects of regular exercise might well depend on the severity of the aortic obstruction, we investigated the effects of exercise on mild as well as severe TAC. We employed a type of exercise which we previously showed to exert a beneficial effect on post-MI remodeling and dysfunction (Figure 9).⁹ The results of the present study contrast with the beneficial effects of exercise on LV hypertrophy and dysfunction reported for ischemic,¹⁰ systemic hypertensive^{14,15} and hypertrophic⁴¹ cardiomyopathy. Experimental studies in Dahl salt-sensitive or spontaneously hypertensive rats, have generally shown beneficial effects of regular treadmill exercise^{11,12} or swimming^{13,42} on cardiac function, fibrosis, the expression of hypertrophy marker genes and survival although not on LV hypertrophy per se. In contrast, Schulz et al.³⁷ reported that excessive long-term (up to 16 months) wheel running aggravated cardiac hypertrophy and dysfunction, fibrosis and expression of hypertrophy marker genes in spontaneously hypertensive female rats. In the present study, eight weeks of voluntary wheel running had no significant effect on LV hypertrophy and remodeling in either mTAC or sTAC mice. In contrast, while LV function was well maintained in mTAC_{EX}, a trend towards aggravated LV dysfunction and backward failure was apparent in sTAC_{EX} mice. These effects of exercise in sTAC mice could not be explained by alterations in myofilament function, as F_{max} and pCa_{50} were not altered. Interestingly, a decrease in F_{pas} was noted, which was however not associated with a reduction in LV end-diastolic pressure. The latter may, at least in part, be related to an increase in collagen I content in the sTAC_{EX} mice, which may have offset the exercise-induced lowering of

passive cardiomyocyte stiffness. Survival rate was not significantly altered by exercise training but tended to improve with exercise in mTAC and sTAC mice. This trend towards an improved survival with exercise without improvements in LV function is in agreement with another rodent study of pressure-overload hypertrophy¹¹ and indicates that exercise could potentially improve survival in models of pressure-overload hypertrophy without beneficial effects on LV function.

An explanation for the lack of a beneficial effect is not readily found. However, it should be noted that the effects of exercise training on the development of LV dysfunction and hypertrophy depend at least in part on the mode, frequency and intensity of exercise.^{10,37} For example, dynamic exercise, which exposes the heart to a volume-overload reverses LV remodeling and improves cardiac function in patients with heart failure.^{10,43} In contrast, when static and dynamic exercises are combined (resulting in more pronounced increases in systemic pressure) the beneficial effects of physical training are no longer observed.¹⁰ Since dynamic exercise in the presence of an aortic stenosis will result in exaggerated increases in LV systolic pressures⁶ this will likely add a pronounced static component to the exercise response. It is thus possible that the excessive increase in LV systolic workload that occurs in response to acute exercise may have offset the positive effects of the 8-week voluntary wheel running protocol, which we previously observed in mice with a MI.⁹ Since we have previously shown that eNOS overexpression in part mimics the beneficial effects of exercise training in mice with MI^{18,44} it will be of interest to evaluate the effects of eNOS overexpression (i.e. the beneficial molecular effects of exercise, but without the hemodynamic overload) on LV hypertrophy and dysfunction in sTAC mice in future studies.

5

Methodological considerations

There are several methodological aspects that may have impacted the results of the present study. First, we employed acute TAC as an experimental model to produce LV pressure-overload, which contrasts with the clinical pressure-overload syndromes, including aortic stenosis and hypertension, that typically develop gradually over a longer period of time. Furthermore, the effects of exercise training on LV function in hypertension are mediated in part via modification of peripheral impedance, which obviously is fixed in the case of aortic constriction. Second, the severity of LV hypertrophy and dysfunction in response to TAC depends on the genetic background,⁴⁵ and we cannot exclude that a similar dependency also exists for the cardiac effects of exercise training following TAC. Third, the effects of exercise may well depend on the type and severity of training. Since C57Bl/6 mice perform very well in voluntary wheel running (in contrast to their poor performance during forced treadmill running),⁴⁶ we subjected our C57Bl/6 mice to voluntary wheel running. Unfortunately, this prevented us to evaluate various exercise intensities, so that we cannot exclude that higher exercise intensities might have resulted in significant effects on LV hypertrophy and function in TAC mice. Importantly, we have previously shown in mice with the same genetic background and using the same voluntary wheel running protocol as employed in the present study, that exercise training mitigated LV dysfunction, fibrosis and pulmonary congestion following MI (Figure 9). These findings indicate that the lack of effect of exercise training in TAC mice is not simply the result of

the genetic background in conjunction with the type of exercise stimulus.

Conclusions

The results of the present study demonstrated that voluntary wheel running failed to improve LV function in mice with either compensated or decompensated pressure-overload LV hypertrophy produced by TAC. Moreover, in severely banded mice, exercise even tended to aggravate global cardiac dysfunction and pulmonary congestion, which contrasts the mitigating effects of voluntary wheel running on LV dysfunction and pulmonary congestion in mice with MI.^{9,18} Taken together, these results indicate that the effects of exercise training on pathologic LV hypertrophy and dysfunction depend critically on the underlying pathology.

Acknowledgment

We gratefully acknowledge the financial support by the Netherlands Heart Foundation (2007B024 and 2005B234) and Erasmus MC (Translational Grant).

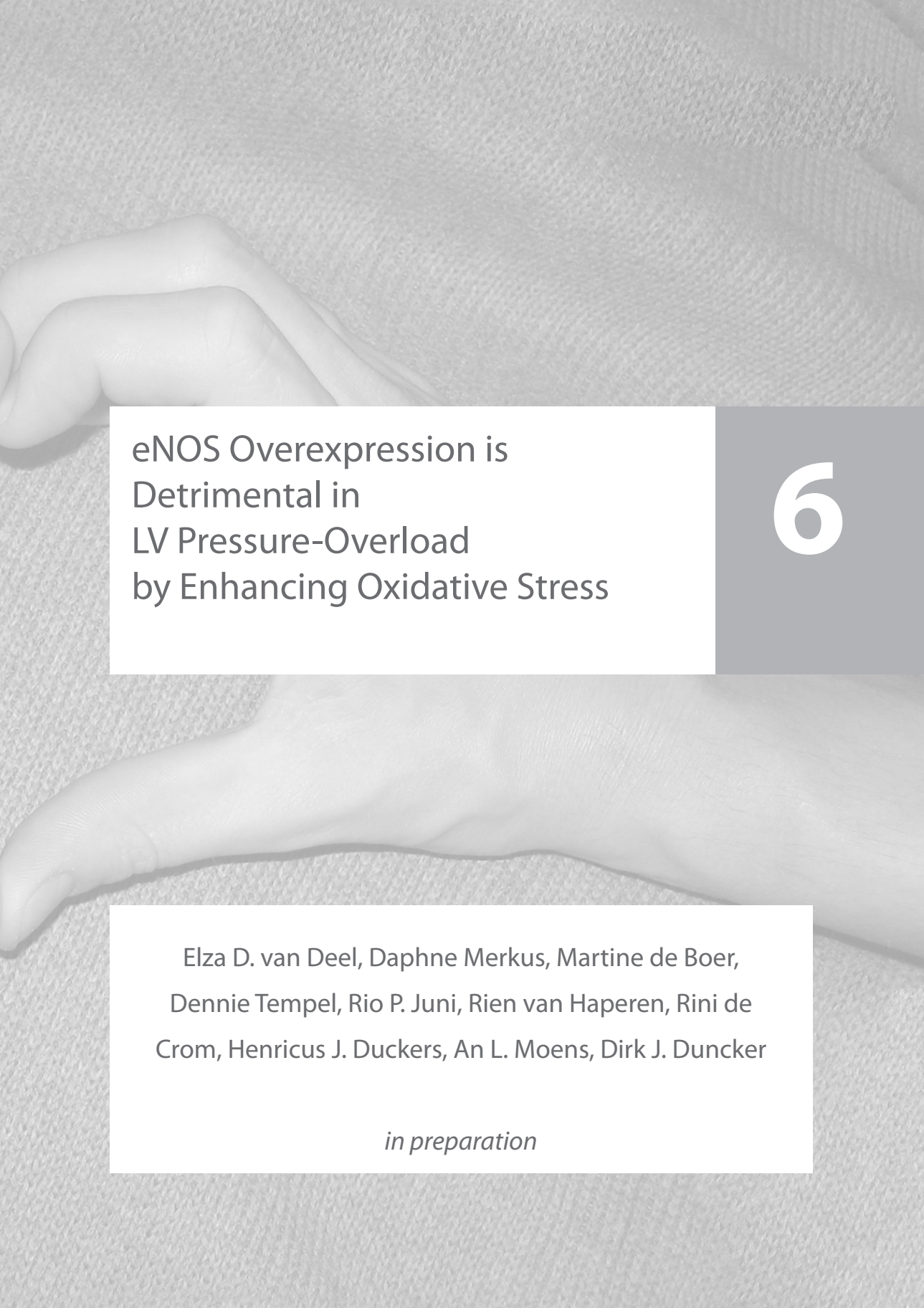
References

1. N. Frey, H.A. Katus, E.N. Olson and J.A. Hill, *Hypertrophy of the heart: a new therapeutic target?*. *Circulation*, 109 (2004), pp. 1580–1589.
2. W. Grossman, D. Jones and L.P. McLaurin, *Wall stress and patterns of hypertrophy in the human left ventricle*. *J Clin Invest*, 56 (1975), pp. 56–64.
3. J. Heineke and J.D. Molkentin, *Regulation of cardiac hypertrophy by intracellular signalling pathways*. *Nat Rev Mol Cell Biol*, 7 (2006), pp. 589–600.
4. L.H. Opie, P.J. Commerford, B.J. Gersh and M.A. Pfeffer, *Controversies in ventricular remodelling*. *Lancet*, 367 (2006), pp. 356–367.
5. J.R. McMullen and G.L. Jennings, *Differences between pathological and physiological cardiac hypertrophy: novel therapeutic strategies to treat heart failure*. *Clin Exp Pharmacol Physiol*, 34 (2007), pp. 255–262.
6. D.J. Duncker, J. Zhang, T.J. Pavik, M.J. Crampton and R.J. Bache, *Effect of exercise on coronary pressure–flow relationship in hypertrophied left ventricle*. *Am J Physiol*, 269 (1995), pp. H271–H281.
7. D.J. Duncker, V.J. de Beer and D. Merkus, *Alterations in vasomotor control of coronary resistance vessels in remodelled myocardium of swine with a recent myocardial infarction*. *Med Biol Eng Comput*, 46 (2008), pp. 485–497.
8. E. Crimi, L.J. Ignarro, F. Cacciatore and C. Napoli, *Mechanisms by which exercise training benefits patients with heart failure*. *Nat Rev Cardiol*, 6 (2009), pp. 292–300.
9. M.C. de Waard, J. van der Velden, V. Bito, S. Ozdemir, L. Biesmans and N.M. Boontje, et al. *Early exercise training normalizes myofilament function and attenuates left ventricular pump dysfunction in mice with a large myocardial infarction*. *Circ Res*, 100 (2007), pp. 1079–1088.
10. M.J. Haykowsky, Y. Liang, D. Pechter, L.W. Jones, F.A. McAlister and A.M. Clark, *A meta-analysis of the effect of exercise training on left ventricular remodeling in heart failure patients: the benefit depends on the type of training performed*. *J Am Coll Cardiol*, 49 (2007), pp. 2329–2336.
11. A.J. Chicco, S.A. McCune, C.A. Emter, G.C. Sparagna, M.L. Rees and D.A. Bolden, et al. *Low-intensity exercise training delays heart failure and improves survival in female hypertensive heart failure rats*. *Hypertension*, 51 (2008), pp. 1096–1102.
12. S.M. MacDonnell, H. Kubo, D.L. Crabbe, B.F. Renna, P.O. Reger and J. Mohara, et al. *Improved myocardial beta-adrenergic responsiveness and signaling with exercise training in hypertension*. *Circulation*, 111 (2005), pp. 3420–3428.
13. M. Miyachi, H. Yazawa, M. Furukawa, K. Tsuboi, M. Ohtake and T. Nishizawa, et al. *Exercise training alters left ventricular geometry and attenuates heart failure in Dahl salt-sensitive hypertensive rats*. *Hypertension*, 53 (2009), pp. 701–707.
14. K. Boman, E. Gerdts, K. Wachtell, B. Dahlöf, M.S. Nieminen and M. Olofsson, et al. *Exercise and cardiovascular outcomes in hypertensive patients in relation to structure and function of left ventricular hypertrophy: the LIFE study*. *Eur J Cardiovasc Prev Rehabil*, 16 (2009), pp. 242–248.
15. P. Palatini, P. Visentin, F. Dorigatti, C. Guarnieri, M. Santonastaso and S. Cozzio, et al. *Regular physical activity prevents development of left ventricular hypertrophy in hypertension*. *Eur Heart J*, 30 (2009), pp. 225–232.
16. S.C. Yap, J.J. Takkenberg, M. Witsenburg, F.J. Meijboom and J.W. Roos-Hesslink, *Aortic stenosis at young adult age*. *Expert Rev Cardiovasc Ther*, 3 (2005), pp. 1087–1098.
17. A. Amery, S. Julius, L.S. Whitlock and J. Conway, *Influence of hypertension on the hemodynamic response to exercise*. *Circulation*, 36 (1967), pp. 231–237.
18. M.C. de Waard, J. van der Velden, N.M. Boontje, D.H. Dekkers, R. van Haperen and D.W. Kuster, et al. *Detrimental effect of combined exercise training and eNOS overexpression on cardiac function after myocardial infarction*. *Am J Physiol Heart Circ Physiol*, 296 (2009), pp. H1513–H1523.
19. H.A. Rockman, R.S. Ross, A.N. Harris, K.U. Knowlton, M.E. Steinhilper and L.J. Field, et al. *Segregation of atrial-specific and inducible expression of an atrial natriuretic factor transgene in an in vivo murine model of cardiac hypertrophy*. *Proc Natl Acad Sci USA*, 88 (1991), pp. 8277–8281.
20. P.S. Pagel, J.P. Kampine, W.T. Schmeling and D.C. Wartier, *Alteration of left ventricular diastolic function by desflurane, isoflurane, and halothane in the chronically instrumented dog with autonomic nervous system blockade*. *Anesthesiology*, 74 (1991), pp. 1103–1114.
21. L.C. Junqueira, W. Cossermelli and R. Brentani, *Differential staining of collagens type I, II and III by Sirius Red*

- and polarization microscopy. Arch Histol Jpn, 41 (1978), pp. 267–274.
22. I. Lenaerts, V. Bito, F.R. Heinzel, R.B. Driesen, P. Holemans and J. D'Hooge, et al. *Ultrastructural and functional remodeling of the coupling between Ca²⁺ influx and sarcoplasmic reticulum Ca²⁺ release in right atrial myocytes from experimental persistent atrial fibrillation.* Circ Res, 105 (2009), pp. 876–885.
 23. J. van der Velden, Z. Papp, R. Zaremba, N.M. Boontje, J.W. de Jong and V.J. Owen, et al. *Increased Ca²⁺-sensitivity of the contractile apparatus in end-stage human heart failure results from altered phosphorylation of contractile proteins.* Cardiovasc Res, 57 (2003), pp. 37–47.
 24. J.P. Konhilas, *What we know and do not know about sex and cardiac disease.* J Biomed Biotechnol, 2010 (2010), p. 562051.
 25. A.L. Moens, J.S. Leyton-Mange, X. Niu, R. Yang, O. Cingolani and E.K. Arkenbout, et al. *Adverse ventricular remodeling and exacerbated NOS uncoupling from pressure-overload in mice lacking the beta3-adrenoreceptor.* J Mol Cell Cardiol, 47 (2009), pp. 576–585.
 26. P. Zhang, X. Xu, X. Hu, E.D. van Deel, G. Zhu and Y. Chen, *Inducible nitric oxide synthase deficiency protects the heart from systolic overload-induced ventricular hypertrophy and congestive heart failure.* Circ Res, 100 (2007), pp. 1089–1098.
 27. T. Nagayama, S. Hsu, M. Zhang, N. Koitabashi, D. Bedja and K.L. Gabrielson, et al. *Sildenafil stops progressive chamber, cellular, and molecular remodeling and improves calcium handling and function in hearts with pre-existing advanced hypertrophy caused by pressure overload.* J Am Coll Cardiol, 53 (2009), pp. 207–215.
 28. J. van der Velden, D. Merkus, B.R. Klarenbeek, A.T. James, N.M. Boontje and D.H. Dekkers, et al. *Alterations in myofilament function contribute to left ventricular dysfunction in pigs early after myocardial infarction.* Circ Res, 95 (2004), pp. e85–e95.
 29. X. Loyer, A.M. Gomez, P. Milliez, M. Fernandez-Velasco, P. Vangheluwe and L. Vinet, et al. *Cardiomyocyte overexpression of neuronal nitric oxide synthase delays transition toward heart failure in response to pressure overload by preserving calcium cycling.* Circulation, 117 (2008), pp. 3187–3198.
 30. B. Schwarz, E. Percy, X.M. Gao, A.M. Dart, G. Richardt and X.J. Du, *Altered calcium transient and development of hypertrophy in beta2-adrenoceptor overexpressing mice with and without pressure overload.* Eur J Heart Fail, 5 (2003), pp. 131–136.
 31. R.J. van Oort, J.L. Respress, N. Li, C. Reynolds, A.C. De Almeida and D.G. Skapura, et al. *Accelerated development of pressure overload-induced cardiac hypertrophy and dysfunction in an RyR2-R176Q knockin mouse model.* Hypertension, 55 (2010), pp. 932–938.
 32. N. Bowling, R.A. Walsh, G. Song, T. Estridge, G.E. Sandusky and R.L. Fouts, et al. *Increased protein kinase C activity and expression of Ca²⁺-sensitive isoforms in the failing human heart.* Circulation, 99 (1999), pp. 384–391.
 33. H. Wang, J.E. Grant, C.M. Doede, S. Sadayappan, J. Robbins and J.W. Walker, *PKC-beta11 sensitizes cardiac myofilaments to Ca²⁺ by phosphorylating troponin I on threonine-144.* J Mol Cell Cardiol, 41 (2006), pp. 823–833.
 34. D.J. Duncker, N.M. Boontje, D. Merkus, A. Versteilen, J. Krysiak and G. Mearini, et al. *Prevention of myofilament dysfunction by beta-blocker therapy in postinfarct remodeling.* Circ Heart Fail, 2 (2009), pp. 233–242.
 35. I. Morano, K. Hadicke, H. Haase, M. Bohm, E. Erdmann and M.C. Schaub, *Changes in essential myosin light chain isoform expression provide a molecular basis for isometric force regulation in the failing human heart.* J Mol Cell Cardiol, 29 (1997), pp. 1177–1187.
 36. N. Hamdani, V. Kooij, S. van Dijk, D. Merkus, W.J. Paulus and C.D. Remedios, et al. *Sarcomeric dysfunction in heart failure.* Cardiovasc Res, 77 (2008), pp. 649–658.
 37. R.L. Schultz, J.G. Swallow, R.P. Waters, J.A. Kuzman, R.A. Redetzke and S. Said, et al. *Effects of excessive long-term exercise on cardiac function and myocyte remodeling in hypertensive heart failure rats.* Hypertension, 50 (2007), pp. 410–416.
 38. J. Chambers, *Aortic stenosis.* BMJ, 330 (2005), pp. 801–802.
 39. J. Scharhag, T. Meyer, I. Kindermann, G. Schneider, A. Urhausen and W. Kindermann, *Bicuspid aortic valve: evaluation of the ability to participate in competitive sports: case reports of two soccer players.* Clin Res Cardiol, 95 (2006), pp. 228–234.
 40. P. Zeppilli, M. Bianco, S. Bria and V. Palmieri, *Bicuspid aortic valve: an innocent finding or a potentially life-threatening anomaly whose complications may be elicited by sports activity?.* J Cardiovasc Med (Hagerstown), 7 (2006), pp. 282–287.
 41. J.P. Konhilas, P.A. Watson, A. Maass, D.M. Boucek, T. Horn and B.L. Stauffer, et al. *Exercise can prevent and*

- reverse the severity of hypertrophic cardiomyopathy.* Circ Res, 98 (2006), pp. 540–548.
42. C.D. Garcarena, O.A. Pinilla, M.B. Nolly, R.P. Laguens, E.M. Escudero and H.E. Cingolani, et al. *Endurance training in the spontaneously hypertensive rat: conversion of pathological into physiological cardiac hypertrophy.* Hypertension, 53 (2009), pp. 708–714.
 43. A. Mezzani, U. Corra and P. Giannuzzi, *Central adaptations to exercise training in patients with chronic heart failure.* Heart Fail Rev, 13 (2008), pp. 13–20.
 44. S.P. Jones, J.J. Greer, R. van Haperen, D.J. Duncker, R. de Crom and D.J. Lefer, *Endothelial nitric oxide synthase overexpression attenuates congestive heart failure in mice.* Proc Natl Acad Sci USA, 100 (2003), pp. 4891–4896.
 45. C.J. Barrick, M. Rojas, R. Schoonhoven, S.S. Smyth and D.W. Threadgill, *Cardiac response to pressure overload in 129S1/SvImJ and C57BL/6J mice: temporal- and background-dependent development of concentric left ventricular hypertrophy.* Am J Physiol Heart Circ Physiol, 292 (2007), pp. H2119–H2130.
 46. I. Lerman, B.C. Harrison, K. Freeman, T.E. Hewett, D.L. Allen and J. Robbins, et al. *Genetic variability in forced and voluntary endurance exercise performance in seven inbred mouse strains.* J Appl Physiol, 92 (2002), pp. 2245–2255.





eNOS Overexpression is
Detrimental in
LV Pressure-Overload
by Enhancing Oxidative Stress

6

Elza D. van Deel, Daphne Merkus, Martine de Boer,
Dennie Tempel, Rio P. Juni, Rien van Haperen, Rini de
Crom, Henricus J. Duckers, An L. Moens, Dirk J. Duncker

in preparation

Abstract

Physical exercise training has been shown to protect against left ventricular (LV) dysfunction following a myocardial infarction (MI) but not following transverse aortic constriction (TAC) induced pressure-overload. This disparity may be due to exacerbated systolic loading during exercise as a consequence of the fixed stenosis. Since the cardioprotective effects of physical exercise training following myocardial infarction (MI) are mediated through endothelial nitric oxide synthase (eNOS), selective upregulation of eNOS potentially harnesses the beneficial effects of exercise without the concomitant detrimental effects of exaggerated hemodynamic loading. To investigate the influence of eNOS expression level on TAC-induced LV hypertrophy and dysfunction wildtype, eNOS knock-out as well as eNOS transgenic mice were subjected to 8 weeks of TAC. Interestingly, not elevation but rather loss of eNOS expression protected the heart against pressure-overload induced cardiac remodeling, dysfunction, fibrosis and pulmonary congestion whereas additional eNOS exerted deleterious effects. Reversal of detrimental effects of eNOS overexpression with antioxidant-treatment reveals that eNOS overexpression aggravates TAC-induced cardiac remodeling and dysfunction by elevating oxidative stress, likely as a result of eNOS-uncoupling.

In conclusion, in contrast to the beneficial effects of eNOS after MI, elevated eNOS levels adversely affect the remodeling process associated with TAC due to enhanced oxidative stress.

Introduction

Paradoxically, improved treatment of cardiovascular diseases has reduced acute mortality but in combination with progressive aging of the population, highly increased the number of heart failure patients.¹ The two major risk factors involved (myocardial infarction (MI) and increased impedance of left ventricular (LV) outflow by hypertension or aortic stenosis) both induce LV hypertrophy that, although initiated as a compensatory mechanism, in the long term contributes to the progression towards heart failure.²⁻⁴ In contrast, physical exercise training induces physiological LV hypertrophy that is not accompanied by LV dysfunction and protects against the development of heart failure.⁵ Accordingly, we previously demonstrated exercise training to mitigate LV dysfunction in mice after MI.⁶ Subsequently, we showed that the protective effects of exercise after MI were mimicked by endothelial nitric oxide synthase (eNOS) overexpression⁷⁻⁸ and abrogated in eNOS knock out mice,⁹ illustrating the critical role of eNOS in the beneficial effects of exercise. eNOS exerts its protective effects by producing nitric oxide (NO) that has numerous cardiovascular effects but mainly evokes cardioprotection by reducing afterload, improving contractile performance, stimulating angiogenesis, reducing fibrosis and apoptosis and suppressing pathological hypertrophy.¹⁰

In contrast to the beneficial effects of exercise after MI, we recently also found that exercise failed to protect against LV hypertrophy and dysfunction in a mouse model of pressure-overload through transverse aortic constriction (TAC).¹¹ Evidently, the beneficial effects of exercise training critically depend on the underlying pathology. A potential explanation for the lack of beneficial exercise effect after TAC, is exaggerated systolic loading of the LV during exercise as a consequence of the fixed stenosis.¹² We therefore hypothesize that in pressure-overload upregulation of eNOS could harness the beneficial effects of exercise while avoiding exaggerated hemodynamic loading.

However, the role of eNOS in pressure-overload hypertrophy remains controversial because it on the one hand exerts antioxidant and antihypertrophic effects by producing NO yet contributes to cardiovascular disease when functionally uncoupled and instead of NO produces super oxide.¹³

Several studies have investigated the effect of eNOS in pressure-overload by using eNOS knockout (eNOS-Ko) mice, but failed to reach consensus. In one study eNOS-Ko mice developed aggravated LV hypertrophy and dysfunction after TAC¹⁴ whereas others report mitigated TAC-induced LV hypertrophy and dysfunction in eNOS-Ko mice that was explained by prevention of eNOS uncoupling and reactive oxygen species (ROS) production.¹⁵ A potential explanation suggested for opposite findings in eNOS-Ko mice is a difference in severity of the hypertrophic response and causative pressure-overload.¹⁵ However, this clarification is difficult to substantiate with results obtained in separate laboratories. Furthermore, whether additional eNOS evokes cardiac protection in pressure-overload, or quite the contrary, exacerbates eNOS uncoupling and concomitant ROS production, has so far not been studied.

Consequently, the aim of the present study is to elucidate the effect of eNOS expression

level on cardiac hypertrophy and function in mild and severe pressure-overload in eNOS-Ko, wildtype (Wt) and eNOS overexpressing transgenic (eNOS-Tg) mice. Additionally, we set out to study whether the effects of additional eNOS are influenced by eNOS uncoupling and ROS generation.

Methods

All experiments were performed in accordance with the "Guiding Principles in the Care and Use of Animals" as approved by the Council of the American Physiological Society and with prior approval of the Animal Care Committee of the Erasmus MC Rotterdam. A total of 342 mice (24.6 ± 0.3 gr) of either sex entered the study.

Experimental procedure

eNOS-Ko mice were obtained from Jackson Laboratory. The generation of eNOS-Tg mice has been previously described¹⁶ and littermates C57Bl/6 of transgenic eNOS mice were used as Wt controls. 65 eNOS Ko, 76 Wt and 68 eNOS Tg mice underwent mild TAC (mTAC), severe TAC (sTAC) or a sham operation as previously described.¹¹ Additionally, sTAC was induced or a sham operation performed in 58 Wt and 65 eNOS-Tg mice that were randomized to receive the anti-oxidant N-acetylcystein (NAC) (1mg/ml in drinking water), or vehicle to study the effects of eNOS overexpression on ROS production in pressure-overload hypertrophy.

Eight weeks after surgery, echocardiographic and hemodynamic measurements were performed under isoflurane anesthesia. All mice were ventilated and anesthetized with 2.5% isoflurane and M-mode LV echocardiography was performed with an Aloka SSD 4000 echo device (Aloka; Tokyo, Japan) using a 12-MHz probe. LV diameters at end diastole (LVEDD) and end systole (LVESD) were measured, and fractional shortening was calculated. Aortic pressure distal to the stenosis was measured through a PE10 catheter in the left carotid artery. A 1.4-Fr microtipped manometer (Millar Instruments; Houston, Texas, USA) was inserted in the right carotid artery to record aortic pressure proximal to the stenosis and subsequently advanced into the LV to measure LV pressure (LVP) and calculate the maximum rate of rise ($LV \text{ dP/dt}_{\text{max}}$) and fall ($LV \text{ dP/dt}_{\text{min}}$) of LVP, the rate of rise of LVP at a pressure of 40 mmHg ($LV \text{ dP/dt}_{\text{P40}}$) and the time constant of LV pressure decay (τ) as previously described.¹¹ At the end of each experiment LV, right ventricle (RV), wet and dry lung weights and tibia length (TL) were determined and LV tissue samples were stored for histological and molecular analysis.

Histomorphometry

Paraffin embedded LV tissue was serially sectioned into 4- μm slices. Subsequently, gomorri staining was performed to measure cardiomyocyte cross-sectional area (CSA). Capillary density was determined by Lectin staining and interstitial fibrosis was measured using Picro Sirius Red staining. LV sections of 6 mice per group were analysed with a quantitative image analysis system (Clemex Technologies).

Gene expression analysis

Total RNA was extracted from 6 frozen LV sample per group using the RNeasy kit (Qiagen, The Netherlands) and RNA quantity was verified by optical dosimetry (Nanodrop®, Isogen Life Science, The Netherlands). Isolated RNA was reverse transcribed into cDNA (IscripT, Biorad, The Netherlands) and analyzed by real-time fluorescence assessment of SYBR Green signal in the iCycler iQ Detection system (Bio-Rad, The Netherlands). Primer sets for myocardial hypertrophy marker genes atrial natriuretic peptide (ANP), brain natriuretic peptide (BNP), α -skeletal actin (α -SKA), and eNOS were employed. mRNA levels were corrected for the housekeeping gene hypoxanthine guanine phosphoribosyl transferase (HPRT) and normalized to Wt sham values.

eNOS protein level and dimer-to-monomer ratio

Low temperature SDS-PAGE was performed for detection of eNOS monomer and dimer.¹³ The protein samples were subjected to SDS-PAGE with 7% self-made SDS-Tris gels run overnight. Gels and buffers were equilibrated at 4°C before electrophoresis, and the buffer tank was placed in an ice bath during electrophoresis to maintain the low temperature. Subsequent to SDS-PAGE, the proteins were transferred for 3 hours to nitrocellulose membranes. The blots were then probed as routine western blot with primary NOS3 antibody (1:5000, Santa Cruz Biotechnology, Inc, Heidelberg, Germany) and secondary rabbit anti-mouse IgG antibody conjugated with HRP (1:1000, Santa Cruz Biotechnology, Inc, Heidelberg, Germany), and eNOS dimer and monomer bands were detected by enhanced chemiluminescence substrate (Perkin Elmer) with LAS 3000 CCD camera (Fujifilm). The images were then analyzed with ImageJ (NIH).

Statistical analysis

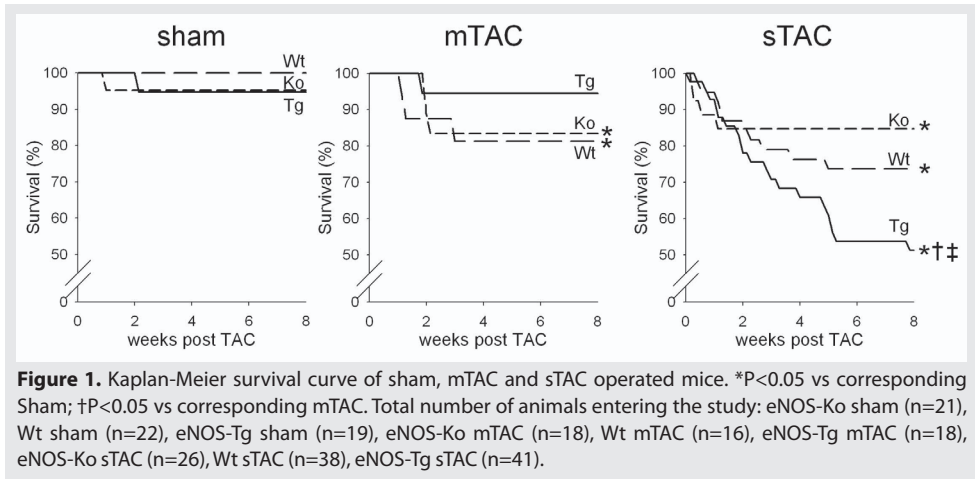
All data were tested using 2-way (eNOS expression level x stenosis) ANOVA followed by post-hoc testing with a Student-Newman-Keuls test. A value of $P \leq 0.05$ was considered statistically significant (two-tailed). Data are presented as means \pm SEM.

All groups contained similar numbers of male and female mice. Similar as previously described,¹¹ we did not observe an influence of sex on the effects of TAC and/or eNOS expression level on survival and LV hypertrophy or dysfunction. Consequently, we pooled male and female mice for final analysis.

Results

Influence of TAC and eNOS on survival rate

Lack or overexpression of eNOS did not affect mortality in sham operated animals (Fig.1.) while mTAC resulted in an 17% mortality in eNOS-Ko and 19% in Wt mice but no significant mortality in eNOS-Tg (5%). while sTAC induced mortality in all groups (15% eNOS-Ko, 26% Wt and 49% eNOS-Tg). Interestingly, sTAC-induced mortality was aggravated by eNOS overexpression and accordingly more severe in eNOS-Tg (49%) than in eNOS-Ko mice (15%).



Cardiac remodeling and dysfunction

eNOS expression levels did not affect bodyweight (Table 1) but tibia length was slightly larger in Wt and eNOS-Tg mice than in eNOS-Ko sham mice. Lack of eNOS resulted in elevated LV systolic pressure (LVSP) and mean arterial pressure (MAP) proximal and distal to the stenosis, while eNOS overexpression decreased LVSP and proximal and distal MAP (Fig. 2 and Table 1). Heart rate (HR), LV weight and geometry or LV systolic and diastolic function were not affected by eNOS expression level in sham operated mice.

Surprisingly, although there was an inverse relationship between eNOS expression and increase in LV afterload, LV hypertrophy by mTAC and sTAC was most pronounced in eNOS-Tg mice. Accordingly, mTAC only induced LV dilation in Wt and eNOS-Tg mice but not in eNOS-Ko. In addition, mTAC reduced LV dp/dt_{p40} and LV dp/dt_{min} in eNOS-Tg mice but did not affect these parameters in eNOS-Ko and Wt animals. Again, in sTAC the aggravation of LV remodeling (LV weight and diameter), systolic function ($dp/dt/P40$), diastolic function (dp/dt_{min} and τ) and pulmonary congestion (lung fluid weight and RV weight) was more severe with increasing eNOS expression.

LV histopathology

Cardiomyocyte CSA, capillary density and interstitial fibrosis were all unaffected by eNOS expression level in sham operated animals (Fig. 3). mTAC did not increase cardiomyocyte CSA but resulted in a higher capillary density in eNOS-Tg mice compared to eNOS-Ko animals. Interestingly, although myocyte hypertrophy in response sTAC was independent of genotype, sTAC only produced capillary rare fraction and interstitial fibrosis in Wt and eNOS-Tg but not in eNOS-Ko mice (Fig. 3).

Expression of hypertrophy markers

Since the strongest effects on LV remodeling and dysfunction were seen in sTAC mice and consequently there was no sign of pulmonary congestion in mTAC mice, we elected to explore alterations in gene expression produced by TAC in sham and sTAC mice only (Fig. 4). In sham operated mice lack of eNOS resulted in elevated BNP expression levels

Table 1. Anatomical and Functional data

		eNOS-Ko	Wt	eNOS-Tg
Anatomical data				
Body weight (g)	sham	24.0 ± 0.9	26.7 ± 1.2	25.3 ± 0.7
	mTAC	24.2 ± 1.1	25.5 ± 1.0	25.5 ± 1.1
	sTAC	23.7 ± 1.0	26.7 ± 1.0	23.6 ± 0.9 †
Tibia length (cm)	sham	1.79 ± 0.01	1.83 ± 0.01 ‡	1.82 ± 0.01 ‡
	mTAC	1.81 ± 0.01	1.85 ± 0.01	1.83 ± 0.01
	sTAC	1.79 ± 0.01	1.87 ± 0.01*‡	1.82 ± 0.01 §
LV weight (mg)	sham	94 ± 4	93 ± 3	96 ± 3
	mTAC	119 ± 6 *	133 ± 8 *	147 ± 10 *
	sTAC	157 ± 7 *†	179 ± 7 *‡§	195 ± 8 *†§
RV weight (mg)	sham	22 ± 1	23 ± 1	23 ± 1
	mTAC	22 ± 1	23 ± 1	26 ± 2
	sTAC	30 ± 2 *†	34 ± 2 *†	39 ± 3 *†§
Lung fluid weight (mg)	sham	103 ± 2	114 ± 4	126 ± 8
	mTAC	103 ± 3	135 ± 12	133 ± 10
	sTAC	180 ± 20 *†	201 ± 22 *†	250 ± 22 *†§
LV wall thickness (mm)	sham	1.16 ± 0.05	1.14 ± 0.05	1.07 ± 0.04
	mTAC	1.17 ± 0.03	1.15 ± 0.06	1.19 ± 0.06
	sTAC	1.38 ± 0.04	1.31 ± 0.06	1.22 ± 0.05 ‡
LV weight / body weight	sham	3.9 ± 0.1	3.5 ± 0.1 †	3.8 ± 0.1 §
	mTAC	5.0 ± 0.2 *	5.3 ± 0.3 *	5.8 ± 0.3 *
	sTAC	6.7 ± 0.3 *†	6.9 ± 0.3 *†	8.4 ± 0.4 *†§
Functional data				
Heart Rate (bpm)	sham	550 ± 8	558 ± 15	560 ± 18
	mTAC	547 ± 10	554 ± 21	539 ± 18
	sTAC	542 ± 12	527 ± 10	538 ± 14
MAP prox (mmHg)	sham	104 ± 3	87 ± 4 ‡	71 ± 4 ‡§
	mTAC	110 ± 8	99 ± 3	77 ± 3 ‡§
	sTAC	93 ± 5 †	84 ± 4 ‡§	75 ± 3 ‡
ΔSP (abs)	sham	0 ± 3	0 ± 2	-2 ± 1
	mTAC	37 ± 6 *	43 ± 4 *	37 ± 4 *
	sTAC	49 ± 4 *†	52 ± 5 *	49 ± 3 *
LV dp/dt _{max} (mmHg·s ⁻¹)	sham	8646 ± 645	8884 ± 621	9177 ± 757
	mTAC	8897 ± 304	8204 ± 512	6870 ± 460*‡
	sTAC	6997 ± 472*†	6486 ± 346*†	5028 ± 328*†§
LVEDP (mmHg)	sham	4.8 ± 0.6	4.4 ± 0.6	3.8 ± 0.6
	mTAC	7.0 ± 1.0	7.6 ± 1.6	5.3 ± 0.6
	sTAC	14.1 ± 1.5 *†	13.2 ± 1.4 *†	16.9 ± 2.7 *†

MAP prox, mean arterial pressure proximal to the stenosis; ΔSP, systolic pressure gradient over the stenosis; LVEDP, LV end diastolic pressure. eNOS-Ko sham (n=20), Wt sham (n=22), eNOS Tg sham (n=18), eNOS-KO mTAC (n=15), Wt mTAC (n=13), eNOS-Tg mTAC (n=17), eNOS-Ko sTAC (n=20), WT sTAC (n=27), eNOS-Tg sTAC (n=18). *P<0.05 vs corresponding sham; †P<0.05 vs corresponding mTAC; ‡P<0.05 vs corresponding eNOS-Ko; §P<0.05 vs corresponding Wt.

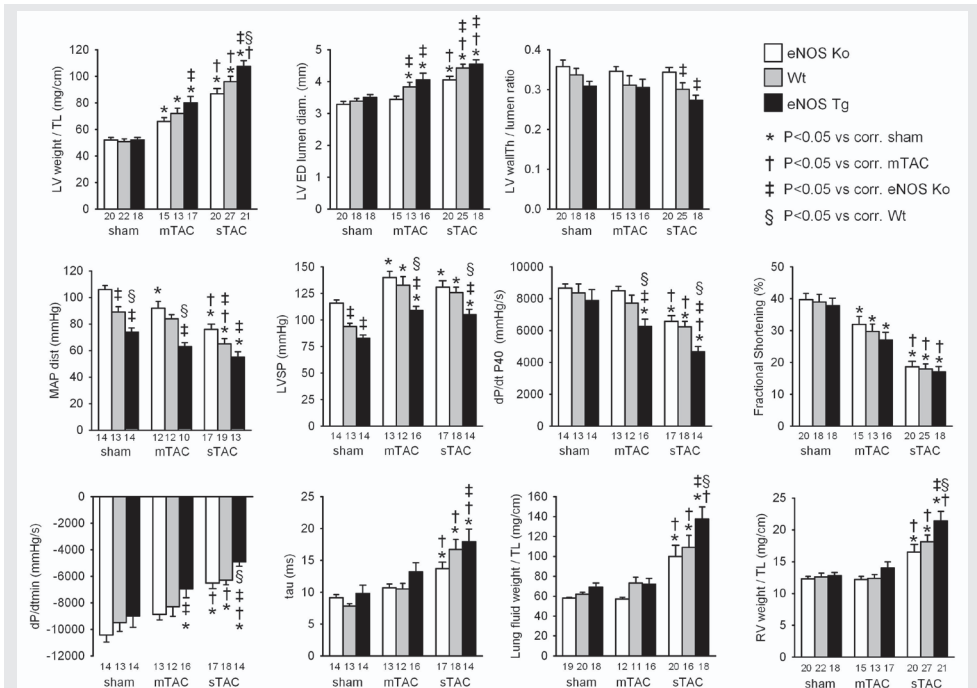


Figure 2. Effect of TAC and eNOS on LV mass and geometry, hemodynamic parameters and lung fluid weight (lung wet weight minus lung dry weight) in eNOS-Ko (white bars), Wt (grey bars) and eNOS-Tg (black bars) mice. MAP dist, mean aortic pressure distal to the stenosis; LVSP, LV systolic pressure. *P<0.05 vs corresponding Sham †P<0.05 vs corresponding mTAC; ‡P<0.05 vs corresponding eNOS-Ko; §P<0.05 vs corresponding Wt. Number of animals is indicated below each bar.

compared to eNOS overexpression. Similarly, ANP and α -SKA expression tended to be higher in sham operated eNOS-Ko mice but this failed to reach statistical significance (P=0.1 for both genes). Following sTAC, ANP and α -SKA expression was markedly elevated but unaffected by eNOS expression level. Conversely, sTAC only increased BNP expression level in Wt and eNOS-Tg mice but not in eNOS-Ko animals (Fig. 4).

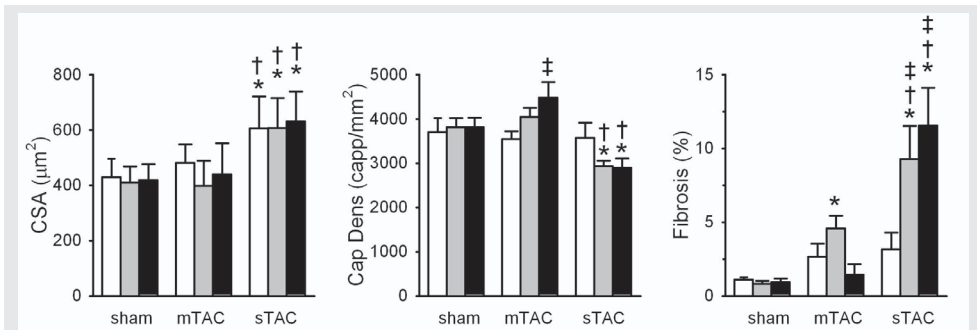
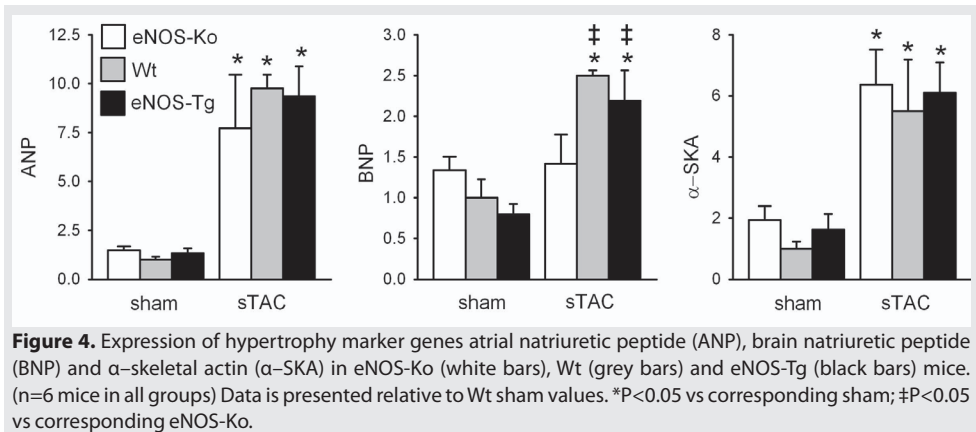


Figure 3. Histological analyses of the effect of TAC and eNOS expression level on cardiomyocyte cross sectional area (CSA), capillary density and fibrosis in eNOS-Ko (white bars), Wt (grey bars) and eNOS-Tg (black bars) mice. (n=6 mice in all groups) *P<0.05 vs corresponding Sham †P<0.05 vs corresponding mTAC; ‡P<0.05 vs corresponding eNOS-Ko



eNOS and eNOS uncoupling

To evaluate the effect of pressure-overload on eNOS levels and eNOS uncoupling ratio's we choose to compare only the more extreme phenotype of sTAC with sham operated animals in Wt and eNOS-Tg mice (Fig. 5). Overexpression of eNOS not only elevated eNOS mRNA and protein levels but also resulted in a trend towards improved eNOS coupling ($p=0.3$) in sham operated mice. Surprisingly, although sTAC increased eNOS protein level, elevated eNOS mRNA expression and total protein levels were no longer observed in eNOS-Tg after sTAC. Furthermore, sTAC tended to induce eNOS uncoupling in eNOS-Tg mice ($p=0.2$).

Effects of NAC treatment and eNOS overexpression on survival and cardiac hypertrophy and dysfunction

Because of the only modest effects of mTAC in Wt and eNOS-Tg mice we elected to include only sham and sTAC samples for the evaluation of NAC treatment. NAC had no effect on survival (Fig. 6), cardiac geometry or function or histology markers in sham operated Wt and eNOS-Tg mice (Fig. 7). In contrast, to the lack of effects of ROS scavenging in Wt

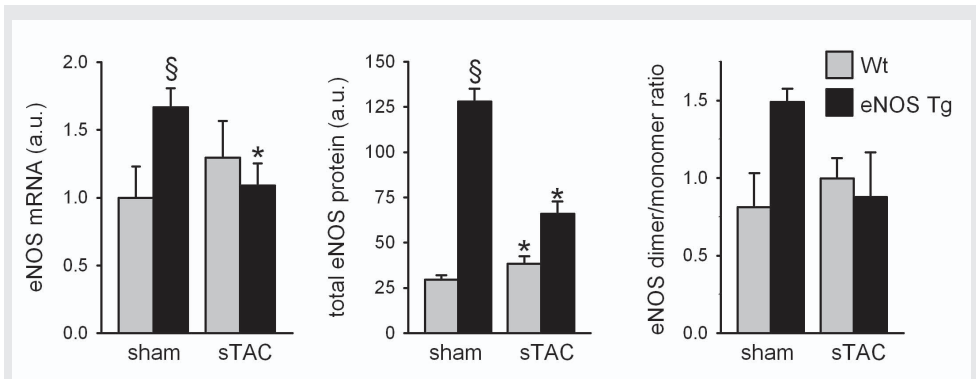


Figure 5. eNOS expression and protein levels and monomer/dimer ratios in Wt (grey bars) and eNOS-Tg (black bars) mice. (n=6 mice in RNA groups, n=2 in protein groups) Data is presented in arbitrary units (a.u.). *P<0.05 vs corresponding sham; §P<0.05 vs corresponding Wt.

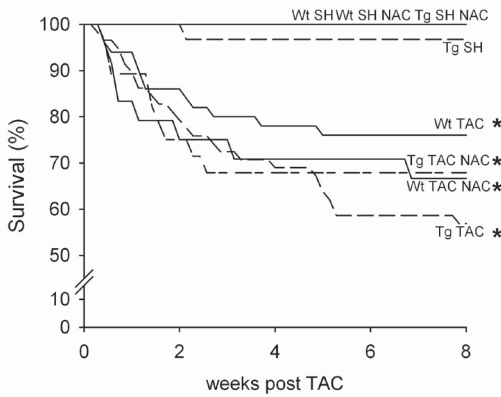


Figure 6. Kaplan-Meier survival curve of sham and sTAC operated Wt and eNOS-Tg mice with or without NAC treatment. * $P < 0.05$ vs corresponding Sham. Total number of animals entering the study: Wt sham (n=33), eNOS-Tg sham (n=31), Wt sham NAC (n=11), eNOS-Tg sham NAC (n=8), Wt sTAC (n=50), eNOS-Tg sTAC (n=48), Wt sTAC NAC (n=24), eNOS-Tg sTAC NAC (n=28).

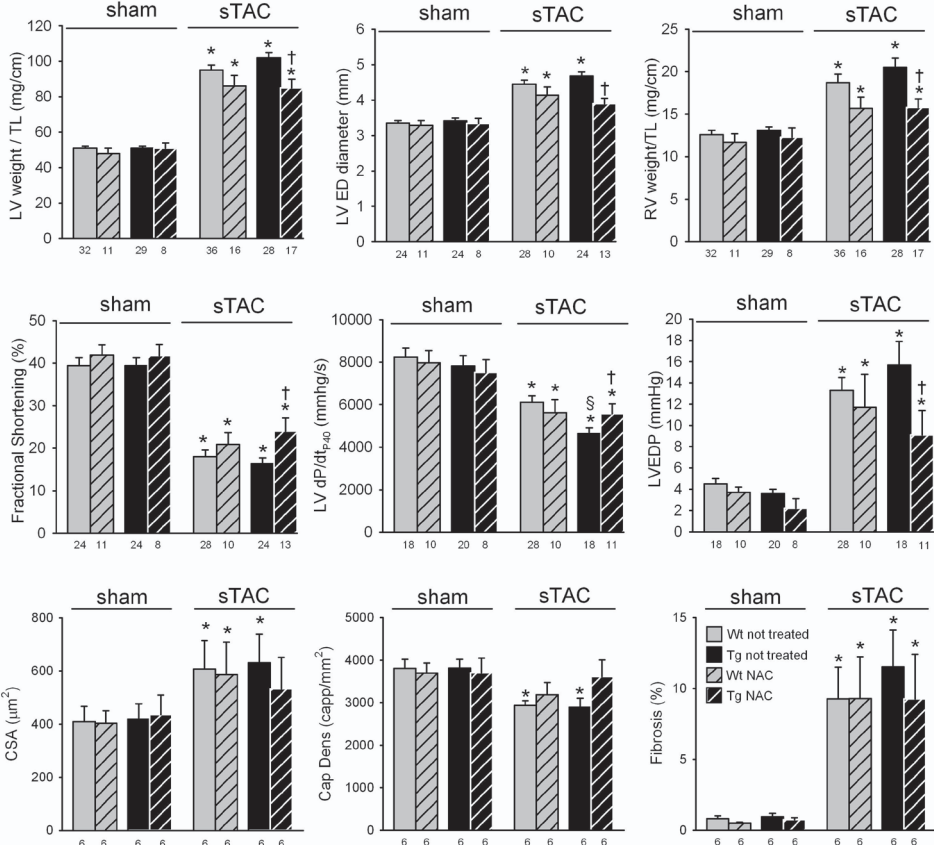
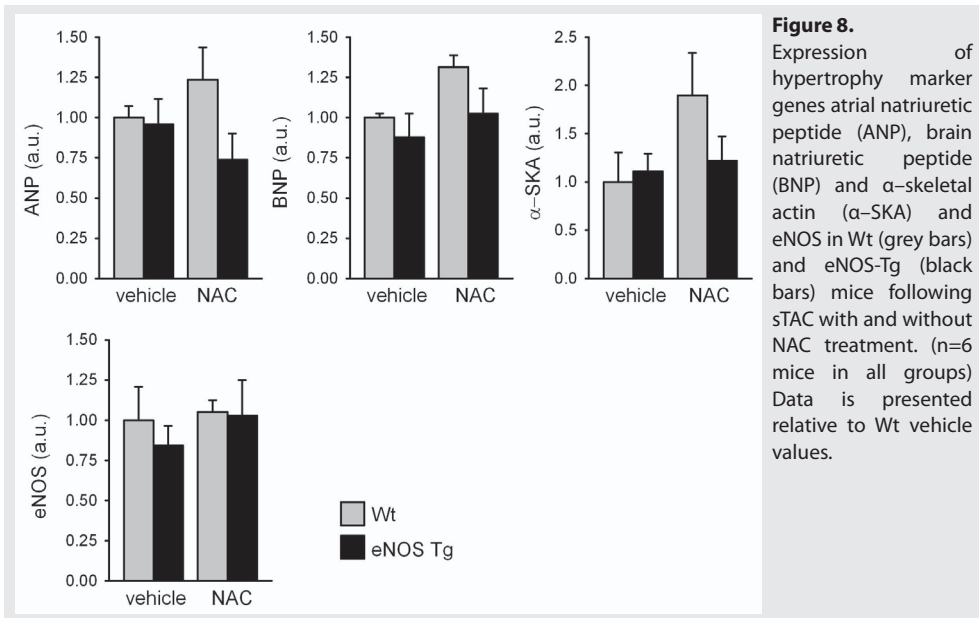


Figure 7. Effect of TAC and eNOS on LV mass and geometry, hemodynamic parameters, RV mass, cardiomyocyte cross sectional area (CSA), capillary density and fibrosis in Wt (grey bars) and eNOS-Tg (black bars) mice without additional treatment (open bars) or treated with NAC (hatched bars). * $P < 0.05$ vs corresponding Sham † $P < 0.05$ vs corresponding not treated; § $P < 0.05$ vs. corresponding Wt. Number of animals is indicated below each bar.

mice, NAC in eNOS-Tg mice prevented detrimental effects of eNOS overexpression after sTAC by reducing pressure-overload induced LV hypertrophy and dilation and improving systolic function (fractional shortening and LV dp/dtP40) and LVEDP as well secondary RV hypertrophy (Fig. 7). Additionally, NAC treatment maintained capillary density in both Wt and eNOS-Tg mice but only prevented a significantly increase in CSA following sTAC in eNOS-Tg mice without affecting interstitial fibrosis in either genotype.

Effects of NAC treatment on gene expression

Following sTAC, RNA expression levels of hypertrophic marker genes, ANP, BNP and α -SKA were not affected by NAC treatment (Fig. 8) although trends towards reduced expression of hypertrophic marker genes in NAC treated eNOS-Tg vs. Wt could be established (ANP: $p=0.08$, BNP: $p=0.1$, α -SKA: $p=0.2$). Likewise, eNOS expression levels after sTAC were unaffected by ROS scavenging (Fig. 8).



Discussion

The present study demonstrates that eNOS expression aggravates LV hypertrophy and dysfunction in a dose dependent manner in mild as well as severe pressure overload. Accordingly, reductions in capillary density, interstitial fibrosis and elevated BNP expression level were mitigated in eNOS-Ko mice compared to Wt and eNOS-Tg animals. Secondly, scavenging of ROS attenuated LV hypertrophy and dysfunction in eNOS-Tg but not in Wt mice. These results indicate that eNOS expression does not reduce but rather elevates pressure-overload induced ROS, and explain why deletion of eNOS is protective and overexpression of eNOS is detrimental in TAC induced pressure-overload hypertrophy and dysfunction.

Effects of eNOS on pressure- overload LV hypertrophy and dysfunction

In agreement with recent data from our laboratory,¹¹ mTAC elevated LVSP and induced moderate LV hypertrophy and dilation with maintained global LV function and minimal effects on fibrosis in Wt mice. Conversely, 8 weeks of sTAC produced robust LV remodeling, and dysfunction with concomitant capillary rare fraction, fibrosis and elevated expression of hypertrophic marker genes. Decompensated LV hypertrophy in sTAC also explains why LVSP was not further elevated in sTAC compared to mTAC.

Consistent with prior observations, eNOS gene deletion and overexpression respectively, induced hypertension and hypotension without influencing basal cardiac function.^{7,17} Accordingly eNOS expression level had no effect on cardiomyocyte cross-sectional area, capillary density and interstitial fibrosis under baseline conditions. eNOS-Ko mice have been described to develop LV hypertrophy¹⁸ but this was not observed in the present study. However, similar to results from the present study others did not observe LV hypertrophy in eNOS-Ko sham mice but demonstrate elevated levels of natriuretic peptides in these mice,¹⁹ albeit ANP increase failed to reach statistical significance in the present study. Interestingly, sham eNOS-Tg mice not only produce more eNOS but eNOS also tended to be better coupled in these mice compared to corresponding wildtype animals.

6

A clear relationship between eNOS expression level and pressure-overload induced LV remodeling, dysfunctional and secondary pulmonary congestion was observed in mTAC as well as sTAC. Interestingly, in spite of aggravate dysfunction eNOS overexpression did evoke beneficial affects on capillary density in mTAC that was lost in sTAC. Additionally, in sTAC we demonstrated an inverse relationship between eNOS expression level and survival and showed that eNOS gene deletion normalized BNP expression but not ANP and α -SKA. Furthermore, sTAC not only reduced eNOS mRNA and protein level but also tended to result in eNOS uncoupling in eNOS-Tg mice.

The effects of loss of eNOS on the cardiac response to TAC have been previously studied but produced conflicting results. One group found eNOS deficiency to aggravate pressure-overload hypertrophy from TAC^{14,20} that was contradicted by results from another study demonstrating loss of eNOS to protect the heart against the consequences of pressure-overload.¹⁵ A difference in severity of pressure-overload was proposed as a possible explanation for this discrepancy¹⁵ but this was so far never further investigated. Therefore in this study we investigated the effects of loss as well as overexpression of eNOS in severe and mild pressure-overload through aortic constriction. Interestingly, we found loss of eNOS to not only protect the heart against severe but also against mild pressure-overload. Furthermore, eNOS overexpression in TAC did not exhibit the beneficial effects on cardiac dysfunction observed in MI,⁷⁻⁸ but in contrast aggravated LV remodeling and dysfunction following mild as well as severe TAC. Apparently, the described divergent effects of eNOS on pressure-overload hypertrophy are not explained by overload severity. However it should be noted that in spite of the same degree of stenosis, wildtype littermate mice in the studies in which eNOS deficiency was protective (chapter 6 and ¹⁵) developed more LV hypertrophy (~100%) in response to TAC compared to mice in which loss of eNOS was detrimental^{14,20} that increased heart weight by 50% in response to TAC.

The diverse hypertrophic response to TAC indicates that perhaps a difference in genetic background influenced the cardiac hypertrophic response and consequently the effects of eNOS on LV hypertrophy in these mice. The absence of additive protection by elevated eNOS levels in sTAC can easily be explained by the reduction of eNOS mRNA and protein expression to Wt levels following sTAC. A potential mechanism how eNOS overexpression aggravated cardiac remodeling and dysfunction following TAC could be found in eNOS uncoupling and ROS production. eNOS uncoupling has been described as a result of TAC¹³ and potential mechanism for protection against pressure-overload LV hypertrophy and dysfunction in eNOS-Ko mice.¹⁵ And although in the present study we did not observe eNOS uncoupling by TAC in Wt animals, a trend towards TAC induced eNOS uncoupling in eNOS-Tg mice was observed that reduces NO bioavailability and aggravates oxidative stress.

Effects of ROS scavaging on pressure-overload induced LV hypertrophy and dysfunction

Excessive ROS generation is one of the important mechanisms contributing to pathological cardiac remodeling.²¹⁻²² In the normal heart, nicotinamide-adenine dinucleotide phosphate oxidase, xanthine oxidase and mitochondrial electron transport, are the main sources of ROS while detrimental effects of ROS are prevented by antioxidant systems like superoxide dismutases.²³⁻²⁴ However, in pressure-overload ROS production overwhelms the antioxidant defense mechanism, resulting in oxidative stress. Subsequently, oxidative stress targets the NO pathway by upregulation of phosphodiesterase type 5²⁵ which decreases cGMP bioavailability and by stimulating eNOS uncoupling. When eNOS uncouples and shifts from a dimer to a monomer state it no longer produces NO but instead turns into an important source of super oxide (O_2^-) and as such instigates a vicious cycle of ROS production. Accordingly, prevention of eNOS uncoupling by tetrahydrobiopterin (BH4) administration reversed LV hypertrophy in mice following TAC.¹³

NAC antioxidant treatment has been reported to attenuate pressure-overload induced LV hypertrophy.²⁶ In contrast others found only trends towards cardio protective effects of ROS scavenging in wildtype mice subjected to pressure-overload,^{13,15,27} which was confirmed by observations in the present study. In eNOS-Tg mice subjected to sTAC, NAC reduced LV hypertrophy, prevented LV dilation and improved cardiac function, demonstrating that increased ROS production contributed to the adverse response to pressure-overload in mice with elevated eNOS levels. Accordingly, the beneficial effects of ROS scavenging on cardiac hypertrophy in eNOS-Tg mice were accompanied by a global trend towards normalisation of hypertrophic marker gene expression (Fig. 8). Protection against pressure-overload induced LV hypertrophy by increasing cGMP (the downstream product of the eNOS pathway) bioavailability without upregulation of eNOS^{25,28} and the trend towards eNOS uncoupling following TAC in eNOS-Tg mice, further indicate that the detrimental effects of eNOS overexpression are caused by a defect in eNOS itself.

Conclusions

The results of the present study show that eNOS overexpression failed to attenuate LV remodeling and dysfunction after TAC but instead turned out to be detrimental, whereas

lack of eNOS proved to be cardioprotective in pressure-overload hypertrophy. Reversal of aggravated pressure-overload induced LV hypertrophy and dysfunction in eNOS-Tg mice by ROS scavenging shows that the detrimental effects of eNOS overexpression are caused by elevated ROS production, likely as a result of eNOS uncoupling.

Future studies should address the role of eNOS uncoupling in adverse effects of eNOS overexpression on pressure-overload induced hypertrophy more specifically by inhibiting eNOS uncoupling directly via BH4 treatment and investigate whether rescue of annihilating of eNOS overexpression by TAC unmasks beneficial effects of eNOS.

Acknowledgements

The authors are grateful to Shanti Tel for her assistance with histological analysis. This work was financial supported by the Dutch Heart Foundation (2007B024).

Conflict of interest

None declared

References

1. Schocken, D.D., et al., *Prevention of heart failure: a scientific statement from the American Heart Association Councils on Epidemiology and Prevention, Clinical Cardiology, Cardiovascular Nursing, and High Blood Pressure Research; Quality of Care and Outcomes Research Interdisciplinary Working Group; and Functional Genomics and Translational Biology Interdisciplinary Working Group*. *Circulation*, 2008. **117**(19): p. 2544-65.
2. Frey, N., et al., *Hypertrophy of the heart: a new therapeutic target?* *Circulation*, 2004. **109**(13): p. 1580-9.
3. McMullen, J.R. and G.L. Jennings, *Differences between pathological and physiological cardiac hypertrophy: novel therapeutic strategies to treat heart failure*. *Clin Exp Pharmacol Physiol*, 2007. **34**(4): p. 255-62.
4. Selvetella, G., et al., *Adaptive and maladaptive hypertrophic pathways: points of convergence and divergence*. *Cardiovasc Res*, 2004. **63**(3): p. 373-80.
5. Haykowsky, M.J., et al., *A meta-analysis of the effect of exercise training on left ventricular remodeling in heart failure patients: the benefit depends on the type of training performed*. *J Am Coll Cardiol*, 2007. **49**(24): p. 2329-36.
6. de Waard, M.C., et al., *Early exercise training normalizes myofibrillar function and attenuates left ventricular pump dysfunction in mice with a large myocardial infarction*. *Circ Res*, 2007. **100**(7): p. 1079-88.
7. de Waard, M.C., et al., *Detrimental effect of combined exercise training and eNOS overexpression on cardiac function after myocardial infarction*. *Am J Physiol Heart Circ Physiol*, 2009. **296**(5): p. H1513-23.
8. Jones, S.P., et al., *Endothelial nitric oxide synthase overexpression attenuates congestive heart failure in mice*. *Proc Natl Acad Sci U S A*, 2003. **100**(8): p. 4891-6.
9. de Waard, M.C., et al., *Beneficial effects of exercise training after myocardial infarction require full eNOS expression*. *J Mol Cell Cardiol*, 2010. **48**(6): p. 1041-9.
10. Tirziu, D. and M. Simons, *Endothelium-driven myocardial growth or nitric oxide at the crossroads*. *Trends Cardiovasc Med*, 2008. **18**(8): p. 299-305.
11. van Deel, E.D., et al., *Exercise training does not improve cardiac function in compensated or decompensated left ventricular hypertrophy induced by aortic stenosis*. *J Mol Cell Cardiol*, 2011. **50**(6): p. 1017-25.
12. Duncker, D.J., et al., *Effect of exercise on coronary pressure-flow relationship in hypertrophied left ventricle*. *Am J Physiol*, 1995. **269**(1 Pt 2): p. H271-81.
13. Moens, A.L., et al., *Reversal of cardiac hypertrophy and fibrosis from pressure overload by tetrahydrobiopterin: efficacy of recoupling nitric oxide synthase as a therapeutic strategy*. *Circulation*, 2008. **117**(20): p. 2626-36.
14. Ichinose, F., et al., *Pressure overload-induced LV hypertrophy and dysfunction in mice are exacerbated by congenital NOS3 deficiency*. *Am J Physiol Heart Circ Physiol*, 2004. **286**(3): p. H1070-5.
15. Takimoto, E., et al., *Oxidant stress effects from nitric oxide synthase-3 uncoupling stimulates cardiac pathologic remodeling from chronic pressure load*. *J Clin Invest*, 2005. **115**(5): p. 1221-31.
16. van Haperen, R., et al., *Reduction of blood pressure, plasma cholesterol, and atherosclerosis by elevated endothelial nitric oxide*. *J Biol Chem*, 2002. **277**(50): p. 48803-7.
17. Massion, P.B. and J.L. Balligand, *Modulation of cardiac contraction, relaxation and rate by the endothelial nitric oxide synthase (eNOS): lessons from genetically modified mice*. *J Physiol*, 2003. **546**(Pt 1): p. 63-75.
18. Liu, Y.H., et al., *Effect of ACE inhibitors and angiotensin II type 1 receptor antagonists on endothelial NO synthase knockout mice with heart failure*. *Hypertension*, 2002. **39**(2 Pt 2): p. 375-81.
19. Bubikat, A., et al., *Local atrial natriuretic peptide signaling prevents hypertensive cardiac hypertrophy in endothelial nitric-oxide synthase-deficient mice*. *J Biol Chem*, 2005. **280**(22): p. 21594-9.
20. Buys, E.S., et al., *Cardiomyocyte-restricted restoration of nitric oxide synthase 3 attenuates left ventricular remodeling after chronic pressure overload*. *Am J Physiol Heart Circ Physiol*, 2007. **293**(1): p. H620-7.
21. Seddon, M., Y.H. Looi, and A.M. Shah, *Oxidative stress and redox signalling in cardiac hypertrophy and heart failure*. *Heart*, 2007. **93**(8): p. 903-7.
22. Takimoto, E. and D.A. Kass, *Role of oxidative stress in cardiac hypertrophy and remodeling*. *Hypertension*, 2007. **49**(2): p. 241-8.
23. van Deel, E.D., et al., *Extracellular superoxide dismutase protects the heart against oxidative stress and hypertrophy after myocardial infarction*. *Free Radic Biol Med*, 2008. **44**(7): p. 1305-13.
24. Tsutsui, H., S. Kinugawa, and S. Matsushima, *Oxidative Stress and Heart Failure*. *Am J Physiol Heart Circ Physiol*, 2011.
25. Lu, Z., et al., *Oxidative stress regulates left ventricular PDE5 expression in the failing heart*. *Circulation*, 2010. **121**(13): p. 1474-83.
26. Byrne, J.A., et al., *Contrasting roles of NADPH oxidase isoforms in pressure-overload versus angiotensin II-*

- induced cardiac hypertrophy*. *Circ Res*, 2003. **93**(9): p. 802-5.
27. Chess, D.J., et al., *The antioxidant tempol attenuates pressure overload-induced cardiac hypertrophy and contractile dysfunction in mice fed a high-fructose diet*. *Am J Physiol Heart Circ Physiol*, 2008. **295**(6): p. H2223-30.
 28. Takimoto, E., et al., *Chronic inhibition of cyclic GMP phosphodiesterase 5A prevents and reverses cardiac hypertrophy*. *Nat Med*, 2005. **11**(2): p. 214-22.



Extracellular Superoxide Dismutase
Deficiency Exacerbates Pressure
Overload–Induced Left Ventricular
Hypertrophy and Dysfunction

7

Zhongbing Lu*, Xin Xu*, Xinli Hu, Guangshuo Zhu, Ping
Zhang, Elza D. van Deel, Joel P. French, John T. Fassett,
Tim D. Oury, Robert J. Bache, Yingjie Chen

*The first 2 authors contributed equally to this work.

Hypertension 2008; 51(1):19-25.

Abstract

Extracellular superoxide dismutase (SOD) contributes only a small fraction to total SOD activity in the normal heart but is strategically located to scavenge free radicals in the extracellular compartment. To examine the physiological significance of extracellular SOD in the response of the heart to hemodynamic stress, we studied the effect of extracellular SOD deficiency on transverse aortic constriction (TAC)-induced left ventricular remodeling. Under unstressed conditions extracellular SOD deficiency had no effect on myocardial total SOD activity, the ratio of glutathione:glutathione disulfide, nitrotyrosine content, or superoxide anion production but resulted in small but significant increases in myocardial fibrosis and ventricular mass. In response to TAC for 6 weeks, extracellular SOD-deficient mice developed more severe left ventricular hypertrophy (heart weight increased 2.56-fold in extracellular SOD-deficient mice as compared with 1.99-fold in wild-type mice) and pulmonary congestion (lung weight increased 2.92-fold in extracellular SOD-deficient mice as compared with 1.84-fold in wild-type mice). Extracellular SOD-deficient mice also had more ventricular fibrosis, dilation, and a greater reduction of left ventricular fractional shortening and rate of pressure development after TAC. TAC resulted in greater increases of ventricular collagen I, collagen III, matrix metalloproteinase-2, matrix metalloproteinase-9, nitrotyrosine, and superoxide anion production. TAC also resulted in a greater decrease of the ratio of glutathione:glutathione disulfide in extracellular SOD-deficient mice. The finding that extracellular SOD deficiency had minimal impact on myocardial overall SOD activity but exacerbated TAC induced myocardial oxidative stress, hypertrophy, fibrosis, and dysfunction indicates that the distribution of extracellular SOD in the extracellular space is critically important in protecting the heart against pressure overload.

Introduction

Congestive heart failure (CHF) because of a variety of conditions is associated with depressed antioxidant reserves and increased products of oxygen free radical reactions, suggesting that oxidative stress might contribute to contractile dysfunction in the failing heart.¹ Superoxide dismutase (SOD) is the first line of defense against free radical attack. Three SOD isozymes have been identified, including a copper/zinc-containing SOD (SOD1), which is primarily cytosolic in location, a mitochondrial manganese SOD (SOD2), and an extracellular SOD (SOD3). SOD3 is a glycoprotein secreted into the extracellular fluid by fibroblasts that bind to sulfated polysaccharides, such as heparin and heparan sulfate,^{2,3} as well as to other matrix components.^{4,5} As a result, SOD3 binds to the surface of endothelial cells and the extracellular matrix, which has a high abundance of heparan sulfate.⁶ Several recent studies have demonstrated that SOD3 expression is decreased in the failing heart, and this was associated with endothelial dysfunction.⁷⁻⁹ In addition, patients in whom SOD3 binding to endothelial cells is decreased as the result of substitution of arginine-213 by glycine (R213G) have an increased incidence of hypertension¹⁰ and an increased risk of ischemic heart disease,^{10,11} suggesting that impaired SOD3 binding can increase the vulnerability to cardiovascular disease. However, because SOD3 has a minimal impact on total myocardial SOD activity, it is uncertain whether SOD3 can influence the response of the heart to hemodynamic overload. To address this question, we examined the effect of SOD3 gene deletion (SOD3^{-/-}) on myocardial oxidative stress and the development of left ventricular (LV) hypertrophy and CHF in hearts exposed to systolic overload produced by transverse aortic constriction (TAC). Here we report that SOD3^{-/-} had no effect on LV function or oxidative stress under normal conditions but resulted in evidence of increased oxidative stress in response to TAC, and this was associated with more severe LV dilation and contractile dysfunction, as well as greater myocardial hypertrophy and fibrosis. The findings imply that the specific distribution of SOD3 is important in protecting the overloaded heart.

7

Methods

Mice and TAC-Induced Systolic Overload

Male C57BL/6 (Taconic, Germantown, NY) and SOD3^{-/-} mice (congenic with the Taconic C57BL/6 strain)^{3,12} 8 to 10 weeks of age were used. This study was approved by the animal care and use committee of the University of Minnesota. The TAC procedure was performed on wild-type (n=19) and SOD3^{-/-} mice (n=25) using the minimally invasive suprasternal approach described by Hu et al.¹³ Body weight and age-matched wild-type mice (n=12) and SOD3^{-/-} mice (n=8) were used as controls.

Echocardiography and Evaluation of LV Hemodynamics

Mice were anesthetized with 1.5% isoflurane. Echocardiographic images were obtained with a Visualsonics high-resolution Vevo 660 system as described previously (n=8 to 13 mice each group).¹⁴ For aortic and LV pressure measurement, a 1.2-F pressure catheter (Scisense Inc) was introduced through the right common carotid artery into the

ascending aorta and then advanced into the LV for measurement of systolic and end-diastolic pressures and positive and negative LV rate of pressure development (dp/dt_{\max}) as described previously.¹⁴

Western Blots, Chemical Analysis, and Histological Analysis

The detailed methods for Western blot, chemical analysis for SOD activity, superoxide anion production, the ratio of glutathione (GSH):glutathione disulfide (GSSG), and thiobarbituric acid reactive substances (TBARS) content are included in the online supplementary data (please see <http://hyper.ahajournals.org>). Tissue sections (8 μm) from the central portion of the LV were stained with Sirius red (Sigma) for fibrosis and fluorescein isothiocyanate-conjugated wheat germ agglutinin (AF488, Invitrogen) to evaluate myocyte size. For mean myocyte size, the cross-sectional area of ≥ 120 cells per sample and 4 samples per group was averaged. The percentage of fibrosis was determined as described previously.¹⁵

Data and Statistical Analysis

All of the values are expressed as mean \pm SE. Statistical significance was defined as $P < 0.05$. One-way ANOVA was used to test each variable for differences among the treatment groups with StatView (SAS Institute Inc). If ANOVA demonstrated a significant effect, pairwise posthoc comparisons were made with Fisher's least significant difference test.

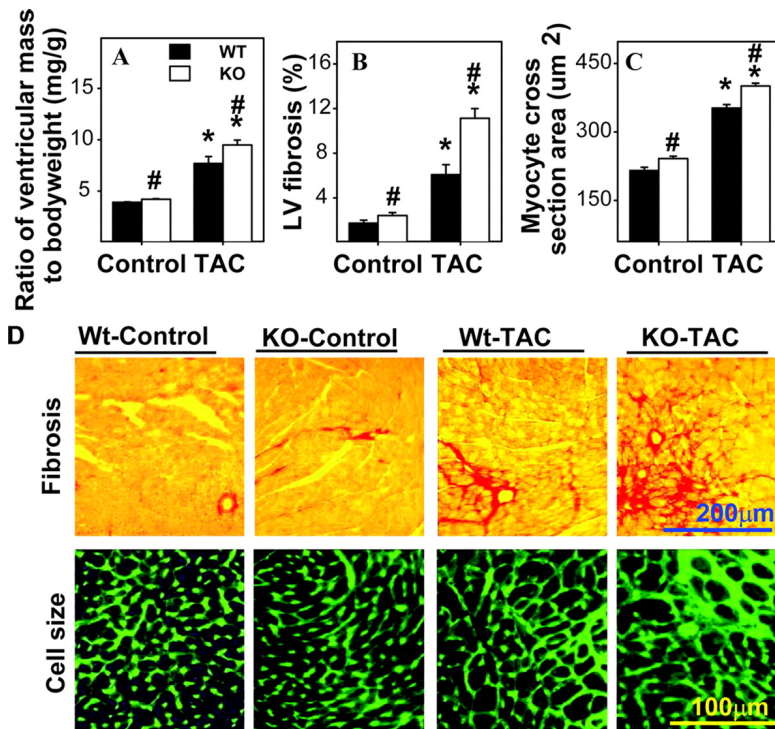


Figure 1. SOD3^{-/-} exacerbates TAC-induced ventricular hypertrophy (A), myocardial fibrosis (B and D), and cardiac myocyte hypertrophy (C and D). * $P < 0.05$ vs the corresponding control; # $P < 0.05$ vs wild-type mice (Wt).

Results

SOD3^{-/-} Exacerbated TAC-Induced Ventricular Hypertrophy and Fibrosis

Under control conditions, ventricular weight and the ratio of ventricular weight:body weight were slightly but significantly increased in SOD3^{-/-} mice as compared with wild-type mice (Figure 1 and Table 1). Histological staining of LV tissue showed that SOD3^{-/-} mice had a slight but significant increase of ventricular fibrosis and the cardiac myocyte cross-sectional area in comparison with wild-type mice under control conditions (Figure 1). TAC for 6 weeks resulted in a significantly greater increase of ventricular weight and the ratio of ventricular weight:body weight in the SOD3^{-/-} mice versus the controls (Figure 1A and Table 1). TAC resulted in a significantly greater increase in the cardiac myocyte cross-sectional area and myocardial fibrosis in the SOD3^{-/-} mice as compared with the wild-type mice (Figure 1B through 1D), indicating that the greater LV hypertrophy in the SOD3^{-/-} mice in response to TAC resulted from increases of both myocyte size and ventricular fibrosis. The fibrosis after TAC occurred predominantly in a perivascular location (Figure 1B and 1D). Consistent with the increased fibrosis, TAC resulted in a significantly greater increase of ventricular collagen I and collagen III protein content in the SOD3^{-/-} than in the wild-type mice (Figure 2A and 2B). In addition, a significant increase of myocardial matrix metalloproteinase (MMP)-2 and MMP-9 protein content was observed in the SOD3^{-/-} mice both under control conditions and after TAC (Figure 2A and 2B). Although the mortality rate tended to be higher in the SOD3^{-/-} mice in the first week after TAC, this difference was not significant, and total mortality rate during the 6-week period after TAC was not different between SOD3^{-/-} (48%) and wild-type mice (47%).

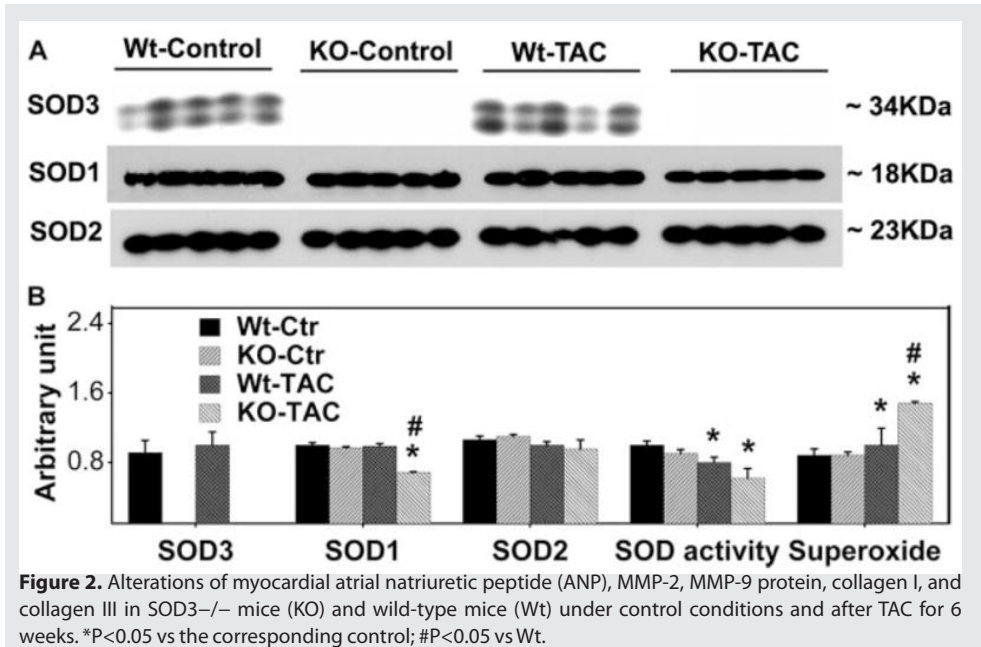
Table 1. Anatomic and Functional Data for Wild-Type and SOD3^{-/-} Mice

Parameter	Wt-Control	SOD3 ^{-/-} Control	Wt-TAC	SOD3 ^{-/-} TAC
Body weight, g	26.0 ± 0.6	25.7 ± 0.6	26.8 ± 1.4	26.7 ± 0.5
Ventricular mass, mg	102 ± 1.6	108 ± 2.1 [†]	199 ± 7.5 [*]	256 ± 9.2 ^{††}
Ratio of ventricular mass/body weight, mg/g	3.92 ± 0.04	4.21 ± 0.05 [†]	7.69 ± 0.68 [*]	9.49 ± 0.47 ^{††}
Lung mass, mg	134 ± 1.4	135 ± 5.7	238 ± 45 [*]	406 ± 40 ^{††}
Ratio of lung mass/body weight, mg/g	5.17 ± 0.11	5.23 ± 0.12	9.6 ± 2.4 [*]	15.4 ± 1.6 ^{††}
Heart rate, bpm	542 ± 22	534 ± 9.0	506 ± 23 [*]	503 ± 13 ^{††}
LV end-systolic diameter, mm	2.11 ± 0.11	2.35 ± 0.12	4.23 ± 0.24 [*]	5.06 ± 0.13 ^{††}
LV end-diastolic diameter, mm	3.96 ± 0.11	4.15 ± 0.05	5.08 ± 0.12 [*]	5.74 ± 0.11 ^{††}
LV fractional shortening, %	71.7 ± 1.7	66.7 ± 2.1	30.6 ± 4.9 [*]	22.4 ± 1.5 ^{††}
LV ejection fraction, %	84.8 ± 1.6	80.5 ± 1.8	41.4 ± 5.6	31.5 ± 2.0
LV posterior wall thickness at end diastole, mm	0.65 ± 0.01	0.68 ± 0.01	0.89 ± 0.04 [*]	0.88 ± 0.02 [†]
LV posterior wall thickness at end systole, mm	1.04 ± 0.02	1.10 ± 0.01	1.14 ± 0.05	1.08 ± 0.03
Mean aortic pressure, mmHg	74.4 ± 3.8	73.9 ± 3.7	112 ± 6.0 [*]	97.7 ± 5.4 ^{††}
Systolic LV pressure, mmHg	96.0 ± 2.1	98.8 ± 3.0	168 ± 10.1 [†]	138 ± 8.1 ^{††}
LV end diastolic pressure, mmHg	7.4 ± 1.2	6.5 ± 0.9	35.6 ± 2.2 [*]	42.9 ± 1.8 ^{††}
LV dP/dt _{max} , mmHg/s	8341 ± 451	8230 ± 644	5596 ± 536 [*]	4134 ± 536 ^{††}
LV dP/dt _{min} , mmHg/s	-6739 ± 768	-7256 ± 315	-5781 ± 444 [*]	-4176 ± 477 ^{††}

**P*<0.05 vs corresponding control conditions; †*P*<0.05 vs wild-type mice.

SOD3^{-/-} Exacerbated TAC-Induced LV Dysfunction

Aortic pressure, LV systolic pressure, and LV dP/dt_{max} were not different between wild-type mice and SOD3^{-/-} mice under control conditions. TAC caused significant increases of LV



systolic pressure in both wild-type and SOD3^{-/-} mice (Table 1). Six weeks after TAC, LV peak systolic pressure, LV dp/dt_{max} , and LV dp/dt_{min} were significantly less in SOD3^{-/-} mice as compared with wild-type mice, indicating LV dysfunction (Table 1). The lower LV systolic pressure in the SOD3^{-/-} mice 6 weeks after TAC could not be ascribed to a lesser initial pressure overload in these mice, because the identical TAC procedure was performed on both groups by the same surgeon randomly on the same days, and the SOD3^{-/-} mice developed more LV hypertrophy after TAC than did the wild-type mice.

Echocardiographic imaging of the heart 6 weeks after TAC demonstrated significant increases of LV end-systolic diameter and LV end-diastolic diameter in both SOD3^{-/-} and wild-type mice in comparison with mice of similar body weight without TAC (Table 1). However, the degree of LV dilatation, assessed as LV end-diastolic diameter, was significantly greater in SOD3^{-/-} mice than in wild-type mice. TAC caused significant increases in LV end-diastolic wall thickness that were similar in SOD3^{-/-} and wild-type mice (Table 1); the greater increase in LV mass in the SOD3^{-/-} mice was accounted for by the increased LV chamber diameter in these animals. Systolic dysfunction was more severe in the SOD3^{-/-} mice, as demonstrated by greater decreases of LV systolic shortening fraction and ejection fraction after TAC in the SOD3^{-/-} mice (Table 1), as well as a greater increase in end-systolic diameter, as compared with the wild-type mice (Table 1).

TAC resulted in significantly greater increases in lung weight and ratio of lung weight:body weight in SOD3^{-/-} versus wild-type mice (Table 1), suggesting more pulmonary congestion in the SOD3^{-/-} mice. In addition, SOD3^{-/-} also exacerbated the TAC-induced increase of myocardial atrial natriuretic peptide (Figure 2A and 2B). Taken together, these

data indicate that the SOD3^{-/-} mice developed more LV dysfunction in response to the sustained pressure overload produced by TAC.

SOD3^{-/-} Had No Apparent Effect on Oxidative Stress in Normal Hearts

As anticipated, SOD3 was undetectable in the SOD3^{-/-} mice (Figure 3), and SOD3^{-/-} did not affect myocardial SOD1 or SOD2 protein content under control conditions (Figure 3). Total myocardial SOD activity and myocardial superoxide anion content were not different between wild-type and SOD3^{-/-} mice under control conditions (Figure 3), consistent with previous reports that SOD3 contributes only a small fraction to overall myocardial SOD activity.^{2,16} In addition, myocardial TBARS and nitrotyrosine were not different between SOD3^{-/-} mice and wild-type mice under control conditions (Figure 4). Both myocardial GSH and GSSG were decreased in the SOD3^{-/-} mice, but the ratio of GSH:GSSG was not different between wild-type and SOD3^{-/-} mice. Myocardial catalase protein content was also not different between wild-type and SOD3^{-/-} mice (data not shown). These findings indicate that SOD3^{-/-} had no detectable effect on oxidative stress in the normal heart.

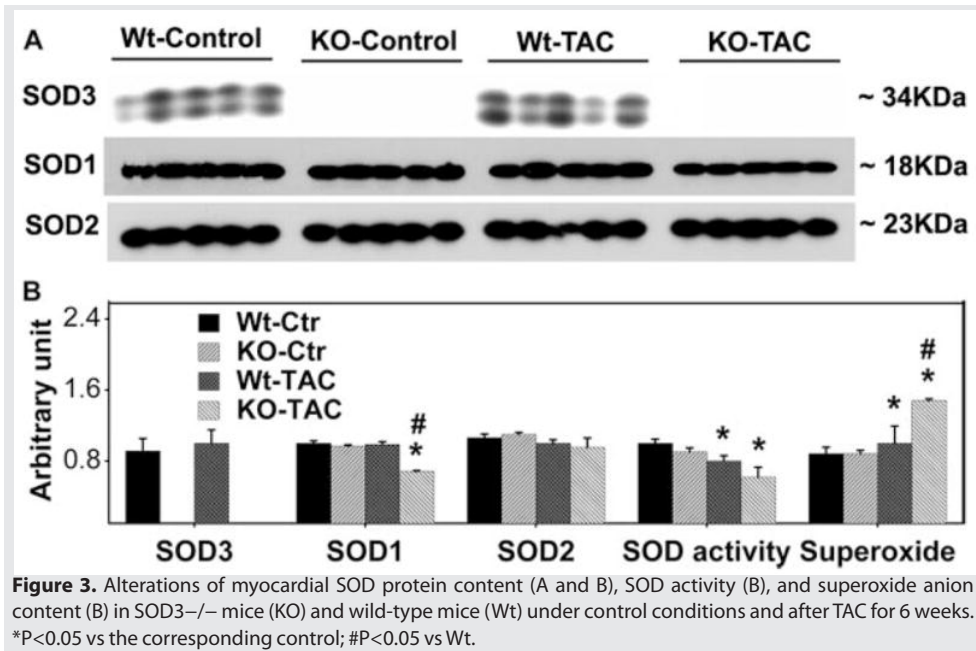


Figure 3. Alterations of myocardial SOD protein content (A and B), SOD activity (B), and superoxide anion content (B) in SOD3^{-/-} mice (KO) and wild-type mice (Wt) under control conditions and after TAC for 6 weeks. *P<0.05 vs the corresponding control; #P<0.05 vs Wt.

SOD3^{-/-} Exacerbated TAC-Induced Evidence of Myocardial Oxidative Stress

In comparison with wild-type mice, the ratio of myocardial GSH:GSSG was significantly decreased in SOD3^{-/-} mice 6 weeks after TAC (Figure 4). TAC caused increases of myocardial TBARS and nitrotyrosine content both in wild-type mice and in SOD3^{-/-} mice, but these increases were significantly greater in the SOD3^{-/-} mice than in the wild-type mice (Figure 4). Consistent with a greater increase of oxidative stress in SOD3^{-/-} mice after TAC, TAC significantly increased myocardial superoxide production in the SOD3^{-/-} mice as compared with wild-type mice (in vitro assay; Figure 3). After TAC, myocardial SOD activity was significantly decreased both in wild-type mice and in SOD3^{-/-} mice with no

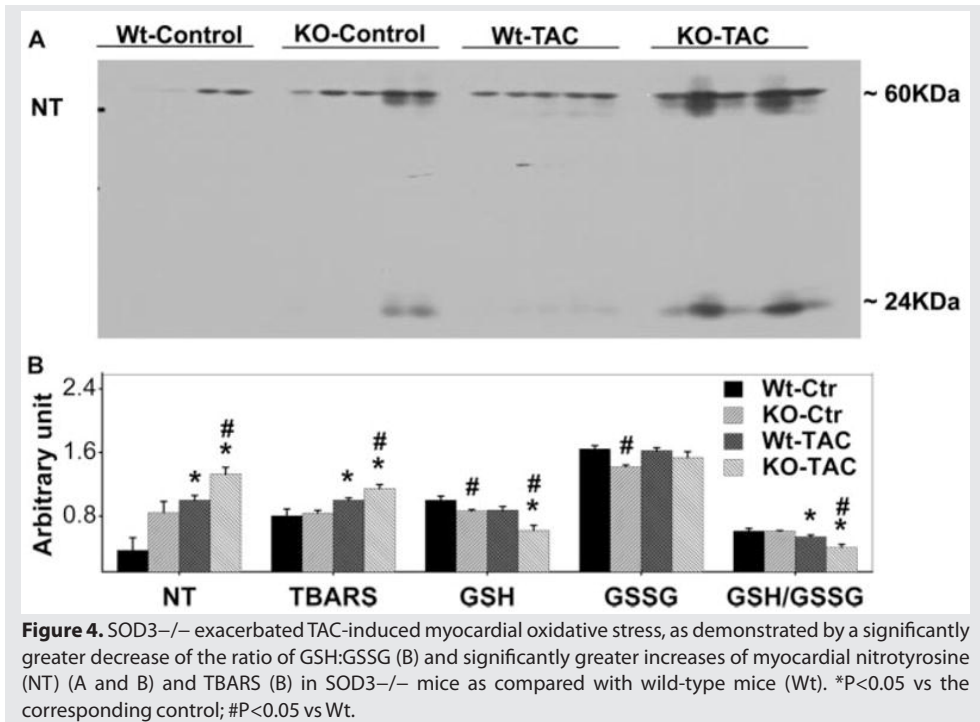


Figure 4. SOD3^{-/-} exacerbated TAC-induced myocardial oxidative stress, as demonstrated by a significantly greater decrease of the ratio of GSH:GSSG (B) and significantly greater increases of myocardial nitrotyrosine (NT) (A and B) and TBARS (B) in SOD3^{-/-} mice as compared with wild-type mice (Wt). *P<0.05 vs the corresponding control; #P<0.05 vs Wt.

7 difference between the groups (Figure 3). Myocardial catalase protein content was not different between wild-type and SOD3^{-/-} mice after TAC (data not shown). Taken together, the data indicate a greater degree of myocardial oxidative stress in SOD3^{-/-} mice than in control mice after TAC.

Discussion

The major new findings of this study are that SOD3^{-/-} had no detectable effect on ventricular SOD activity, indicators of myocardial oxidative stress, or LV function in the unstressed heart but exacerbated LV oxidative stress, hypertrophy, dilation, fibrosis, and dysfunction in response to pressure overload produced by TAC. These findings imply that the specific distribution of SOD3, rather than its contribution to total SOD activity, is critically important in protecting the heart from hemodynamic overload. To our knowledge, these findings provide the first direct evidence that extracellular SOD exerts a critical role in protecting the heart against pressure overload-induced oxidative stress and contractile dysfunction.

In the present study SOD3^{-/-} had no effect on ventricular SOD activity under control conditions. This is consistent with previous reports that SOD3 contributes minimally to overall SOD activity in the heart.^{2,16} Although myocardial TBARS and nitrotyrosine content, the ratio of GSH:GSSG, and superoxide anion production were unchanged in the SOD3^{-/-}

mice under unstressed conditions, the findings of mild but significant increases of ventricular fibrosis, myocyte hypertrophy, and the ratio of ventricular mass:body weight indicate that the absence of SOD3 did have a modest negative impact on the heart under control conditions. Therefore, the inability to detect increased oxidative stress in the hearts of SOD3^{-/-} mice under control conditions likely indicates that the methods were not sensitive enough to detect a small increase of oxidative stress in the SOD3^{-/-} hearts. The increased myocardial fibrosis in the SOD3^{-/-} mice under control conditions is analogous to previous reports indicating that SOD3 has antifibrotic functions in the lung.^{5,12} An increase of myocardial fibrosis is often associated with a parallel increase of MMP protein content and activity.^{2,16} The greater increase of collagen I, collagen III, MMP-2, and MMP-9 in the SOD3^{-/-} hearts after TAC is consistent with the greater degree of myocardial fibrosis in this strain.

Although no previous reports have directly examined the effect of SOD3^{-/-} on systolic overload-induced LV hypertrophy and CHF, there is evidence that abnormalities of SOD3 can contribute to cardiovascular disease. In patients with coronary artery disease, both SOD activity in coronary artery segments and endothelium-bound SOD3 released by bolus injection of heparin were decreased.^{8,9} The lack of SOD3 exacerbates angiotensin-induced hypertension and vascular oxidative stress and attenuates vascular NO bioavailability.¹⁷⁻¹⁹ It is consequently not surprising that SOD3 deficiency would have a role in the development of vascular disease or hypertension. The present findings demonstrate that SOD3 also exerts protective effects when the heart is exposed to systolic overload.

The decrease of the GSH:GSSG ratio and the increases of TBARS, nitrotyrosine, and myocardial superoxide anion production in the SOD3^{-/-} mice exposed to TAC in the present study are consistent with previous reports demonstrating that oxidative stress is increased in the failing heart.^{1,14,20,21} Thus, in animals with aortic constriction, the development of heart failure was associated with increases of myocardial nitrotyrosine,^{14,21} TBARS, and superoxide^{14,21,22} and a decrease of the ratio of GSH:GSSG.^{22,23} Several sources for increased oxidative stress have been identified in the failing heart, including the mitochondrial respiratory chain,²⁴ uncoupled endothelial NO synthase,^{14,21} reduced nicotinamide-adenine dinucleotide phosphate oxidase,²⁵ and xanthine oxidase.²⁶ There are several sources of superoxide in the endothelium where SOD3 has its principal site of action. We reported recently that systolic overload produced by TAC in mice caused increased expression of myocardial inducible NO synthase (iNOS) and endothelial NO synthase monomer (a structure that generates superoxide rather than NO), whereas iNOS deletion or selective pharmacological iNOS inhibition with 1400 W decreased markers of oxidative stress and improved LV function, suggesting that either iNOS uncoupling or iNOS-induced endothelial NO synthase uncoupling contributed to the increased oxidative stress and development of CHF in the wild-type mice.^{2,16} Furthermore, administration of BH4 to prevent NOS uncoupling,^{14,21} selective inhibition of xanthine oxidase, or reduced nicotinamide-adenine dinucleotide phosphate oxidase has been reported to attenuate oxidative stress and ventricular dysfunction in this model of cardiac overload.

Although there is evidence of increased free radical production in the failing heart, there

is also evidence that decreased antioxidant reserves contribute to the increased oxidative stress in several models of myocardial dysfunction. Thus, CHF is associated with decreased SOD3 protein content and activity,^{8,9,27} and overexpression of SOD3 has been reported to protect the heart against ischemia-reperfusion injury²⁸ and to reduce postinfarct LV remodeling.²⁹ The present study shows that a decrease of SOD3 is not only a consequence of CHF but could also contribute to the development of CHF. The decrease of myocardial SOD activity and SOD1 protein content after TAC is consistent with previous reports in pressure overload–induced heart failure in guinea pigs,²⁰ and myocardial infarct–induced heart failure rats.³⁰ The significant decrease of SOD1 in SOD3^{-/-} mice after TAC may partially contribute to the increased ventricular oxidative stress in SOD3^{-/-} mice after TAC, although the molecular mechanism for the decrease of SOD1 in SOD3^{-/-} mice after TAC is not clear. Oxidative stress has been shown to impair mitochondrial metabolism and contractile function, so it is reasonable that increased oxidative stress could exacerbate the contractile dysfunction in the SOD3^{-/-} mice.

A limitation of the present study is that the effect of SOD3^{-/-} on ventricular structure and function was only studied at baseline and 6 weeks after TAC so that information about changes in kinetics between wild-type and SOD3^{-/-} mice cannot be determined. It should be pointed out that, because SOD3 was knocked out from these mice since conception, the mice have had a lifetime to adapt to the loss of SOD3, which might have allowed them to preserve LV function under basal conditions. Therefore, by using the global SOD3^{-/-} mice, we may underestimate the physiological significance of SOD3 in regulating normal ventricular function.

The finding that SOD3^{-/-} exacerbated TAC-induced LV oxidative stress, hypertrophy, dilation, fibrosis, and contractile dysfunction indicates that SOD3 provides an important protective effect against oxidative stress and contractile dysfunction when the heart is exposed to chronic pressure overload.

Perspectives

SOD3 is strategically located to scavenge free radicals in the extracellular compartment. However, it was not clear whether SOD3 can abrogate oxidative stress or modify ventricular remodeling after pressure overload. The present finding demonstrates for the first time that SOD3^{-/-} exacerbated LV oxidative stress, hypertrophy, dilation, fibrosis, and dysfunction in response to pressure overload produced by TAC, indicating that SOD3 is critically important in protecting the heart from hemodynamic overload. These findings provide the first direct evidence that a reduction of extracellular SOD is not only a consequence of CHF but could also contribute to its development. Therefore, it is anticipated that strategies to decrease extracellular oxidative stress may protect the heart from pressure overload–induced ventricular hypertrophy and CHF.

Acknowledgments

We are grateful to Dr Stefan Marklund of Umea University, Umea, Sweden, for supplying breeding pairs of SOD3^{-/-} mice and comments for the discussion.

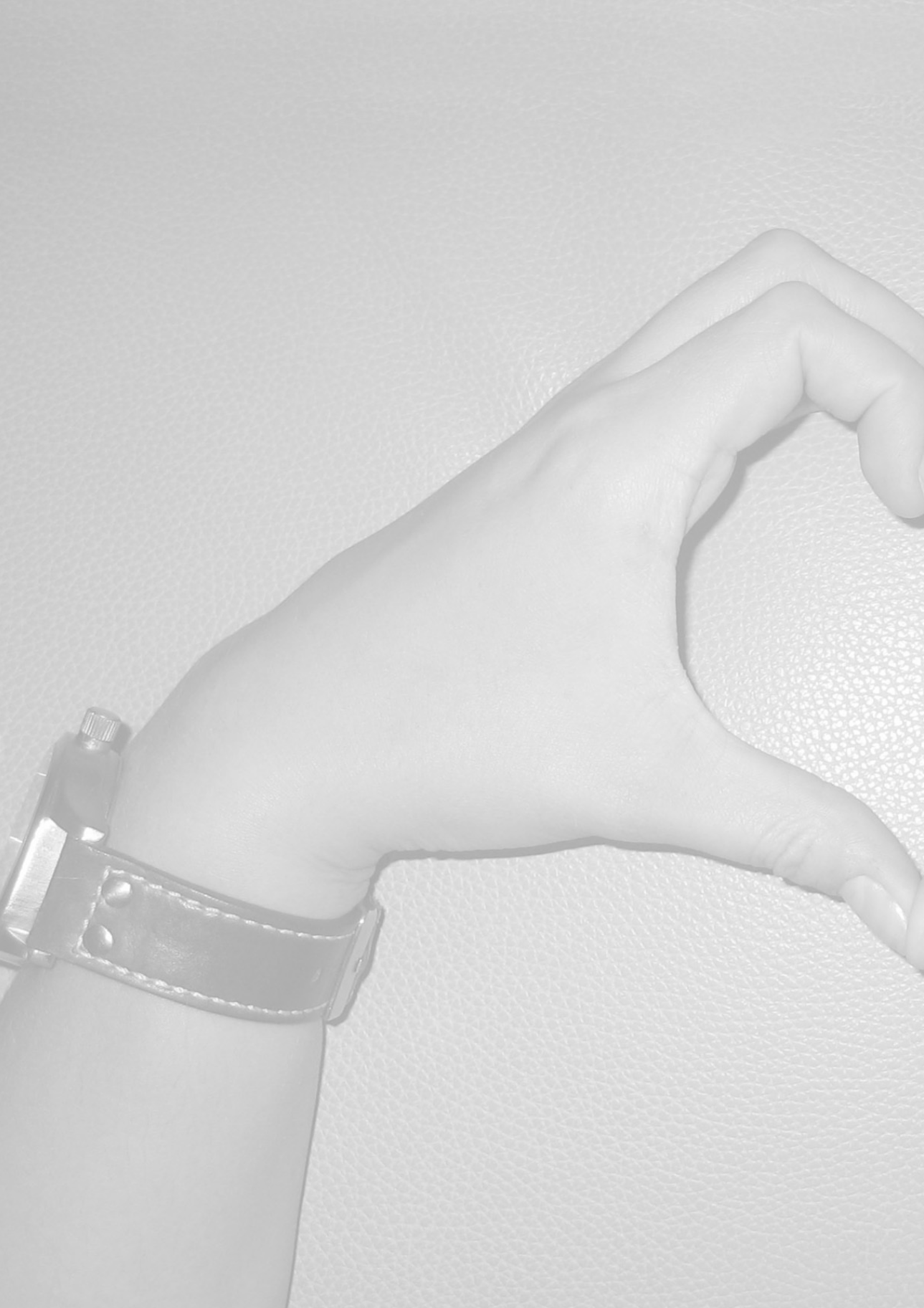
Sources of Funding

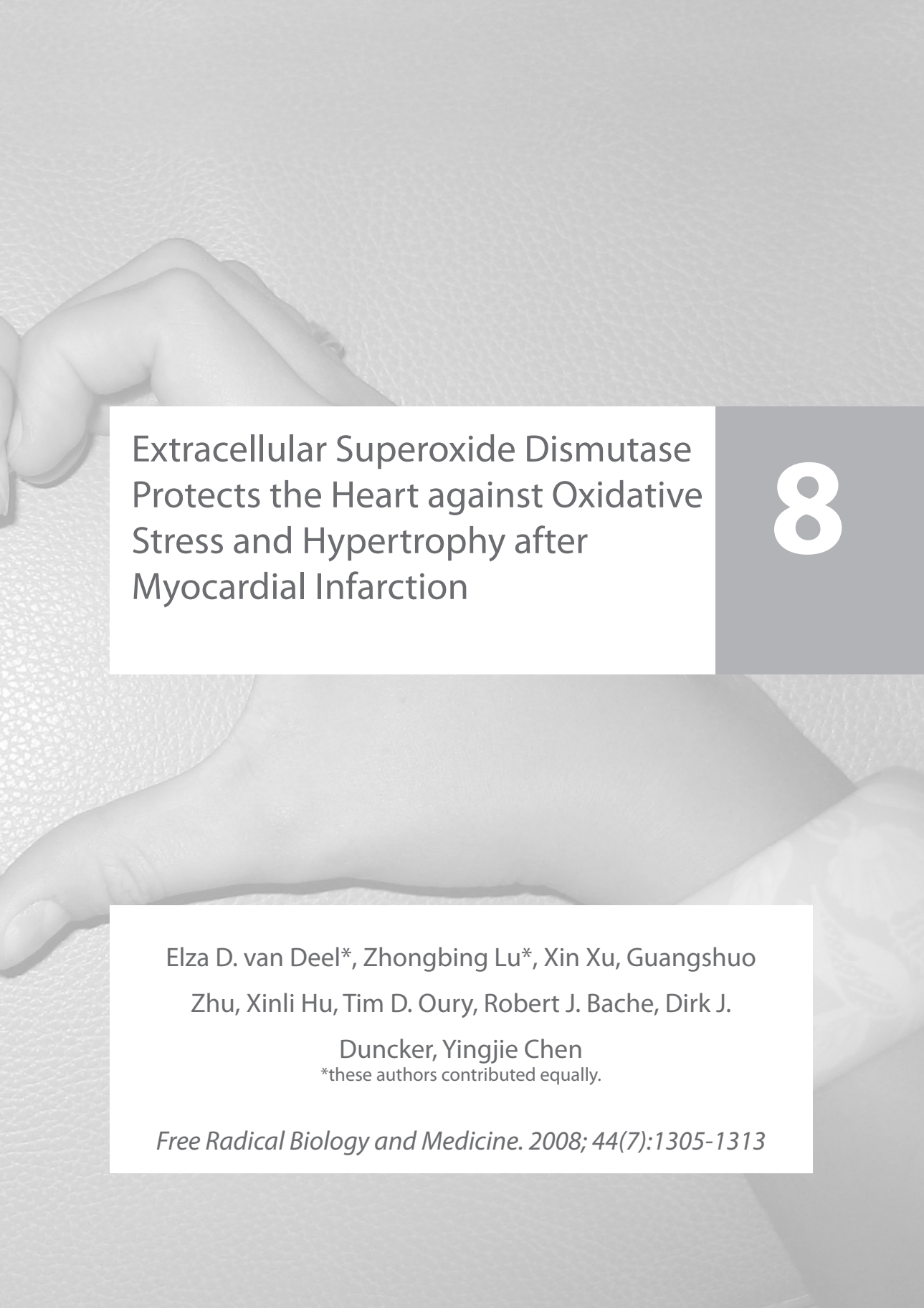
This study was supported by National Heart, Lung, and Blood Institute grants HL71790 (Y.C.), HL21872 (R.J.B.), and HL63700 (T.D.O.) from the National Institutes of Health. P.Z. is recipient of a scientist development award from the American Heart Association. X.X. is a recipient of a postdoctoral fellowship award from the American Heart Association. J.T.F. is a recipient of a Scientist Developer Award from the American Heart Association.

References

1. Giordano FJ. *Oxygen, oxidative stress, hypoxia, and heart failure*. J Clin Invest. 2005; 115: 500–508.
2. Marklund SL. *Extracellular superoxide dismutase and other superoxide dismutase isoenzymes in tissues from nine mammalian species*. Biochem J. 1984; 222: 649–655.
3. Carlsson LM, Jonsson J, Edlund T, Marklund SL. *Mice lacking extracellular superoxide dismutase are more sensitive to hyperoxia*. Proc Natl Acad Sci U S A. 1995; 92: 6264–6268.
4. Petersen SV, Oury TD, Ostergaard L, Valnickova Z, Wegrzyn J, Thogersen IB, Jacobsen C, Bowler RP, Fattman CL, Crapo JD, Enghild JJ. *Extracellular superoxide dismutase (EC-SOD) binds to type I collagen and protects against oxidative fragmentation*. J Biol Chem. 2004; 279: 13705–13710.
5. Fattman CL, Schaefer LM, Oury TD. *Extracellular superoxide dismutase in biology and medicine*. Free Radic Biol Med. 2003; 35: 236–256.
6. Sandstrom J, Carlsson L, Marklund SL, Edlund T. *The heparin-binding domain of extracellular superoxide dismutase C and formation of variants with reduced heparin affinity*. J Biol Chem. 1992; 267: 18205–18209.
7. Chen Y, Hou M, Li Y, Traverse JH, Zhang P, Salvemini D, Fukai T, Bache RJ. *Increased superoxide production causes coronary endothelial dysfunction and depressed oxygen consumption in the failing heart*. Am J Physiol Heart Circ Physiol. 2005; 288: H133–H141.
8. Landmesser U, Merten R, Spiekermann S, Buttner K, Drexler H, Hornig B. *Vascular extracellular superoxide dismutase activity in patients with coronary artery disease: relation to endothelium-dependent vasodilation*. Circulation. 2000; 101: 2264–2270.
9. Landmesser U, Spiekermann S, Dikalov S, Tatge H, Wilke R, Kohler C, Harrison DG, Hornig B, Drexler H. *Vascular oxidative stress and endothelial dysfunction in patients with chronic heart failure: role of xanthine oxidase and extracellular superoxide dismutase*. Circulation. 2002; 106: 3073–3078.
10. Juul K, Tybjaerg-Hansen A, Marklund S, Heegaard NH, Steffensen R, Sillesen H, Jensen G, Nordestgaard BG. *Genetically reduced antioxidative protection and increased ischemic heart disease risk: the Copenhagen City Heart Study*. Circulation. 2004; 109: 59–65.
11. Yamada H, Yamada Y, Adachi T, Fukatsu A, Sakuma M, Futenma A, Kakumu S. *Protective role of extracellular superoxide dismutase in hemodialysis patients*. Nephron. 2000; 84: 218–223.
12. Fattman CL, Tan RJ, Tobolewski JM, Oury TD. *Increased sensitivity to asbestos-induced lung injury in mice lacking extracellular superoxide dismutase*. Free Radic Biol Med. 2006; 40: 601–607.
13. Hu P, Zhang D, Swenson L, Chakrabarti G, Abel ED, Litwin SE. *Minimally invasive aortic banding in mice: effects of altered cardiomyocyte insulin signaling during pressure overload*. Am J Physiol Heart Circ Physiol. 2003; 285: H1261–H1269.
14. Zhang P, Xu X, Hu X, van Deel ED, Zhu G, Chen Y. *Inducible nitric oxide synthase deficiency protects the heart from systolic overload-induced ventricular hypertrophy and congestive heart failure*. Circ Res. 2007; 100: 1089–1098.
15. Howard CV, Reed MG. *Estimation of component volume and volume fraction*. In: Catherine J, ed. Unbiased Stereology, Three-Dimensional Measurement in Microscopy. Abingdon, United Kingdom: BIOS Scientific Publishers; 2005: 17–64.
16. Marklund SL. *Extracellular superoxide dismutase in human tissues and human cell lines*. J Clin Invest. 1984; 74: 1398–1403.
17. Gongora MC, Qin Z, Laude K, Kim HW, McCann L, Folz JR, Dikalov S, Fukai T, Harrison DG. *Role of extracellular superoxide dismutase in hypertension*. Hypertension. 2006; 48: 473–481.
18. Jung O, Marklund SL, Geiger H, Pedrazzini T, Busse R, Brandes RP. *Extracellular superoxide dismutase is a major determinant of nitric oxide bioavailability: in vivo and ex vivo evidence from eCSOD-deficient mice*. Circ Res. 2003; 93: 622–629.
19. Welch WJ, Chabrashvili T, Solis G, Chen Y, Gill PS, Aslam S, Wang X, Ji H, Sandberg K, Jose P, Wilcox CS. *Role of extracellular superoxide dismutase in the mouse angiotensin slow pressor response*. Hypertension. 2006; 48: 934–941.
20. Dhalla AK, Singal PK. *Antioxidant changes in hypertrophied and failing guinea pig hearts*. Am J Physiol. 1994; 266: H1280–H1285.
21. Takimoto E, Champion HC, Li M, Ren S, Rodriguez ER, Tavazzi B, Lazzarino G, Paolocci N, Gabrielson KL, Wang Y, Kass DA. *Oxidant stress from nitric oxide synthase-3 uncoupling stimulates cardiac pathologic*

- remodeling from chronic pressure load.* J Clin Invest. 2005; 115: 1221–1231.
22. Jacob MH, Pontes MR, Araujo AS, Barp J, Irigoyen MC, Llesuy SF, Ribeiro MF, Bello-Klein A. *Aortic-banding induces myocardial oxidative stress and changes in concentration and activity of antioxidants in male Wistar rats.* Life Sci. 2006; 79: 2187–2193.
 23. Saraiva RM, Minhas KM, Zheng M, Pitz E, Treuer A, Gonzalez D, Schuleri KH, Vandegaer KM, Barouch LA, Hare JM. *Reduced neuronal nitric oxide synthase expression contributes to cardiac oxidative stress and nitroso-redox imbalance in ob/ob mice.* Nitric Oxide. 2007; 16: 331–338.
 24. Ide T, Tsutsui H, Kinugawa S, Utsumi H, Kang D, Hattori N, Uchida K, Arimura K, Egashira K, Takeshita A. *Mitochondrial electron transport complex I is a potential source of oxygen free radicals in the failing myocardium.* Circ Res. 1999; 85: 357–363.
 25. Gupte SA, Levine RJ, Gupte RS, Young ME, Lionetti V, Labinskyy V, Floyd BC, Ojaimi C, Bellomo M, Wolin MS, Recchia FA. *Glucose-6-phosphate dehydrogenase-derived NADPH fuels superoxide production in the failing heart.* J Mol Cell Cardiol. 2006; 41: 340–349.
 26. Berry CE, Hare JM. *Xanthine oxidoreductase and cardiovascular disease: molecular mechanisms and pathophysiological implications.* J Physiol. 2004; 555: 589–606.
 27. Iida S, Chu Y, Francis J, Weiss RM, Gunnett CA, Faraci FM, Heistad DD. *Gene transfer of extracellular superoxide dismutase improves endothelial function in rats with heart failure.* Am J Physiol Heart Circ Physiol. 2005; 289: H525–H532.
 28. Li Q, Bolli R, Qiu Y, Tang XL, Murphree SS, French BA. *Gene therapy with extracellular superoxide dismutase attenuates myocardial stunning in conscious rabbits.* Circulation. 1998; 98: 1438–1448.
 29. Li Q, Bolli R, Qiu Y, Tang XL, Guo Y, French BA. *Gene therapy with extracellular superoxide dismutase protects conscious rabbits against myocardial infarction.* Circulation. 2001; 103: 1893–1898.
 30. Hill MF, Singal PK. *Antioxidant and oxidative stress changes during heart failure subsequent to myocardial infarction in rats.* Am J Pathol. 1996; 148: 291–300.





Extracellular Superoxide Dismutase
Protects the Heart against Oxidative
Stress and Hypertrophy after
Myocardial Infarction

8

Elza D. van Deel*, Zhongbing Lu*, Xin Xu, Guangshuo
Zhu, Xinli Hu, Tim D. Oury, Robert J. Bache, Dirk J.
Duncker, Yingjie Chen

*these authors contributed equally.

Free Radical Biology and Medicine. 2008; 44(7):1305-1313

Abstract

Extracellular superoxide dismutase (EC-SOD) contributes only a small fraction to total SOD activity in the heart but is strategically located to scavenge free radicals in the extracellular compartment. EC-SOD expression is decreased in myocardial-infarction (MI)-induced heart failure, but whether EC-SOD can abrogate oxidative stress or modify MI-induced ventricular remodeling has not been previously studied. Consequently, the effects of EC-SOD gene deficiency (EC-SOD KO) on left ventricular (LV) oxidative stress, hypertrophy, and fibrosis were studied in EC-SOD KO and wild-type mice under control conditions, and at 4 and 8 weeks after permanent coronary artery ligation. EC-SOD KO had no detectable effect on LV function in normal hearts but caused small but significant increases of LV fibrosis. At 8 weeks after MI, EC-SOD KO mice developed significantly more LV hypertrophy (LV mass increased 1.64-fold in KO mice compared to 1.35-fold in wild-type mice; $p < 0.01$) and more fibrosis and myocyte hypertrophy which was more prominent in the peri-infarct region than in the remote myocardium. EC-SOD KO mice had greater increases of nitrotyrosine in the peri-infarct myocardium, and this was associated with a greater reduction of LV ejection fraction, a greater decrease of sarcoplasmic or endoplasmic reticulum calcium²⁺ ATPase, and a greater increase of atrial natriuretic peptide in the peri-infarct zone compared to wild-type mice. EC-SOD KO was associated with more increases of phosphorylated p38 (p-p38^{Thr180/Tyr182}), p42/44 extracellular signal-regulated kinase (p-Erk^{Thr202/Tyr204}), and c-Jun N-terminal kinase (p-JNK^{Thr183/Tyr185}) both under control conditions and after MI, indicating that EC-SOD KO increases activation of mitogen-activated protein kinase signaling pathways. These findings demonstrate that EC-SOD plays an important role in protecting the heart against oxidative stress and infarction-induced ventricular hypertrophy.

Introduction

Left ventricular (LV) hypertrophy and dysfunction after myocardial infarction (MI) is associated with increased production of reactive oxygen species (ROS) and depressed antioxidant reserves, suggesting that oxidative stress might contribute to ventricular remodeling and development of ventricular hypertrophy and congestive heart failure (CHF).¹ Superoxide dismutase (SOD) is the first line of defense against ROS. Three SOD isozymes have been identified, including a copper/zinc-containing SOD (CuZn-SOD) which is primarily cytosolic in location, a mitochondrial manganese SOD (Mn-SOD), and extracellular SOD (EC-SOD). EC-SOD is a glycoprotein secreted into the extracellular fluid by cells such as fibroblasts, endothelial cells, and smooth muscle cells that binds to sulfated polysaccharides such as heparin and heparan sulphate^{2,3} and other matrix components.^{4,5} As a result, EC-SOD binds to the surface of endothelial cells and the extracellular matrix which has a high abundance of heparan sulfate.⁶ Patients in whom EC-SOD binding to endothelial cells is decreased as the result of substitution of arginine-213 by glycine (R213G) have an increased incidence of hypertension⁷ and increased risk of ischemic heart disease,^{7,8} implying that impaired EC-SOD binding or decreased myocardial EC-SOD content can increase the vulnerability to cardiovascular disease. Several recent studies have demonstrated that EC-SOD expression is decreased in the failing heart, and this was associated with evidence of increased myocardial oxidative stress and endothelial dysfunction.^{9,10,11} However, whether EC-SOD can influence ventricular oxidative stress and remodeling after MI remains unknown. Here we examined the effect of EC-SOD gene deletion (EC-SOD^{-/-}) on myocardial oxidative stress and cardiac remodeling following MI. EC-SOD^{-/-} had no effect on LV function under normal conditions but resulted in slight but significant myocyte hypertrophy and myocardial fibrosis that was associated with activation of the mitogen-activated protein kinase (MAPK) signaling cascades. MI resulted in evidence of increased oxidative stress that was greater in the EC-SOD^{-/-} mice and was associated with more myocardial hypertrophy and fibrosis and a more prominent decrease of ejection fraction than in the wild-type mice. These findings provide the first direct evidence that EC-SOD exerts a significant protective effect against myocardial-infarction-induced oxidative stress and ventricular remodeling.

Methods

Mice

Male C57BL/6 mice (Taconic, Germantown, NY) and EC-SOD^{-/-} mice (congenic with the Taconic C57BL/6 strain of mice,^{3,12} 8–10 weeks of age, were used. The investigation conforms with the Guide for the Care and Use of Laboratory Animals published by the US National Institutes of Health (NIH Publication No. 85-23, revised 1996).

Experimental procedure

MI was produced by permanent ligation of the left anterior descending coronary artery in wild-type ($N = 33$) and EC-SOD^{-/-} ($N = 35$) mice. Mice were anesthetized and instrumented for hemodynamic measurements at 4 or 8 weeks after MI. Body-weight- and age-matched

wild-type mice ($N = 17$) and EC-SOD^{-/-} mice ($N = 22$) were used as controls for functional analysis after sham surgery.

Echocardiography

Mice were anesthetized with 1.5% isoflurane. Echocardiographic images were obtained with a Visualsonics high-resolution Veve 660 system as previously described.¹³ LV cross-sectional area at end diastole (LVCSA_d) and at end systole (LVCSA_s), LV long axis diameter at end diastole (LVD_d) or at end systole (LVD_s), and LV short axis wall thickness were measured. LV ejection fraction (LVEF) was calculated by the cubic method: $LVEF = [(LVCSA_d) \times (LVD_d)^2 - (LVCSA_s) \times (LVD_s)^2] / (LVCSA_d) \times (LVD_d)^2 \times 100\%$.

Evaluation of aortic pressure and LV hemodynamics

The mice were weighed, anesthetized with 4% isoflurane, intubated using a 24G catheter, and ventilated with a mouse ventilator (HSE Harvard Apparatus; Germany). The ventilation rate was set at 120 breaths per minute with a tidal volume of 250–300 μ l and a positive end expiratory pressure of 4 cm H₂O. Animals were ventilated with a gas mixture of O₂/N₂ (1/2), anesthesia was maintained using 2.5% isoflurane, and body temperature was maintained at 37 °C by placing the mice on a temperature-controlled heating pad. For hemodynamic measurements, a 1.2F pressure catheter (Scisense Inc., Ontario, Canada) was inserted in the right carotid artery to record aortic pressure and advanced into the LV to measure LV pressure, its first derivative (LV dP/dt), and heart rate (HR).

Hemodynamic data were digitized on-line and processed using IOX data acquisition and analysis software (EMKA Technologies, Falls Church, USA). At least 10 beats during stable hemodynamic conditions were collected for data analysis.

Western blots

LV protein content was analyzed using Western blots as previously described ($N = 4$ samples each group).¹⁴ Primary antibodies against CuZn-SOD, Mn-SOD, EC-SOD, atrial natriuretic peptide (ANP), sarcoplasmic or endoplasmic reticulum calcium²⁺ ATPase (SERCA2a), nitrotyrosine, total c-Jun N-terminal kinase (JNK), phosphorylated JNK (p-JNK^{Thr183/Tyr185}), and catalase were purchased from Transduction Laboratories, Santa Cruz Inc., Abcam Inc., Upstate, and Sigma, respectively. The antibodies against phosphorylated p38 MAP kinase (p-p38^{Thr180/Tyr182}), p42/44 extracellular signal-regulated kinase (ERK), and phosphorylated p42/44 MAP kinase (p-Erk^{Thr202/Tyr204}) were purchased from Cell Signaling.

SOD activity

Total SOD activity of LV homogenates was determined with a Superoxide Anion Detection kit (Calbiochem Co.) according to the manufacturer's instructions and expressed as scavenging ability of the homogenates on superoxide anion ($N = 5$ samples each group).

Histological staining and measurement of fibrosis

Frozen tissue sections (8 μ m) from the central portion of the LV were stained with H&E (Sigma) for overall morphology, Sirius red for fibrosis, and fluorescein-isothiocyanate-conjugated wheat germ agglutinin (AF488; Invitrogen) to evaluate myocyte size. For mean

myocyte size, the short axis diameter and cross-sectional area of at least 120 cells/sample (from four areas) and at least four samples of each group were averaged. The percentage volume fibrosis was determined using the method described in Unbiased Stereology.¹⁵

Data and statistical analyses

All values were expressed as mean \pm SE. Statistical significance was defined as $p < 0.05$. One-way analysis of variance (ANOVA) was used to test each variable for differences among the treatment groups with StatView (SAS Institute Inc.). If the ANOVA demonstrated a significant effect, post hoc pairwise comparisons were made with Fisher's least significant difference test.

Results

EC-SOD^{-/-} exacerbated MI-induced ventricular hypertrophy and fibrosis

Under control conditions, LV weight and the ratio of LV weight to body weight (an index of ventricular hypertrophy) were slightly but significantly greater in the EC-SOD^{-/-} mice than in the wild-type mice (Figure 1, Table 1). At 8 weeks after MI we observed significant myocardial hypertrophy indicated by increases of ventricular weight and the ratio of ventricular weight to body weight or to tibia length, in both wild-type and EC-SOD^{-/-} mice, but the degree of hypertrophy was significantly greater in the EC-SOD^{-/-} mice than in the wild-type mice (Figure 1A, 1B and 1C). This was also true 4 weeks after MI (Table 1). Myocardial infarct size was not different between wild-type and EC-SOD^{-/-} mice (Table 1). The MI-induced mortality was not different between EC-SOD^{-/-} and wild-type mice (8 of 33 wild-type mice and 8 of 35 EC-SOD^{-/-} mice died during the post-MI period).

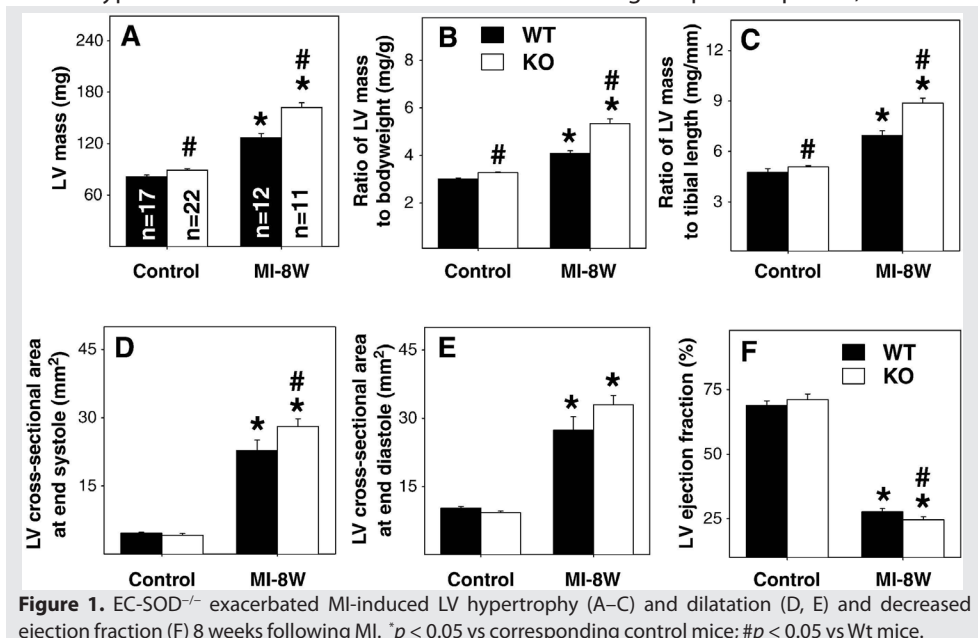


Table 1. Anatomic and functional data for wild-type (Wt) and EC-SOD^{-/-} (KO) mice during control conditions and 4 weeks or 8 weeks after myocardial infarction

Parameters	Strain	Control	MI-4 weeks	MI-8 weeks
Body weight (g)	Wt	28.1 ± 0.84	29.7 ± 1.5	31.1 ± 0.68*
	KO	28.0 ± 0.54	29.9 ± 0.87	30.5 ± 0.68*
Heart mass (mg)	Wt	105 ± 2.2	153 ± 7.0*	160 ± 6.0*
	KO	115 ± 2.3#	185 ± 13*#	201 ± 7.0*#
Heart mass/body weight (mg/g)	Wt	3.9 ± 0.04	5.3 ± 0.27*	5.1 ± 0.16*
	KO	4.2 ± 0.04#	6.2 ± 0.44*#	6.6 ± 0.24*#
Heart mass/tibia length (mg/mm)	Wt	6.2 ± 0.25	8.7 ± 0.42*	8.8 ± 0.33*
	KO	6.4 ± 0.11	10.0 ± 0.65*#	11.0 ± 0.37*#
LV posterior wall thickness at end diastole (mm)	Wt	0.65 ± 0.01	NA	1.0 ± 0.04*
	KO	0.73 ± 0.01	NA	0.99 ± 0.02*
LV posterior wall thickness at end systole (mm)	Wt	0.95 ± 0.01	NA	1.2 ± 0.03*
	KO	0.98 ± 0.14	NA	1.3 ± 0.02*#
Heart rate (bpm)	Wt	506 ± 14	503 ± 14	516 ± 16
	KO	513 ± 19	481 ± 9.8	503 ± 13
Mean aortic pressure (mm Hg)	Wt	75 ± 2.8	69 ± 4.3*	65 ± 2.5*
	KO	77 ± 2.6	75 ± 2.7*	65 ± 2.2*
LV systolic pressure (mm Hg)	Wt	96 ± 2.0	85 ± 4.2*	82 ± 2.9*
	KO	97 ± 2.6	88 ± 2.5*	83 ± 2.5*
LV end diastolic pressure (mm Hg)	Wt	7.5 ± 1.5	11.4 ± 3.4*	12.2 ± 2.5*
	KO	6.6 ± 0.8	12.9 ± 2.3*	12.1 ± 3.5*
LV dP/dt _{max} (mm Hg/s)	Wt	8341 ± 377	5545 ± 691*	5090 ± 423*
	KO	7809 ± 612	4626 ± 305*	4536 ± 432*
LV dP/dt _{min} (mm Hg/s)	Wt	-6739 ± 576	-4983 ± 491*	-4542 ± 387*
	KO	-6833 ± 366	-4140 ± 250*	-4214 ± 471*
Infarct area (%)	Wt	0	41.3 ± 1.6*	37.5 ± 2.3*
	KO	0	40.0 ± 1.3*	37.7 ± 0.78

NA, not available.

**p* < 0.05 compared with corresponding control conditions; # *p* < 0.05 compared with wild-type mice.

Histological staining of LV tissue was performed on EC-SOD^{-/-} and wild-type mice under control conditions and 8 weeks after MI. The EC-SOD^{-/-} mice had slightly but significantly more fibrosis than the wild-type mice under control conditions (Figures 2A and 2B). MI resulted in significant increases of fibrosis in both the peri-infarct and the remote zones, and this was significantly greater in the EC-SOD^{-/-} mice (Figure 2A and 2B). MI caused myocyte hypertrophy in both the peri-infarct and the remote zones that was significantly greater in the EC-SOD^{-/-} mice than in the wild-type mice (Figures 2A and 2C). Thus, the greater ventricular mass in the EC-SOD^{-/-} mice in response to MI was the result of increases of both myocyte size and ventricular fibrosis.

Aortic pressure, LV systolic pressure, and LV dP/dt_{max} were not different between wild-type mice and EC-SOD^{-/-} mice under control conditions. At both 4 and 8 weeks after MI, we observed small but significant decreases of LV systolic pressure, mean aortic pressure, LV dP/dt_{max}, and LV dP/dt_{min} in both wild-type mice and EC-SOD^{-/-} mice. MI for 4 and 8 weeks

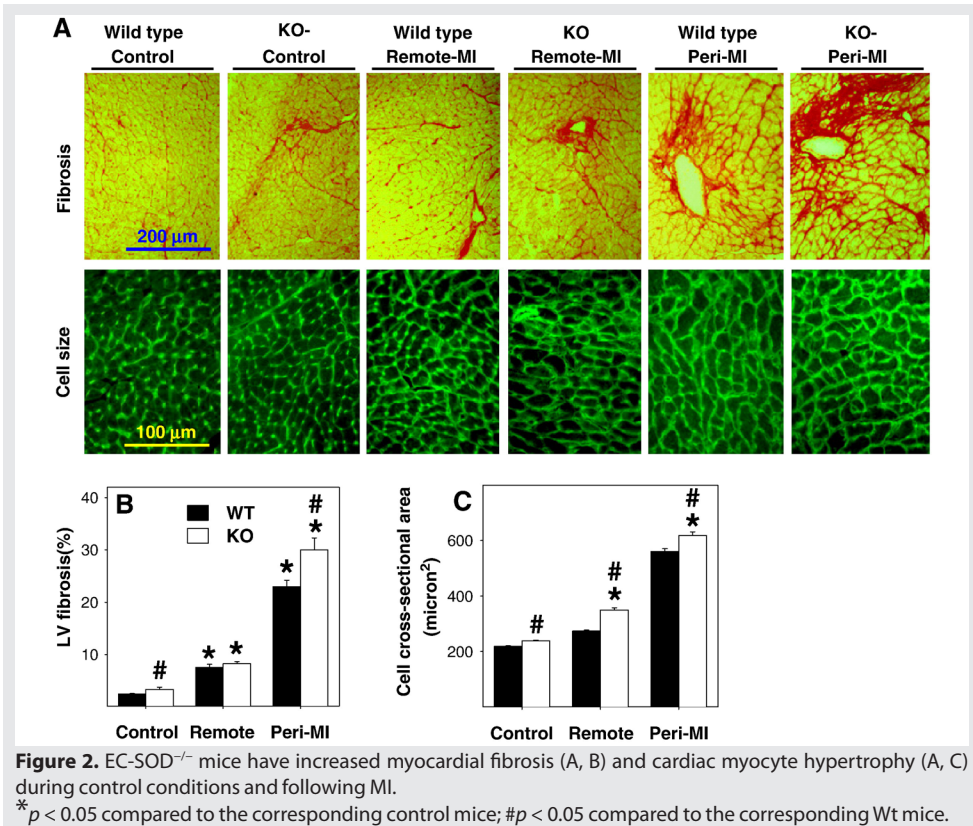
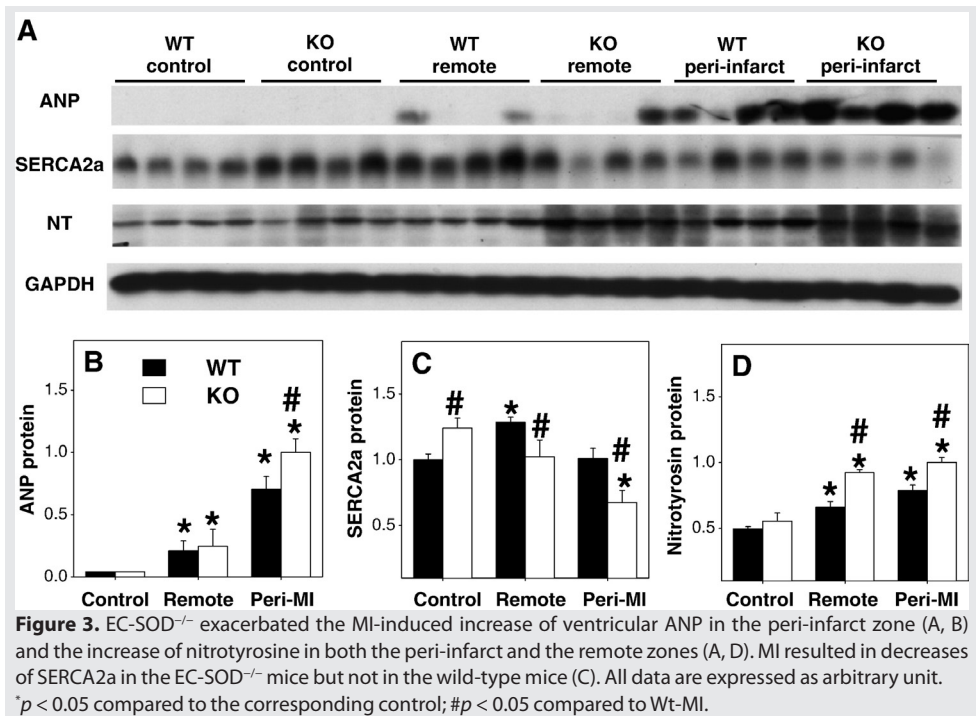


Figure 2. EC-SOD^{-/-} mice have increased myocardial fibrosis (A, B) and cardiac myocyte hypertrophy (A, C) during control conditions and following MI.

**p* < 0.05 compared to the corresponding control mice; #*p* < 0.05 compared to the corresponding Wt mice.

tended to cause greater decreases of LV $\text{dP/dt}_{\text{max}}$ and LV $\text{dP/dt}_{\text{min}}$ in EC-SOD^{-/-} mice than in wild-type mice, but these differences were not significant (Table 1). Echocardiographic imaging of the heart 8 weeks after MI demonstrated significant increases of LV cross-sectional area at end diastole in both EC-SOD^{-/-} and wild-type mice in comparison with sham-operated mice (Figure 1E), indicating MI-induced LV dilation. The increase of LV cross-sectional area at end diastole tended to be greater in the EC-SOD^{-/-} mice than in the wild-type mice (*p* = 0.06). At 8 weeks after MI, LV cross-sectional area at end systole was significantly increased in both EC-SOD^{-/-} and wild-type mice in comparison with sham-operated mice (Figure 1D), but this increase was 19% greater (*p* < 0.05) in the EC-SOD^{-/-} mice than in the wild-type mice, indicating that MI caused more ventricular remodeling in the EC-SOD^{-/-} mice. However, LV cross-sectional area at end diastole was also increased in the EC-SOD^{-/-} mice, so that MI caused only a slightly greater decrease of LV ejection fraction in the EC-SOD^{-/-} than in the wild-type mice (Figure 1F, Table 1). Overall, the echocardiographic and LV pressure measurements demonstrated that EC-SOD^{-/-} only moderately exacerbated the MI-induced LV dysfunction.

ANP is a sensitive biochemical marker for LV hypertrophy and/or ventricular remodeling. Myocardial ANP levels were increased in both wild-type and EC-SOD^{-/-} mice 8 weeks after MI; this increase was greater in the peri-infarct zone than in the remote zone where it was



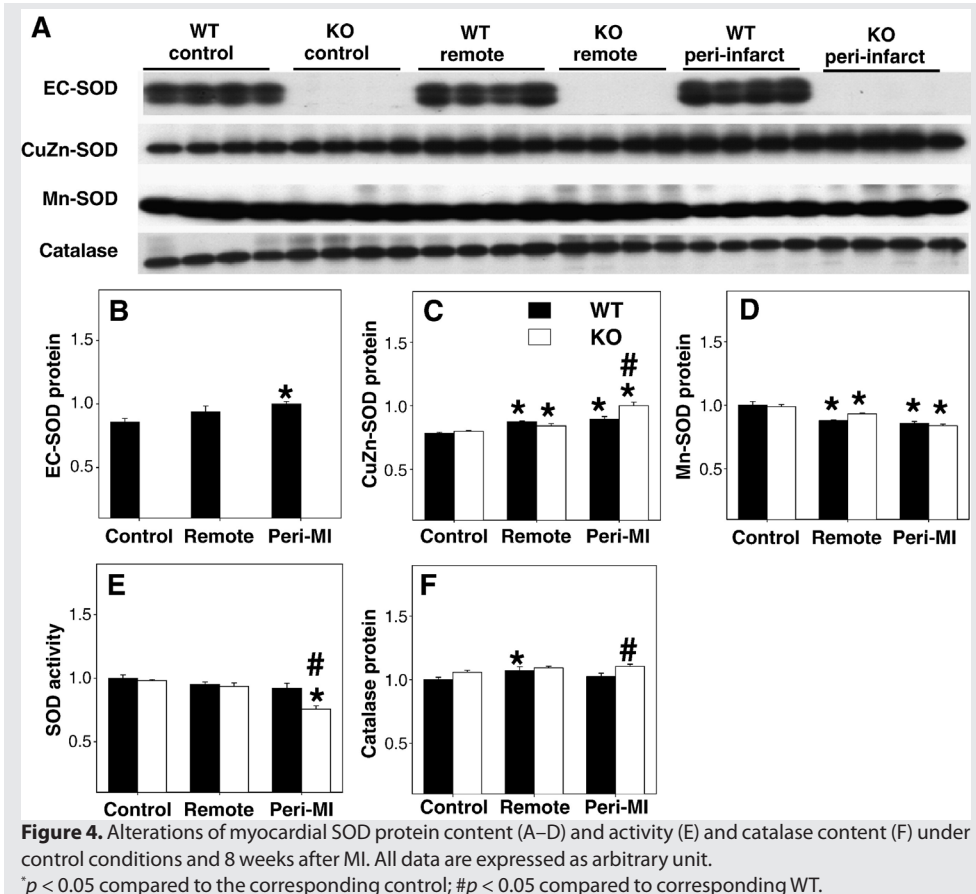
significantly greater in the EC-SOD^{-/-} mice than in the wild-type mice (Figure 3A and 3B). SERCA2a, which pumps calcium from the cytosol back into the sarcoplasmic reticulum at the end of systole, is generally decreased in the setting of heart failure. Under control conditions SERCA2A was significantly higher in EC-SOD^{-/-} mice than in wild-type mice. In the wild-type mice SERCA2A was significantly increased in the remote zone 8 weeks after MI but was unchanged in the peri-infarct zone. SERCA2a was significantly lower in both the remote and the peri-infarct zones of the EC-SOD^{-/-} mice compared to wild-type mice 8 weeks after MI (Figure 3A and 3C). Taken together, these data are consistent with more prominent myocardial hypertrophy and fibrosis in the EC-SOD^{-/-} mice after MI.

EC-SOD^{-/-} exacerbated MI-induced myocardial oxidative stress

As anticipated, EC-SOD was undetectable in the EC-SOD^{-/-} mice (Figure 4A and 4B). EC-SOD^{-/-} did not affect myocardial CuZn-SOD or Mn-SOD protein content under control conditions (Figure 4A, 4C, and 4D). Total myocardial SOD activity was not different between wild type mice and EC-SOD^{-/-} mice under control conditions (Figure 4E), consistent with previous reports that EC-SOD contributes only minimally to overall myocardial SOD activity.^{2,16} Myocardial nitrotyrosine contents were not different between EC-SOD^{-/-} mice and wild-type mice under control conditions (Figure 3A and 3D). Myocardial catalase protein content was not different between wild-type and EC-SOD^{-/-} mice (Figure 4A and 4F) under control conditions.

MI caused significant increases of myocardial nitrotyrosine in both the remote and the

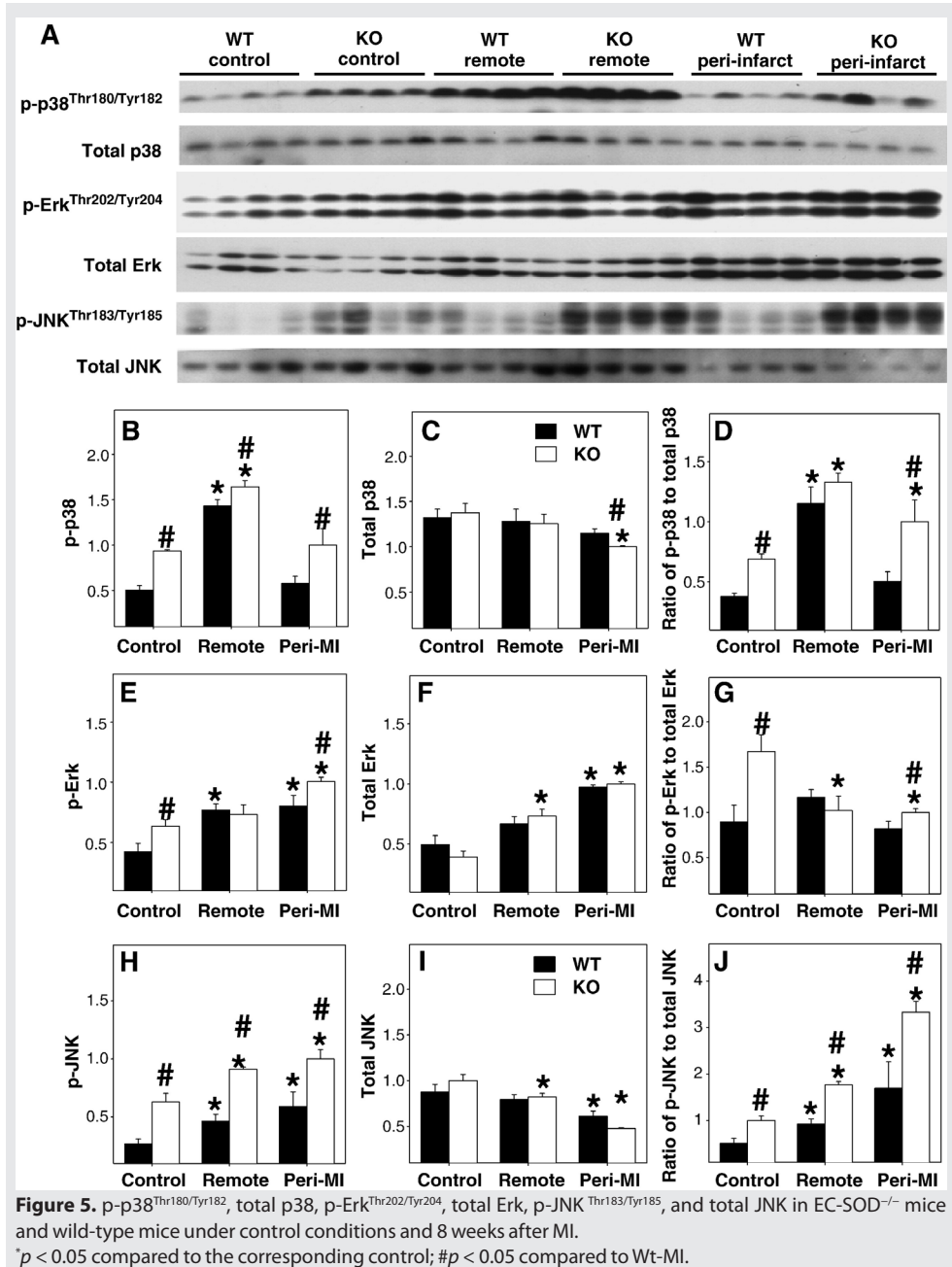
peri-infarct zones of wild-type and EC-SOD^{-/-} mice, and these increases were significantly greater in the EC-SOD^{-/-} mice than in the wild-type mice (Figure 3A and 3D), indicating increased myocardial oxidative stress in EC-SOD^{-/-} mice after MI. SOD activity in the peri-infarct zone was significantly decreased in the EC-SOD^{-/-} mice 8 weeks after MI but not in the wild-type mice (Figure 4E). Myocardial catalase protein content was not different between wild-type and EC-SOD^{-/-} mice during control conditions and did not change significantly after MI (Figure 4F).



EC-SOD^{-/-} alters activation of mitogen-activated protein kinases

MAPKs are major targets of reactive oxygen species,¹⁷ and the development of ventricular hypertrophy or heart failure is often associated with increased oxidative stress and activation of MAPK.¹⁸ To elucidate whether EC-SOD^{-/-} alters MAPK signaling in the normal or infarcted heart, total and phosphorylated p-38, JNK, and ERK were determined (Figure 5). In control noninfarcted hearts EC-SOD^{-/-} was associated with significant increases of p-p38^{Thr180/Tyr182}, p-Erk^{Thr202/Tyr204}, and p-JNK^{Thr183/Tyr185} and the ratios of the phosphorylated to total proteins. MI caused significant increases of p-p38^{Thr180/Tyr182} and p-JNK^{Thr183/Tyr185} and the ratios of p-p38 to total p38 and of p-JNK to total JNK in the remote zone; in the peri-

infarct region the increase in p-JNK also occurred in both groups of mice but the increase of p-p38 occurred only in the EC-SOD^{-/-} mice. p-Erk^{Thr202/Tyr204} increased following MI but, due to an increase in total Erk, the ratio of p-Erk to total ERK was little changed in either the remote or the peri-infarct zones (Figure 5).



Discussion

The major new findings of this study are that (i) following MI, EC-SOD^{-/-} hearts sustained more hypertrophy and fibrosis than wild-type hearts, with a greater increase of LV cross section at end systole and a greater decrease of LV ejection fraction, (ii) MI caused a greater increase in oxidative stress, as indicated by nitrotyrosine, in EC-SOD^{-/-} hearts than in wild-type hearts, and (iii) EC-SOD^{-/-} resulted in activation of myocardial MAPK signaling pathways in both unstressed and infarcted hearts. To the best of our knowledge, these findings provide the first evidence that EC-SOD exerts a protective effect against MI-induced ventricular remodeling and modulates activation of the MAPK signaling pathway.

The unchanged myocardial SOD activity in the EC-SOD^{-/-} mice under control conditions is consistent with previous reports that EC-SOD contributes minimally to overall SOD activity in the heart.^{2,16} Nevertheless, the small, but significant, increase of myocardial fibrosis and ventricular mass and the activation of MAPK signaling pathways in the EC-SOD^{-/-} mice under control conditions indicate that the loss of superoxide scavenging activity in the extracellular compartment has a significant influence on signaling related to myocyte hypertrophy and collagen deposition. The lack of change in myocardial nitrotyrosine content in the EC-SOD^{-/-} mice under unstressed conditions may be explained by insufficient sensitivity of the assays for detecting small changes in these measurements. The increase of cardiac fibrosis in the EC-SOD^{-/-} mice is analogous to previous reports that EC-SOD exerts antifibrotic activity in the lung.^{5,12}

The increases of nitrotyrosine in the mice subjected to MI in the present study are consistent with previous reports demonstrating increased oxidative stress in the failing heart.^{1,13,19,20} Thus, in animals with aortic constriction or MI, the development of heart failure was associated with increases of myocardial nitrotyrosine^{13,20} and myocardial superoxide production.^{13,20,21} Several sources for increased superoxide production have been identified in the failing heart, including the mitochondrial respiratory chain,²² uncoupled nitric oxide synthase,^{13,20} NADPH oxidase,²³ and xanthine oxidase.²⁴ We recently reported that systolic overload produced by transverse aortic constriction in mice caused increased expression of the monomeric forms of myocardial iNOS and eNOS (a structure that generates superoxide rather than NO).¹³ Furthermore, iNOS deletion or selective pharmacologic inhibition of iNOS decreased markers of oxidative stress and improved LV function, suggesting that either iNOS-induced eNOS uncoupling or iNOS uncoupling contributed to the increased oxidative stress and development of CHF in the wild-type mice.^{13,20} Furthermore, administration of BH4 to prevent NOS uncoupling²⁰ or selective inhibition of xanthine oxidase or NADPH oxidase has been reported to attenuate oxidative stress and ventricular dysfunction in this model of cardiac overload.

In addition to increased free radical production in the failing heart, there is evidence that decreased antioxidant reserves contribute to increased oxidative stress. Thus, CHF is associated with decreased EC-SOD protein content or activity^{9,10,11} and overexpression of EC-SOD has been reported to protect the heart against ischemia–reperfusion injury^{25,26} (an effect not enhanced by administration of catalase, demonstrating that protection was

dependent upon removal of superoxide but not hydrogen peroxide). In contrast to these previous reports in failing hearts, in the present study EC-SOD protein was significantly increased in the peri-infarct region, and SOD1 protein was increased in both the peri-infarct and the remote regions of the infarcted hearts. The failure to find decreases of SOD protein in the present study likely occurred because the mice were studied relatively early, when LV dysfunction produced by MI had not yet resulted in congestive heart failure.

Nevertheless, we did find a small but significant decrease of SOD activity in the peri-infarct region of the EC-SOD^{-/-} mice after MI, with no change in the remote region. This decrease of SOD activity limited to the peri-infarct zone is consistent with previous reports of myocardial infarct in rats.²⁷ Furthermore, myocyte hypertrophy and fibrosis were more prominent in the peri-infarct region than in the remote myocardium. This greater structural abnormality was not likely the result of ischemia in the peri-infarct region because the perfusion boundary between adjacent coronary perfusion beds has a sharp transition from hypoperfusion in the infarct region to normal perfusion in the adjacent myocardium.²⁸ However, local activation of stretch-activated signaling could explain the greater hypertrophy and fibrosis in the peri-infarct region. Tethering of the noncontractile infarct to adjacent viable myocardium amplifies wall stresses in the peri-infarct region, and biomechanical strain can trigger stretch-activated signaling pathways in cardiomyocytes.²⁹ This might also account for the significantly greater increase of ANP protein in the peri-infarct region compared to the remote region. The concept that stretch-activated signaling pathways can be turned on regionally is supported by studies in rats 6 weeks post infarction where substantial differences in mRNA levels for ANP, endothelin-1, and IGF-1 were found in the peri-infarct zone and the remote myocardium,³⁰ with highest expression in regions that were subjected to high mechanical stresses. The findings of evidence for increased oxidative stress, fibrosis, myocyte hypertrophy, and ANP expression in the peri-infarct zone are similar to findings in the myocardium of hearts with overt heart failure. These findings are of interest because of evidence that the peri-infarct region can progressively expand over time and thereby contribute to the transition from compensated hypertrophy to heart failure.³¹ Thus, with sufficient time, it is possible that the remote zone would gradually take on characteristics seen in the peri-infarct region. This evolution toward heart failure appeared more prominent in the EC-SOD^{-/-} mice, where the degree of ventricular hypertrophy was significantly greater at 8 weeks post infarct than at 4 weeks, than in the wild-type mice which showed no increase in hypertrophy between 4 and 8 weeks post infarct.

The MAPK cascades (in which MAPKs are activated by phosphorylation by upstream MAPK kinases) are important regulatory pathways in cardiac pathophysiology.^{32,33} The most widely investigated MAPKs in the heart are the ERK1/2, JNKs, and p38-MAPKs. ROS are known to activate myocardial MAPK signaling pathways, and reducing oxidative stress attenuates MAPK signaling.³⁴⁻³⁶ In the present study, the increases of p-p38^{Thr180/Tyr182}, p-ERK^{Thr202/Tyr204}, and p-JNK^{Thr183/Tyr185} in the EC-SOD^{-/-} hearts during control conditions, compared with the wild-type hearts, suggests that increased oxidative stress in the EC-SOD^{-/-} hearts was able to activate these pathways even during unstressed conditions. ERK1/2 are activated by oxidative stress in cardiac myocytes.³⁵⁻³⁷ Constitutive activation

of ERK1/2 by cardiac-specific overexpression of their upstream regulator MAPK kinase 1^{38,39} or RAS⁴⁰ results in ventricular hypertrophy or congestive heart failure, indicating that activation of the ERK signaling pathway causes ventricular hypertrophy. ROS also activates p38 and JNK.^{35,36} Activation of p38 by TAK1 induced ventricular hypertrophy.⁴¹ Tenhunen et al.⁴² injected adenovirus encoding wild-type p38-MAPK α together with a constitutively activated upstream kinase into the hearts of rats; the hearts overexpressing p38 MAPK had increased expression of genes related to cell cycle progression and inflammation together with large areas of fibrosis. This observation, which is consistent with the established link between the p38 MAPK pathway and the inflammatory responses in other organ systems, is similar to the findings in the peri-infarct region in the present study. In addition, specific activation of JNKs by overexpression of activated MKK3 or MKK6 induces ventricular dilation and congestive heart failure.⁴³ Taken together, these findings suggest that activation of the MAPK signaling pathway as the result of increased myocardial oxidative stress in EC-SOD^{-/-} mice in the present study may have contributed to the myocyte hypertrophy, fibrosis, or dysfunction observed in this strain both under control conditions and after MI.

In summary, EC-SOD^{-/-} caused slight but significant myocyte hypertrophy and fibrosis in the unstressed heart that was associated with activation of the MAPK signaling pathway. In response to coronary occlusion, EC-SOD^{-/-} mice developed more LV hypertrophy than wild-type mice, with a greater decrease of ejection fraction. The degree of fibrosis and myocyte hypertrophy was significantly greater in the peri-infarct region of the EC-SOD^{-/-} mice than in the wild-type mice, and this was associated with significantly greater ANP protein and significantly less SERCA2a, implying greater dysfunction in this region of the EC-SOD^{-/-} mice. The data indicate that EC-SOD plays important roles in protecting the heart against oxidative stress and infarction-induced ventricular hypertrophy.

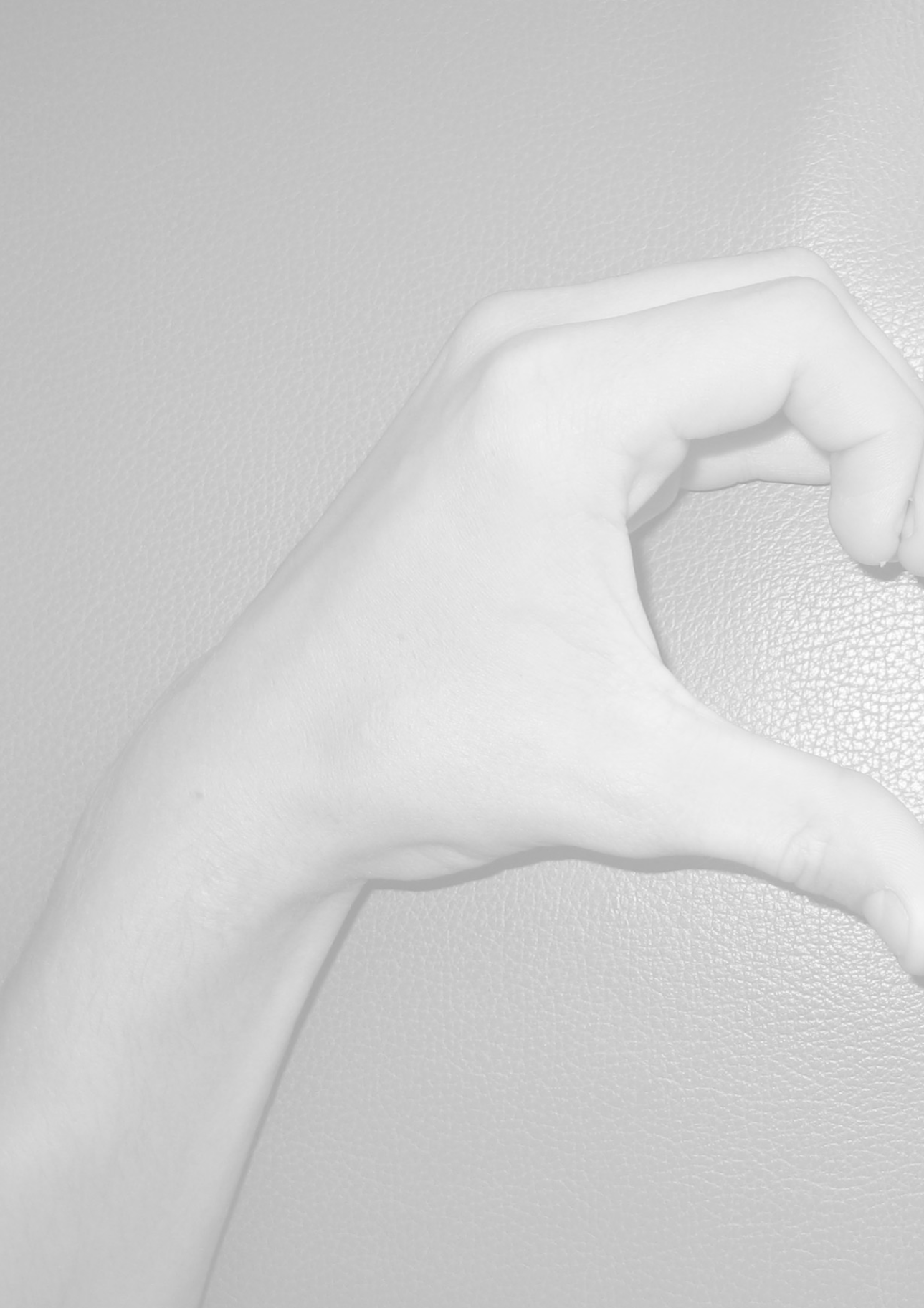
Acknowledgments

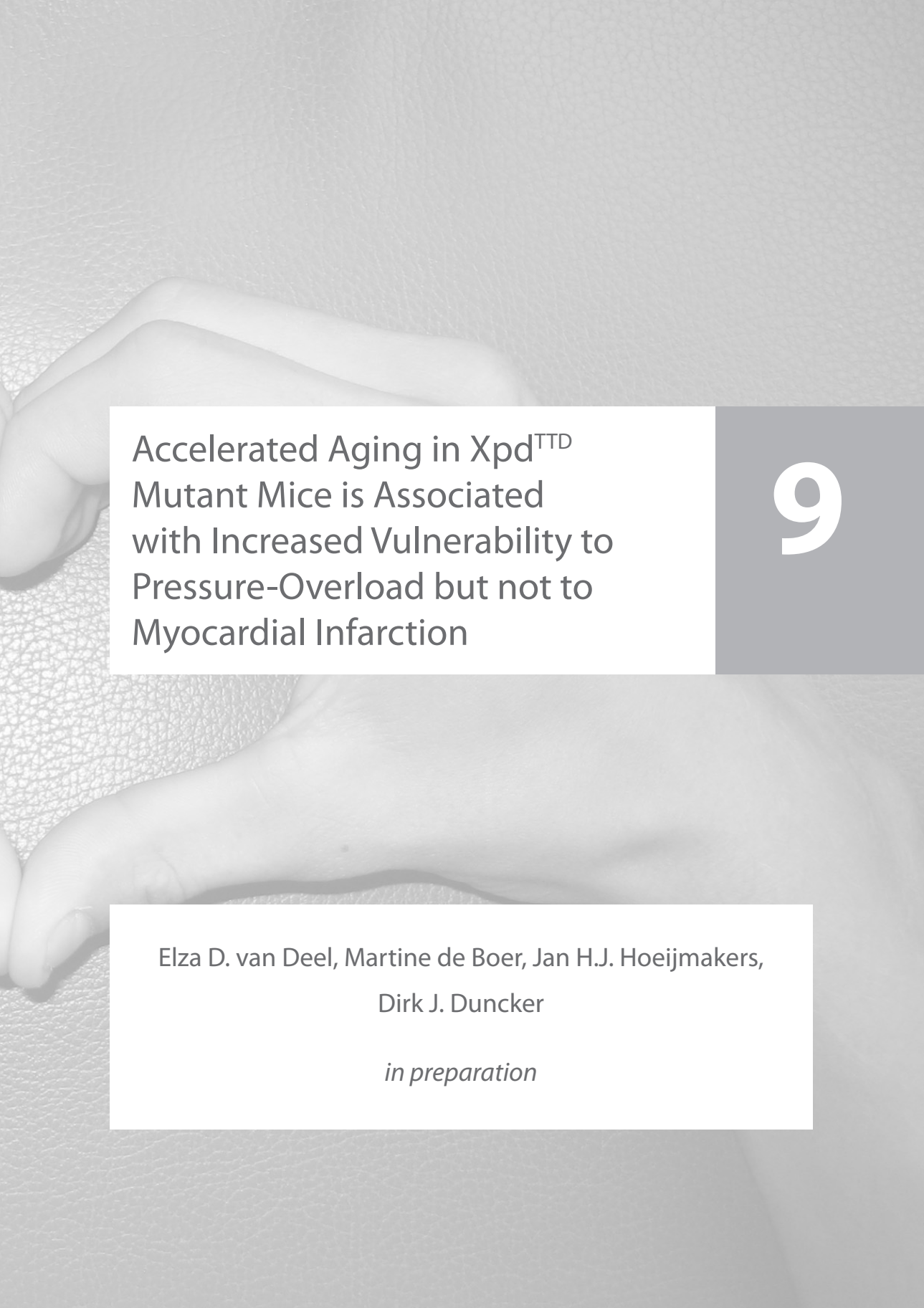
We are grateful to Dr. Stefan Marklund of Umea University, Umea, Sweden for supply of breeding pairs of EC-SOD^{-/-} mice. This study was supported by NHLBI Grants HL71790 (Y.C.), HL21872 (R.J.B.), and HL63700 (T.D.O.) from the National Institutes of Health.

References

1. F.J. Giordano, *Oxygen, oxidative stress, hypoxia, and heart failure*. *J. Clin. Invest.*, 115 (2005), pp. 500–508.
2. S.L. Marklund, *Extracellular superoxide dismutase and other superoxide dismutase isoenzymes in tissues from nine mammalian species*. *Biochem. J.*, 222 (1984), pp. 649–655.
3. L.M. Carlsson, J. Jonsson, T. Edlund and S.L. Marklund, *Mice lacking extracellular superoxide dismutase are more sensitive to hyperoxia*. *Proc. Natl. Acad. Sci. U. S. A.*, 92 (1995), pp. 6264–6268.
4. S.V. Petersen, T.D. Oury, L. Ostergaard, Z. Valnickova, J. Wegrzyn, I.B. Thogersen, C. Jacobsen, R.P. Bowler, C.L. Fattman, J.D. Crapo and J.J. Enghild, *Extracellular superoxide dismutase (EC-SOD) binds to type I collagen and protects against oxidative fragmentation*. *J. Biol. Chem.*, 279 (2004), pp. 13705–13710.
5. C.L. Fattman, L.M. Schaefer and T.D. Oury, *Extracellular superoxide dismutase in biology and medicine*. *Free Radic. Biol. Med.*, 35 (2003), pp. 236–256.
6. J. Sandstrom, L. Carlsson, S.L. Marklund and T. Edlund, *The heparin-binding domain of extracellular superoxide dismutase C and formation of variants with reduced heparin affinity*. *J. Biol. Chem.*, 267 (1992), pp. 18205–18209.
7. K. Juul, A. Tybjaerg-Hansen, S. Marklund, N.H. Heegaard, R. Steffensen, H. Sillesen, G. Jensen and B.G. Nordestgaard, *Genetically reduced antioxidative protection and increased ischemic heart disease risk: The Copenhagen City Heart Study*. *Circulation*, 109 (2004), pp. 59–65.
8. H. Yamada, Y. Yamada, T. Adachi, A. Fukatsu, M. Sakuma, A. Futenma and S. Kakumu, *Protective role of extracellular superoxide dismutase in hemodialysis patients*. *Nephron*, 84 (2000), pp. 218–223.
9. Y. Chen, M. Hou, Y. Li, J.H. Traverse, P. Zhang, D. Salvemini, T. Fukai and R.J. Bache, *Increased superoxide production causes coronary endothelial dysfunction and depressed oxygen consumption in the failing heart*. *Am. J. Physiol. Heart Circ. Physiol.*, 288 (2005), pp. H133–H141. |
10. U. Landmesser, R. Merten, S. Spiekermann, K. Buttner, H. Drexler and B. Hornig, *Vascular extracellular superoxide dismutase activity in patients with coronary artery disease: relation to endothelium-dependent vasodilation*. *Circulation*, 101 (2000), pp. 2264–2270.
11. U. Landmesser, S. Spiekermann, S. Dikalov, H. Tatge, R. Wilke, C. Kohler, D.G. Harrison, B. Hornig and H. Drexler, *Vascular oxidative stress and endothelial dysfunction in patients with chronic heart failure: role of xanthine-oxidase and extracellular superoxide dismutase*. *Circulation*, 106 (2002), pp. 3073–3078.
12. C.L. Fattman, R.J. Tan, J.M. Tobolewski and T.D. Oury, *Increased sensitivity to asbestos-induced lung injury in mice lacking extracellular superoxide dismutase*. *Free Radic. Biol. Med.*, 40 (2006), pp. 601–607.
13. P. Zhang, X. Xu, X. Hu, E.D. van Deel, G. Zhu and Y. Chen, *Inducible nitric oxide synthase deficiency protects the heart from systolic overload-induced ventricular hypertrophy and congestive heart failure*. *Circ. Res.*, 100 (2007), pp. 1089–1098. |
14. Y. Chen, Y. Li, P. Zhang, J.H. Traverse, M. Hou, X. Xu, M. Kimoto and R.J. Bache, *Dimethylarginine dimethylaminohydrolase and endothelial dysfunction in failing hearts*. *Am. J. Physiol. Heart Circ. Physiol.*, 289 (2005), pp. H2212–H2219.
15. C.V. Howard and M.G. Reed, *Estimation of component volume and volume fraction*, J. Catherine, Editor, *Unbiased Stereology, Three-dimensional measurement in microscopy*, BIOS Scientific Publishers, Abingdon, Oxon (2005), pp. 17–64.
16. S.L. Marklund, *Extracellular superoxide dismutase in human tissues and human cell lines*. *J. Clin. Invest.*, 74 (1984), pp. 1398–1403.
17. D.K. Das, N. Maulik and R.M. Engelman, *Redox regulation of angiotensin II signaling in the heart*. *J. Cell Mol. Med.*, 8 (2004), pp. 144–152.
18. J. Heineke and J.D. Molkentin, *Regulation of cardiac hypertrophy by intracellular signalling pathways*. *Nat. Rev., Mol. Cell Biol.*, 7 (2006), pp. 589–600.
19. A.K. Dhalla and P.K. Singal, *Antioxidant changes in hypertrophied and failing guinea pig hearts*. *Am. J. Physiol.*, 266 (1994), pp. H1280–H1285.
20. E. Takimoto, H.C. Champion, M. Li, S. Ren, E.R. Rodriguez, B. Tavazzi, G. Lazzarino, N. Paolucci, K.L. Gabrielson, Y. Wang and D.A. Kass, *Oxidant stress from nitric oxide synthase-3 uncoupling stimulates cardiac pathologic remodeling from chronic pressure load*. *J. Clin. Invest.*, 115 (2005), pp. 1221–1231.
21. M.H. Jacob, M.R. Pontes, A.S. Araujo, J. Barp, M.C. Irigoyen, S.F. Llesuy, M.F. Ribeiro and A. Bello-Klein, *Aortic-banding induces myocardial oxidative stress and changes in concentration and activity of antioxidants in male Wistar rats*. *Life Sci.*, 79 (2006), pp. 2187–2193.
22. T. Ide, H. Tsutsui, S. Kinugawa, H. Utsumi, D. Kang, N. Hattori, K. Uchida, K. Arimura, K. Egashira and A. Takeshita, *Mitochondrial electron transport complex I is a potential source of oxygen free radicals in the*

- failing myocardium*. *Circ. Res.*, 85 (1999), pp. 357–363.
23. S.A. Gupte, R.J. Levine, R.S. Gupte, M.E. Young, V. Lionetti, V. Labinskyy, B.C. Floyd, C. Ojaimi, M. Bellomo, M.S. Wolin and F.A. Recchia, *Glucose-6-phosphate dehydrogenase-derived NADPH fuels superoxide production in the failing heart*. *J. Mol. Cell Cardiol.*, 41 (2006), pp. 340–349.
 24. C.E. Berry and J.M. Hare, *Xanthine oxidoreductase and cardiovascular disease: molecular mechanisms and pathophysiological implications*. *J. Physiol.*, 555 (2004), pp. 589–606.
 25. Q. Li, R. Bolli, Y. Qiu, X.L. Tang, S.S. Murphree and B.A. French, *Gene therapy with extracellular superoxide dismutase attenuates myocardial stunning in conscious rabbits*. *Circulation*, 98 (1998), pp. 1438–1448.
 26. S. Iida, Y. Chu, J. Francis, R.M. Weiss, C.A. Gunnnett, F.M. Faraci and D.D. Heistad, *Gene transfer of extracellular superoxide dismutase improves endothelial function in rats with heart failure*. *Am. J. Physiol. Heart Circ. Physiol.*, 289 (2005), pp. H525–H532.
 27. M.F. Hill and P.K. Singal, *Antioxidant and oxidative stress changes during heart failure subsequent to myocardial infarction in rats*. *Am. J. Pathol.*, 148 (1996), pp. 291–300.
 28. S.M. Factor, E.H. Sonnenblick and E.S. Kirk, *The histologic border zone of acute myocardial infarction— islands or peninsulas?*. *Am. J. Pathol.*, 92 (1978), pp. 111–124.
 29. B.M. Jackson, J.H. Gorman, I.S. Salgo, S.L. Moainie, T. Plappert, J. St, L.H. Edmunds and R.C. Gorman, *Border zone geometry increases wall stress after myocardial infarction: contrast echocardiographic assessment*. *Am. J. Physiol. Heart Circ. Physiol.*, 284 (2003), pp. H475–H479.
 30. J.P. Loennechen, A. Stoylen, V. Beisvag, U. Wisloff and O. Ellingsen, *Regional expression of endothelin-1, ANP, IGF-1, and LV wall stress in the infarcted rat heart*. *Am. J. Physiol. Heart Circ. Physiol.*, 280 (2001), pp. H2902–H2910.
 31. B.M. Jackson, J.H. Gorman, S.L. Moainie, T.S. Guy, N. Narula, J. Narula, M.G. John-Sutton, L.H. Edmunds and R.C. Gorman, *Extension of borderzone myocardium in postinfarction dilated cardiomyopathy*. *J. Am. Coll. Cardiol.*, 40 (2002), pp. 1160–1167.
 32. J. Heineke and J.D. Molkentin, *Regulation of cardiac hypertrophy by intracellular signalling pathways*. *Nat. Rev., Mol. Cell Biol.*, 7 (2006), pp. 589–600.
 33. A. Clerk, T.E. Cullingford, S.J. Fuller, A. Giraldo, T. Markou, S. Pikkariainen and P.H. Sugden, *Signaling pathways mediating cardiac myocyte gene expression in physiological and stress responses*. *J. Cell. Physiol.*, 212 (2007), pp. 311–322.
 34. M. Sano, K. Fukuda, T. Sato, H. Kawaguchi, M. Suematsu, S. Matsuda, S. Koyasu, H. Matsui, K. Yamauchi-Takahara, M. Harada, Y. Saito and S. Ogawa, *ERK and p38 MAPK, but not NF-kappaB, are critically involved in reactive oxygen species-mediated induction of IL-6 by angiotensin II in cardiac fibroblasts*. *Circ. Res.*, 89 (2001), pp. 661–669.
 35. M. Yoshizumi, K. Tsuchiya and T. Tamaki, *Signal transduction of reactive oxygen species and mitogen-activated protein kinases in cardiovascular disease*. *J. Med. Invest.*, 48 (2001), pp. 11–24.
 36. K. Tanaka, M. Honda and T. Takabatake, *Redox regulation of MAPK pathways and cardiac hypertrophy in adult rat cardiac myocyte*. *J. Am. Coll. Cardiol.*, 37 (2001), pp. 676–685.
 37. R. Aikawa, I. Komuro, T. Yamazaki, Y. Zou, S. Kudoh, M. Tanaka, I. Shiojima, Y. Hiroi and Y. Yazaki, *Oxidative stress activates extracellular signal-regulated kinases through Src and Ras in cultured cardiac myocytes of neonatal rats*. *J. Clin. Invest.*, 100 (1997), pp. 1813–1821.
 38. P.H. Sugden and A. Clerk, *Cellular mechanisms of cardiac hypertrophy*. *J. Mol. Med.*, 76 (1998), pp. 725–746.
 39. O.F. Bueno and J.D. Molkentin, *Involvement of extracellular signal-regulated kinases 1/2 in cardiac hypertrophy and cell death*. *Circ. Res.*, 91 (2002), pp. 776–781.
 40. J.J. Hunter, N. Tanaka, H.A. Rockman, J. Ross and K.R. Chien, *Ventricular expression of a MLC-2v-ras fusion gene induces cardiac hypertrophy and selective diastolic dysfunction in transgenic mice*. *J. Biol. Chem.*, 270 (1995), pp. 23173–23178.
 41. D. Zhang, V. Gausin, G.E. Taffet, N.S. Belaguli, M. Yamada, R.J. Schwartz, L.H. Michael, P.A. Overbeek and M.D. Schneider, *TAK1 is activated in the myocardium after pressure overload and is sufficient to provoke heart failure in transgenic mice*. *Nat. Med.*, 6 (2000), pp. 556–563.
 42. O. Tenhunen, J. Rysa, M. Ilves, Y. Soini, H. Ruskoaho and H. Leskinen, *Identification of cell cycle regulatory and inflammatory genes as predominant targets of p38 mitogen-activated protein kinase in the heart*. *Circ. Res.*, 99 (2006), pp. 485–493.
 43. P. Liao, D. Georgakopoulos, A. Kovacs, M. Zheng, D. Lerner, H. Pu, J. Saffitz, K. Chien, R.P. Xiao, D.A. Kass and Y. Wang, *The in vivo role of p38 MAP kinases in cardiac remodeling and restrictive cardiomyopathy*. *Proc. Natl. Acad. Sci. U. S. A.*, 98 (2001), pp. 12283–12288.





Accelerated Aging in Xpd^{TTD}
Mutant Mice is Associated
with Increased Vulnerability to
Pressure-Overload but not to
Myocardial Infarction

9

Elza D. van Deel, Martine de Boer, Jan H.J. Hoeijmakers,
Dirk J. Duncker

in preparation

Abstract

Heart failure has become a global disease epidemic that particularly affects the elderly. Interestingly, a number of non-pathologic structural and functional cardiac changes in aging, strikingly resemble alterations typically observed in heart failure. Aging is closely linked to DNA damage. Potentially DNA damage and subsequent aging reduces cardiac reserve and increases the vulnerability of the heart to hemodynamic overload, thereby aggravating and the development of heart failure. To test this concept we subjected DNA repair deficient Xpd^{TTD} mice that exhibit accelerated aging to the two major risk factor for heart failure, myocardial infarction (MI) and pressure-overload through a transverse aortic constriction (TAC). At 3 months of age Xpd^{TTD} mice show a similar survival response following MI and mild TAC as wildtype littermates but demonstrate increased mortality following severe TAC. In 1 year old Xpd^{TTD} mice survival following MI was unaltered compared to Xpd^{TTD} mice at age 3 months. In contrast severe TAC markedly decreased survival in 12 months old Xpd^{TTD} animals compared to wildtype littermates and Xpd^{TTD} mice of 3 months of age. Moreover, mild TAC that produced compensated LV hypertrophy accompanied by well maintained cardiac function without inducing significant mortality in 1 year old wildtype littermates, also markedly increased mortality in the 1 year old prematurely aged mice. In conclusion, TAC, but not MI induced mortality is aggravated in the aging heart. These findings suggest that the type of cardiac-overload rather than the severity, critically determines the cardiac pathological response in the aging heart.

Introduction

Despite ongoing research and promising new therapies, the prevalence of heart failure (HF) is still increasing.¹⁻² Globally over 23 million people are affected by the disease,³ indicating HF has become a chronic disease epidemic. Paradoxically, improved treatment of cardiovascular disease has reduced acute mortality over the past decades but highly increased the number of patients that develop HF over time. Furthermore, general advances in medicine, public health and food production have considerably increased life span in developed countries. Importantly, large cohort studies like the Framingham Heart Study, the Rochester Epidemiologic Project in Olmsted County and the Rotterdam Study consistently show that the incidence and prevalence of HF increases with age,⁴⁻⁶ reaching 1% in those 55-64 years of age and 10% in those aged over 85 years in the Rotterdam Study. These observations indicate that, age, apart from preceding cardiovascular disease, is an important risk factor that predisposes the heart to failure.

Interestingly, aging induces a number of non-pathologic structural and functional cardiac changes that resemble alterations typically observed in heart failure.⁷ First the total number of cardiomyocytes declines with age. This in turn leads to replacement hypertrophy of the remaining cardiomyocytes and interstitial deposition of collagen (i.e. cardiac fibrosis).⁸⁻⁹ Additionally, aging results in impaired Ca^{2+} handling and decreased cardiac responsiveness to beta-adrenergic stimulation.⁸⁻⁹ These aging-associated changes may affect cardiac function only minimally under non-pathological conditions but likely reduce cardiac reserve, hence increasing vulnerability of the heart to develop cardiac failure. This concept is supported by, clinical trials showing that age is an important predictor of mortality in HF patients.¹⁰

Although the complex process of aging is still incompletely understood, there is growing evidence that aging is at least in part the consequence of cumulative DNA damage in combination with inadequate repair of genomic injury.¹¹⁻¹⁴ The nucleotide excision repair pathway is one of the genome maintenance pathways and involves the DNA helicase subunit Xpd that is implicated in opening the DNA helix around a DNA lesion as one of the steps in the recognition and excision of a DNA injury. Some inherited mutations in Xpd cause the human progeroid repair syndrome trichothiodystrophy (TTD) in which genome maintenance is compromised and consequent time-dependent accumulation of DNA damage from internal and external stressors is associated with gradual functional decline and aging. Accordingly, accumulation of DNA-damage as a consequence of impaired DNA repair results in premature and accelerated aging in the the Xpd^{TTD} mouse-model that mimicks the TTD phenotype as a consequence of an XPD point mutation.¹⁵

One of the major sources of damage within the cell are reactive oxygen species (ROS).¹² ROS are generated by normal cellular respiration but when insufficiently balanced by antioxidants can over time cause cumulative damage to biomolecules, including DNA. Because cardiomyocytes contain relatively high numbers of mitochondria, the heart may be particularly vulnerable to ROS-induced DNA damage and concomitant aging.

However, at present medical treatment of elderly HF patients is not adjusted for age but based on results from clinical trials in younger patients.¹⁶ Furthermore comorbid diseases constitute an additional complication in the treatment of aged patients.¹⁷ A better understanding of age-associated cardiac alterations is therefore essential for improved treatment and impedance of cardiac aging and subsequent reduction of the prevalence of heart failure.

To elucidate how DNA-damage induced aging influences cardiac vulnerability to pathological stimuli and heart failure we studied cardiac hypertrophy and dysfunction following the two major underlying pathologies of heart failure, myocardial infarction (MI) and pressure-overload from transverse aortic constriction (TAC), 3 months old (3mo) and 12 months old (12mo) wildtype (Wt) mice and Xpd^{TTD} mutant mice that undergo accelerated aging.

Methods

All experiments were performed in accordance with the “Guiding Principles in the Care and Use of Animals” as approved by the Council of the American Physiological Society and with prior approval of the Animal Care Committee of the Erasmus MC Rotterdam. A total of 63 3mo Wt, 69 3mo Xpd^{TTD} and 67 12mo Wt and 66 12mo Xpd^{TTD} mice entered the study and were randomly assigned to one of the experimental groups.

Experimental procedure

The generation of Xpd^{TTD} mice has been previously described¹⁵ and littermates C57Bl/6 of mutant Xpd^{TTD} mice were used as Wt controls. All mice were weighed, sedated with 4% isoflurane, intubated and connected to a pressure-controlled ventilator (SAR-830/P; CWE), set at 90 breaths per minute with a peak inspiratory pressure of 18 cm H₂O and a positive end expiratory pressure of 4 cm H₂O. A gas mixture of O₂/N₂ (1:2 vol/vol) containing 2.5% isoflurane was used to maintain anesthesia. Body temperature was kept at 37°C and buprenorphine (50 µg/kg) was injected s.c. for postsurgical analgesia. Myocardial infarction was induced by ligation of the left coronary artery in 29 Wt and 29 Xpd^{TTD} mice using a 7-0 suture as previously described.¹⁸ In 30 Wt and 29 Xpd^{TTD} mice the aorta was constricted between the truncus brachiocephalicus and the arteria carotis communis sinistra using a 25G needle to a mild transverse aortic constriction (mTAC) and in 37 Wt and 44 Xpd^{TTD} mice using a 27G needle to produce a severe transverse aortic constriction (sTAC) as previously described.¹⁹ Buprenorphine (0.05 mg/kg) was administered (s.c.) for pain relief, and saline was injected to aid recovery. Age-matched sham operated mice (n=67) underwent an identical surgical procedures- except for ligation of the coronary artery or constriction of the aorta.

One week following sham, MI or TAC procedure, M-mode LV echocardiography was performed under 2.5% isoflurane anesthesia. LV diameter was measured with an Aloka SSD 4000 echo device (Aloka; Tokyo, Japan) using a 12-MHz probe. LV diameters at end

diastole (LVEDD) and end systole (LVESD) were measured, and fractional shortening was calculated. Eight weeks after surgery, the mice were again anesthetized with 2.5% isoflurane and ventilated to perform M-mode LV echocardiography and hemodynamic measurements. A PE10 catheter was inserted in the left carotid artery to measure systemic aortic pressure and a 1.4-Fr microtipped manometer (Millar Instruments; Houston, Texas, USA) was inserted in the right carotid artery to, when applicable, record aortic pressure proximal to the stenosis. Subsequently, the manometer was advanced into the left ventricle (LV) to measure LV pressure, its first derivative (LV dp/dt), the time constant of LV pressure decay (τ), and heart rate. At the end of each experiment mice were sacrificed and the LV, right ventricular and wet and dry lungs weight as well as tibia length (TL) measured. LV tissue samples were stored for histological and molecular analysis.

Statistical analysis

All data have been expressed as mean \pm SEM. Statistical significance ($P < 0.05$) for changes in cardiac response to overload and aging was determined by three-way (age \times genetic mutation \times hypertrophic stimulus) followed by two-way (genetic mutation \times hypertrophic stimulus) and (age \times hypertrophic stimulus) ANOVA and when appropriate post-hoc testing with a Student-Newman-Keuls test.

All groups contained comparable numbers of male and female mice. Similar as previously described,¹⁹ we did not observe an influence of gender on the effects of mutation and/or hypertrophic stimulus and/or age on the responses of survival and LV hypertrophy or dysfunction. Consequently, we pooled males and females for final analysis.

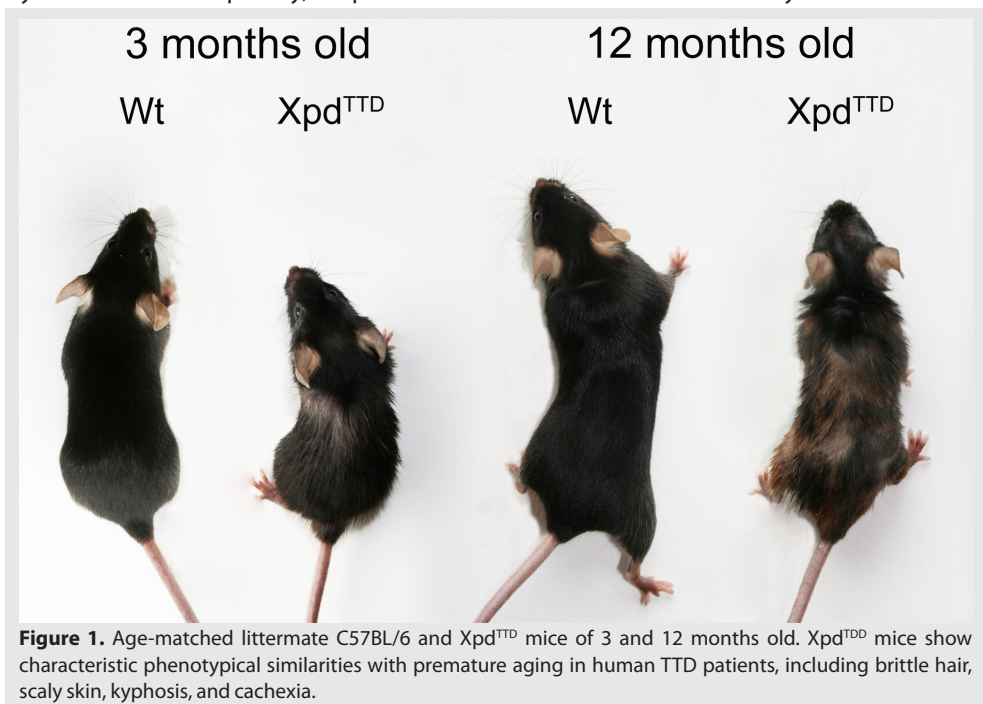


Figure 1. Age-matched littermate C57BL/6 and Xpd^{TTD} mice of 3 and 12 months old. Xpd^{TTD} mice show characteristic phenotypic similarities with premature aging in human TTD patients, including brittle hair, scaly skin, kyphosis, and cachexia.

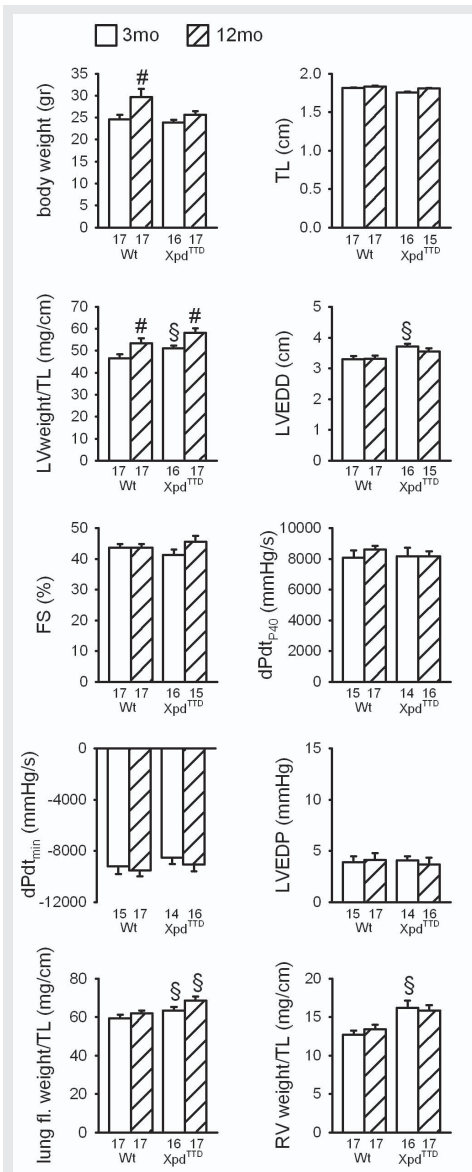


Figure 2. Effect of natural aging from 3 (open bars) to 12 months (hatched bars) on body weight, tibia length (TL), LV mass and geometry, hemodynamic parameters and lung fluid weight (lung wet weight minus lung dry weight) in Wt and Xpd^{TTD} mice. LVEDD, LV end diastolic diameter; FS, Fractional shortening; LVEDP, LV end diastolic pressure. § P<0.05 vs. corresponding Wt; # P<0.05 vs. corresponding 3 months old mice. Number of animals is indicated below each bar.

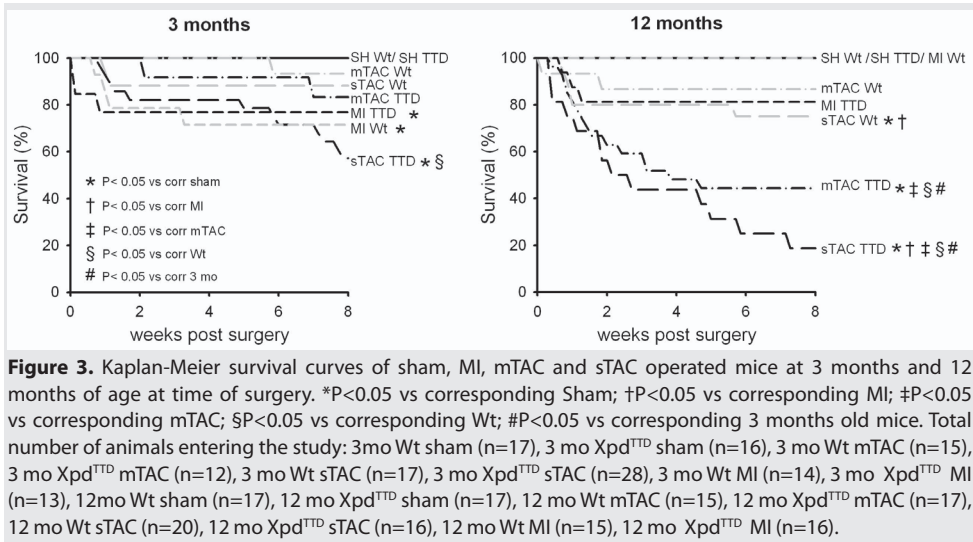
Results

Effects of natural and accelerated aging on cardiac geometry and function

Natural aging from 3 to 12 months was accompanied by an increase in bodyweight in sham-operated Wt mice but not in sham Xpd^{TTD} animals (Fig. 1 and 2). However, in spite of an unchanged tibia length, LV weight relative to tibia length was increased by natural aging in both Wt and Xpd^{TTD} mice, without affecting LV function. Like natural aging, accelerated aging as a result of deficient DNA repair elevated relative LV weight in 3 mo sham mice but also induced LV dilation and pulmonary congestion. However, the effects of accelerated aging were only still statistical significant in 12mo Xpd^{TTD} mice for long edema with a strong trend towards RV hypertrophy (P=0.06) (Fig. 2).

Influence of impaired DNA repair and cardiac overload on survival rate

Impaired DNA-repair did not affect mortality in 3mo sham or mTAC operated animals (Fig. 3). Likewise, sTAC did not influence survival in 3mo Wt mice but conversely induced robust mortality (43%) in 3mo Xpd^{TTD} mice. Mortality rates following MI were similar in 3mo Wt (29%) and Xpd^{TTD} mice (23%). Sham surgery did not induce mortality in both Wt and Xpd^{TTD} animals that were operated at 12 months of age. However, mTAC, that did not induce significant mortality in 12mo Wt mice, markedly increased mortality in Xpd^{TTD} animals (66%). Similarly, mortality in 12mo Wt mice following sTAC (25%) was severely aggravated in 12mo Xpd^{TTD} animals (81%). Moreover, natural aging from 3 to 12 months increased the mortality response to mTAC and sTAC in Xpd^{TTD} animals (Fig. 3). Interestingly, 12mo Wt and Xpd^{TTD} mice were protected against MI-induced mortality, although there was a strong trend towards



MI induced mortality in Xpd^{TTD} mice ($P=0.06$).

Cardiac remodeling and dysfunction following 1 week of cardiac overload

One week of mTAC and sTAC did not affect LV geometry but mildly reduced fractional shortening in 3mo Wt mice (Fig. 4). Conversely, in response to sTAC 3mo Xpd^{TTD} mice develop LV dilation and an aggravated reduction of fractional shortening compared to mTAC. In 12mo Wt mice mTAC and sTAC comparably reduce fractional shortening but only sTAC induces LV dilation. In addition, sTAC-induced aggravation of LV dilation and dysfunction were more severe in 12mo Xpd^{TTD} mice than in 12mo Wt mice. Additionally, MI increased LV end diastolic diameter and reduced fractional shortening similarly in 3mo and 12mo Wt and Xpd^{TTD} animals (Fig. 4).

Cardiac remodeling and dysfunction following 8 weeks of cardiac overload

In Wt mice that underwent surgery at 3 months of age, 8 weeks of mTAC produced mild hypertrophy accompanied by a mild reduction of fractional shortening (Fig. 5). In contrast, sTAC markedly increased LV weight and wall thickness, induced LV dilation and systolic as well as diastolic dysfunction and pulmonary edema (lung fluid weight and RV weight) in 3mo Wt mice (Fig. 5 and Table 1). Accelerated aging as a result of DNA repair deficiency did not affect LV hypertrophy or dilation but tended to slightly deteriorate LV dysfunction and pulmonary edema.

Additionally, the response to mTAC, sTAC was not aggravated in 12mo Xpd^{TTD} animals compared to 12mo Wt mice (data not shown). However, the very high mortality rates in 12mo Xpd^{TTD} mice following mTAC and sTAC resulted in self-selection mortality causing data obtained from the surviving animals not to allow meaningful analyses.

MI-induced adverse LV remodeling and dysfunction was unaffected by natural (data not shown) or accelerated aging due to deficient DNA repair (Fig. 5).

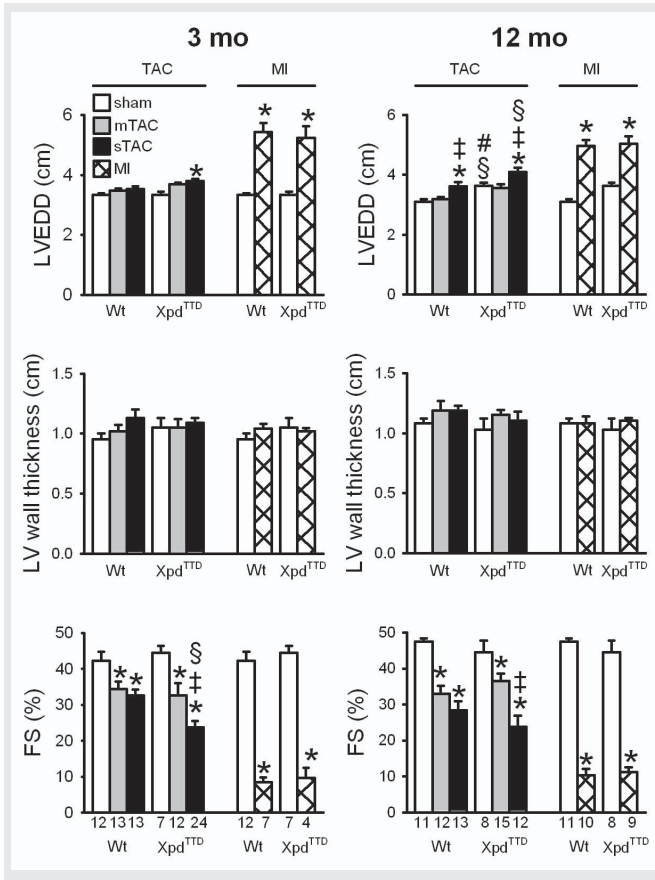


Figure 4. Effect of impaired DNA repair and 1 week of cardiac-overload by mTAC (grey bars), sTAC (black bars) and MI (double hatched bars) on left ventricular (LV) geometry and function, determined by LV echography in 3 and 12 months old Wt and Xpd^{TTD} mice. LVEDD, LV end diastolic diameter; FS, fractional shortening. *P<0.05 vs corresponding sham; †P<0.05 vs corresponding mTAC, §P<0.05 vs corresponding Wt; # P<0.05 vs. corresponding 3 months old mice. The number of animals is indicated below FS bars.

Discussion

9

A key contributor to the complex mechanism of aging is ROS-induced accumulation of DNA damage.²⁰ Accordingly, cumulative DNA damage associated with aging may potentially increase the susceptibility of organs like the heart to pathological stimuli. The present study is the first to evaluate and compare the influence of DNA repair deficiency (resulting in premature ageing) on cardiac vulnerability in the two major risk factors for heart failure, myocardial infarction and pressure-overload. The main findings were that impaired DNA repair 1) increases mortality following mTAC and sTAC but not MI; 2) increased heart weight and LV chamber size at 3 months of age; 3) and aggravated LV dilation and dysfunction in 3mo and 12mo animals in response to 1 week of sTAC. The implications of these findings will be discussed below.

Effects of aging on adverse cardiac remodeling and dysfunction

Heart failure is the most important reason for hospitalization among older adults and mortality rates are higher in elderly than in the younger heart failure patients.²¹

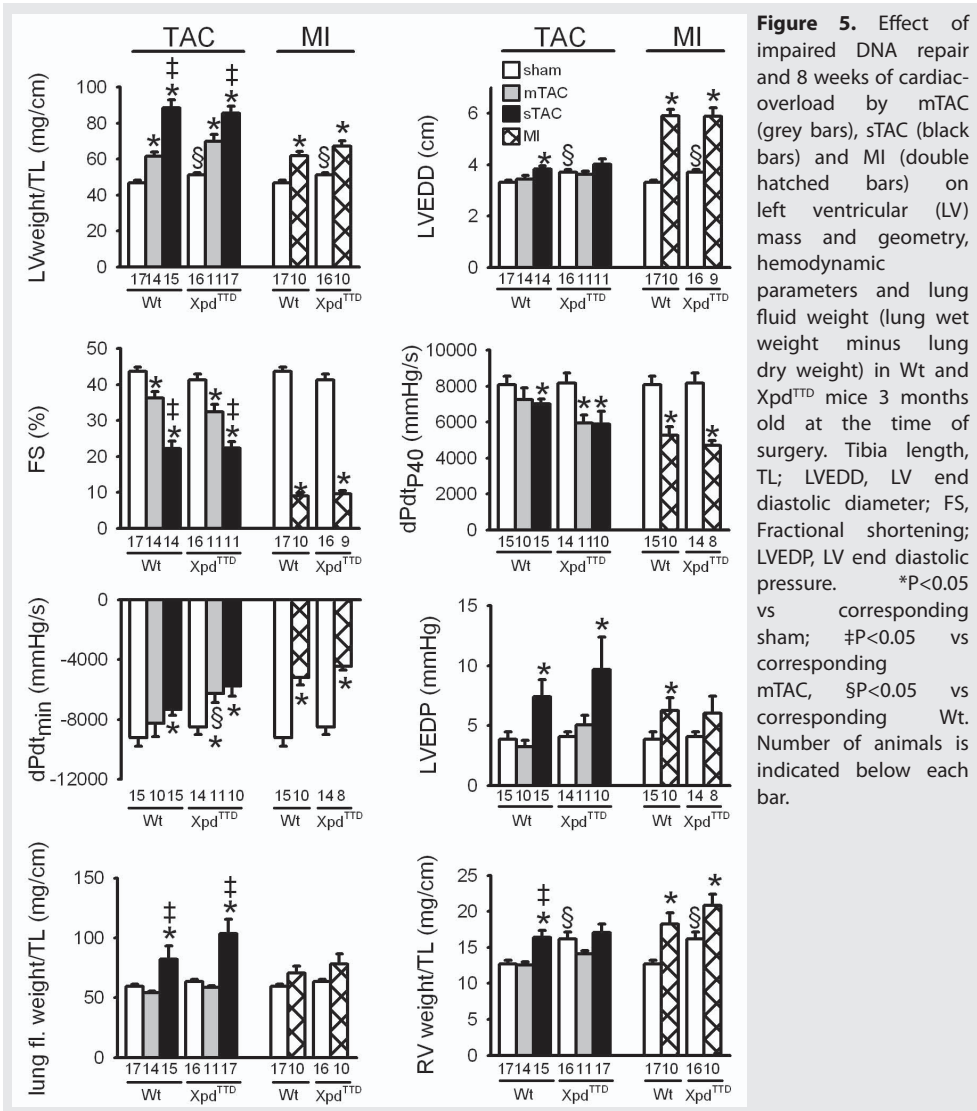


Figure 5. Effect of impaired DNA repair and 8 weeks of cardiac-overload by mTAC (grey bars), sTAC (black bars) and MI (double hatched bars) on left ventricular (LV) mass and geometry, hemodynamic parameters and lung fluid weight (lung wet weight minus lung dry weight) in Wt and Xpd^{TTD} mice 3 months old at the time of surgery. Tibia length, TL; LVEDD, LV end diastolic diameter; FS, Fractional shortening; LVEDP, LV end diastolic pressure. *P<0.05 vs corresponding sham; #P<0.05 vs corresponding mTAC, §P<0.05 vs corresponding Wt. Number of animals is indicated below each bar.

Similarly detrimental effects of aging on cardiac reserve have been described in several experimental animal models for the two most important underlying causes of heart failure: myocardial infarction²²⁻²³ and pressure-overload.²⁴⁻²⁵ However, it is still unknown what mechanisms are involved in the increased vulnerability to HF with aging and whether these mechanisms are similar in the various underlying aetiologies. The present study demonstrates that already at 3 months of age, DNA repair deficiency increased heart weight and size. Although cardiac function is still well maintained in these animals, the mild cardiac hypertrophy could be a compensatory mechanism for cellular damage because of impaired DNA repair that would explain the increased mortality in response to sTAC in 3mo Xpd^{TTD} mice compared to 3mo Wt animals.

Table 1. Anatomical and functional data of at baseline 3 months old mice at 8 weeks follow-up

		Wt	Xpd ^{TTD}
Anatomical data			
Number of animals in group	sham	17	16
	mTAC	14	11
	sTAC	15	17
	MI	10	10
Body weight (g)	sham	24.6 ± 1.1	23.9 ± 0.6
	mTAC	24.4 ± 0.8	22.2 ± 0.8
	sTAC	24.6 ± 0.8	21.7 ± 0.7 §
	MI	25.6 ± 1.2	24.1 ± 0.8
LV weight (mg)	sham	85 ± 3	90 ± 3
	mTAC	113 ± 5 *	122 ± 7 *
	sTAC	163 ± 8 *†‡	150 ± 6 *†‡
	MI	112 ± 4 *	117 ± 5 *
RV weight (mg)	sham	23 ± 1	29 ± 2
	mTAC	23 ± 1 †	25 ± 1 †
	sTAC	30 ± 2 *‡	30 ± 2 †
	MI	33 ± 3 *	36 ± 3 *
LV wall thickness (mm)	sham	1.01 ± 0.04	1.05 ± 0.06
	mTAC	1.06 ± 0.04	1.19 ± 0.07
	sTAC	1.23 ± 0.07 *	1.25 ± 0.08 *
	MI	1.26 ± 0.14 *	1.38 ± 0.14 *
Functional data			
Heart Rate (bpm)	sham	528 ± 10	548 ± 12
	mTAC	548 ± 9	537 ± 10
	sTAC	550 ± 9	540 ± 17
	MI	526 ± 16	526 ± 7
MAP systemic (mmHg)	sham	83 ± 3	78 ± 3
	mTAC	72 ± 4 †	69 ± 5 §
	sTAC	59 ± 4 †	69 ± 7 §
	MI	69 ± 5 *	61 ± 5 *
Tau (ms)	sham	8.9 ± 0.6	9.0 ± 0.9
	mTAC	10.3 ± 0.7 †	11.3 ± 0.9
	sTAC	12.7 ± 1.7 *	13.1 ± 0.9
	MI	15.4 ± 1.8 *	13.9 ± 1.3 *

MAP, mean arterial pressure.

*P<0.05 vs corresponding sham; †P<0.05 vs corresponding sTAC; §P<0.05 vs corresponding Wt.

In contrast to clinical studies that consistently show an exponential increase of mortality rates following acute MI with age²⁶⁻³⁰ because of increase in occurrence of cardiac rupture^{26,31-32} and arrhythmias,²⁸ natural aging from 3 to 12 months, or deficient DNA repair (resulting in accelerated ageing) did not aggravate MI-associated mortality in Wt and Xpd^{TTD} mice. Additionally, 12mo Wt and Xpd^{TTD} mice developed less LV dilation in response to MI than 3mo mice. This might indicate reduced degradation of extra cellular matrix proteins³³⁻³⁴ that would contribute to the prevention of LV dilation and infarct rupture.³⁵ However, future studies will be needed to confirm these speculations. Interestingly, mTAC, which did not induce significant mortality in 1 year old Wt mice, markedly increased mortality in DNA repair deficient mice. Likewise, following severe aortic constriction mortality was robustly increased in 12mo accelerated aged mice compared to Wt littermates and furthermore markedly deteriorated compared to 3 months old DNA repair deficient mice. Accordingly, already 1 week following sTAC when most Xpd^{TTD} were still alive, sTAC induces more severe LV dilation in 12mo Xpd^{TTD} mice than in 12mo Wt mice. Taken together these findings show that mortality in Xpd^{TTD} mice in response to mTAC as well as sTAC but not to MI was increased compared to Wt mice.

These observations suggest that the type of cardiac-overload, rather than the degree of cardiac dysfunction, critically determines the cardiac pathological response and the susceptibility to overload.

Mechanisms underlying the divergent interactions between ageing and TAC and MI induced cardiac remodeling

The question remains why accelerated aging as a result of cumulative DNA damage would markedly increase cardiac vulnerability to aortic stenosis without affecting the survival rate in MI. A potential mechanism underlying the divergent effects of cumulative DNA damage on cardiac vulnerability could be the level of oxidative stress. Under pathological conditions increased ROS production is the major inducer of DNA damage.³⁶ However, the mechanism of ROS production is not identical in the distinct etiologies. In the TAC model an important source of ROS is eNOS uncoupling.³⁷⁻³⁸ Oxidative stress causes eNOS uncoupling, i.e. shift from a dimeric to a monomeric form that no longer produces NO but forms superoxide instead.³⁹⁻⁴⁰ Consequently, eNOS uncoupling reduces bioavailability of NO and increases ROS production that, in turn, aggravates eNOS uncoupling and results in a vicious cycle of ROS-induced ROS release.⁴¹⁻⁴² The elevated ROS levels result in oxidative damage to DNA, membranes, proteins and other macromolecules, not only stimulating cardiac remodeling and failure⁴³⁻⁴⁴ but also contributing to the progression of aging.²⁰

Consequently, oxidative stress plays an important role in both aging and heart failure. Hence, TAC-mediated increased oxidative stress and DNA damage could synergistically contribute to the increased cardiac vulnerability to TAC in our mouse model of impaired DNA repair. Furthermore, by impairing Ca²⁺ handling and modulating ion channels in cardiomyocytes, TAC-induced ROS production may predispose the pressure-overloaded heart to arrhythmias.⁴⁵ Increased susceptibility to arrhythmias would also explain why survival rates already drop rapidly early after mTAC and sTAC in accelerated aged mice while LV hypertrophy and dysfunction are still relatively modest (Fig 3). Additionally it is

possible that the development of LV hypertrophy and dysfunction are blunted in Xpd^{TTD} mice as a result of a survival response to accumulation of DNA damage.⁴⁶

Limitations to the study and future directions

The mechanisms behind the increased cardiac vulnerability to pressure overload with aging are currently difficult to evaluate because the very high mortality rates likely resulted in self-selection explaining why the few TAC mice that survived the 8 week follow-up period failed to exhibit severe cardiac remodeling and dysfunction. Future studies, that will involve cardiac functional measurements 1-2 weeks following TAC, when cardiac remodeling is still in progress and most mice still alive, are needed to obtain better insight in the effect of cumulative DNA damage and accelerated aging on LV remodeling and dysfunction. Moreover, the potential role of increased vulnerability to cardiac arrhythmias in DNA damage induced accelerated aging should be investigated by continuously measuring ECG, via Holter monitoring, in Wt and Xpd^{TTD} mice subjected to TAC.

Potential clinical implications

As clinical trials have generally excluded elderly people, management of cardiovascular disease in elderly is principally based on evidence from younger patient cohorts.¹⁶ Besides fundamental animal research on the mechanism behind increased vulnerability to develop HF with aging, clinical trials focusing on management of HF in elderly are needed. Prevention of cellular and DNA damage by reducing oxidative stress while preventing eNOS uncoupling by tetrahydrobiopterin treatment or folic acid supplementation⁴⁷ or physical exercise induced eNOS and antioxidant stimulation⁴⁸ are promising potential targets in elderly HF patients.

The striking observation in mice in the present study, that accelerated aging as a consequence of deficient DNA repair reduced survival of pressure-overload through a mild as well as a severe aortic stenosis but not to MI, demonstrates clearly that not all forms of heart failure are similar. Furthermore, this indicates that the effect of DNA damage induced aging on vulnerability to cardiac-overload, critically depends on the type of underlying etiology rather than the degree of cardiac overload.

References

1. Curtis, L.H., et al., Incidence and prevalence of heart failure in elderly persons, 1994-2003. *Arch Intern Med*, 2008. 168(4): p. 418-24.
2. McCullough, P.A., et al., Confirmation of a heart failure epidemic: findings from the Resource Utilization Among Congestive Heart Failure (REACH) study. *J Am Coll Cardiol*, 2002. 39(1): p. 60-9.
3. Bui, A.L., T.B. Horwich, and G.C. Fonarow, Epidemiology and risk profile of heart failure. *Nat Rev Cardiol*, 2011. 8(1): p. 30-41.
4. Levy, D., et al., Long-term trends in the incidence of and survival with heart failure. *N Engl J Med*, 2002. 347(18): p. 1397-402.
5. Lloyd-Jones, D.M., et al., Lifetime risk for developing congestive heart failure: the Framingham Heart Study. *Circulation*, 2002. 106(24): p. 3068-72.
6. Mosterd, A., et al., Prevalence of heart failure and left ventricular dysfunction in the general population; The Rotterdam Study. *Eur Heart J*, 1999. 20(6): p. 447-55.
7. Oxenham, H. and N. Sharpe, Cardiovascular aging and heart failure. *Eur J Heart Fail*, 2003. 5(4): p. 427-34.
8. Bernhard, D. and G. Laufer, The aging cardiomyocyte: a mini-review. *Gerontology*, 2008. 54(1): p. 24-31.
9. Lakatta, E.G. and D. Levy, Arterial and cardiac aging: major shareholders in cardiovascular disease enterprises: Part II: the aging heart in health: links to heart disease. *Circulation*, 2003. 107(2): p. 346-54.
10. Lee, D.S., et al., Predicting mortality among patients hospitalized for heart failure: derivation and validation of a clinical model. *JAMA*, 2003. 290(19): p. 2581-7.
11. Garinis, G.A., et al., DNA damage and ageing: new-age ideas for an age-old problem. *Nat Cell Biol*, 2008. 10(11): p. 1241-7.
12. Johnson, F.B., D.A. Sinclair, and L. Guarente, Molecular biology of aging. *Cell*, 1999. 96(2): p. 291-302.
13. Kirkwood, T.B., Understanding the odd science of aging. *Cell*, 2005. 120(4): p. 437-47.
14. Hoeijmakers, J.H., DNA damage, aging, and cancer. *N Engl J Med*, 2009. 361(15): p. 1475-85.
15. de Boer, J., et al., Premature aging in mice deficient in DNA repair and transcription. *Science*, 2002. 296(5571): p. 1276-9.
16. Shih, H., et al., The aging heart and post-infarction left ventricular remodeling. *J Am Coll Cardiol*, 2011. 57(1): p. 9-17.
17. Imazio, M., et al., Management of heart failure in elderly people. *Int J Clin Pract*, 2008. 62(2): p. 270-80.
18. van Deel, E.D., et al., Extracellular superoxide dismutase protects the heart against oxidative stress and hypertrophy after myocardial infarction. *Free Radic Biol Med*, 2008. 44(7): p. 1305-13.
19. van Deel, E.D., et al., Exercise training does not improve cardiac function in compensated or decompensated left ventricular hypertrophy induced by aortic stenosis. *J Mol Cell Cardiol*, 2011. 50(6): p. 1017-25.
20. Harman, D., Aging: a theory based on free radical and radiation chemistry. *J Gerontol*, 1956. 11(3): p. 298-300.
21. Roger, V.L., et al., Heart disease and stroke statistics--2011 update: a report from the American Heart Association. *Circulation*, 2011. 123(4): p. e18-e209.
22. Bujak, M., et al., Aging-related defects are associated with adverse cardiac remodeling in a mouse model of reperfusion myocardial infarction. *J Am Coll Cardiol*, 2008. 51(14): p. 1384-92.
23. Przyklenk, K., et al., Aging mouse hearts are refractory to infarct size reduction with post-conditioning. *J Am Coll Cardiol*, 2008. 51(14): p. 1393-8.
24. Boluyt, M.O., et al., Cardiac adaptations to aortic constriction in adult and aged rats. *Am J Physiol*, 1989. 257(2 Pt 2): p. H643-8.
25. Sopko, N.A., et al., Bone marrow support of the heart in pressure overload is lost with aging. *PLoS One*, 2010. 5(12): p. e15187.
26. French, J.K., et al., Mechanical complications after percutaneous coronary intervention in ST-elevation myocardial infarction (from APEX-AMI). *Am J Cardiol*, 2010. 105(1): p. 59-63.
27. Maggioni, A.P., et al., Age-related increase in mortality among patients with first myocardial infarctions treated with thrombolysis. The Investigators of the Gruppo Italiano per lo Studio della Sopravvivenza nell'Infarto Miocardico (GISSI-2). *N Engl J Med*, 1993. 329(20): p. 1442-8.
28. Ornato, J.P., et al., Factors associated with the occurrence of cardiac arrest during hospitalization for acute myocardial infarction in the second national registry of myocardial infarction in the US. *Resuscitation*, 2001. 48(2): p. 117-23.
29. White, H.D., et al., Age and outcome with contemporary thrombolytic therapy. Results from the GUSTO-I trial. Global Utilization of Streptokinase and TPA for Occluded coronary arteries trial. *Circulation*, 1996.

- 94(8): p. 1826-33.
30. Alexander, K.P., et al., Acute coronary care in the elderly, part II: ST-segment-elevation myocardial infarction: a scientific statement for healthcare professionals from the American Heart Association Council on Clinical Cardiology: in collaboration with the Society of Geriatric Cardiology. *Circulation*, 2007. 115(19): p. 2570-89.
 31. Moreno, R., et al., Primary angioplasty reduces the risk of left ventricular free wall rupture compared with thrombolysis in patients with acute myocardial infarction. *J Am Coll Cardiol*, 2002. 39(4): p. 598-603.
 32. Yang, Y., et al., Age-related differences in postinfarct left ventricular rupture and remodeling. *Am J Physiol Heart Circ Physiol*, 2008. 294(4): p. H1815-22.
 33. Jugdutt, B.I., Ventricular remodeling after infarction and the extracellular collagen matrix: when is enough enough? *Circulation*, 2003. 108(11): p. 1395-403.
 34. Spinale, F.G., Myocardial matrix remodeling and the matrix metalloproteinases: influence on cardiac form and function. *Physiol Rev*, 2007. 87(4): p. 1285-342.
 35. Kandam, V., et al., Early activation of matrix metalloproteinases underlies the exacerbated systolic and diastolic dysfunction in mice lacking TIMP3 following myocardial infarction. *Am J Physiol Heart Circ Physiol*, 2010. 299(4): p. H1012-23.
 36. Bertram, C. and R. Hass, Cellular responses to reactive oxygen species-induced DNA damage and aging. *Biol Chem*, 2008. 389(3): p. 211-20.
 37. Moens, A.L., et al., Reversal of cardiac hypertrophy and fibrosis from pressure overload by tetrahydrobiopterin: efficacy of recoupling nitric oxide synthase as a therapeutic strategy. *Circulation*, 2008. 117(20): p. 2626-36.
 38. Takimoto, E., et al., Oxidant stress from nitric oxide synthase-3 uncoupling stimulates cardiac pathologic remodeling from chronic pressure load. *J Clin Invest*, 2005. 115(5): p. 1221-31.
 39. Balligand, J.L., O. Feron, and C. Dessy, eNOS activation by physical forces: from short-term regulation of contraction to chronic remodeling of cardiovascular tissues. *Physiol Rev*, 2009. 89(2): p. 481-534.
 40. Munzel, T., et al., Vascular consequences of endothelial nitric oxide synthase uncoupling for the activity and expression of the soluble guanylyl cyclase and the cGMP-dependent protein kinase. *Arterioscler Thromb Vasc Biol*, 2005. 25(8): p. 1551-7.
 41. Landmesser, U., et al., Oxidation of tetrahydrobiopterin leads to uncoupling of endothelial cell nitric oxide synthase in hypertension. *J Clin Invest*, 2003. 111(8): p. 1201-9.
 42. Zinkevich, N.S. and D.D. Gutterman, ROS-induced ROS release in vascular biology: redox-redox signaling. *Am J Physiol Heart Circ Physiol*, 2011. 301(3): p. H647-53.
 43. Seddon, M., Y.H. Looi, and A.M. Shah, Oxidative stress and redox signalling in cardiac hypertrophy and heart failure. *Heart*, 2007. 93(8): p. 903-7.
 44. Lu, Z., et al., Extracellular superoxide dismutase deficiency exacerbates pressure overload-induced left ventricular hypertrophy and dysfunction. *Hypertension*, 2008. 51(1): p. 19-25.
 45. Nediani, C., et al., Nitric oxide/reactive oxygen species generation and nitroso/redox imbalance in heart failure: from molecular mechanisms to therapeutic implications. *Antioxid Redox Signal*, 2011. 14(2): p. 289-331.
 46. Susa, D., et al., Congenital DNA repair deficiency results in protection against renal ischemia reperfusion injury in mice. *Aging Cell*, 2009. 8(2): p. 192-200.
 47. Zhang, Y., et al., Modulating endothelial nitric oxide synthase: a new cardiovascular therapeutic strategy. *Am J Physiol Heart Circ Physiol*, 2011. 301(3): p. H634-46.
 48. Golbidi, S. and I. Laher, Molecular mechanisms in exercise-induced cardioprotection. *Cardiol Res Pract*, 2011. 2011: p. 972807.





General Discussion

10

Heart failure is a global health problem with increasing prevalence characterized by maladaptive cardiac remodeling and dysfunction.¹ The progression of heart failure is strongly influenced by the balance between nitric oxide (NO) and reactive oxygen species (ROS): the nitroso-redox balance.²⁻³ Disturbance of this delicate balance results in elevated ROS levels and impaired bioavailability of NO and consequently predisposes the heart to failure by promoting pathological cardiac hypertrophy and dilation⁴ and reducing cardiac function⁵ (Figure 1).

NO in heart failure

Since the discovery of endothelial-derived relaxing factor in 1980⁶ the crucial role of NO in maintaining normal cardiovascular function has been well established.^{5,7-9} In spite of well described cardioprotective effects of NO,^{7,9-10} the role of NOS in the cardiovascular system remains controversial as both adaptive as well as maladaptive effects have been ascribed to NOS. NOS produced NO is known to stimulate vasodilation, cardiac function and attenuate pathological remodeling.⁷ However, in pathology, oxidation or reduction of the eNOS cofactor tetrahydrobiopterin (BH4) causes NOS to uncouple from a dimeric to a monomeric form that no longer produces NO but forms superoxide instead.^{7,11} Subsequently, NOS produced superoxide shifts the nitroso-redox balance even further by scavenging of NO and forming peroxynitrite oxidants that further uncouple NOS.² Consequently NOS uncoupling reduces bioavailability of NO and increases ROS production that further aggravates NOS uncoupling and results in a vicious cycle of ROS induced ROS release.¹²⁻¹³

In this thesis we have investigated the role of two NOS isoforms in the development of heart failure; inducible NOS (iNOS) and endothelial NOS (eNOS). Besides being an important component of the immune defence mechanism,¹⁴ we demonstrated in **chapter 2** that iNOS also plays a role in pressure-overload induced LV remodeling and dysfunction as a result of iNOS uncoupling-induced oxidative stress. Additionally, also eNOS uncoupling contributed to pressure-overload induced cardiac hypertrophy and dysfunction (**chapter 2**). Accordingly, under non pathological conditions, overexpression of coupled eNOS provoked cardioprotective effects like reduction of cholesterol levels and blood pressure resulting in a reduction in atherosclerotic lesions (**chapter 3**). Subsequently, we established in **chapter 4** that the reduced blood pressure observed in eNOS overexpressing mice was indeed the consequence of eNOS-induced systemic vasodilation. However, the high level of eNOS overexpression only induced moderate vasodilation as a consequence of a compensatory mechanism of reduced soluble guanylyl cyclase activity (**chapter 4**).

In healthy conditions eNOS expression is activated and upregulated by exercise enhanced shear stress and mechanical stretch.⁷ Increased eNOS expression potentially protects the heart by increasing cardiac oxygen supply,¹⁵⁻¹⁶ promoting cardiac relaxation and filling^{5,17-18} and increasing myocardial contractile force.^{7,19} Additionally exercise induced activation of the PI3K/Akt pathway not only stimulates eNOS but concurrently induces physiological hypertrophy that further enhances cardiac function.²⁰ These beneficial effects of physical

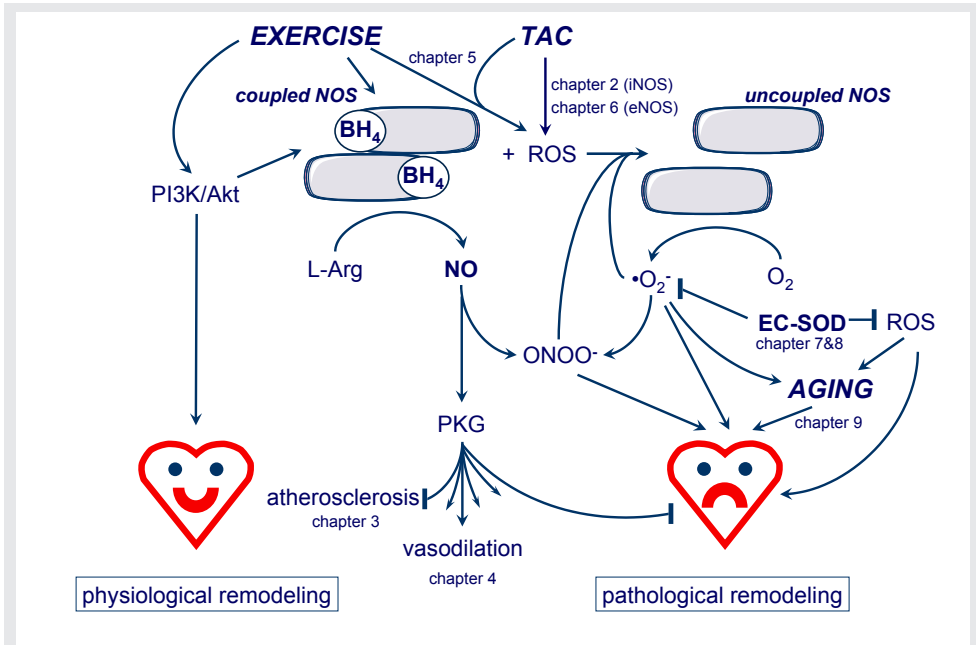


Figure 1. Schematic overview of the effects of the interaction between eNOS and ROS on cardiac remodeling described in this thesis.

exercise on cardiac function and the development of physiological hypertrophy have provoked the idea that exercise training might be therapeutic in improving cardiac function and reversing pathological remodeling in heart failure patients.²¹ However, data on the influence of physical exercise on LV remodeling remain highly inconclusive and appear to be influenced by several factors like the type of exercise training performed, the timing of onset of training and the underlying pathology of heart failure. The differential effects of different types of exercise was nicely illustrated in a meta-analysis by Haykowsky et al. which demonstrated that aerobic training but not strength training or combined aerobic and strength training improved cardiac function and reversed LV remodeling in heart failure patients.²² Secondly, careful examination of several human and animal MI studies suggests that the timing of onset of the training protocol can significantly influence the potential protective effects of exercise. Following a large MI, the majority of studies reported that exercise had beneficial effects²³⁻²⁹ or no effect³⁰⁻³⁴ on cardiac function and dilation when started late after MI, although negative effects were reported in one study.³⁵ However when exercise was started early after a large MI most studies reported that exercise had either no³⁶⁻⁴³ or even detrimental effects^{35,44-45} on LV remodeling and dysfunction although some studies also described attenuated remodeling by exercise.⁴⁶⁻⁴⁷ Additionally, etiology seems a critical determinant of cardiac exercise effects. Since the pressure overloaded, volume overloaded and infarcted heart are characterized by different remodeling phenotypes and underlying molecular signalling pathways, it is not surprising that exercise training differently affects these distinct pathologies. In fact, studies that directly compared ischemic and non-ischemic heart failure show that exercise-induced reversal of LV remodeling and improvement of cardiac function and exercise capacity is

more profound in non-ischemic than in ischemic heart failure patients.⁴⁸⁻⁴⁹ Accordingly, the majority of human and animal studies,⁵⁰⁻⁵⁸ but not all,⁵⁹⁻⁶² examining the effect of exercise training on hypertension demonstrate positive effects of exercise training on LV remodeling while only one study of voluntary wheel running in spontaneous hypertensive rats⁶³ describes detrimental effects of exercise on LV remodeling and dysfunction. Besides hypertension, pressure-overload to the heart can also be induced by obstruction of the LV outflow track as occurs in aortic stenosis.⁶⁴ Therefore, in **chapter 5** we investigated whether exercise training also protects the heart against pathological remodeling in response to a transverse aortic constriction (TAC). In contrast to the mainly beneficial effects of exercise in hypertension induced pressure-overload hypertrophy,⁵⁰⁻⁵⁸ we and others⁶⁵⁻⁶⁷ found that exercise training had no protective effect on remodeling and dysfunction in aortic constriction. The critical dependence of beneficial exercise effects on cardiac dysfunction are underlined by comparing data from our own lab of mouse models for MI^{38,46} and pressure-overload from TAC (**chapter 5**) (Figure 2). A first

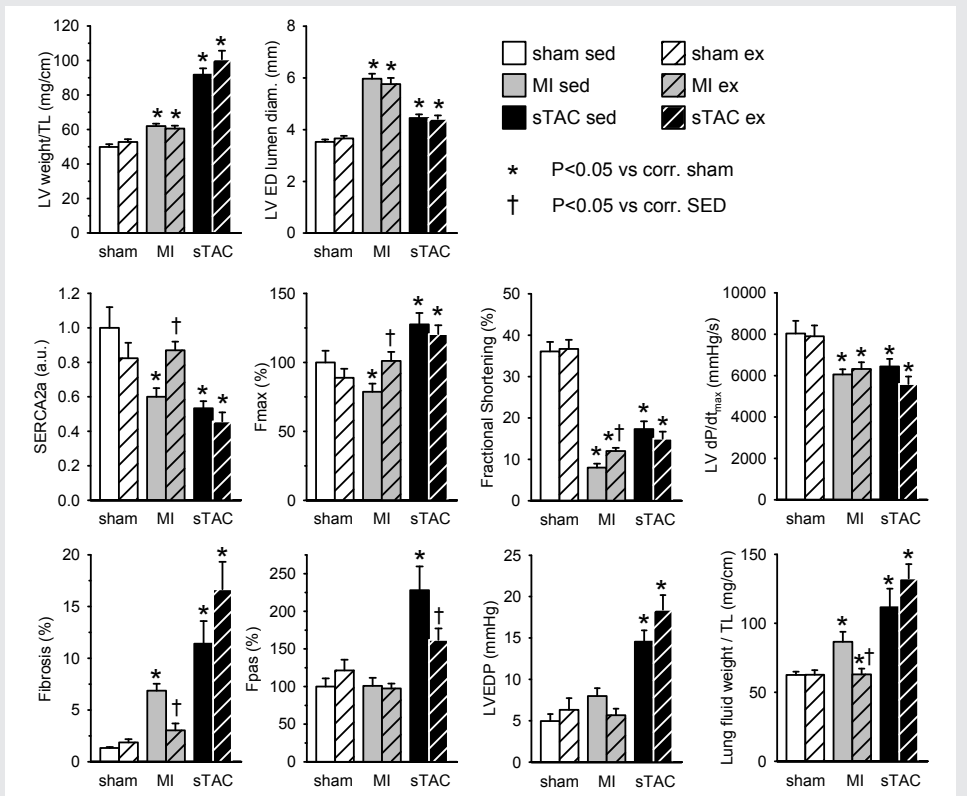


Figure 2. Effects of aetiology and exercise on left ventricular (LV) remodeling and function as well as pulmonary congestion following MI (data from de Waard et al. [38, 46]) and sTAC (chapter 5). Physical exercise training (hatched bars) attenuates cardiac dysfunction and congestion in response to myocardial infarction (MI) (grey bars) but does not exert beneficial cardiac effects following severe transverse aortic constriction (sTAC) (black bars). TL, tibia length; ED, end diastolic, SERCA, sarcoplasmic reticulum calcium ATPase; Fmax, maximal force; Fpas, passive force; LVEDP, LVED pressure. *P<0.05 vs corresponding sham; †P<0.05 vs corresponding sedentary animals.

indication that the cardiac response to these two forms of overload is not identical comes from the etiology dependent decrease of cardiac compliance (fibrosis, passive force and LV end diastolic pressure) and concomitant pulmonary congestion that was much more severe in TAC than in MI. Secondly, although 8 weeks of exercise training mildly improved cardiac function and mitigated pulmonary congestion in mice with an MI, the identical exercise protocol did not attenuate cardiac dysfunction or pulmonary congestion in the pressure-overloaded TAC model. The loss of beneficial exercise effects in the presence of a fixed aortic stenosis is likely the result of prevention of an exercise-induced reduction of peripheral resistance⁶⁸ by the fixed stenosis. In contrast, in the presence of a stenotic aorta, the fixed stenosis causes a marked increase in systolic pressure during exercise⁶⁹ that worsens the overload during exercise and may consequently abrogate the beneficial effects of exercise training.

Potentially, pharmacological or genetic tools that harness the beneficial effects of exercise on cardiac remodeling and dysfunction without the detrimental effects of exercise-induced exacerbated systolic loading could prove to be more effective in heart failure patients than exercise. Since the protective effects of physical exercise are principally mediated by increased eNOS activity,^{46,70} the influence of the eNOS-pathway on cardiac remodeling and dysfunction has been the subject of many studies. Indeed experiments in eNOS overexpressing^{46,71} and eNOS deficient mice⁷² demonstrate protective effects of eNOS against adverse cardiac remodeling and dysfunction following MI. However, in another form of cardiac remodeling, where hypertrophy and dysfunction are induced by cardiac pressure-overload through a fixed stenosis of the aorta, the effects of eNOS are less clear. One group found eNOS deficiency to aggravate pressure-overload hypertrophy from TAC⁷³⁻⁷⁴ that was contradicted by results from another study demonstrating loss of eNOS to protect the heart against the consequences of pressure-overload.⁷⁵ A difference in severity of pressure-overload was proposed as a possible explanation for this discrepancy⁷⁵ but this was so far never further investigated. To obtain better insight in the role of eNOS in pressure-overload we studied in **chapter 6** the effect of loss as well as overexpression of eNOS in severe and mild pressure-overload through aortic constriction. Interestingly, we found loss of eNOS not only to protect the heart against severe but also against mild pressure-overload. Furthermore, eNOS overexpression in TAC did not exhibit the beneficial effects on cardiac dysfunction observed in MI^{46,71}, but in contrast aggravated LV remodeling and dysfunction following mild as well as severe TAC. Apparently, the described divergent effects of eNOS on pressure-overload hypertrophy are not explained by overload severity. However it should be noted that in spite of the same degree of stenosis, wildtype littermate mice in the studies in which eNOS deficiency was protective (**chapter 6** and ref. 75) developed more LV hypertrophy (~100%) in response to TAC compared to mice in which loss of eNOS was detrimental⁷³⁻⁷⁴ that increased heart weight by 50% in response to TAC. The diverse hypertrophic response to TAC indicates that perhaps a difference in genetic background influenced the cardiac hypertrophic response and consequently the effects of eNOS on LV hypertrophy in these mice. An overview of data from our laboratory (chapter 6 and ref. 46,70), illustrating the opposite effects of eNOS expression level on cardiac remodeling and dysfunction in response to the two major forms of cardiac overload (MI and pressure-overload), is given in Figure 3.

Additionally, aggravation of the TAC-induced LV hypertrophy and dysfunction by eNOS, was demonstrated to be the result of pressure-overload induced eNOS-uncoupling and concomitant enhanced ROS production.⁷⁵ Accordingly, we demonstrated in **chapter 6** that detrimental effects of eNOS overexpression on LV hypertrophy and dysfunction in response to TAC can be abrogated by anti-oxidant treatment. Accordingly, although numbers of animals are limited (n=2) we demonstrated a trend towards increased eNOS-uncoupling in eNOS overexpressing mice following TAC (p=0.2). Since prevention of eNOS uncoupling by treatment with BH4 has been described to attenuated pressure-overload hypertrophy⁷⁵⁻⁷⁶ targeting eNOS uncoupling in heart failure has a high potential for effective treatment of heart failure patients.⁷⁷ Additionally, attenuation of TAC-induced adverse remodeling by inhibiting degradation of cGMP by phosphodiesterase type 5 further illustrates the potential protective properties of the NO-cGMP-pathway in pathological cardiac remodeling.⁷⁸⁻⁷⁹

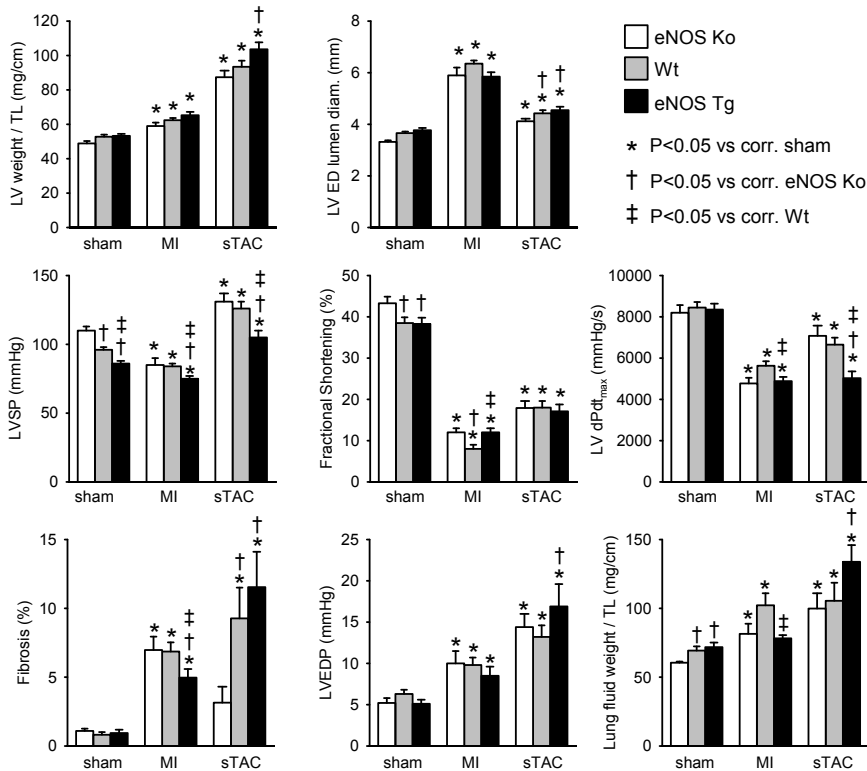


Figure 3. Effects of aetiology and eNOS expression level on left ventricular (LV) remodeling and function as well as pulmonary congestion in eNOS knock out (Ko) (white bars), wildtype (Wt) (grey bars) and eNOS overexpressing (Tg) (black bars) mice following MI (data from de Waard et al. [46, 70]) and sTAC (chapter 6). eNOS overexpression attenuated LV function and pulmonary congestion in response to myocardial infarction (MI), but in contrast aggravated cardiac dysfunction and congestion following severe transverse aortic constriction (sTAC). Moreover, detrimental effects of TAC induced pressure-overload were attenuated by loss of eNOS. TL, tibia length; ED, end diastolic; LVSP, LV systolic pressure; LVEDP, LVED pressure. *P<0.05 vs corresponding sham; †P<0.05 vs corresponding eNOS Ko; ‡P<0.05 vs corresponding Wt.

Oxidative stress in heart failure

Increased oxidative stress plays an important role in the pathophysiology of heart failure.²⁻⁸⁰ Because of their high metabolic activity mitochondria rich cardiomyocytes form a particularly active source of ROS.⁸¹ ROS contribute to the progression of HF by impairing cardiac function through modifying proteins critical for excitation-contraction coupling,⁸¹⁻⁸² stimulating adverse cardiac remodeling by inducing cell damage and cell death⁸³ and activating hypertrophic signaling pathways^{80,84} and inducing cardiac fibrosis.⁸⁵ In healthy physiology, diverse nonenzymatic and enzymatic antioxidants protect cells against ROS induced damage by degrading ROS to non toxic molecules.⁸⁶ Nonenzymatic antioxidants include vitamins E and C,⁸⁷ whereas well characterized enzymatic antioxidants are superoxide dismutases (SODs) that scavenge the oxygen radical superoxide ($O_2^{\cdot-}$).⁸⁸ However, under pathological conditions ROS production can overwhelm the antioxidant defense mechanisms, resulting in oxidative stress.

In the interaction between oxidative stress and NO the role of the antioxidant EC-SOD is particularly interesting. Colocalization of EC-SOD with eNOS across the LV wall,⁸⁹ increased NO bioavailability by EC-SOD⁹⁰ and stimulation of EC-SOD expression by NO,⁹¹ demonstrate a strong interaction between NO and EC-SOD and imply a functional role for EC-SOD in the regulation of the nitroso-redox balance. Accordingly, EC-SOD protected the heart against TAC (**chapter 7**) and MI-induced (**chapter 8**) myocardial oxidative stress, hypertrophy, fibrosis and dysfunction. Additionally in response to pressure-overload EC-SOD deficiency markedly increased myocardial fibrosis and aggravated concomitant pulmonary congestion whereas in MI loss of EC-SOD aggravated the already high fibrosis content in the border zone of the infarction but did not affect fibrosis in the surviving tissue. These data show that EC-SOD protects against cardiac hypertrophy and dysfunction by mitigating etiology dependent and independent features.

Oxidative stress is not only important in cardiovascular diseases but also plays a role in aging.⁹² Accumulation of ROS induces damage to DNA, proteins and lipids that impairs cell function and eventually results in cell death.⁹³ Interestingly, aging induces a number of non-pathologic structural and functional cardiac changes that resemble alterations typically observed in heart failure⁹⁴ like reduced number of cardiomyocytes,⁹⁵ hypertrophy of the remaining cardiomyocytes, cardiac fibrosis⁹⁵⁻⁹⁶ and reduced contractile function.⁹⁵⁻⁹⁶ These changes may affect cardiac function only minimally under non pathological conditions but likely result in reduced cardiac reserve and increased vulnerability of the heart to develop cardiac failure. Accordingly, clinical trials have shown that age is an important predictor for mortality in heart failure patients.⁹⁷ Interestingly, we found in **chapter 9** that the effects of DNA damage-induced aging on the response to cardiac overload are highly dependent on the underlying etiology. In the Xpd^{TTD} mouse model,⁹⁸ cardiac remodeling and dysfunction as well as mortality as a result of MI were unaffected by cumulative DNA damage induced aging. In contrast, 1 year of accelerated aging had detrimental effects on survival after severe aortic constriction compared to wildtype 1 year old mice and younger Xpd^{TTD} mice with less cumulative DNA damage. Moreover, mild aortic constriction produced modest LV hypertrophy and dysfunction in

young Xpd^{TTD} mice and old wildtype littermates, but resulted in pronounced mortality in 1 year old Xpd^{TTD} animals. Clearly, TAC-induced mortality is aggravated in the aged heart. In exercise and eNOS overexpression, the detrimental effects of TAC compared to MI are likely caused by a more severe disturbance of the nitroso-redox balance in TAC than in MI. Hence, etiology dependence of the elevation in ROS production might also explain why mortality in TAC Xpd^{TTD} mice is aggravated while mortality in MI Xpd^{TTD} mice is not affected. Consequently, the influence of accelerated aging by accumulated DNA damage on the vulnerability of the heart to pathological overload is critically determined by the type of cardiac-overload and the associated underlying pathology.

Future perspectives

In this thesis we investigated the influence of the delicate balance between NO and ROS on cardiac remodeling. Better understanding and potential regulation of this balance holds promise for improved treatment of many cardiovascular diseases including pathological remodeling and heart failure.⁷⁷ However, these discoveries also unmasked the challenging tight interplay between NO and ROS and complex cross-talk with numerous cellular signalling pathways² (Figure 1). Further investigation is needed before the potential of NO and ROS scavenging can be optimally employed in clinical treatment.

Current pharmacological therapy in heart failure patients consists of angiotensin converting enzyme (ACE)-inhibitors, beta blockers and diuretics.⁹⁹⁻¹⁰¹ Additional agents to optimize therapy include angiotensin receptor blockers (ARBs) and aldosterone antagonists. ACE-inhibitors, ARBs and aldosterone antagonists all act on the renin-angiotensin-aldosterone system (RAAS) and exert their effect by preventing vasoconstriction, sodium and water retention, aldosterone and vasopressin release and stimulation of sympathetic tone. Additionally, RAAS inhibitors beneficially influence cardiac remodeling by impeding cardiac fibrosis, inflammation and cell growth. Beta blockers block the action of endogenous catecholamines on the beta adrenergic receptor and decrease renin secretion which both reduce congestion. Additionally, beta blockers attenuate pathological remodeling by reducing myocardial hypertrophy and fibrosis.¹⁰² Finally, diuretics restore and maintain normal volume status in patients with signs of fluid overload, and consequently prevent the development of secondary right ventricular remodeling. However, these treatments primarily focus on systolic dysfunction as observed after myocardial infarction while guidelines for patients with an aortic stenosis that develop systolic but also marked diastolic heart failure, only recommend follow-up until the onset of symptoms¹⁰³⁻¹⁰⁴ at which surgical intervention needs to be performed promptly because of the high increase in mortality after the onset of severe symptoms.⁶⁴ Because symptom onset is subjective and often rapidly progressive it would be favorable to prevent or slow down the development of severe symptoms by pharmacological treatment in order to delay or even avert the necessity for surgical intervention. Unfortunately, no medical treatment is capable of reducing the progression of aortic stenosis induced LV hypertrophy and dysfunction so far.¹⁰⁵

Cardioprotective potential of eNOS

The research described in this thesis as well as numerous other animal studies suggest an important role for the nitroso-redox balance in the progression of pressure-overload induced cardiac failure in response to an aortic stenosis.^{73-75,106-110} However, the potency for eNOS as therapeutic tool remains controversial because eNOS can exert protective as well as detrimental effects on cardiac remodeling. Future studies are required to investigate how increased eNOS expression by physical exercise or pharmacological stimulation can be beneficial in pressure-overload hypertrophy in response to an aortic stenosis without provoking detrimental eNOS-uncoupling.

A potent inducer of eNOS expression and activation is physical exercise.⁷ Yet, patients with moderate to severe aortic stenosis are recommended to avoid competitive sports to reduce the risk of sudden death.¹¹¹ Nevertheless, until recently no clinical study investigated whether exercise restriction is actually beneficial for patients with an aortic stenosis.¹¹² Recently, one study compared patients after balloon valvuloplasty for aortic stenosis that were or were not recommended to avoid sport activities.¹¹³ In line with results described in **chapter 5** of this thesis, the outcomes of this study suggest that there is no clear association between exercise and sudden death in aortic stenosis,¹¹³ yet effects of exercise on cardiac remodeling in these patients were not assessed.

Previously we showed in MI that beneficial exercise effects depend on eNOS by demonstrating that the beneficial effects of exercise require full eNOS expression⁷⁰ and can be mimicked through overexpression of eNOS.^{46,71} Lack of beneficial effects of exercise (**chapter 5**) as well as eNOS (**chapter 6**) in the TAC model and normalisation of adverse effects of eNOS overexpression with antioxidant treatment (**chapter 6**) implies that the absence of beneficial effects of exercise training in the TAC model is not simply the result of exacerbated systolic loading during exercise. Likely, elevated ROS production, as a result of eNOS uncoupling also at least partly contributed to the loss of protective exercise effects in pressure-overload through TAC. Hence, it would be interesting to examine whether physical exercise is capable of exerting its beneficial effects on cardiac remodeling in the presence of an aortic stenosis when eNOS uncoupling and concomitant ROS production are prevented. However, so far clinical trials attempting to prevent eNOS uncoupling by administering a synthetic BH4 analog or by restoring the bioavailability of BH4 through folic acid treatment, failed to demonstrate beneficial effects.⁷⁷ The lack of cardioprotection by attempting to prevent eNOS uncoupling could potential be explained by insufficient dosage or instability of BH4.⁷⁷ However, further research is required to better understand how modulation of the nitroso-redox balance to can be optimized to attenuate cardiac remodeling and dysfunction induced by aortic stenosis.

Cardioprotective potential of antioxidant therapy

Many animal studies have demonstrated prevention of oxidant stress to attenuate LV remodeling.¹¹⁴⁻¹¹⁹ However, so far large clinical trials of antioxidant treatment have not been able to produce improvements in heart failure patients¹²⁰⁻¹²² and some trials even demonstrated increased risk of developing heart failure with antioxidant supplementation.¹²³⁻¹²⁴ Possible explanations for the lack of beneficial antioxidant effects

are the use of suboptimal dose, wrong antioxidant strategy or the lack of individually tailored therapy.⁸¹ Additionally, scavenging of all ROS will also affect ROS activated signalling pathways that are required for normal healthy cellular physiology. Hence, indiscriminate removal of ROS not only eliminates deleterious effects of ROS but also compromises intrinsic cardioprotective mechanisms. The potential of specifically targeting certain ROS producing enzymes is supported by the antioxidant properties of successful drugs already in use like ACE-inhibitors that inhibit NADPH oxidase activation.^{80,125} Because NADPH oxidase is an important initiator of eNOS uncoupling,² ACE-inhibitors would also help to restore the balance between ROS and NO. An additional possible target that could specifically beneficially modulate the nitroso-redox balance is EC-SOD. Indeed in **chapters 7 and 8** of this thesis we already demonstrated that EC-SOD is an important contributor to cardioprotection in the failing heart. The strong interaction between eNOS and EC-SOD is illustrated by EC-SOD colocalization with eNOS,⁸⁹ EC-SOD mediated increase in NO bioavailability⁹⁰ as well as NO stimulated EC-SOD expression,⁹¹ and suggests that the beneficial effects of EC-SOD involve restoration of the balance between NO and ROS. Consequently, novel EC-SOD mimetics that remove ROS in a site-specific manner may evoke more pronounced beneficial effects on cardiac remodeling and dysfunction in heart failure patients than non-selective antioxidants.

Cardioprotective potential of reducing oxidative stress in aging

ROS induced cellular damage is not only linked to cardiac pathophysiology but also associated with aging.⁹² Because myocyte damage in aging subsequently reduces cardiac functional reserve, aging is an important risk factor for the development of heart failure.¹²⁶ Consequently, reduction of cellular damage, particularly DNA damage, forms a highly potent target for attenuating the detrimental effects of aging on the failing heart. Particularly elderly patients with aortic stenosis potentially benefit from such a treatment, since aortic valve replacement is generally not considered in elderly patients with aortic stenosis because of the increase in the operative risk with age.¹⁰⁵ Because pharmacological restoration of the nitroso-redox balance, or selective inhibition of ROS in elderly patients, not only tackles direct overload induced cardiovascular pathology but also targets the detrimental effects of aging, selective reduction of oxidative stress and improvement of NO bioavailability presents a promising new strategy for treatment of aged heart failure patients. Therefore, clinical trials studying these compounds should consider enrolling this important patient group of elderly patients that are currently challenging to treat.

10 For a better understanding of the mechanism behind the influence of oxidative stress and DNA damage on aging and heart failure, future studies need to extend current knowledge. Preliminary results described in **chapter 9** revealed that accelerated aging through cumulative DNA damage particularly compromises the pressure-overloaded heart. Even a mild aortic stenosis, that in normal mice induced moderated LV hypertrophy associated with well maintained cardiac function, induced robust mortality in the prematurely aged mice. The fact that this increased mortality is not observed in response to MI suggests that an etiology specific mechanism the increased vulnerability to pressure-overload in aging. By comparing previous results from our laboratory^{46,70} with results from chapter 6 of this thesis (Figure 3) we can speculate that TAC, likely as a result of eNOS-uncoupling, induces

more oxidative stress in the myocardium than MI. Accordingly, eNOS uncoupling resulting in oxidative stress has been described to be an important contributor to LV hypertrophy and dysfunction in the TAC model.⁷⁶ Higher ROS levels in TAC and causative ROS-mediated DNA damage most likely explain the different effects of DNA repair deficiency on the increased vulnerability to cardiac overload in TAC and MI. However, the mechanisms behind the increased cardiac vulnerability to pressure overload with aging are currently difficult to evaluate because the very high mortality rates resulted in self-selection that may explain why the surviving TAC mice did not exhibit severe cardiac remodeling and dysfunction. Future studies, that will involve cardiac functional measurements 2 weeks following TAC when cardiac remodeling is still in progress and most mice are still alive, are required to obtain better insight in the effect of cumulative DNA damage and accelerated aging on LV remodeling and dysfunction.

In addition, the studies in this thesis clearly demonstrate the important role of the nitroso-redox balance in cardiac pathological remodeling and dysfunction. Modulation of the balance between NO and ROS, holds promising potential for attenuating cardiac vulnerability in aging. Elevated expression of eNOS, for example through physical exercise, combined with pharmacological prevention of eNOS uncoupling could provide a promising new therapeutic strategy to attenuate the development and progression of cardiac remodeling and failure in aging.

Furthermore, TAC induced ROS production may predispose the pressure-overloaded heart to arrhythmias, by impairing Ca^{2+} handling and modulating ion channels in cardiomyocytes.² In contrast to MI mice in which infarct rupture is an important contributor to mortality,¹²⁷ cardiac arrhythmias are the most likely cause of sudden death in TAC mice. Consequently, it would be of great interest to measure ECG and ion channel function in wildtype and Xpd^{TTD} TAC mice to investigate whether premature aged mice are indeed prone to develop fatal cardiac arrhythmias and consequently show reduced survival following TAC.

Additionally, like in human patients where multiple non-cardiac coexisting chronic conditions contribute to the development of heart failure, Xpd^{TTD} mice are also affected by several age-related diseases that are most overt in the liver, kidney and lymphoid tissue¹²⁸ and can influence the progression of heart failure. Although this similarity between elderly humans and the Xpd^{TTD} mouse makes this mouse an elegant model for global DNA damage induced accelerated aging, it is not possible to study isolated cardiac aging effects in these mice. In order to evaluate the influence of exclusive cardiomyocyte aging, a mouse model with cardio-specific aging should be generated in which increased cardiac vulnerability to hemodynamic overload with age can be studied without non cardiac age-related influences.

In conclusion, the research presented in this thesis clearly demonstrates the important role of the balance between eNOS and ROS in the development of heart failure and presents new insight in potential novel treatment strategies that increase NO bioavailability while selectively scavenging ROS. Although substantial additional research will be required to

fully comprehend the complex intertwined systems of oxidative stress and NO-signalling, it is clear that controlled modulation of the nitroso-redox balance is a promising target to prevent and attenuate cardiac remodeling and dysfunction. Moreover, this strategy is potentially particularly beneficial for elderly patients with aortic stenosis that are currently challenging to treat.¹²⁹

References

1. Bui, A.L., T.B. Horwich, and G.C. Fonarow, *Epidemiology and risk profile of heart failure*. *Nat Rev Cardiol*, 2011. **8**(1): p. 30-41.
2. Nediani, C., et al., *Nitric oxide/reactive oxygen species generation and nitroso/redox imbalance in heart failure: from molecular mechanisms to therapeutic implications*. *Antioxid Redox Signal*, 2011. **14**(2): p. 289-331.
3. Hare, J.M. and J.S. Stamler, *NO/redox disequilibrium in the failing heart and cardiovascular system*. *J Clin Invest*, 2005. **115**(3): p. 509-17.
4. Otani, H., *The role of nitric oxide in myocardial repair and remodeling*. *Antioxid Redox Signal*, 2009. **11**(8): p. 1913-28.
5. Massion, P.B., et al., *Nitric oxide and cardiac function: ten years after, and continuing*. *Circ Res*, 2003. **93**(5): p. 388-98.
6. Furchgott, R.F. and J.V. Zawadzki, *The obligatory role of endothelial cells in the relaxation of arterial smooth muscle by acetylcholine*. *Nature*, 1980. **288**(5789): p. 373-6.
7. Balligand, J.L., O. Feron, and C. Dessy, *eNOS activation by physical forces: from short-term regulation of contraction to chronic remodeling of cardiovascular tissues*. *Physiol Rev*, 2009. **89**(2): p. 481-534.
8. Forstermann, U. and W.C. Sessa, *Nitric oxide synthases: regulation and function*. *Eur Heart J*, 2011.
9. Jugdutt, B.I., *Nitric oxide and cardiovascular protection*. *Heart Fail Rev*, 2003. **8**(1): p. 29-34.
10. Jones, S.P. and R. Bolli, *The ubiquitous role of nitric oxide in cardioprotection*. *J Mol Cell Cardiol*, 2006. **40**(1): p. 16-23.
11. Munzel, T., et al., *Vascular consequences of endothelial nitric oxide synthase uncoupling for the activity and expression of the soluble guanylyl cyclase and the cGMP-dependent protein kinase*. *Arterioscler Thromb Vasc Biol*, 2005. **25**(8): p. 1551-7.
12. Landmesser, U., et al., *Oxidation of tetrahydrobiopterin leads to uncoupling of endothelial cell nitric oxide synthase in hypertension*. *J Clin Invest*, 2003. **111**(8): p. 1201-9.
13. Zinkevich, N.S. and D.D. Gutterman, *ROS-induced ROS release in vascular biology: redox-redox signaling*. *Am J Physiol Heart Circ Physiol*, 2011. **301**(3): p. H647-53.
14. Lowenstein, C.J. and E. Padalko, *iNOS (NOS2) at a glance*. *J Cell Sci*, 2004. **117**(Pt 14): p. 2865-7.
15. Duncker, D.J. and R.J. Bache, *Regulation of coronary blood flow during exercise*. *Physiol Rev*, 2008. **88**(3): p. 1009-86.
16. Gielen, S., G. Schuler, and V. Adams, *Cardiovascular effects of exercise training: molecular mechanisms*. *Circulation*, 2010. **122**(12): p. 1221-38.
17. Feron, O., et al., *Modulation of the endothelial nitric-oxide synthase-caveolin interaction in cardiac myocytes. Implications for the autonomic regulation of heart rate*. *J Biol Chem*, 1998. **273**(46): p. 30249-54.
18. Shah, A.M., et al., *8-bromo-cGMP reduces the myofilament response to Ca²⁺ in intact cardiac myocytes*. *Circ Res*, 1994. **74**(5): p. 970-8.
19. Seddon, M., A.M. Shah, and B. Casadei, *Cardiomyocytes as effectors of nitric oxide signalling*. *Cardiovasc Res*, 2007. **75**(2): p. 315-26.
20. McMullen, J.R., et al., *Phosphoinositide 3-kinase(p110alpha) plays a critical role for the induction of physiological, but not pathological, cardiac hypertrophy*. *Proc Natl Acad Sci U S A*, 2003. **100**(21): p. 12355-60.
21. Shabetai, R., *Beneficial effects of exercise training in compensated heart failure*. *Circulation*, 1988. **78**(3): p. 775-6.
22. Haykowsky, M.J., et al., *A meta-analysis of the effect of exercise training on left ventricular remodeling in heart failure patients: the benefit depends on the type of training performed*. *J Am Coll Cardiol*, 2007. **49**(24): p. 2329-36.
23. Giannuzzi, P., et al., *Antiremodeling effect of long-term exercise training in patients with stable chronic heart failure: results of the Exercise in Left Ventricular Dysfunction and Chronic Heart Failure (ELVD-CHF) Trial*. *Circulation*, 2003. **108**(5): p. 554-9.
24. Orenstein, T.L., et al., *Favorable left ventricular remodeling following large myocardial infarction by exercise training. Effect on ventricular morphology and gene expression*. *J Clin Invest*, 1995. **96**(2): p. 858-66.
25. Wisloff, U., et al., *Aerobic exercise reduces cardiomyocyte hypertrophy and increases contractility, Ca²⁺ sensitivity and SERCA-2 in rat after myocardial infarction*. *Cardiovasc Res*, 2002. **54**(1): p. 162-74.
26. Zhang, L.Q., et al., *Sprint training restores normal contractility in postinfarction rat myocytes*. *J Appl Physiol*, 2000. **89**(3): p. 1099-105.

27. Jain, M., et al., *Angiotensin II receptor blockade attenuates the deleterious effects of exercise training on post-MI ventricular remodelling in rats*. Cardiovasc Res, 2000. **46**(1): p. 66-72.
28. Leosco, D., et al., *Exercise promotes angiogenesis and improves beta-adrenergic receptor signalling in the post-ischaemic failing rat heart*. Cardiovasc Res, 2008. **78**(2): p. 385-94.
29. Wisloff, U., et al., *Superior cardiovascular effect of aerobic interval training versus moderate continuous training in heart failure patients: a randomized study*. Circulation, 2007. **115**(24): p. 3086-94.
30. Libonati, J.R., *Exercise and diastolic function after myocardial infarction*. Med Sci Sports Exerc, 2003. **35**(9): p. 1471-6.
31. Musch, T.I., et al., *Endurance training in rats with chronic heart failure induced by myocardial infarction*. Circulation, 1986. **74**(2): p. 431-41.
32. Sullivan, M.J., M.B. Higginbotham, and F.R. Cobb, *Exercise training in patients with severe left ventricular dysfunction. Hemodynamic and metabolic effects*. Circulation, 1988. **78**(3): p. 506-15.
33. Belardinelli, R., et al., *Effects of exercise training on left ventricular filling at rest and during exercise in patients with ischemic cardiomyopathy and severe left ventricular systolic dysfunction*. Am Heart J, 1996. **132**(1 Pt 1): p. 61-70.
34. Palevo, G., et al., *Resistance exercise training improves heart function and physical fitness in stable patients with heart failure*. J Cardiopulm Rehabil Prev, 2009. **29**(5): p. 294-8.
35. Gaudron, P., et al., *Effect of endurance training early or late after coronary artery occlusion on left ventricular remodeling, hemodynamics, and survival in rats with chronic transmural myocardial infarction*. Circulation, 1994. **89**(1): p. 402-12.
36. Alhaddad, I.A., et al., *Early exercise after experimental myocardial infarction: effect on left ventricular remodeling*. Coron Artery Dis, 1998. **9**(6): p. 319-27.
37. Bito, V., et al., *Early exercise training after myocardial infarction prevents contractile but not electrical remodelling or hypertrophy*. Cardiovasc Res, 2010. **86**(1): p. 72-81.
38. de Waard, M.C., et al., *Early exercise training normalizes myofilament function and attenuates left ventricular pump dysfunction in mice with a large myocardial infarction*. Circ Res, 2007. **100**(7): p. 1079-88.
39. Dubach, P., et al., *Effect of high intensity exercise training on central hemodynamic responses to exercise in men with reduced left ventricular function*. J Am Coll Cardiol, 1997. **29**(7): p. 1591-8.
40. Dubach, P., et al., *Effect of exercise training on myocardial remodeling in patients with reduced left ventricular function after myocardial infarction: application of magnetic resonance imaging*. Circulation, 1997. **95**(8): p. 2060-7.
41. Giannuzzi, P., et al., *Long-term physical training and left ventricular remodeling after anterior myocardial infarction: results of the Exercise in Anterior Myocardial Infarction (EAMI) trial*. EAMI Study Group. J Am Coll Cardiol, 1993. **22**(7): p. 1821-9.
42. Myers, J., et al., *Exercise training and myocardial remodeling in patients with reduced ventricular function: one-year follow-up with magnetic resonance imaging*. Am Heart J, 2000. **139**(2 Pt 1): p. 252-61.
43. Otsuka, Y., et al., *Exercise training without ventricular remodeling in patients with moderate to severe left ventricular dysfunction early after acute myocardial infarction*. Int J Cardiol, 2003. **87**(2-3): p. 237-44.
44. Jugdutt, B.I., B.L. Michorowski, and C.T. Kappagoda, *Exercise training after anterior Q wave myocardial infarction: importance of regional left ventricular function and topography*. J Am Coll Cardiol, 1988. **12**(2): p. 362-72.
45. Kubo, N., et al., *Exercise at ventilatory threshold aggravates left ventricular remodeling in patients with extensive anterior acute myocardial infarction*. Am Heart J, 2004. **147**(1): p. 113-20.
46. de Waard, M.C., et al., *Detrimental effect of combined exercise training and eNOS overexpression on cardiac function after myocardial infarction*. Am J Physiol Heart Circ Physiol, 2009. **296**(5): p. H1513-23.
47. Xu, X., et al., *Effects of exercise training on cardiac function and myocardial remodeling in post myocardial infarction rats*. J Mol Cell Cardiol, 2008. **44**(1): p. 114-22.
48. Delagardelle, C., et al., *Reverse remodelling through exercise training is more pronounced in non-ischemic heart failure*. Clin Res Cardiol, 2008. **97**(12): p. 865-71.
49. Webb-Peploe, K.M., et al., *Different response of patients with idiopathic and ischaemic dilated cardiomyopathy to exercise training*. Int J Cardiol, 2000. **74**(2-3): p. 215-24.
50. Boman, K., et al., *Exercise and cardiovascular outcomes in hypertensive patients in relation to structure and function of left ventricular hypertrophy: the LIFE study*. Eur J Cardiovasc Prev Rehabil, 2009. **16**(2): p. 242-8.
51. Ernter, C.A., et al., *Low-intensity exercise training delays onset of decompensated heart failure in spontaneously hypertensive heart failure rats*. Am J Physiol Heart Circ Physiol, 2005. **289**(5): p. H2030-8.
52. Garcarena, C.D., et al., *Endurance training in the spontaneously hypertensive rat: conversion of pathological*

- into physiological cardiac hypertrophy. *Hypertension*, 2009. **53**(4): p. 708-14.
53. Kokkinos, P.F., et al., *Effects of regular exercise on blood pressure and left ventricular hypertrophy in African-American men with severe hypertension*. *N Engl J Med*, 1995. **333**(22): p. 1462-7.
 54. Kolwicz, S.C., et al., *Left ventricular remodeling with exercise in hypertension*. *Am J Physiol Heart Circ Physiol*, 2009. **297**(4): p. H1361-8.
 55. Lee, Y.I., et al., *Effects of exercise training on pathological cardiac hypertrophy related gene expression and apoptosis*. *Eur J Appl Physiol*, 2006. **97**(2): p. 216-24.
 56. MacDonnell, S.M., et al., *Improved myocardial beta-adrenergic responsiveness and signaling with exercise training in hypertension*. *Circulation*, 2005. **111**(25): p. 3420-8.
 57. Pfeffer, M.A., et al., *Ventricular morphology and pumping ability of exercised spontaneously hypertensive rats*. *Am J Physiol*, 1978. **235**(2): p. H193-9.
 58. Turner, M.J., et al., *Effect of endurance exercise training on left ventricular size and remodeling in older adults with hypertension*. *J Gerontol A Biol Sci Med Sci*, 2000. **55**(4): p. M245-51.
 59. Chicco, A.J., et al., *Low-intensity exercise training delays heart failure and improves survival in female hypertensive heart failure rats*. *Hypertension*, 2008. **51**(4): p. 1096-102.
 60. Miyachi, M., et al., *Exercise training alters left ventricular geometry and attenuates heart failure in Dahl salt-sensitive hypertensive rats*. *Hypertension*, 2009. **53**(4): p. 701-7.
 61. Morris, R.T., et al., *Exercise training prevents development of cardiac contractile dysfunction in hypertensive TG (mREN-2)27 rats*. *J Am Soc Hypertens*, 2007. **1**(6): p. 393-9.
 62. Stewart, K.J., et al., *Exercise effects on cardiac size and left ventricular diastolic function: relationships to changes in fitness, fatness, blood pressure and insulin resistance*. *Heart*, 2006. **92**(7): p. 893-8.
 63. Schultz, R.L., et al., *Effects of excessive long-term exercise on cardiac function and myocyte remodeling in hypertensive heart failure rats*. *Hypertension*, 2007. **50**(2): p. 410-6.
 64. Ross, J., Jr. and E. Braunwald, *Aortic stenosis*. *Circulation*, 1968. **38**(1 Suppl): p. 61-7.
 65. Dowell, R.T., et al., *Heart functional responses to pressure overload in exercised and sedentary rats*. *Am J Physiol*, 1976. **230**(1): p. 199-204.
 66. Emter, C.A. and C.P. Baines, *Low-intensity aerobic interval training attenuates pathological left ventricular remodeling and mitochondrial dysfunction in aortic-banded miniature swine*. *Am J Physiol Heart Circ Physiol*, 2010. **299**(5): p. H1348-56.
 67. Ljungqvist, A., G. Unge, and S. Carlsson, *The myocardial capillary vasculature in exercising animals with increased cardiac pressure load*. *Acta Pathol Microbiol Scand A*, 1976. **84**(3): p. 244-6.
 68. Hambrecht, R., et al., *Effects of exercise training on left ventricular function and peripheral resistance in patients with chronic heart failure: A randomized trial*. *JAMA*, 2000. **283**(23): p. 3095-101.
 69. Duncker, D.J., et al., *Alpha 1-adrenergic tone does not influence the transmural distribution of myocardial blood flow during exercise in dogs with pressure overload left ventricular hypertrophy*. *Basic Res Cardiol*, 1995. **90**(1): p. 73-83.
 70. de Waard, M.C., et al., *Beneficial effects of exercise training after myocardial infarction require full eNOS expression*. *J Mol Cell Cardiol*, 2010. **48**(6): p. 1041-9.
 71. Jones, S.P., et al., *Endothelial nitric oxide synthase overexpression attenuates congestive heart failure in mice*. *Proc Natl Acad Sci U S A*, 2003. **100**(8): p. 4891-6.
 72. Scherrer-Crosbie, M., et al., *Endothelial nitric oxide synthase limits left ventricular remodeling after myocardial infarction in mice*. *Circulation*, 2001. **104**(11): p. 1286-91.
 73. Buys, E.S., et al., *Cardiomyocyte-restricted restoration of nitric oxide synthase 3 attenuates left ventricular remodeling after chronic pressure overload*. *Am J Physiol Heart Circ Physiol*, 2007. **293**(1): p. H620-7.
 74. Ichinose, F., et al., *Pressure overload-induced LV hypertrophy and dysfunction in mice are exacerbated by congenital NOS3 deficiency*. *Am J Physiol Heart Circ Physiol*, 2004. **286**(3): p. H1070-5.
 75. Takimoto, E., et al., *Oxidant stress from nitric oxide synthase-3 uncoupling stimulates cardiac pathologic remodeling from chronic pressure load*. *J Clin Invest*, 2005. **115**(5): p. 1221-31.
 76. Moens, A.L., et al., *Reversal of cardiac hypertrophy and fibrosis from pressure overload by tetrahydrobiopterin: efficacy of recoupling nitric oxide synthase as a therapeutic strategy*. *Circulation*, 2008. **117**(20): p. 2626-36.
 77. Zhang, Y., et al., *Modulating endothelial nitric oxide synthase: a new cardiovascular therapeutic strategy*. *Am J Physiol Heart Circ Physiol*, 2011. **301**(3): p. H634-46.
 78. Lu, Z., et al., *Oxidative stress regulates left ventricular PDE5 expression in the failing heart*. *Circulation*, 2010. **121**(13): p. 1474-83.
 79. Takimoto, E., et al., *Chronic inhibition of cyclic GMP phosphodiesterase 5A prevents and reverses cardiac hypertrophy*. *Nat Med*, 2005. **11**(2): p. 214-22.

80. Seddon, M., Y.H. Looi, and A.M. Shah, *Oxidative stress and redox signalling in cardiac hypertrophy and heart failure*. Heart, 2007. **93**(8): p. 903-7.
81. Sawyer, D.B., *Oxidative stress in heart failure: what are we missing?* Am J Med Sci, 2011. **342**(2): p. 120-4.
82. Chiamvimonvat, N., et al., *Functional consequences of sulfhydryl modification in the pore-forming subunits of cardiovascular Ca²⁺ and Na⁺ channels*. Circ Res, 1995. **76**(3): p. 325-34.
83. Tsutsui, H., S. Kinugawa, and S. Matsushima, *Oxidative Stress and Heart Failure*. Am J Physiol Heart Circ Physiol, 2011.
84. Afanas'ev, I., *ROS and RNS signaling in heart disorders: could antioxidant treatment be successful?* Oxid Med Cell Longev, 2011. **2011**: p. 293769.
85. Siwik, D.A., et al., *Inhibition of copper-zinc superoxide dismutase induces cell growth, hypertrophic phenotype, and apoptosis in neonatal rat cardiac myocytes in vitro*. Circ Res, 1999. **85**(2): p. 147-53.
86. Mates, J.M., *Effects of antioxidant enzymes in the molecular control of reactive oxygen species toxicology*. Toxicology, 2000. **153**(1-3): p. 83-104.
87. Powers, S.K. and M.J. Jackson, *Exercise-induced oxidative stress: cellular mechanisms and impact on muscle force production*. Physiol Rev, 2008. **88**(4): p. 1243-76.
88. Zelko, I.N., T.J. Mariani, and R.J. Folz, *Superoxide dismutase multigene family: a comparison of the CuZn-SOD (SOD1), Mn-SOD (SOD2), and EC-SOD (SOD3) gene structures, evolution, and expression*. Free Radic Biol Med, 2002. **33**(3): p. 337-49.
89. Brahmajothi, M.V. and D.L. Campbell, *Heterogeneous basal expression of nitric oxide synthase and superoxide dismutase isoforms in mammalian heart : implications for mechanisms governing indirect and direct nitric oxide-related effects*. Circ Res, 1999. **85**(7): p. 575-87.
90. Jung, O., et al., *Extracellular superoxide dismutase is a major determinant of nitric oxide bioavailability: in vivo and ex vivo evidence from ecSOD-deficient mice*. Circ Res, 2003. **93**(7): p. 622-9.
91. Fukai, T., et al., *Regulation of the vascular extracellular superoxide dismutase by nitric oxide and exercise training*. J Clin Invest, 2000. **105**(11): p. 1631-9.
92. Harman, D., *Aging: a theory based on free radical and radiation chemistry*. J Gerontol, 1956. **11**(3): p. 298-300.
93. Bertram, C. and R. Hass, *Cellular responses to reactive oxygen species-induced DNA damage and aging*. Biol Chem, 2008. **389**(3): p. 211-20.
94. Oxenham, H. and N. Sharpe, *Cardiovascular aging and heart failure*. Eur J Heart Fail, 2003. **5**(4): p. 427-34.
95. Bernhard, D. and G. Laufer, *The aging cardiomyocyte: a mini-review*. Gerontology, 2008. **54**(1): p. 24-31.
96. Lakatta, E.G. and D. Levy, *Arterial and cardiac aging: major shareholders in cardiovascular disease enterprises: Part II: the aging heart in health: links to heart disease*. Circulation, 2003. **107**(2): p. 346-54.
97. Lee, D.S., et al., *Predicting mortality among patients hospitalized for heart failure: derivation and validation of a clinical model*. JAMA, 2003. **290**(19): p. 2581-7.
98. de Boer, J., et al., *Premature aging in mice deficient in DNA repair and transcription*. Science, 2002. **296**(5571): p. 1276-9.
99. Dickstein, K., et al., *ESC guidelines for the diagnosis and treatment of acute and chronic heart failure 2008: the Task Force for the diagnosis and treatment of acute and chronic heart failure 2008 of the European Society of Cardiology. Developed in collaboration with the Heart Failure Association of the ESC (HFA) and endorsed by the European Society of Intensive Care Medicine (ESICM)*. Eur J Heart Fail, 2008. **10**(10): p. 933-89.
100. Heart Failure Society of, A., et al., *HFSA 2010 Comprehensive Heart Failure Practice Guideline*. J Card Fail, 2010. **16**(6): p. e1-194.
101. Tamargo, J. and J. Lopez-Sendon, *Novel therapeutic targets for the treatment of heart failure*. Nat Rev Drug Discov, 2011. **10**(7): p. 536-55.
102. Landmesser, U., K.C. Wollert, and H. Drexler, *Potential novel pharmacological therapies for myocardial remodelling*. Cardiovasc Res, 2009. **81**(3): p. 519-27.
103. Bonow, R.O., et al., *2008 Focused update incorporated into the ACC/AHA 2006 guidelines for the management of patients with valvular heart disease: a report of the American College of Cardiology/American Heart Association Task Force on Practice Guidelines (Writing Committee to Revise the 1998 Guidelines for the Management of Patients With Valvular Heart Disease): endorsed by the Society of Cardiovascular Anesthesiologists, Society for Cardiovascular Angiography and Interventions, and Society of Thoracic Surgeons*. Circulation, 2008. **118**(15): p. e523-661.
104. Vahanian, A., et al., *Guidelines on the management of valvular heart disease: The Task Force on the Management of Valvular Heart Disease of the European Society of Cardiology*. Eur Heart J, 2007. **28**(2): p.

- 230-68.
105. lung, B., *Management of asymptomatic aortic stenosis*. Heart, 2011. **97**(3): p. 253-9.
 106. Cave, A., et al., *NADPH oxidase-derived reactive oxygen species in cardiac pathophysiology*. Philos Trans R Soc Lond B Biol Sci, 2005. **360**(1464): p. 2327-34.
 107. Henderson, B.C., et al., *Oxidative remodeling in pressure overload induced chronic heart failure*. Eur J Heart Fail, 2007. **9**(5): p. 450-7.
 108. Moens, A.L., et al., *Adverse ventricular remodeling and exacerbated NOS uncoupling from pressure-overload in mice lacking the beta3-adrenoreceptor*. J Mol Cell Cardiol, 2009. **47**(5): p. 576-85.
 109. Ruetten, H., et al., *Concentric left ventricular remodeling in endothelial nitric oxide synthase knockout mice by chronic pressure overload*. Cardiovasc Res, 2005. **66**(3): p. 444-53.
 110. Sindhu, R.K., et al., *Effects of aortic coarctation on aortic antioxidant enzymes and NADPH oxidase protein expression*. Life Sci, 2005. **76**(8): p. 945-53.
 111. Bonow, R.O., et al., *Task Force 3: valvular heart disease*. J Am Coll Cardiol, 2005. **45**(8): p. 1334-40.
 112. Rome, J.J., *Exercise restriction to prevent sudden death in congenital aortic stenosis: whom are we treating?* J Am Coll Cardiol, 2010. **56**(23): p. 1947-8.
 113. Brown, D.W., et al., *Sudden unexpected death after balloon valvuloplasty for congenital aortic stenosis*. J Am Coll Cardiol, 2010. **56**(23): p. 1939-46.
 114. Chess, D.J., et al., *The antioxidant tempol attenuates pressure overload-induced cardiac hypertrophy and contractile dysfunction in mice fed a high-fructose diet*. Am J Physiol Heart Circ Physiol, 2008. **295**(6): p. H2223-30.
 115. Dhalla, A.K., M.F. Hill, and P.K. Singal, *Role of oxidative stress in transition of hypertrophy to heart failure*. J Am Coll Cardiol, 1996. **28**(2): p. 506-14.
 116. Khanna, A.K., J. Xu, and M.R. Mehra, *Antioxidant N-acetyl cysteine reverses cigarette smoke-induced myocardial infarction by inhibiting inflammation and oxidative stress in a rat model*. Lab Invest, 2011.
 117. Prasad, K., et al., *Oxidative stress as a mechanism of cardiac failure in chronic volume overload in canine model*. J Mol Cell Cardiol, 1996. **28**(2): p. 375-85.
 118. Sia, Y.T., et al., *Beneficial effects of long-term use of the antioxidant probucol in heart failure in the rat*. Circulation, 2002. **105**(21): p. 2549-55.
 119. Tsujimoto, I., et al., *The antioxidant edaravone attenuates pressure overload-induced left ventricular hypertrophy*. Hypertension, 2005. **45**(5): p. 921-6.
 120. Heart Protection Study Collaborative, G., *MRC/BHF Heart Protection Study of antioxidant vitamin supplementation in 20,536 high-risk individuals: a randomised placebo-controlled trial*. Lancet, 2002. **360**(9326): p. 23-33.
 121. Lonn, E., et al., *Effects of long-term vitamin E supplementation on cardiovascular events and cancer: a randomized controlled trial*. JAMA, 2005. **293**(11): p. 1338-47.
 122. Yusuf, S., et al., *Vitamin E supplementation and cardiovascular events in high-risk patients. The Heart Outcomes Prevention Evaluation Study Investigators*. N Engl J Med, 2000. **342**(3): p. 154-60.
 123. Marchioli, R., et al., *Vitamin E increases the risk of developing heart failure after myocardial infarction: Results from the GISSI-Prevenzione trial*. J Cardiovasc Med (Hagerstown), 2006. **7**(5): p. 347-50.
 124. Miller, E.R., 3rd, et al., *Meta-analysis: high-dosage vitamin E supplementation may increase all-cause mortality*. Ann Intern Med, 2005. **142**(1): p. 37-46.
 125. Thomson, M.J., M.P. Frenneaux, and J.C. Kaski, *Antioxidant treatment for heart failure: friend or foe?* QJM, 2009. **102**(5): p. 305-10.
 126. Dai, D.F. and P.S. Rabinovitch, *Cardiac aging in mice and humans: the role of mitochondrial oxidative stress*. Trends Cardiovasc Med, 2009. **19**(7): p. 213-20.
 127. Sane, D.C., W.S. Mozingo, and R.C. Becker, *Cardiac rupture after myocardial infarction: new insights from murine models*. Cardiol Rev, 2009. **17**(6): p. 293-9.
 128. Wijnhoven, S.W., et al., *Accelerated aging pathology in ad libitum fed Xpd(TTD) mice is accompanied by features suggestive of caloric restriction*. DNA Repair (Amst), 2005. **4**(11): p. 1314-24.
 129. lung, B., et al., *Decision-making in elderly patients with severe aortic stenosis: why are so many denied surgery?* Eur Heart J, 2005. **26**(24): p. 2714-20.





Summary

11

Summary

Left ventricular (LV) remodeling in response to cardiac-overload is an impressive example of the body's capability to adapt to unfavorable circumstances and initially enables the heart to cope with exacerbated loading. However, in spite of the apparent appropriateness of the process, LV remodeling ultimately results in cardiac dilation and dysfunction and predisposes the heart to failure. The mechanisms underlying the progression of the compensated remodeled heart to heart failure are incompletely understood but recent evidence suggests a critical role for an imbalance between protective nitric oxide (NO) molecules and destructive reactive oxygen species (ROS) in the progression of heart failure. The studies presented in this thesis were carried out to obtain a better understanding of the effects of NO synthases (NOSs) and oxidative stress on LV remodeling and dysfunction in mouse models for the two major risk factors for heart failure, myocardial infarction (MI) and pressure-overload.

The importance of NOS in the cardiovascular system has been extensively studied but remains controversial since NOS represents a double edged sword able to stimulate cardiac protection as well as pathology. Under basal conditions NOS produces nitric oxide (NO) which is important for endothelial and myocyte function but also protects against cardiac hypertrophy. However, under certain conditions the dimer NOS can uncouple into two monomers and become a source of ROS by produce superoxide instead of NO. Particularly the NOS isoform inducible NOS (iNOS) is well know for its destructive properties because, next to potential ROS generation when uncoupled, iNOS is capable to locally produce high toxic amounts of NO. Accordingly, iNOS deficiency attenuated cardiac hypertrophy, dilation, fibrosis and dysfunction following tranverse aortic constriction (TAC) by consequent prevention of iNOS uncoupling (**chapter 2**). Similar mitigation of LV remodeling and pulmonary congestion by selective pharmacological iNOS inhibition suggests that iNOS inhibition might be effective for treatment of systolic-overload induced cardiac remodeling.

The residual LV hypertrophy and dysfunction following TAC in iNOS deficient mice was in part due to endothelial NOS (eNOS) uncoupling. Like iNOS, eNOS has the potential to produce protective NO molecules as well as detrimental ROS depending on the circumstances. To further elucidate the role of eNOS in pathological remodeling we first studied in **chapter 3** the cardiovascular effects of increased eNOS activity in a transgenic mouse model overexpressing human eNOS. Elevated eNOS expression decreased blood pressure, plasma cholesterol and concomitant atherosclerotic lesions. Interestingly, in spite of a 10 fold increase of eNOS protein content, eNOS overexpression did not greatly reduce systemic vascular resistance (**chapter 4**). The mild effects of marked elevated eNOS levels on vasomotor tone were explained by blunted NO responsiveness as a result of reduced guanylyl cyclase activity, without evidence of eNOS uncoupling or adaptations in other vasoregulatory pathways (**chapter 4**). Upregulation of eNOS expression and activity cannot only be achieved by genetic modification but can also be induced by physical exercise. Therefore, we investigated in **chapter 5** the potential protective effects of exercise training on pressure-overload induced cardiac remodeling

and dysfunction. In contrast to previous observations in MI, exercise did not attenuate cardiac hypertrophy, dilation or dysfunction following TAC-induced pressure-overload, but instead aggravated the response to pressure-overload. Consequently, the protective effects of physical exercise training on pathological remodeling critically depend on the underlying etiology of remodeling. The lack of beneficial effects of exercise in TAC are likely explained by exacerbated systolic loading of the LV during exercise as a consequence of the fixed aortic stenosis. Potentially, eNOS overexpression by genetic modification harnesses the beneficial effects of eNOS without exercise-induced aggravate systolic loading. Accordingly, in **chapter 6** we investigated the influence of eNOS expression level on pressure-overload induced LV hypertrophy and dysfunction. For this purpose we used wildtype and eNOS deficient knock-out as well as eNOS overexpressing transgenic mice. Interestingly, not elevation but rather loss of eNOS expression protected the heart against pressure-overload induced cardiac remodeling, dysfunction, fibrosis and pulmonary congestion whereas additional eNOS exerted deleterious effects. Apparently, elevated eNOS levels differently affect the remodeling process resulting from MI compared to the remodeling in response to TAC. Reversal of detrimental effects of eNOS overexpression with antioxidant-treatment reveals that eNOS overexpression, aggravates cardiac remodeling and dysfunction by elevating oxidative stress, likely as a result of eNOS-uncoupling.

We investigated the role of oxidative stress in pathological remodeling in **chapter 7 and 8** of this thesis more directly by studying the physiological significance of the antioxidant extracellular superoxide dismutase (EC-SOD) in LV remodeling and dysfunction from pressure-overload through TAC or after MI in EC-SOD deficient mice. Under unstressed conditions, loss of the anti-oxidative property of EC-SOD did not affect total SOD activity or superoxide production. However, lack of EC-SOD exacerbated TAC-induced (**chapter 7**) and MI-induced (**chapter 8**) myocardial oxidative stress, hypertrophy, dysfunction and fibrosis, indicating the critical importance of EC-SOD in the extracellular space for cardiac protection of the overloaded heart. Additionally, these studies reveal that cardiac fibrosis, LV end diastolic pressure and pulmonary congestion appear to be further increased in TAC than in MI and consequently stronger influenced by EC-SOD in TAC (**chapter 7**) compared to MI (**chapter 8**). Evidently, the antioxidant EC-SOD targets common as well as etiology-specific cardiac abnormalities while protecting the heart against ROS mediated cardiac hypertrophy and dysfunction in both MI and TAC.

An important aspect of the detrimental effects of oxidative stress is ROS-induced cumulative DNA damage. DNA damage in turn is also closely linked to cellular aging. Interestingly, a number of non-pathologic structural and functional cardiac changes in aging, including hypertrophy, fibrosis and apoptosis, strikingly resemble alterations typically observed in heart failure. This raises the question whether DNA damage and subsequent aging would reduce cardiac reserve and increase the vulnerability of the heart to pathological stimuli and the development of heart failure. To investigate whether the cumulative DNA damage indeed causes the heart to be more sensitive to cardiac overload we studied in **chapter 9** the impact of DNA damage on MI and TAC-induced cardiac remodeling. For this purpose we used mice that exhibit accelerated aging as a result of cumulated DNA

damage and defective DNA transcription caused by a DNA repair defect. At 3 months of age these mice, referred to as Xpd^{TTD}, show a similar survival response following MI and mTAC as wildtype littermates but demonstrate increased mortality following sTAC. In 1 year old Xpd^{TTD} mice survival following MI was unaltered compared to 3 months aged young Xpd^{TTD} mice. In contrast sTAC markedly decreased survival in old Xpd^{TTD} animals compared to wildtype littermates and young Xpd^{TTD} mice. Moreover mTAC, that produced compensated LV hypertrophy accompanied by well maintained cardiac function and low mortality in 1 year old wildtype littermates, also markedly increased mortality in the 1 year old prematurely aged mice. Evidently, not the severity but much more the type of cardiac-overload, critically determines the cardiac pathological response.

Together, the research described in this thesis demonstrates the prominent influences of NO and ROS in cardiac remodeling and dysfunction and illustrates how the the balance between NO and ROS production is critically determined by the underlying pathology. The sensitivity of this balance is particularly highlighted by the detrimental effects of exercise and eNOS overexpression through elevated ROS production in TAC versus protective effects of exercise and eNOS overexpression through elevated NO production in MI. Additionally, the important etiology dependency of the role of ROS in cardiac failure is demonstrated in DNA repair deficient mice, which are more vulnerable to aortic stenosis but not to MI. Stimulation of NO and oxidant scavenging hold promising potential in treatment of pathological remodeling, particularly in elderly patients suffering from an aortic stenosis, provided that NOS induced ROS production is prohibited. Furthermore, the research described in this thesis urges caution to extrapolate results obtained in one subgroup of heart failure patients to heart failure patients with different etiologies.





Nederlandse Samenvatting

Nederlandse Samenvatting

Een mooi voorbeeld van de aanpassingsmogelijkheden van het lichaam aan ongunstige omstandigheden is remodeleren van het linker ventrikel (LV) die het hart in staat stelt te compenseren voor een verhoogde belasting. Hoewel dit proces een goedbedoelde poging is om de pompfunctie van het LV in stand te houden, leidt LV remodeleren uiteindelijk tot dilatatie en verminderde functie van het LV en een verhoogd risico voor het ontwikkelen van hartfalen. Het mechanisme achter de progressie van LV remodeleren naar hartfalen wordt nog niet volledig begrepen, maar recent onderzoek suggereert een belangrijke rol voor de balans tussen beschermende stikstofmonoxide (NO) moleculen en beschadigende reactieve zuurstofsoorten (ROS). In dit proefschrift is geprobeerd een beter inzicht te krijgen in de effecten van het NO producerende enzym NO synthase (NOS) en oxidatieve stress op LV remodelering en disfunctie in muismodellen voor de twee belangrijkste risicofactoren voor hartfalen, het myocard infarct (MI) en drukoverbelasting van het hart.

De rol van NOS in het cardiovasculaire systeem is uitgebreid bestudeerd maar blijft desondanks onvolledig begrepen, omdat NOS zowel beschermende als beschadigende processen kan stimuleren. Onder normale omstandigheden draagt het door NOS gevormde NO bij aan endotheel en myocyte functie en beschermt NO tegen de ontwikkeling van hypertrofie. Echter, onder bepaalde omstandigheden kan de dimeer NOS ontkoppelen en veranderen in een monomere vorm. Ontkoppeld NOS produceert niet langer NO maar produceert het vrije radicaal superoxide waardoor niet alleen de productie van NO verminderd maar ook de aanmaak van ROS wordt verhoogd.

Voornamelijk de induceerbare NOS isovorm (iNOS) is bekend om zijn beschadigende eigenschappen, omdat iNOS naast ROS productie in ontkoppelde vorm ook plaatselijk hele hoge toxische hoeveelheden NO kan produceren. In overeenstemming hiermee vonden we dat iNOS deficiënte muizen minder LV remodelering, disfunctie en fibrose ontwikkelden na cardiale drukoverbelasting als gevolg van een transverse aorta constrictie (TAC), doordat er geen iNOS ont koppeling plaats vond in deze muizen (**hoofdstuk 2**). Een vergelijkbare vermindering van LV remodeleren en pulmonale congestie door middel van farmacologische remming van iNOS suggereert dat remming van iNOS zou kunnen worden toegepast voor de behandeling van cardiale remodelering als gevolg van drukoverbelasting.

De resterende LV hypertrofie en disfunctie na TAC in de iNOS deficiënte muizen wordt deels veroorzaakt door ont koppeling van endotheliale NOS (eNOS). Net als iNOS is eNOS in staat om afhankelijk van de omstandigheden zowel NO als ROS te produceren. Om een beter inzicht te krijgen in de rol van eNOS in het cardiovasculaire systeem en in het bijzonder in pathologische LV remodelering zijn in **hoofdstuk 3** van dit proefschrift allereerst de cardiovasculaire effecten van verhoogde eNOS expressie onderzocht in een transgeen muismodel dat het humane eNOS gen tot overexpressie brengt. Verhoogde eNOS expressie leidde tot een lagere bloeddruk en plasma cholesterol spiegels met als gevolg daarvan verminderde atherosclerotische laesies. Interessant genoeg leidde de eNOS

overexpressie, ondanks een tienvoudige hoeveelheid eNOS eiwit, maar tot een bescheiden daling in de systemische vaatweerstand (**hoofdstuk 4**). De milde effecten van de sterk verhoogde hoeveelheid eNOS op de vaattonus konden in **hoofdstuk 4** worden verklaard door een verminderde gevoeligheid voor NO als gevolg van een verlaagde activiteit van gunayl cyclase zonder aanwijzingen voor compensatoire aanpassingen van andere vaattonus regulerende systemen of voor eNOS ontkoppeling. Naast het verhogen van eNOS expressie met behulp van genetische modificatie, wordt eNOS expressie normaliter in het lichaam verhoogd als reactie op fysieke inspanning. Om die reden hebben we in **hoofdstuk 5** de mogelijk beschermende invloed van inspanningstraining op cardiale remodellering en disfunctie als gevolg van drukoverbelasting door TAC onderzocht. In tegenstelling tot eerdere resultaten na een MI, beschermd inspanningstraining niet tegen TAC geïnduceerde LV hypertrofie, dilatatie en disfunctie. Blijkbaar zijn de beschermende effecten van fysieke inspanningstraining op het hart sterk afhankelijk van het onderliggende ziektebeeld dat de LV remodellering veroorzaakt. Een mogelijke verklaring voor het uitblijven van positieve effecten van inspanningstraining in TAC is verergerde systolische belasting van het hart tijdens de inspanning als gevolg van de vaste aorta stenose. Verhoogde eNOS expressie door middel van genetische modificatie zou daarom mogelijk de positieve effecten van inspanningstraining kunnen nabootsen zonder de verergerde systolische belasting die gepaard gaat met inspanningstraining. Daarom zijn in **hoofdstuk 6** de invloed van eNOS expressie op LV hypertrofie en disfunctie als gevolg van drukoverbelasting onderzocht in eNOS-deficiënte en normale muizen en muizen die eNOS tot overexpressie brengen. Anders dan in eerste instantie verwacht, beschermd niet de overexpressie maar juist het verlies van eNOS het hart tegen de drukoverbelasting geïnduceerde cardiale remodellering en disfunctie, fibrose en pulmonale congestie. Klaarblijkelijk beïnvloedt een verhoogd eNOS gehalte het remodelleringsproces anders in MI dan in TAC. Het feit dat de negatieve effecten van eNOS overexpressie konden worden voorkomen door behandeling met anti-oxidanten suggereert dat eNOS overexpressie cardiale remodellering en disfunctie verergerd door middel van oxidatieve stress, waarschijnlijk als gevolg van eNOS ontkoppeling.

In **hoofdstuk 7 en 8** van dit proefschrift hebben we de rol van oxidatieve stress op pathologische remodellering meer direct onderzocht door het belang van het antioxidant enzym extra cellulair superoxide dismutase (EC-SOD) in LV remodellering na TAC en MI te bestuderen in EC-SOD deficiënte muizen. Onder normale omstandigheden had verlies van de anti-oxidatieve effecten van EC-SOD geen effect op de totale SOD activiteit of superoxide productie. Echter, EC-SOD deficiëntie verergerde TAC geïnduceerde (**hoofdstuk 7**) en MI geïnduceerde (**hoofdstuk 8**) myocardiale oxidatieve stress, LV hypertrofie, disfunctie en fibrose. Dit betekent dat EC-SOD in de extracellulaire ruimte een belangrijke rol speelt in de bescherming van het overbelaste hart. Verder laten deze studies zien dat fibrose, verhoging van de LV eind diastolische druk en pulmonale congestie in grotere mate worden veroorzaakt door TAC dan door MI en ook sterker worden beïnvloed door EC-SOD in TAC (**hoofdstuk 7**) dan in MI (**hoofdstuk 8**). Kennelijk beschermt EC-SOD tegen cardiale remodellering en disfunctie als gevolg van ROS in TAC en MI door het bestrijden van deels gemeenschappelijke en ziektebeeld specifieke pathologische mechanismen.

Een belangrijk aspect van de negatieve effecten van oxidatieve stress is de door ROS veroorzaakte DNA schade. Cumulatieve DNA schade is sterk gerelateerd aan cellulaire veroudering. Opmerkelijk genoeg vertoont het verouderde hart een aantal structurele en functionele eigenschappen die sterk overeenkomen met veranderingen in het falende hart, zoals hypertrofie, fibrose en apoptose. Dit leidt tot de vraag of DNA schade en daarop volgende veroudering mogelijk de cardiale reserve van het hart verminderen en daarmee de gevoeligheid van het hart voor pathologische stimuli en het ontwikkelen van hartfalen verhogen. Om te onderzoeken of cumulatieve DNA schade het hart inderdaad meer gevoelig maakt voor cardiale overbelasting is in **hoofdstuk 9** het effect van DNA schade op LV remodellering na MI en TAC bestudeerd. Hiervoor is gebruik gemaakt van een muismodel dat, als gevolg van cumulatieve DNA schade en deficiënte DNA transcriptie veroorzaakt door een DNA reparatie defect, versnelt verouderd. Op een leeftijd van 3 maanden vertonen deze muizen, die Xpd^{TTD} muizen genoemd worden, eenzelfde mortaliteit na MI en milde TAC als de normale nestgenoten maar een verhoogde mortaliteit na ernstige TAC. De overleving na MI was niet veranderd in 1 jaar oude Xpd^{TTD} muizen vergeleken met de jongere 3 maanden oude Xpd^{TTD} dieren. Daarentegen was de mortaliteit in 1 jaar oude versneld verouderde muizen veel hoger na ernstige TAC dan in 3 maanden oude Xpd^{TTD} muizen en 1 jaar oude normale muizen. Bovendien resulteerde milde TAC in 1 jaar oude normale muizen niet tot significante mortaliteit, maar in 1 jaar oude Xpd^{TTD} muizen wel tot een duidelijk verminderde overleving. Blijkbaar is niet de ernst maar veel meer de vorm van overbelasting bepalend voor de cardiale pathologische reactie.

Samengevat beschrijft het onderzoek in dit proefschrift de belangrijke invloed van NO en ROS op cardiale remodellering en disfunctie en illustreert het hoe de balans tussen NO en ROS productie in hoge mate bepaald wordt door het onderliggende ziektebeeld. De gevoeligheid van deze balans wordt vooral duidelijk geïllustreerd door de duale rol van eNOS dat, anders dan eerder waargenomen in MI, nadelig bleek te zijn in TAC en leidde tot oxidatieve stress in plaats van bescherming door verhoogde NO productie. Stimulatie van NO productie en het wegvangen van zuurstofradicalen zijn daarom veelbelovende kandidaat-mechanismen om in de toekomst patiënten te kunnen behandelen tegen pathologische remodellering. In het bijzonder oudere patiënten die leiden aan een aorta stenose en momenteel moeilijk te behandelen zijn, zouden kunnen profiteren van verhoogde NO productie mits ROS productie door NOS voorkomen wordt. Daarnaast maant het onderzoek in dit proefschrift tot voorzichtigheid om resultaten, verkregen in een bepaalde subpopulatie van hartfalenpatiënten, te extrapoleren naar hartfalenpatiënten in het algemeen, aangezien de effecten van een bepaalde behandeling sterk afhankelijk blijken te zijn van de onderliggende oorzaak van hartfalen.





PhD Portfolio
List of Publications
Curriculum Vitae

PhD Portfolio

Name PhD Student Elza Dianne van Deel
 ErasmusMC Departments Experimental Cardiology and Genetics
 Research School: Cardiovascular Research School COEUR
 Postgraduate school of Molecular Medicine (Mol Med)
 Erasmus MC, Rotterdam, the Netherlands

PhD period 2007-2012
 Promotors: Prof.dr. D.J. Duncker
 Prof.dr. H.J.H. Hoeijmakers

Education

2006-2007 MSc in Clinical Research, Nihes, Erasmus MC Rotterdam, the Netherlands
 1995-1999 BSc in Medical Biology, Higher Laboratory Education, Rotterdam the Netherlands

PhD Training

	Year	ECTS
Molecular biology and recombinant DNA technology	1999	1.5
Laboratory Animal Science	1999	4.5
Microsurgery	2001	0.5
Radiation hygiene level 5	2003	2
Radiation hygiene level 4	2003	4.5
COEUR Research Seminars	2003-2012	4.4
COEUR Courses 1, 2, 3, 4, 5, 6, 8	2003-2011	10.5
Statistics	2006	6
Biomedical English Writing and Communication	2006	1.5
Philosophy of Science	2006	1.5
Cardiac Function and Adaptation NHS	2008	2
Vascular Biology NHS	2009	2
Molecular and Cell Biology	2009	2

Teaching

Supervising: MSc and BSc students	2001-2011	4.2
Lecturing: Junior Medschool for high school graduates, Experimental Cardiology Research	2009-2011	0.5
Lecturing: Medical students, Adverse Cardiac Remodeling 2010		0.5

Committees

PhD committee of the Erasmus MC University	2008-2012	2
Organization of the Dutch-German Cardiology meeting	2010	1
COEUR-PhD-day committee	2010	0.5

Symposia and Conferences

ECTS 36.2

Oral presentations

- 2004 Dutch society for microcirculation and vascular biology meeting, Breda the Netherlands
- 2005 Joint meeting of the Dutch society for microcirculation and vascular biology and the Dutch hypertension society, Vught, the Netherlands
- 2005 Young Physiologist symposium of the Dutch physiology society, Papendal, the Netherlands
- 2007 Dutch Society for microcirculation and vascular biology, Amsterdam, the Netherlands
- 2008 Dutch Society for microcirculation and vascular biology, Ermelo, the Netherlands
- 2008 PhD-training course of the Netherlands Heart Foundation, Papendal, the Netherlands
- 2008 Young Physiologist symposium of the Dutch physiology society, Papendal, the Netherlands
- 2008 COEUR Research Seminar of Aging, Rotterdam, the Netherlands
- 2010 Dutch Society for microcirculation and vascular biology, Biesenmortel, the Netherlands
- 2010 Harlan TAC meeting, Horst, the Netherlands
- 2010 Young Physiologist symposium of the Dutch physiology society, Maastricht, the Netherlands
- 2011 ICar-VU Symposium on at the Free University of Amsterdam, Amsterdam, the Netherlands
- 2011 Experimental Biology, Washington, USA

Poster presentations

- 2004 Netherlands Physiology Society Heart Function Symposium, Amsterdam, the Netherlands
- 2005 Experimental Biology, San Diego, USA
- 2007 Experimental Biology Washington, USA
- 2007 American Heart Association, Scientific Meeting, Chicago, USA
- 2008 Science-day of the Dutch Heart Foundation, Amsterdam, the Netherlands
- 2008 Joint Conference of Physiological Science, Beijing, China
- 2009 ESC Summer School on Cardiovascular Sciences, Nice, France
- 2009 Young Physiologist symposium of the Dutch physiology society, Papendal, the Netherlands
- 2009 American Heart Association, Scientific Meeting, Washington, USA
- 2009 Dutch-German Joint Meeting of the Molecular Cardiology Groups Hamburg, Germany
- 2010 Experimental Biology, Los Angeles, USA
- 2010 Dutch-German Joint Meeting of the Molecular Cardiology Groups, Rotterdam, the Netherlands
- 2011 Experimental Biology, Washington, USA
- 2011 Dutch-German Joint Meeting of the Molecular Cardiology Groups, Ulm, Germany
- 2011 ESC International Conference on Heart Failure with Preserved Ejection Fraction, Budapest, Hungary
- 2011 American Heart Association, Scientific Meeting, Orlando, USA
- 2011 Young Physiologist symposium of the Dutch physiology society, Nijmegen, the Netherlands

Awards

- 2005 Young investigator award of the Netherlands society for microcirculation and vascular biology and the Dutch hypertension society
- 2008 1st prize for the presentation at the PhD-training course of the Netherlands Heart Foundation
- 2008 3rd prize for the oral presentation at the Young Physiologist symposium of the Dutch physiology society
- 2009 2nd prize in the poster presentation of at the Young Physiologist symposium of the Dutch physiology society
- 2010 3rd prize for the oral presentation at the Young Physiologist symposium of the Dutch physiology society
- 2011 Best Oral Presentation on the ICar-VU Symposium at the Free University of Amsterdam

Grants

- 2011 UNESCO-L'Oréal International Fellowships for Young Women in Life-Sciences 2012

List of publications

Full papers

- **van Deel ED**, de Boer M, Kuster DW, Boontje NM, Holemans P, Sipido KR, van der Velden J, Duncker DJ; Exercise training does not improve cardiac function in compensated or decompensated left ventricular hypertrophy induced by aortic stenosis. *J Mol Cell Cardiol.* 2011;50(6):1017-25.
- Pol CJ, Muller A, Zuidwijk MJ, **van Deel ED**, Kaptein E, Saba A, Marchini M, Zucchi R, Visser TJ, Paulus WJ, Duncker DJ, Simonides WS; Left-ventricular remodeling after myocardial infarction is associated with a cardiomyocyte-specific hypothyroid condition. *Endocrinology.* 2011;152(2):669-79.
- Cheng C, Noorderloos M, **van Deel ED**, Tempel D, den Dekker W, Wagtmans K, Duncker DJ, Soares MP, Laman JD, Duckers HJ; Dendritic cell function in transplantation arteriosclerosis is regulated by heme oxygenase 1. *Circ Res.* 2010;106(10):1656-66.
- Thornton AS, De Castro CA, **van Deel E**, van Beusekom HM, Jordaens L; An in vivo comparison of radiofrequency cardiac lesions formed by standard and magnetically steered 4 mm tip catheters. *Neth Heart J.* 2010;18(2):66-71.
- Bito V, de Waard MC, Biesmans L, Lenaerts I, Ozdemir S, **van Deel E**, Abdel-Mottaleb Y, Driesen R, Holemans P, Duncker DJ, Sipido KR; Early exercise training after myocardial infarction prevents contractile but not electrical remodelling or hypertrophy. *Cardiovasc Res.* 2010;86(1):72-81.
- Giuseppe D'Ancona, Joost M. Hartman, Fabio Bartolozzi, **Elza van Deel**, Dirk J.G.M. Duncker, Ad J.J.C. Bogers, Michele Pilato and Arie P. Kappetein; Epicardial coronary artery Doppler: validation in the animal model. *Interact Cardiovasc Thorac Surg.* 2008;7(4):634-7.
- **Elza D. van Deel**, Zhongbing Lu, Xin Xu, Xinli Hu, Guangshuo Zhu, John Fassett, Ping Zhang, Tim D. Oury, Robert J Bache, Dirk J. Duncker, Yingjie Chen; Extra cellular superoxide dismutase protects the heart against oxidative stress and hypertrophy after myocardial infarction. *Free Radical Bio Med.* 2008;44(7):1305-13.
- Zhongbing Lu; Xin Xu; Xinli Hu; Guangshuo Zhu; Ping Zhang; **Elza D. van Deel**; Joel P. French; John T. Fassett; Tim D. Oury; Robert J. Bache; Yingjie Chen; Extracellular superoxide dismutase deficiency exacerbates pressure overload-induced left ventricular hypertrophy and dysfunction. *Hypertension.* 2008;51(1):19-25.
- **Elza D. van Deel**, Daphne Merkus, Rien van Haperen, Monique C. de Waard, Rini de Crom, and Dirk J. Duncker; Vasomotor control in mice overexpressing human endothelial nitric oxide synthase. *Am J Physiol Heart Circ Physiol.* 2007;293(2):H1144-53.

- Ping Zhang, Xin Xu, Xinli Hu, **Elza D. van Deel**, Guangshuo Zhu, Yingjie Chen; Inducible Nitric Oxide Synthase Deficiency Protects the Heart From Systolic Overload-Induced Ventricular Hypertrophy and Congestive Heart Failure. *Circ Res.* 2007; 100(7): 1089-98.
- GA Pop, ZY Chang, CJ Slager, BJ Kooij, **ED van Deel**, L Moraru, J Quak, GC Meijer, DJ Duncker; Catheter-based impedance measurements in the right atrium for continuously monitoring hematocrit and estimating blood viscosity changes; an in vivo feasibility study in swine. *Biosens Bioelectron.* 2004;19(12):1685-93.
- R van Haperen, C Cheng, BM Mees, **E van Deel**, M de Waard, LC van Damme, T van Gent, T van Aken, R Krams, DJ Duncker, R de Crom; Functional expression of endothelial nitric oxide synthase fused to green fluorescent protein in transgenic mice. *Am J Pathol.* 2003;163(4): 1677-86.
- R van Haperen, M de Waard, **E van Deel**, B Mees, M Kutryk, T van Aken, J Hamming, F Grosveld, DJ Duncker, R de Crom; Reduction of blood pressure, plasma cholesterol, and atherosclerosis by elevated endothelial nitric oxide. *J Biol Chem.* 2002;277(50): 48803-7.

Book Chapters

- Luc Jordaens, Paul Knops, Bruno Schwagten, Geert P. Kimman, **Elza van Deel**, Wim van der Giessen, Heleen van Besuekom; AVNRT Cryoablation and Comparison with RF Ablation, Cryoablation of Cardiac Arrhythmias edited by Audrius J. Bredikis and David J. Wilber; Philadelphia, Elsevier Inc, 2011, p 128-142.
- Duncker DJ, van Haperen R, **van Deel E**, de Waard M, Mees B, de Crom R.; Endothelial nitric oxide synthase in cardiovascular homeostasis and disease. *The Physiological Genomics of the Critically Ill Mouse*, edited by Ince C. Dordrecht/Boston/London: Kluwer Academic, 2004, p. 291-310.

Published Abstracts

- **Elza D. van Deel**, Martine de Boer, Rio P. Juni, Daphne Merkus, Rien van Haperen, Rini de Crom, An L. Moens, Dirk J. Duncker; eNOS induced oxidative stress exacerbates pressure-overload induced LV hypertrophy and dysfunction and masks beneficial effects of eNOS overexpression. *Circulation* 2011; 124
- M. Stok, H. de Boer, T.P. de Visser, A.J.J. Reuser, **E. van Deel**, D.J. Duncker, N.P. van Til, G. Wagemaker; Towards hematopoietic stem cell gene therapy for the treatment of Pompe disease. *Neuromuscular Disorders* 2011;21, Pag 715

- **Elza D. van Deel**, Martine de Boer, Daphne Merkus, Rien van Haperen, Rini de Crom, Dirk J. Duncker; Beneficial effect of eNOS overexpression on pressure overload induced cardiac hypertrophy and dysfunction unmasked by ROS scavenging. *The FASEB Journal*. 2011;25:1093.9
- Martine de Boer, **Elza D. van Deel**, Gijsbertus T.J. van der Horst, Jan H.J. Hoeijmakers, Dirk J. Duncker; The effects of aging on the cardiac response to hemodynamic overload depend critically on the underlying pathology *The FASEB Journal*. 2011;25:5478
- Dennie Tempel; Martine de Boer; **Elza van Deel**; Remco Haasdijk; Robert Herpers; Dirk J Duncker; Stefan Schulte-Merker; Caroline Cheng; Henricus J Duckers; Apelin Signaling, a Novel Cardiac Specific Regulatory Pathway in Progenitor Cell Trafficking after Myocardial Infarction in Mice. *Circulation* 2010; 122 A18958
- **Elza D. van Deel**, Martine de Boer, Nicky M. Boontje, Monique de Waard, Jolanda van der Velden, Dirk J. Duncker; Diverse effects of exercise on myofilament function in pathologic left ventricular hypertrophy and dysfunction. *The FASEB Journal* 2010; 24: 619.15
- Martine de Boer, **Elza D. van Deel**, Gijsbertus T.J. van der Horst, Jan H.J. Hoeijmakers, Dirk J. Duncker; The Effects of Pressure Overload on Cardiac Geometry and Function are Aggravated by Aging. *The FASEB Journal* 2010; 24: 596.2
- **Elza D. van Deel**, Monique C. de Waard, Martine de Boer, Diederik Kuster and Dirk J. Duncker; Beneficial Effects of Regular Physical Exercise on LV Remodeling and Hypertrophy Depend Critically on the Underlying Cause of Hypertrophy and Remodeling. *Circulation* 2009;120:S818
- Annemarie M Noordeloos, C Cheng, **E van Deel**, D Tempel, M L Simoons, B Lambrecht, D J Duncker and H J Duckers; Heme Oxygenase 1 Expression in Dendritic Cells Drives Cd4+ T Cell Activation in Transplantation Atherosclerosis. *Circulation*. 2008;118:S_863
- Christine J. Pol, **Elza D. van Deel**, Alice Muller, Theo J. Visser, Dirk J. Duncker and Warner S. Simonides. Left ventricular myocardial infarction in mice induces sustained cardiac deiodinase type III activity. *J Mol Cell Cardio* 2008;50(6):1017-25.
- **Elza D. van Deel**, Martine de Boer, Rien van Haperen, Rini de Crom, Daphne Merkus, Dirk J. Duncker; eNOS overexpression fails to protect against pressure overload induced LV hypertrophy and dysfunction. *Acta Physiologica Sinica*, 2008, 60 (Suppl.1): 93
- **Elza D. van Deel**, Zhongbing Lu, Xin Xu, Gunagshuo Zhu, Xinli Hu, John Fassett, Ping Zhang, Tim D. Oury, Robert J Bache, Dirk J. Duncker, Yingjie Chen; Critical role of extracellular SOD for protecting the heart against myocardial hypertrophy and dysfunction after myocardial infarction. *Circulation* 2007; 116:II_290

- Annemarie Noordeloos, **Elza van Deel**, Denise Hermes, Maarten L Simoons, Dirk J Duncker, Caroline Cheng and Henricus J Duckers; Heme Oxygenase-1 expression in Dendritic Cells determines the Outcome of Transplantation Arteriosclerosis. *Circulation*. 2007;116:II_146
- **Elza D van Deel**, Monique C de Waard, Daphne Merkus, Dirk J Duncker; Exercise training ameliorates left ventricular dysfunction after myocardial infarction but not left ventricular dysfunction in pressure overload induced cardiac hypertrophy. *The FASEB Journal* 2007; 21: S92
- **Elza D. van Deel**, Monique C. de Waard, Daphne Merkus, Rien van Haperen, Rini de Crom, Dirk J. Duncker; Altered Systemic Vasomotor Control in Mice Overexpressing Endothelial Nitric Oxide Synthase. *The FASEB Journal* 2005, 19(6) pag. A1244
- Schaar JA, Mastik F, **van Deel ED**, Slager C, Serruys PW, Duncker DJ, van der Steen AFW. The thrombus becomes stiffer in the first 3 hours: In vivo assessment with palpography. *Journal of American College of Cardiology* 2005, 45(3) pag 367A-367A
- M.C. de Waard, **E.D. van Deel**, D. Merkus, R van Haperen, R. de Crom, D.J. Duncker. Beneficial effect of exercise training on cardiac function is lost in mice that overexpress endothelial NO synthase *Circulation*. 2004;110 (17S) pag 299-300.
- M.C. de Waard, **E.D. van Deel**, D. Merkus, A de Vos, R van Haperen, R. de Crom, D.J. Duncker; Exercise training and eNOS overexpression improve left ventricular pump function after myocardial infarction via different mechanisms. *Circulation*. 2003;108 (17S) pag 94-95.
- **Elza D. van Deel**, Monique C. de Waard, René Stubenitsky, Pieter D. Verdouw, Dirk J. Duncker; Influence of Anesthesia and Fluid-supplementation on Heart Rate and Aortic Blood Pressure and Their Stability in FVB Mice. *Basic Research in Cardiology*, Vol. 95, No 6 (2000) pag. 522

Curriculum Vitae

Elza Dianne van Deel werd op 22 maart 1977 geboren te Rotterdam. In 1995 haalde zij haar VWO diploma aan de Gereformeerde Scholengemeenschap Randstad in Rotterdam. In dat zelfde jaar startte ze, in Delft, aan de Hogeschool Rotterdam met de opleiding Hoger Laboratorium Onderwijs en studeerde in juni 1999 af in de richting Medische Biologie. In het laatste jaar deed ze onderzoek bij de Experimentele Cardiologie van het Thoraxcentrum en onderdeel van het ErasmusMC, toen onder leiding van Prof. Dr. P.D. Verdouw, waar ze werkte aan preconditionering van het hart in ratten en het opzetten en ontwikkelen van technieken voor cardiovasculaire metingen in transgene muizen. In september 1999 begon ze als research analist op diezelfde afdeling om het muismodel met overexpressie van humaan endotheliaal NO-synthase te karakteriseren en was ze betrokken bij verschillende cardiologische onderzoeken in diverse varkensmodellen. In 2007, behaalde zij haar "Master of Science in Clinical Research" met de specialisatie "Cardiovascular Sciences" aan het Netherlands Institute for Health Sciences. In 2007 begon Elza ook haar promotieonderzoek bij de Experimentele Cardiologie, onder leiding van Prof.Dr. D.J. Duncker en Prof.Dr. J.H.J. Hoeijmakers, naar de rol van endotheliaal NO-synthase, oxidatieve stress, en de effecten van veroudering als gevolg van DNA schade in de ontwikkeling van hartfalen.



Dankwoord



Dankwoord

Zoals de kaft en stelling 9 van dit proefschrift al proberen aan te geven ben ik me absoluut bewust dat de totstandkoming van dit boekje niet alleen mijn eigen verdienste is, maar dat het niet was gelukt zonder steun van mensen om me heen. En ik ben dan ook heel dankbaar dat ik heel veel mensen mag bedanken!

Als eerste natuurlijk mijn mentor en promotor Dirk "Durk" Duncker. Het is grotendeels dankzij jouw vertrouwen in mij dat dit boekje hier ligt. Bedankt voor alle kansen en vrijheid die je me gegeven hebt en voor de vele werk- maar vaak ook niet-werkgerelateerde gesprekken. Als iemand mensen kan enthousiasmeren voor de wetenschap dan ben jij het! Dus ik ben blij dat je dat ook in de toekomst nog zult blijven doen.

In de laatste periode van mijn promotieonderzoek kreeg ik er zelfs nog een promotor bij. Jan Hoeijmakers, bedankt dat ik mede dankzij u alvast kennis kon maken met de moleculaire kant van de fysiologie.

Mijn promotiecommissie, Jan Danser, Frits Prinzen en Jolanda van der Velden, sorry dat jullie weer eens "bij wijze van hoge uitzondering" iets minder tijd kregen om dit proefschrift te beoordelen, ik heb jullie inbreng bijzonder gewaardeerd. Daarnaast wil ik natuurlijk ook de andere leden van de grote commissie An Moens en Eric Duckers bedanken voor het opponeren en wetenschappelijke inbreng in mijn onderzoek.

The scientific world turned out to be a small world after all and I was lucky enough to spend some lab time abroad to participate with and learn from great international scientists. Dr Chen and Dr Bache thank you so much for giving me the opportunity to spend some time in your lab at the University of Minnesota. This experience has thought me so much more than just that what you can learn behind a microscope. Guangshou, it must have been tough sometimes, to work with such a direct, smart ass Dutch girl but we had a lot of fun. I would also like to express my gratitude to Dr Rockman and Lan Mao from Duke University for teaching me the TAC model that was very important for my research. Dr Laughlin from the University of Missouri, you are an inspiring scientist and I'm happy you agree with me that science and faith go perfectly well together. Belgie is misschien niet zo ver, maar nog steeds buitenland. Professor Karin Sipido bedankt voor de leuke gesprekken in Nice en de experimenten die ik op uw lab in Leuven mocht uitvoeren. Patricia, je hebt gelukkig veel geduld met me gehad, ik begon Western blotten op het laatst zelfs leuk te vinden!

Als echte Rotterdammer zou ik misschien niet zo enthousiast over Amsterdam mogen zijn, maar ik heb het er altijd super naar mijn zin. Naast gezellige borrels in The Basket bij de VU was het altijd een plezier om met Nicky of Max op het lab te zitten. En je weet dat niemand cellen plakt zoals Nicky, alleen die ushimata is er nog steeds niet van gekomen. Jolanda, het is enorm stimulerend en gezellig om met je samen te werken. Positieve Amsterdamse vibes komen ook zeker uit het AMC vol gezellige Brabanders en Limburgers. Ing, no worries, ik heb minstens net zoveel van jou geleerd als jij van mij.

Maar ook van alle andere universiteiten wisten veel van mijn mede OIO's en andere onderzoekers (te veel om hier te noemen) er altijd weer voor te zorgen dat elke cursus,

congres of symposium niet alleen nuttig was maar ook een beetje een spetterende reünie werd.

Dichter bij huis, op het ErasmusMC, zijn er ook een paar collega's van de afdeling Genetica die hier niet mogen ontbreken. Rien, zoals je hopelijk aan dit boekje ziet heb ik echt wel iets gedaan met al je eNOS muizen. Echt heel erg bedankt voor al je hulp! Rini, ook al ben je inmiddels meer met andere zaken bezig, zonder jou had er waarschijnlijk geen eNOS op de voorkant van mijn proefschrift gestaan. Meer recent Renata en Ingrid, bedankt voor het helpen opzetten van de Xpd muizenfok en Erna voor de link met COEUR. Ed, Calinda, Dennis2x, Diana, Henk, Inge, Jessica, John, Jolanda, Marcel, Kim2x, en alle EDC-ers die voor mijn dieren gezorgd hebben, iedereen weet dat jullie werk de basis is van al ons onderzoek.

Mijn collega's van de Experimentele Cardiologie, wil ik natuurlijk bedanken voor de geweldige tijd die ik met jullie heb gehad en voor het laten vervagen van de grens tussen werk en hobby. Maar om niet compleet op te gaan in het meubilair, is het na 12 jaar toch wel eens tijd om te vertrekken. Mirella en René, mijn stagebegeleiders, bedankt voor het mij bijbrengen van de eerste beginselen in het cardiologisch lab, toen ik nog opkeek tegen geleerde AIO's zoals Serge en Sandra en we nog werkten voor DE professor Verdouw. Piet bedankt voor mijn eerste baan en het laten zien dat oudere mannen ook kwajongens kunnen zijn. Monique (mijn eerste student), met veel plezier denk ik terug aan onze gezamenlijke tijd op het muizenlab. Daphne "Par" (wandelande encyclopedie met aanstekelijke lach) en Birgit "Beer" (mijn vriendin-collega), het was altijd goed om bij jullie mijn hart te kunnen luchten. Vincent "Thingy/knuffelheiden" (eerlijk hard ruziemaken met een heerlijke echte goedmaak knuffel... make my day!), Maaïke "mike-je" (altijd de rust zelve, maar ondertussen), Rob (een half jaar bij jou op de kamer = 3 kilo aankomen), Dennie "TD" en Diederik "Didi" (dappere pogingen leren pipetteren), Marc (afzien met 5 vrouwen op de kamer), Shanti "slavendrijver-drijver-trut" (mijn privé analist), Wijnand "Wibi" (de Witte Aap), Mieke (who run the world.....girls!!!), Ihsan (knuffelmarokaan), Caroline en Petra (kokkerellen) Remco en mijn andere MCL collega's (klaar voor de lunch?), Heleen (histologie wordt bijna leuk), Monique (papierwerk en pepernoten), maar ook natuurlijk mijn studenten: Nadine, Jens, Janine, Sander, Jesse en Katja bedankt voor jullie inzet! André, Annemarie, Bianca, Charlotte, Elles, Esther, Ilia, Ilona, Inge, Lau, Liesbeth, Liz, Nienke, Oana, Renate, Richard, Rorry, Roy, Stefan, Stijn, Tuncay, Zhichao: jullie hulpvaardigheid, humor (van soms ietwat dubieus niveau) en gezelligheid ga ik zeker missen.

Maar gelukkig ligt er genoeg leuks in het verschiet. Jeroen, ik verheug me erg op onze samenwerking. Bedankt voor het mogelijk maken van de spannende avonturen die nog gaan komen

Natuurlijk ook mijn paranimfen Martine "Tiny" en Karin "K" onwijs bedankt. Tiny, 6 mei 2010 zal ik nooit meer vergeten. Het is leuk om een maatje te hebben op het lab maar gelukkig zijn we inmiddels veel meer dan dat. K, je hebt een bijzonder plekje in mijn hart en weet me altijd aan het lachen te krijgen, bedankt dat je er altijd was!

Lieve vrienden, jullie zijn onmisbaar en ik hou onwijs veel van jullie. Ann, we lijken gelukkig nog veel meer op elkaar dan dat we verschillend zijn. Ik ben super blij dat ik al 20 jaar alles met je kan delen. De reis van Rotterdam via Rimini en Como, the Outback, the Woolshed via Oostende en weer terug en alles ertussen, had ik niet zonder je willen maken. Anneke, Goe "Judith", Marlies "van der P" onze meidenweekenden zijn altijd weer fantastisch, net zoals helemaal compleet jezelf kunnen zijn en ontzettend veel lol hebben (you can stand under my umbrella!). Kibje/Rica "Henrike" en Niek "Nicole", het voelt gelukkig nog steeds net zo vertrouwd als toen we pubers waren, of misschien nog wel meer. Boebos "Annemarie", he encantó estudiar español en Andalusia contigo, maar wordt ook nog steeds blij in de bar met Chris "Christine", Jes "Jeske" en Roos "Rosanne". Marge "Marjolein", ondanks de afstand blijft het bijzonder. Bas, Douwe, Eva, Henri, Karien, Karine, Marc en Martijn de bijbelstudies en etentjes met mijn oud mede studenten blijven een unieke combinatie van verdieping en plezier. Mika, mijn kleine grote vriend, bedankt dat je altijd een glimlach op mijn gezicht maakt! Oeke "AnnaBrita", ik mis het nog steeds dat we niet meer elke week over de mat rollen. Ruta, een cursus in Nice is altijd nice, en soms krijg je spontaan veel meer dan nieuwe kennis. Joost, onze eerlijke goede gesprekken zijn heel waardevol. Aris, Dorenda, Eline, Klarieke, Marijke, Martijn, Raoul, Rieke, Robert, Wieg en Wout, wie steekt de BBQ aan? Adrienne, gezellige maar zeker geen oppervlakkige wijntjes. Ik ben vast nog iemand vergeten maar het is super om altijd weer te merken dat er zoveel mensen zijn die me zeggen wat ze echt denken en me laten zien dat het leven mooi is.

Onvervangbaar is ook mijn familie. San "Sander", Jolien, Thijmen, TinTin "Martijn", Janne "Dianne", Arjuan "Arjan", Eer "Eric", Janneke, Arn "Arnoud", Len "Lennard", Aar "Arediene", Ax "Aksel", Geann "Geanne", Mark, Gerb "Gerben", Ucje "Marlinda", Li "Lisanne", wees gerust "tante" Elza zal altijd mijn belangrijkste titel blijven. Jullie markeren niet voor niets de hoofdstukken van dit proefschrift. Frans, Koko "Luuk", Bea, Marten en Colin mijn grote broers en zussen, het is heerlijk om soms ook nog gewoon even het kleine zusje te kunnen zijn. Papa en mama, bedankt voor alle mogelijkheden die jullie me altijd hebben gegeven. Ook al hebben jullie me vast niet altijd helemaal begrepen, van jullie heb ik geleerd wat echt waardevol is in het leven. Goud hoar laiverds!

Anton "Os", de grote verrassing die me blijft verrassen, niemand maakt me zo blij als jij doet! Hou van je! CC

Elza